GEOCHEMICAL AND ISOTOPE STUDIES OF ELEMENT DISPERSAL IN THE ENVIRONMENT DURING MINING AND ORE PROCESSING

by

ALLA V. DOLGOPOLOVA

A thesis submitted for the Degree of
Doctor of Philosophy of the University of London

Imperial College London

February 2005

ABSTRACT

The Orlovka-Spokoinoe mining district (Transbaikalia, Russia) was used to assess sources and pathways of potentially toxic elements released during mining and processing of Ta-Nb-Sn-W ores. Samples of geological (rocks), anthropogenic (ore concentrates, tailings, gasoline) and environmental (lichens, leaves) origins were studied. Element ratios, REE patterns and Pb and Zn isotopes were used as innovative diagnostic tools to trace natural and anthropogenic sources of dust and Pb and Zn within the mining site.

Initially, analytical development of high temperature and pressure microwave digestion technique for leaves and lichens (that have a high ash content and thus are difficult to digest) was required. Complete recovery of Pb and Zn was achieved at pressure of 350 Psi and optimised amount of HF (0.8ml).

Analytical protocols for high precision Pb isotope ratio measurements on MC-ICP-MS resulted in internal precision of <100 ppm ($\pm 2\sigma$) and long-term reproducibility below 350 ppm ($\pm 2\sigma$) for all Pb isotope ratios in all matrices. Mass bias correction using optimised $^{205}Tl/^{203}Tl$ ratios achieved accuracies below 80 ppm for all ratios.

Geological metal sources within the mining site were then geochemically characterised. Zr/Hf, Y/Ho, Rb/Sr showed continuous fractionation during evolution of granites, whereas REE patterns reflected in addition alteration processes. Pb isotopes characterised the geologic suite and defined two possible sources of granites: i) a mixture of upper crust-mantle source or ii) a type II enriched mantle source.

REE patterns were further used to trace dust within the mining site and identified tailings and host rocks as the main dust sources. Pb and Zn normalised to lithogenic elements demonstrated that tailings, barren granites and host rocks are potential sources of Pb and Zn. However, Pb isotopes indicated that long-range aerosols are the dominant Pb source. Zn isotopes showed isotopic variability between geological and environmental samples with lighter shifts measured in the geologic suite and a heavier range typical for lichens.

ACKNOWLEDGEMENTS

I am very grateful to Dominik Weiss, Chris Stanley and Reimar Seltmann for their continuous support, guidance and encouragement throughout the project. Dominik is especially acknowledged for his time and help with MC-ICP-MS measurements. Reimar and Chris are particularly thanked for inspiring discussions.

I highly appreciate financial support that I have received from the Royal School of Mines, Imperial College London (ICL) and Department of Mineralogy, The Natural History Museum (NHM) that enabled me to complete the project through ORS Award, Albert Julius Bursary (ICL) and Departmental Research Fund (Department of Mineralogy, NHM). Sue Stone (ICL) is especially thanked for her assistance in Albert Julius Bursary application process.

Many thanks are given to Barry Coles (ICL), especially for the ICP-AES analyses he carried out and for his help with measurements at the MC-ICP-MS. Thomas Mason (ICL) is thanked for his supervision and advice during Zn isotope measurements and fruitful discussions on data interpretation.

Several members of EMMA division (NHM) have provided invaluable input into my project. In particular, I am grateful to John Spratt, Terry Greenwood, Vic Din and Gary Jones for their kind attitude and continuous help during my work in their laboratories. Sara Russell, Eta Mullane and Teresa Jeffries are acknowledged for their help in running the IsoProbe. William Purvis (Department of Botany, NHM) is thanked for his interest in lichens study and valuable advice.

A special mention is to Russian colleagues A.A. Aksyuk, G.P. Zaraisky, A.V. Fedkin (IEM Chernogolovka), V.V. Shatov, G.B. Romanovsky (VSEGEI St. Petersburg), A.A. Kremenetsky and L.I. Ginzburg (IMGRE Moscow) for fruitful discussions and assistance in field sampling.

Finally, my family is especially thanked for their patience, understanding, love and all support provided during all years of the project, I am indebted to my daughter Vlada who has been such a great helper to me. I dedicate this thesis to them.

LIST OF CONTENTS

LIST OF TABLES

LIST OF FIGURES

CHAPTER 2. CLOSED-VESSEL MICROWAVE DIGESTION TECHNIQUE FOR LICHENS AND LEAVES PRIOR DETERMINATION OF TRACE ELEMENTS (Pb, Zn, Cu) AND STABLE Pb ISOTOPE RATIOS

CHAPTER 3. RAPID AND HIGH PRECISION LEAD ISOTOPE MEASUREMENTS IN ENVIRONMENTAL SAMPLES BY MULTI-COLLECTOR PLASMA SOURCE MASS SPECTROMETRY

CHAPTER 4. GEOCHEMICAL CHARACTERISTICS AND LEAD ISOTOPE SYSTEMATICS OF HIGHLY FRACTIONATED Li-F ENRICHED AMAZONITE GRANITES AND RELATED HOST ROCKS OF THE ORLOVKA-SPOKOINOE MINING DISTRICT, EASTERN TRANSBAIKALIA (RUSSIA)

CHAPTER 5. TRACING DUST AND Pb DISPERSAL AT THE ORLOVKA Ta-W MINING AND ORE PROCESSING SITE: INSIGHTS FROM REE PATTERNS AND ELEMENTAL RATIOS

CHAPTER 1. INTRODUCTION

1.1. BACKGROUND OF THE RESEARCH

There is a vast literature documenting elevated metal concentrations in the environment as a result of man's activities. The mining of metalliferous mineral deposits and associated metal processing activities leads to severe perturbations in the cycling of metals in the surface environment (Thornton, 1996). Where ore deposits were mined, local "geochemical explosions" were created, which sharply intensified metal and potentially toxic element supply into all components of the environment. Mass contamination of natural waters, soils, plants and other natural components under the anthropogenic influence of mining activity can lead to disastrous toxicity in plants, animals and people. Contamination arising from such activities is a worldwide problem (Nriagu and Pacyna, 1988).

Information about contamination can be gained from analyses of metal concentrations and speciation alone, but a lot of uncertainties often remain concerning metal sources. This is particularly true for metals with multiple sources and those that are transported large distances from the original source. Metal sources can be assessed using different geochemical tools. Trace element ratios are sensitive indicators to identify fractionation processes and fluid-rock interaction (Bau, 1996), and thus to serve as a tool to discriminate groups of different origin and genesis. For example, Zr/Hf is a good indicator of crystallisation differentiation in magmatic rocks (Linnen and Keppler, 2002). Zr/Hf, Y/Ho and Rb/Sr were used previously as diagnostic ratios to assess the geochemical evolution of the granite intrusions that host the Orlovka deposit (Fedkin 2000; Zaraisky et al., 2000). Other indicative ratios, i.e. Nb/U and Ce/Pb were applied to characterise the composition of the earth's mantle and its evolution (Hoffman et al., 1986). However, use of indicative ratios as geochemical tracers of metal sources within the environment remains poorly addressed.

Rare earth elements (REE) patterns have been used extensively in igneous, sedimentary and metamorphic petrology to trace sources of rocks and minerals during crustal and mantle evolution (Rollinson, 1993). Due to its indicative and similar geochemical behaviour Y, with an ionic radius similar to that of Ho, is sometimes included along with REE. The low atomic number members of the series

are termed the light rare earths (LREE: La, Ce, Pr, Nd, Pm, Sm and Eu) and those with higher atomic numbers the heavy rare earth elements (HREE: Gd, Tb, Dy, Ho, Er, Tm, Yb, Lu, Sc and Y). Studies such as those by Nesbitt (1979) show that whilst the REE are mobilized during weathering, they are reprecipitated at the site of weathering. A more recent studies show, however, that in the case of extreme weathering the degree of weathering of the source can be recognized in the REE chemistry of the derivative sediment (Nesbitt et al., 1990). A number of properties of the REE suggest that they should also be useful in the study of environmental processes as: 1) they are among the least soluble trace elements, and 2) they are relatively immobile during low-grade metamorphism and hydrothermal alterations (Rollinson, 1993). REE patterns were used in a number of environmental geochemical studies e.g., in surface waters (Dinelli et al., 1999) and sewage water (Knappe et al., 1999; Bau et al., 1996) to assess acid mine drainages, in oceanic waters to assess riverine inputs (Elderfield, 1988) or in peat bogs to assess sources of dust (Krachler et al., 2002).

Whereas the concentration and speciation of a metal can vary greatly as it moves through the environment, it often preserves the isotopic composition of its source, which can thus fingerprint its origin. This property has long been used by geologists to trace movement of elements between reservoirs in the earth. For example, Pb isotopes have been widely used to assess the relative contributions of mantle and crustal sources during rock formation (Fletcher 1993; Harmer 1995; Abouchami 2000; Faure, 2001). Lead has four isotopes. The three lead isotopes ^{208}Pb, ^{207}Pb and ^{206}Pb are radiogenic daughter products from the radioactive decay of one isotope of thorium ($^{232}Th \rightarrow {}^{208}Pb$) and two isotopes of uranium ($^{238}U \rightarrow {}^{206}Pb$ and $^{235}U \rightarrow {}^{207}Pb$) (Faure, 1986). The fourth isotope of lead, ^{204}Pb is stable and has no long-lived parent isotope nor does it decay to another isotope. The Pb isotopes are, however, not affected by industrial or biological processes (Ault et al., 1970) and do not fractionate during transport and deposition processes. They therefore retain the isotopic composition of their sources with great potential as source tracers. The use of Pb isotopes to identify and to distinguish between natural and anthropogenic sources of contamination became a routine fingerprinting tool in the last few decades (Rosman et al., 1993, 1994, 1999; Kober et al., 1999; Chiaradia et al., 2000; Luck et al., 2002). Some of these studies have led to conclusions that could not be predicted

from measurements of Pb concentrations alone. For example, a study of children from the site of one of the world's largest Pb mines (Broken Hill, Australia), revealed that high blood Pb levels were not the result of the local mining, but were rather derived from household paint and gasoline fumes (Gulson, 1996).

In recent years there has been growing interest in using Zn isotopes to address problems of environmental contamination. Zn has five stable isotopes, ^{64}Zn, ^{66}Zn, ^{67}Zn, ^{68}Zn and ^{70}Zn, with average atomic abundances of 49.19 %, 27.79 %, 4.04 %, 18.39 % and 0.60 %, respectively (Tanimizu et al., 2002). There are instances of close proximity to sources of contamination (e.g., smelting plants) where the source of Zn is fairly clear-cut, but like many other metals, there are a variety of sources of Zn in the environment. These include natural sources (e.g., soil dust, volcanic material, weathering of Zn-rich rocks) and anthropogenic sources (e.g., sewage sludge, smelting plants, combustion products, mine waste). Although development of Zn isotopes measurements are still at an early stage, the first studies indicated Zn isotopic variability in a variety of geological (carbonates and sulphides) and biological (lobster liver, mussel tissue, phytoplankton and plants) samples (Maréchal et al., 1999; Maréchal et al., 2000; Archer and Vance, 2002; Albarède, 2004; Mason et al., 2003). This permits interpretations of the geochemistry and biochemistry of Zn in the natural environment.

The present investigation of elemental ratios, rare earth element patterns and Pb and Zn isotopes has been made with the aim of establishing diagnostic tools to assess sources and pathways of these elements in the environment of the Orlovka-Spokoinoe mining site, Eastern Transbaikalia, Russia. Mining is a major industrial source of contamination in Eastern Transbaikalia where rare-metal, gold-silver, base-metal, fluorite, and uranium deposits have all been mined during the last century. The Orlovka-Spokoinoe mine and its surroundings, however, are not drastically contaminated by Pb and Zn. The literature concerning dispersion of contamination around mining sites with relatively low concentrations of Pb and Zn is surprisingly limited and therefore the Orlovka-Spokoinoe mining site provides a special opportunity to trace Pb and Zn contamination around a mine with low base-metal concentrations. The geochemically well studied Orlovka-Spokoinoe mining and ore processing plant site has been chosen to extend the knowledge on element distribution within this natural laboratory by using elemental ratios, rare earth

elements (REE) patterns and isotope variations of Pb and Zn of biological and geochemical background (birch leaves, lichens, natural rocks and minerals). The synthesis of these data aims to obtain the main features of the geological and geochemical trends of the mining area and to provide a detailed source assessment of Pb and Zn within the mining site by studying relationships and interaction between geological, anthropogenic and environmental samples.

1.2. AIMS, OBJECTIVES AND NOVELTY OF THE STUDY

The main aim of this study is to examine the utility of the isotope compositions of Pb and Zn, elemental ratios and rare earth elements (REE) patterns for monitoring the sources and pathways of these potentially toxic metals released through mining and ore processing activities within an abandoned mine land at the Orlovka-Spokoinoe mining district in Eastern Transbaikalia, Russia.

The main objectives of the research were identified as follows: 1) to distinguish between geologic sources, anthropogenic products and environmental samples; 2) to discriminate between natural (geogenic) and anthropogenic sources of dust, Pb and Zn within the mining environment; 3) to assess multi-component mixing, and 4) to gain experience, knowledge and new insights for environmental application of the still poorly understood Zn isotope system.

Various samples of geological (minerals and rocks), environmental (birch leaves and lichens) and anthropogenic origin (tailings and ore concentrates) were measured for total elemental concentrations, trace elements concentrations, REE, and Pb and Zn isotopic composition. This data set consequently enabled a detailed source assessment to be made.

The research also includes the analytical development of high temperature and pressure microwave digestion techniques for lichens and leaves and analytical protocols for high precision Pb isotope measurements. Total elemental concentrations of samples were measured using inductively coupled plasma-atomic emission spectrometry (ICP-AES) and Pb and Zn isotopic variations using multi-collector inductively coupled plasma mass spectrometer (MC ICP-MS).

The novelty of the study lies in using a combination of several geochemical tools such as elemental ratios, REE patterns and high-precision Pb and Zn isotopes to assess sources and migration pathways of Pb and Zn within the studied mining site.

REE patterns that were previously extensively used in igneous, sedimentary and metamorphic petrology to trace sources of rocks and minerals during crustal and mantle evolution, for the first time highlighted new possibilities to trace dust pollutants within the mining environment. **Pb isotopes** brought additional insights into the understanding of the formation mechanisms of the Khangilay-Orlovka-Spokoinoe granite plutons and also into the sources of Pb dispersed within the mining site. **Zn isotopes** measured in lichens and a geologic suite from the Orlovka-Spokoinoe mining site exhibited a clear distinction between Zn isotopic variations of geologic and biologic materials.

1.3. THESIS STRUCTURE

Five of the chapters are presented in the form of separate publications. Some of the chapters are already published (Chapters 2, 3 and 4), others are submitted to peer-reviewed journals (Chapters 5 and 6). Because of this format, the chapters have a different layout and their own abstract, introduction, conclusions and references. **Chapter 1** introduces the background of the research together with defined aims and objectives. **Chapter 2** describes the development of microwave acid digestion for lichens and leaves prior to elemental and MC-ICP-MS analysis (Dolgopolova et al., 2004b). **Chapter 3** covers the development of high-precision Pb isotope measurements in environmental samples by MC-ICP-MS (extracts of the chapter are published in Weiss et al., 2004). **Chapter 4** focuses on the chemical characteristics and Pb isotope systematics of ore-bearing granites and host rocks of the Orlovka-Spokoinoe mining site and presents a slightly revised version of Dolgopolova et al., 2004a. **Chapter 5** presents the findings of a study that traces dust and Pb dispersal within the Orlovka-Spokoinoe mining site using REE patterns and elemental ratios (Dolgopolova et al., *submitted a*). **Chapter 6** presents an investigation into use of element and isotope ratios to assess sources and pathways of Pb and Zn dispersed within the Orlovka-Spokoinoe mining site during mining and ore processing (Dolgopolova et al., *submitted b*). Finally, **Chapter 7** summarises the main findings of the project and makes an assessment of why a combination of independent geochemical tools such as element concentrations, element ratios, REE patterns and isotopes is vital for the comprehensive assessment of metal sources within the environment. It also contains recommendations for further research.

Appendix 1 includes photos of the Orlovka-Spokoinoe mining site and the map of the main infrastructure units. A selection of lichens for the environmental study including lichens photos and analytical SEM analyses of silicate particle trapped by lichens) are given in **Appendix 2**. **Appendix 3** provides a background to the sample preparation protocols, including column chemistry procedure prior high-precision Zn isotope measurements by MC-ICP-MS. Tables with full analysis database are listed in **Appendix 4**. Two additional co-authored publications are provided in **Appendix 5**.

1.4. REFERENCES

Abouchami, W., Galer, S.J.G., Hofmann, A.W., 2000. High precision lead isotope systematics of lavas from the Hawaiian scientific drilling project. Chemical Geology 169, 187-209.

Albarède F., 2004. The stable isotope geochemistry of copper and zinc. In: Rosso, J.J. (Ed.), Mineralogical Society of America. Reviews in Mineralogy and Geochemistry 55, 409-427.

Archer, K. and Vance, D., 2002. Large fractionations in Fe, Cu and Zn isotopes associated with Archean microbially-mediated sulphides. Geochimica et Cosmochimica Acta 66 (15A), A26 Suppl.

Ault, W.A., Senechal, R.G., Erlebach, W.E., 1970. Isotopic composition as a natural tracer of lead in the environment. Environmental Science and Technology 4, 305-311.

Bau, M., 1996. Controls on the fractionation of isovalent trace elements in magmatic and aqueous systems: evidence from Y/Ho, Zr/Hf, and lanthanide tetrad effect. Contributions to Mineralogy and Petrology 123, 323-333.

Bau, M. and P. Dulski, 1996. Anthropogenic origin of positive gadolinium anomalies in river waters. Earth Planetary Scientific Letters 143, 245-255.

Chiaradia, M. and Cupelin, F., 2000. Behaviour of airborne lead and temporal variations of its source effects in Geneva (Switzerland): comparison of anthropogenic versus natural processes. Atmospheric Environment 34, 959-971.

Dinelli, E., et al., REE mobility associated to acid mine drainage: Investigations in the Libiola area, northern Italy, in Geochemistry of the Earth's surface, Armannsson, Editor. 1999, Balkema: Rotterdam. p. 173-176.

Dolgopolova, A., Seltmann, R., Kober, B., Weiss, D., Stanley C., Dulski, P., 2004a. Geochemical characteristics and Pb isotope systematics of highly fractionated Li-F enriched amazonite granites and related host rocks of the Orlovka-Spokoinoe mining district, Eastern Transbaikalia (Russia). Trans. Inst. Min. Metall. Section B: Applied Earth Sciences, 113, B83-B99.

Dolgopolova, A., Weiss, D., Seltmann, R., Stanley C., Coles, B., Cheburkin A.K., 2004b. Closed-vessel microwave digestion technique for lichens and leaves prior to determination of trace elements (Pb, Zn, Cu) and stable Pb isotope ratios. International Journal of Environmental Analytical Chemistry 84 (12), 889-899.

Dolgopolova, A., Weiss, D.J., Seltmann, R., Dulski, P. Tracing dust and Pb dispersal at the Orlovka Ta-W mining and ore processing site: insights from REE patterns and elemental ratios. Journal of Hazardous Materials, submitted a.

Dolgopolova, A., Weiss, D.J., Seltmann, R., Kober, B., Mason, T.F.D., Coles, B., Stanley, C.J. Use of element and isotope ratios to assess sources and pathways of Pb and Zn dispersed in the environment during mining and ore processing within the Orlovka-Spokoinoe mining site (Russia). Applied Geochemistry, submitted b.

Elderfield, H., 1988. The oceanic chemistry of the rare earth elements. Phil. Trans. Royal Society London A325, 105-126.

Faure, G. 2001. Origins of igneous rocks: the isotopic evidence. Springer, 496 p.

Faure, G., 1986. Principles of isotope geology. Second edition. John Wiley and Sons, USA, 464 p.

Fedkin, A., 2000. Geochemical evolution and layering of Li-F granites of the Orlovka and Etyka Ta deposits. PhD thesis (in Russian). Moscow State University, Moscow, 163p.

Fletcher, C.J.N., Swainbank, I.G., Colman, T.B., 1993. Metallogenic evolution in Wales: constraints from lead isotope modelling. Journal of the Geological Society, London 150, 77-82.

Gulson, B., Mizon, K., Low, A.J., Korsch, M., Davis, J.J., 1994. Source and pathways of lead in humans from the Broken Hill mining community - an alternative use of exploration methods. Economic Geology 89, 889-908.

Harmer, R.E., Auret, J.M., Eglington B.M., 1995. Lead isotope variations within the Bushveld complex, Southern Africa: a reconnaissance study. Journal of African Earth Sciences 21(4), 595-606.

Hofmann, A.W., Jochum, K.P., Seufert, M., White, W.M., 1986. Nb and Pb in oceanic basalts: new constraints on mantle evolution. Earth and Planetary Science Letters 79, 33-45.

Knappe, A., et al., Gadolinium in aquatic systems as indicator for sewage water contamination, in Geochemistry of the Earth's surface, Armannsson, Editor. 1999, Balkema: Rotterdam. 187-190.

Kober, B., Wessels, M., Bollhoefer, A., Mangini, A., 1999. Pb isotopes in sediments of lake Constance, Central Europe constrain the metal pathways and the contamination history of the catchment, the lake and the regional atmosphere. Geochimica et Cosmochimica Acta 63 (9), 1293-1303.

Krachler, M., et al., 2002. Two thousand years of atmospheric rare earth element (REE) deposition as revealed by an ombrotrophic peat bog profile, Jura Mountains, Switzerland. Journal of Environmental Monitoring 5, 111-121.

Linnen, R.L. and Keppler, H., 2002. Melt composition control of Zr/Hf fractionation in magmatic processes. Geochimica Cosmochimica Acta 66, 3293-3301.

Luck, J.M. and Othman D.B., 2002. Trace element and Pb isotope variability during rainy events in the NW Mediterranean: constraints on anthropogenic and natural sources. Chemical Geology 182, 443-460.

Maréchal, C.N., Télouk, P., Albarède, F., 1999. Precise analysis of copper and Zn isotopes by plasma-source mass spectrometry. Chemical Geology 156, 251-274.

Maréchal, C.N., Nicolas, E., Douchet, C., Albarède, F., 2000. Abundance of Zn isotopes as a marine biogeochemical tracer. Geochemistry Geophysics Geosystems 1, GC000029.

Mason, T.F.D., 2003. High precision transition metal isotope analysis by plasma-source mass spectrometry and implications for low temperature geochemistry. PhD thesis, Imperial College London.

Nesbitt, H.W., 1979. Mobility and fractionation of rare earth elements during weathering of a granodiorite. Nature 279, 206-210.

Nesbitt, H.W., MacRae, N.D., Kronberg, B.I., 1990. Amazon deep-sea fan muds: light REE enriched products of extreme chemical weathering. Earth Planetary Scientific Letters 100, 118-123.

Nriagu, J.O. and Pacyna, J.M., 1988. Quantitative assessment of worldwide contamination of air, water and soils by trace metals. Nature 333, 134-139.

Rollinson, H.R., Using geochemical data: evaluation, presentation, interpretation, 1993: Longman Scientific, 352 pp.

Rosman, K.J.R., Chisholm, W., Boutron, C.F., Candelone, J.P., Gorlach, U., 1993. Isotopic evidence for the source of lead in Greenland snow since the late 1960s. Nature 362, 333-334.

Rosman, K.J.R., Chisholm, W., Boutron, C.F.,' Candelone, J.P., Hong, S., 1994. Isotopic evidence to account for changes in the concentrations of lead in Greenland snow between 1960 and 1988. Geochimica et Cosmochimica Acta 58, 3265-3269.

Rosman, K.J.R., Ly, C., Steinnes, E., 1999. Spatial and temporal variations in isotopic composition of the atmospheric lead in Norwegian moss. Environmental Science and Technology 32, 2542-2548.

Tanimizu, M., Asada, Y., Hirata, T., 2002. Absolute isotopic composition and atomic weight of commercial Zn using inductively coupled plasma mass spectrometry. Analytical Chemistry 74, 5814-5819.

Thornton I., 1996. Impact of mining on the environment; some local, regional and global issues. Applied Geochemistry 11, 355-361.

Weiss, D.J., Kober, B., Dolgopolova, A., Gallagher, K., Spiro, B., Le Roux, G., Mason, T.F.D., Kylander, M., Coles, B.J., 2004. Accurate and precise Pb isotope ratio measurements in environmental samples by MC-ICP-MS. International Journal of Mass Spectrometry 232, 205-215.

Zaraisky, G.P, Aksyuk, A.M., Seltmann, R. and Fedkin, A.V., 2000. Evolution of rare-metal granites and Zr/Hf ratio as an indicator of their crystallization differentiation. In: Yushkin, N.P. (Ed.), Petrography at the Boundary of the XXI Century: Results and Perspectives. Proceed. 2nd Russian Petrography Meeting, Syktyvkar, Geoprint III (in Russian).

CHAPTER 2. CLOSED-VESSEL MICROWAVE DIGESTION TECHNIQUE FOR LICHENS AND LEAVES PRIOR TO DETERMINATION OF TRACE ELEMENTS (Pb, Zn, Cu) AND STABLE Pb ISOTOPE RATIOS

ABSTRACT

A reliable and robust procedure using closed-vessel microwave digestion of lichens and leaves for precise and accurate determination of trace elements (Pb, Zn and Cu) and stable Pb isotope ratios is presented. The method was developed using certified reference material CRM 482 *Pseudovernia furfurea* (Lichens), NIST 1515 (Apple Leaves) and NIST 1547 (Peach Leaves) and tested on lichens from a mining site in Russia. A mixture of 3ml HNO_3, 3ml H_2O_2, 2ml H_2O and 0.8ml HF ensured complete sample dissolution with 100±5% recovery for Pb, Zn and Cu at a maximum temperature of 210°C and pressure of 350 psi. The amount of HF and microwave pressure significantly influenced Pb, Zn and Cu recovery. Comparison between EMMA-XRF and ICP-AES showed good correlation between Pb, Zn and Cu concentrations. Using the newly developed digestion method Pb isotopes in lichens from the mining site were determined with an internal precision better than 0.02%.

Keywords: microwave digestion, acid decomposition, standard reference materials (SRM), lichens, solid particulates, Pb isotopes.

International Journal of Environmental Analytical Chemistry, in print.

Date of submission: 15 January 2004.

Date of acceptance: 28 April 2004.

2.1. INTRODUCTION

The accumulation of trace metals from atmospheric deposition by lichens, mosses and plant leaves is well-documented [1,2,3]. Lichens in particular are regarded as suitable tools for monitoring levels of atmospheric contamination. Because their mineral nutrition depends on both wet and dry depositions from the atmosphere they are able to accumulate and store many substances from the atmosphere [4]. In recent years lichens have been successfully used to assess natural versus anthropogenic sources of airborne particulates using Pb isotopes and therefore to trace atmospheric contamination on local and regional scales [5,6,7].

Although HNO_3 and leaching are sufficient if only contaminant elements are assessed, a complete dissolution of lichens is needed if natural sources are also to be determined. This is of special importance if trace element dispersal is studied in areas with low level contamination where the main carrier of trace and potentially toxic elements might be incorporated in naturally derived sources, for example in silicate phases which are highly resistant to acid attack. These particles are trapped on the surface or within the lichens structure making acid decomposition of lichens different from that of leaves and other botanical samples. Both highly resistant inorganic phases (i.e. siliceous particles) and the organic matrix (lichens) must be completely destroyed to achieve complete dissolution of lichens.

In the last decade closed-vessel microwave-assisted acid decomposition has been widely used for the digestion of lichens [8,9]. This technique has many advantages in comparison with traditional open vessel digestion such as speeding up the sample preparation process, safe operation of the digestion due to fully automated programming, preventing loss of volatile analytes during the digestion and eliminating sample contamination from other samples or the laboratory environment [10-13]. Furthermore, the ability to monitor and control reaction parameters such as temperature and pressure during the digestion process is advantageous in determining the efficiency of sample digestion; the higher temperatures attained under pressure in closed-vessel digestions result in a more complete sample matrix decomposition [10]. For safety reasons 0.5g of plant material is the maximum recommended amount to use in 15 ml vessels for closed-vessel microwave digestion [11]. Any larger sample amount can significantly increase the internal pressure of the

system due to the large production of gaseous degradation products and potentially lead to the rupture of the vessel.

Previously published methods of microwave-assisted digestion of botanical samples vary significantly and depend on the sample matrix and/or analysis targets. Routine decomposition methods involve procedures containing 5-10 ml of HNO_3, 0.5-1 ml of H_2O_2 and up to 0.2 ml of HF mixture [8,9,11,12,14-21]. The main findings were:

1) quantitative recovery of Pb, Zn and Cu concentrations is achieved in lichen standard reference materials;
2) decomposition of lichens included HF to decompose insoluble residues;
3) insufficient amount of HF resulted in lower recovery of Pb, Ni, Cr, Sn, V, Ti, Al and Fe, i.e. those elements that are correlated with the Si content; and
4) during the analysis of real lichen samples characterized by different masses of dust particulate, the use of HF improved accuracy.

However, most of the reported methods required filtering of the digests prior to elemental analysis [8,14,15,17], which suggests incomplete dissolution of the sample matrices even in cases where 0.2ml of HF was added [8,9]. None of the publications have addressed Pb isotope determination in lichens. Consequently, the aim of this study was to improve methods to achieve the complete dissolution of lichens using closed-vessel microwave-assisted digestion for the determination of Pb, Zn and Cu and stable Pb isotope ratios. The existing closed-vessel microwave digestion methods [8,9] were modified by: 1) adjusting the amount of HF added to the sample matrices, 2) increasing the digestion time and 3) optimizing the microwave pressure. Although $HClO_4$ is conventionally used as an effective acid for the breakdown of the organic fractions, the use of this acid was avoided in our experimental development work for safety reasons [22]. To check the accuracy of the method certified standard reference materials of lichens and leaves were included in the study. The modified digestion method was tested on lichens collected from the Orlovka-Spokoinoe mining district in Eastern Transbaikalia, Russia.

The inter-laboratory comparison study for Pb, Zn and Cu contents was performed using inductively coupled plasma atomic emission spectrometry (ICP-AES) and X-ray fluorescence spectrometry (EMMA-XRF). Following the microwave-assisted decomposition procedure, lichens from the mining site were analyzed for Pb isotopes.

2.2. EXPERIMENTAL DEVELOPMENT

2.2.1. Instrumentation

The acid digestions were accomplished using a CEM Microwave Accelerated Reaction System MARS-X with temperature and pressure control. 100 ml Teflon vessels (XP-1500) fitted with screw tops and with a pressure venting system were used as digestion vessels. Prior to their use, all vessels were thoroughly acid-cleaned in the microwave (for 15 min at 150°C) using 5ml of concentrated HNO_3 and 5 ml of Milli-Q H_2O. After cooling, the contents of the vessels were discarded and the vessels were rinsed with Milli-Q deionised H_2O (18 MΩ cm). One vessel out of 12 (i.e. control vessel) monitored pressure and temperature during the digestion, providing constant feedback control of reaction conditions. Pb, Zn and Cu were determined by Fison's Instruments ARL 3508B ICP-AES.

Selected samples were analyzed using energy-dispersive miniprobe multielement analysis (EMMA-XRF); analytical and instrumental details of the measurements are given elsewhere [23,24].

Pb isotopes in lichens were determined using a GVi *IsoProbe* multicollector inductively coupled plasma mass spectrometer (MC-ICP-MS). A CETAC Aridus nebulizer (Omaha, NE, USA) was used for sample uptake for the *IsoProbe*. Details of the measurements are given in [25].

Semi-quantative analysis of siliceous particles on the lichens surface was done using a Jeol 5900LV analytical scanning electron microscope (SEM) equipped with an Oxford Instruments Inca Pentafet energy dispersive X-ray spectrometer (EDS).

Filtered and dried residues from digested lichens were analyzed by X-ray powder Diffraction (XRD). XRD was performed using an Enraf-Nonius PDS120 diffractometer that incorporates an Inel curved, position sensitive detector. Further details of the XRD measurements can be found in [26].

All instruments used for the study are at the Natural History Museum, London apart from the EMMA-XRF facility that is based at the University of Heidelberg.

2.2.2. Samples and reagents

(1) Three certified reference materials NIST 1515 (Apple Leaves), NIST 1547 (Peach Leaves) and CRM 482 #10 *Pseudovernia furfura* (Lichens) were used. The certified concentrations values of Pb, Zn and Cu (μg/g) are given in Table 2.1.

(2) Two lichens species, i.e. *Xanthoparmelia* and *Parmelia ullophyllodes* (n=15) collected from the Orlovka-Spokoinoe mining district in Eastern Transbaikalia (Russia) were used to test the developed digestion method. Lichens study is a part of the environmental geochemical investigations on the Orlovka-Spokoinoe mining site [27].

Table 2.1. Comparison of Pb, Zn and Cu recovery rates in CRM 482 (Lichens), NIST 1547 (Peach Leaves) and NIST 1515 (Apple Leaves) for 3 digestion experiments (Exp. in the Table) tested (see details of the Experiments in Table 2.2). Concentration values (μg/g) were determined by ICP-AES.

Element/ Sample	*Certified values (± 2σ)*	*Exp. I*	*Recovery (%)*	*Exp.II*	*Recovery (%)*	*Exp. III*	*Recovery (%)*
Pb							
Lichens CRM 482	40.9 ± 1.4	28.1 ± 5.1	**68.8**	34.6 ± 3.2	**84.6**	38.1 ± 1.6	**93.2**
Apple leaves NIST 1515	0.5 ± 0.024	0.5 ± 0.07	**97.9**	0.5 ± 0.07	**95.8**	0.5 ± 0.01	**95.7**
Peach leaves NIST 1547	0.9 ± 0.003	0.8 ± 0.03	**86.7**	0.9 ± 0.24	**101**	0.9 ± 0.01	**98.9**
Zn							
Lichens CRM 482	100.6 ± 2.2	62.2 ± 1.8	**61.8**	81.1 ± 1.2	**80.6**	92.6 ± 3.1	**92**
Apple leaves NIST 1515	12.5 ± 0.4	11.6 ± 0.1	**92.6**	11.4 ± 0.4	**91.2**	11.8 ± 0.1	**94.4**
Peach leaves NIST 1547	17.9 ± 0.4	15.9 ± 0.1	**88.6**	15.9 ± 5.6	**88.8**	17.9 ± 0.4	**99.7**
Cu							
Lichens CRM 482	7 ± 0.19	6.1 ± 0.2	**86.3**	6.8 ± 0.2	**97.3**	6.7 ± 0.7	**95.3**
Apple leaves NIST 1515	5.6 ± 0.3	5.2 ± 0.04	**92.3**	5.2 ± 0.2	**91.8**	5.7 ± 0.2	**101**
Peach leaves NIST 1547	3.7 ± 0.4	3.4 ± 0.2	**90.5**	3.6 ± 1.9	**96.5**	3.7 ± 0.4	**98.9**

Analytical grade reagents (Aristar) 69% (v/v) HNO_3, 30% (v/v) H_2O_2 and 48% (v/v) HF were used throughout the study. All working solutions were prepared using high purity water (18 MΩ cm, Millipore).

2.2.3. Sample preparation

Approximately 50g of lichen samples were removed from the birch trees bark using a stainless steel knife. The material was placed in cotton bags, allowed to air dry and transported to the laboratory in sealed plastic bags. In the laboratory rock/bark fragments adhering to the lichens were removed manually using plastic tweezers and wearing latex powder-free gloves and then oven dried overnight at 40°C. The samples were carefully ground in an agate mortar using liquid nitrogen. Samples

were sieved through 100-μm stainless steel sieve, placed in ceramic beakers and dried overnight at 40°C prior to analysis. All materials used were washed, rinsed with distilled water and dried between samples to avoid cross-contamination. After drying, all samples were transferred into acid cleaned plastic bottles using a bony spoon and stored until further use.

2.2.4. Analytical procedures

2.2.4.1. Microwave digestion

Approximately 0.25g of ground sample material was weighed directly into each digestion vessel on an analytical balance. Depending on experimental design 3 to 5 ml of HNO_3 was then added to each vessel (Table 2.2). The mixture of HNO_3 and plant material was allowed to react in the vessel at atmospheric pressure in a vented hood for 20 minutes. Then 3 to 5ml of H_2O_2 (Table 2.2) were added to the sample and samples were allowed to stand for approximately 20 minutes. Depending on the experimental design 0.2–1 ml of HF and 2ml of Milli-Q H_2O in Experiment II were added and samples were subjected to a closed-vessel microwave digestion. The procedure utilized up to 100% of the 1200 W power setting for 70-90 minutes. After the power phase was completed, the vessels were cooled for about 20 minutes, transferred into acid-cleaned Teflon vessels and evaporated till dryness. In total, three digestion procedures were tested (Experiments I, II and III). Details of all experiments are given in Table 2.2.

Table 2.2. Details of three Experiments used in the study.

	Experiment I	**Experiment II**	**Experiment III**
Acids used	5 ml HNO_3+ 5 ml H_2O_2+ 0.2 ml HF	5 ml HNO_3+ 5 ml H_2O_2+ 0.2 – 1ml HF	3 ml HNO_3+ 3 ml H_2O_2+ 2 ml H_2O+ 0.8 ml HF
Pressure, psi	200	200	200-350
Temperature, °C	210	210	210
Total time, min	70	90	90

During all three experiments sample size (0.25 g), acids used (HNO_3, H_2O_2 and HF), maximum temperature (210°C) and pre-digestion procedure prior to microwave acid attack were kept the same. The parameters that varied were: 1) proportions of acids

(5ml HNO_3 and 5 ml H_2O_2 in Experiment I and II, 3ml HNO_3 and 3 ml H_2O_2 in Experiment III); 2) amount of HF (0.2ml in Experiment I, 0.2-1ml in Experiment II and 0.8ml in Experiment III); 3) pressure (200 psi in Experiment I and II and 350psi in Experiment III); 4) digestion time (70 min. in Experiment I and 90 min. in Experiment II and III). In all experiments four sample duplicates were used. For each digestion, reagent blanks were obtained. The blanks were prepared in the same way as the samples. The concentrations obtained for all metals in the blanks were close to the detection limit of the method, indicating that contamination was not a problem in the digestion.

2.2.4.2. Determination of Pb, Zn, Cu concentrations and Pb isotope ratios

After samples were digested and evaporated, they were subsequently redissolved in 5 mls of 1M HCl prior to total element concentration analysis. This ensured a constant chemically stable acid matrix for the ICP-AES analysis. Detection limits for Pb, Zn and Cu were 0.03, 0.001 and 0.001 μg/g respectively. Precision and accuracy were within 10%. Analytical results for the total Pb, Zn and Cu concentrations (μg/g) for three experiments are given in Table 2.1.

Prior to Pb isotope analysis all samples were passed through an ion exchange column with chromatographic Sr resin (EiChrom) to isolate the Pb fraction from the rest of the sample matrix. For this purpose after the microwave digestion samples were dried and redissolved in 2 ml of 2.4M HCl. Pb separation was achieved by using different strengths of HCl during the procedure. Samples were then evaporated to dryness and redissolved in 2% v/v HNO_3 for Pb isotope analysis on MC-ICP-MS. Raw MC-ICP-MS data were corrected for isobaric interferences on ^{204}Pb using ^{200}Hg. Mass discrimination correction was made using NBS 997 Tl as an internal standard. The Pb/Tl ratio was kept to 2:1 during the measurements. The NBS 997 $^{205}Tl/^{203}Tl$ ratio was optimized based on repeated measurements of spiked NBS 981 Pb. Further details of ion exchange procedure and Pb isotope measurements are given in [28].

2.3. RESULTS AND DISCUSSIONS

2.3.1. Amount of HF and digestion time as critical parameters of microwave digestion

In Experiment I 0.2 ml of HF was added, similar to the procedure used by [8] and [9] for the same size of lichen samples. As shown in Table 2.1 the recovery of Pb, Zn and Cu varied between elements and among the samples. Lead recovery was high for the NIST 1515 (Apple Leaves) – 97.9%, moderate for the NIST 1547 (Peach Leaves) – 86.7% and low for the CRM 482 Lichens – (68.8%). Similar recovery rates were observed for Zn and Cu (Table 2.2). The poor recovery in lichens and the presence of visible residues in the final digests can be attributed to an insufficient amount of HF used in the experiment to dissolve the inorganic fraction. Consequently, increase in the amount of HF from 0.2 to 1 ml in Experiment II significantly influenced Pb, Zn and Cu recovery, i.e. by 12% for Cu, 22% for Pb and 30% for Zn. (Figure 2.1). However, the full recovery of all elements was not achieved at this stage. It should be noted that recovery rates for all three elements did not significantly improve when more than 0.8 ml of HF was added because of the formation of fluoride precipitates that is discussed further below.

2.3.2. Fluoride precipitates

When more than 0.8 ml of HF was added to 10 ml of acid mixture and 0.25 g of samples, the formation of whitish residues was observed. Digests were filtered, dried and analysed by semi-quantative scanning electron microscopy (SEM). The SEM analysis showed perfectly shaped needle-like crystals of mostly Ca, Al and F composition and further X-ray powder diffraction (XRD) analysis identified the precipitates as artificial fluorides ($CaAlF_5$). Both high Ca concentrations of up to 4-5% in leaves and lichens and excess of HF led to the formation of artificial fluorides during microwave acid decomposition. The coprecipitation of many incompatible trace elements (eg. Rb, Sr, Y, Cs, Ba, REE, Pb, Th and U) in the structure of insoluble fluorides formed during HF digestion of silicate rocks, hindering the accurate determination of these elements was previously reported [29]. Lower elemental recovery with excess of HF was also reported for peat samples [30]. Similar to lichens, peat contains a significant amount of inorganic fraction derived from soil dust that requires HF to achieve its complete dissolution.

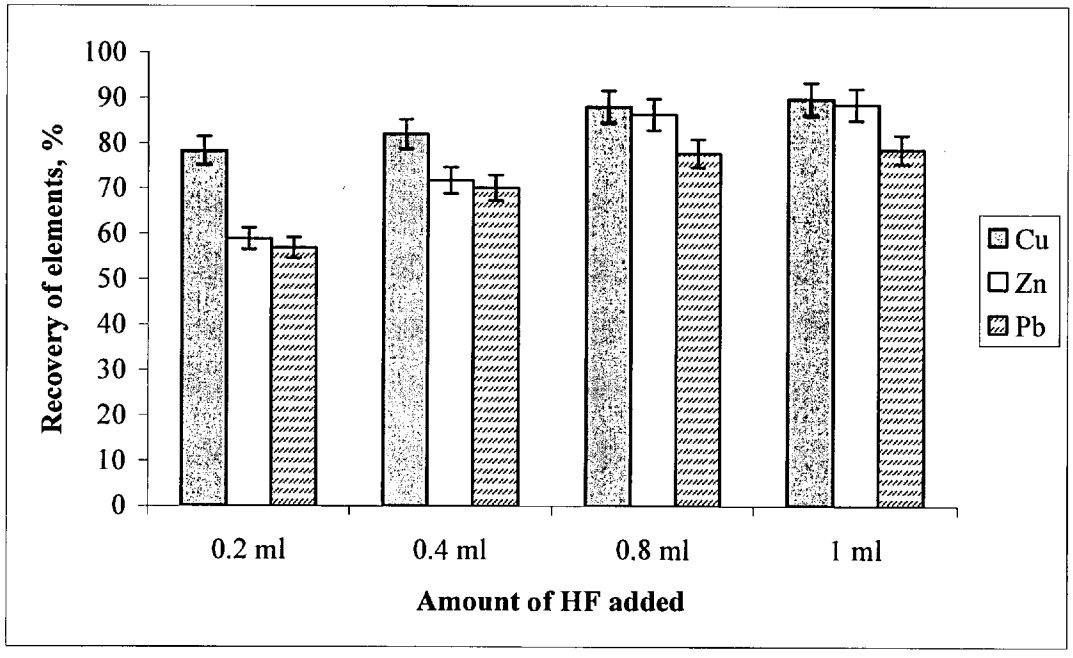

Figure 2.1. Recoveries of Pb, Zn and Cu in CRM 482 *Pseudovernia furfura* lichens as a function of HF amount added to the samples. Lichens were digested under a pressure of 200 psi and temperature of 210°C using a mixture of 5ml HNO_3, 5ml H_2O_2, and 0.2-1ml HF. The error bars show 95% confidence interval, n=4 (n – number of replicates).

2.3.3. Influence of digestion time and pressure on Pb, Zn and Cu recovery

Digestion time is known to influence elemental recovery from botanical samples. For example, Pb recovery improved and stabilized only after about 1.5 h of microwave digestion [16]. The holding digestion time at the final stage of the procedure in Experiment II was increased by 20 minutes after pressure and temperature reached 200 psi and 210°C respectively. As a result, Pb, Zn and Cu concentrations increased on average by ~3% and lead to the recovery of 85-100% for Pb, 81-91% for Zn and 92-97% for Cu. Also previous research compared elemental recovery from peach and orchard leaves using 175 psi and 530 psi of microwave pressure [31] using 0.3 g of material, 5ml of HNO_3 and a final temperature of 175°C. The results of their study showed that the higher pressure lead to 7-9% increase of Pb, Zn and Cu concentrations. In Experiment III the pressure was consequently changed from 200 to 350 psi. At the end of the digestion, resultant solutions were clear and colourless indicating the total decomposition of lichens and leaves matrices. As shown on Figure 2.2 quantitative recovery of 100±5% for Pb, Zn and

Cu was achieved. Recoveries above 100% account for analytical errors only since blanks do not provide any noticeable contribution (see 2.2.4.1).

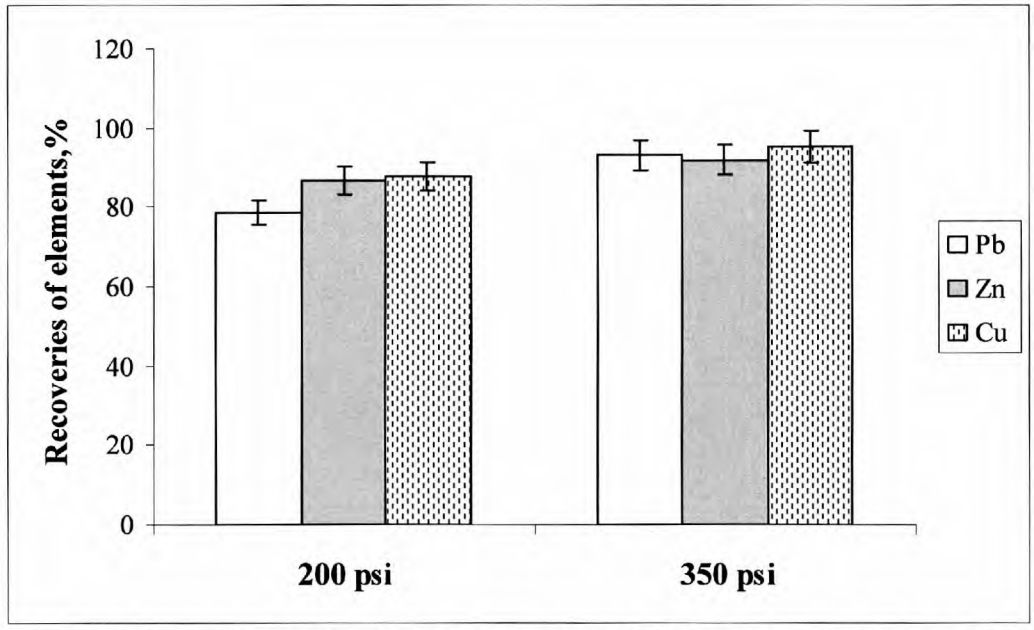

Figure 2.2. Recoveries of Pb, Zn and Cu in CRM 482 *Pseudovernia furfura* lichens as a function of pressure (psi). Lichens were digested under a pressure of 350 psi and temperature of 210°C using a mixture of 3ml HNO_3, 3ml H_2O_2, 2ml H_2O and 0.8ml HF. The error bars show 95% confidence interval, n=4 (n – number of replicates).

2.3.4. Lichens from the Orlovka-Spokoinoe mining district

Lichens collected from different localities (settlement, quarry, tailing pond etc.) of the Orlovka-Spokoinoe mining district (Eastern Transbaikalia, Russia) were digested using the procedure of Experiment III (see Table 2.2 and Table 2.3 for full details of the method). Despite the different density of particles trapped by the lichens (Figures 2.3A, B) and ash content of up to 24%, the microwave acid decomposition of all samples resulted in clear solutions. No filtering or additional treatment of digests was required.

Table 2.3. Heating program of the Experiment III for the digestion of SRM (NIST 1515 Apple Leaves, NIST 1547 Peach Leaves and CRM 482 Lichens).

Stage	Pressure [Psi]	Temperature [^{0}C]	Time [min]
1	20	90	10
2	40	120	10
3	80	160	10
4	200	180	30
5	350	210	30

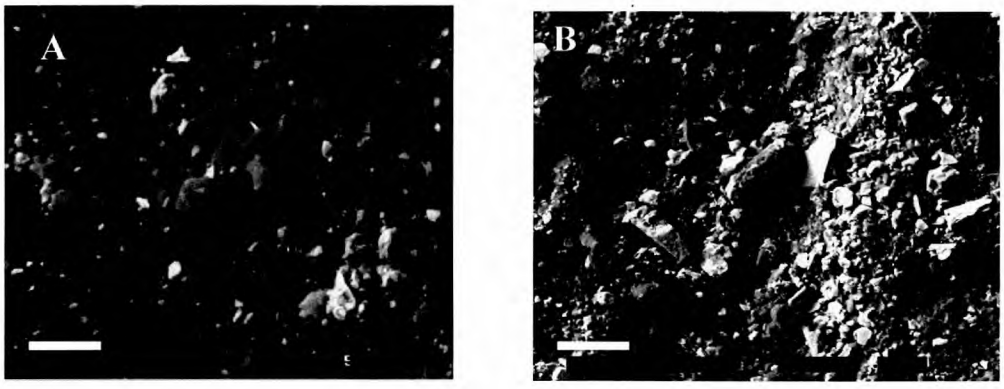

Figures 2.3A, B. Semi-quantative scanning electron microscopy (SEM) images of lichens collected from Orlovka-Spokoinoe mining district (Eastern Transbaikalia, Russia) with siliceous particles on the surface. White bar corresponds to 16.7μm in Figure A and 27μm in Figure B.

Table 2.4 shows Pb, Zn and Cu concentrations in lichens collected from the Orlovka mining district. Pb concentrations ranged between 4-29 μg/g for Pb, 35-98 μg/g for Zn and 6-9 μg/g for Cu.

To further assess the accuracy, Pb, Zn and Cu concentrations were determined in sub- samples by EMMA-XRF at the University of Heidelberg. The two data sets showed a good correlation for Pb, Zn and Cu concentrations with linear regression fit of R^2=0.938-0.999, slope of 0.993-0.999 and intercept of 0.2-0.4. The slope and intercept fell within the 95% confidence interval indicating that regressions showed no statistically significant difference between ICP-AES and XRF data.

Table 2.4 shows Pb isotopes ratios for selected lichen samples from the mining site with the internal precision expressed in ±2σ(%). The error of the internal isotope measurements is below 0.02% for all ratios. The data set will be discussed in detail in a follow-up publication on environmental application of Pb isotopes in lichens from the Orlovka-Spokoinoe mining site.

Table 2.4. Pb, Zn and Cu concentration values (μg/g) determined by ICP-AES and Pb isotope ratios measured by MC-ICP-MS in lichens from the Orlovka-Spokoinoe mining district, Eastern Transbaikalia, Russia.

Sample ID	Samples description	Pb	Zn	Cu	$^{206}Pb/^{204}Pb$	± 2SE (%)	$^{207}Pb/^{204}Pb$	± 2SE (%)	$^{208}Pb/^{204}Pb$	± 2SE (%)
SEL5	Lichens, Orlovka	28.6	97.8	8.9	18.077	0.001	15.572	0.001	38.093	0.001
SEL6	Lichens, Orlovka	9.5	96.1	7.4	18.114	0.001	15.566	0.001	38.120	0.001
L1 C	Lichens, Orlovka	12.6	42.2	6.2	18.113	0.001	15.560	0.001	38.159	0.001
L1 ED	Lichens, Orlovka	8.12	46.2	5.6	18.053	0.001	15.544	0.001	38.077	0.002
L2	Lichens, Orlovka	16.3	35	8.2	18.100	0.001	15.555	0.001	38.113	0.001
TPL1 ED	Lichens, Orlovka	10.3	86.9	6.7	18.299	0.001	15.567	0.001	38.180	0.001
TPL2	Lichens, Orlovka	10.3	82.9	6.7	18.255	0.001	15.563	0.001	38.185	0.001
TPL3	Lichens, Orlovka	9.8	79.3	7.2	18.457	0.001	15.591	0.001	38.330	0.002
TPL4	Lichens, Orlovka	12.6	85.3	8.3	18.806	0.001	15.611	0.001	38.430	0.002
OQL2	Lichens, Orlovka	10.1	38.4	6.2	18.127	0.001	15.564	0.001	38.170	0.001
OQL3	Lichens, Orlovka	9.6	37.8	5.7	18.089	0.001	15.562	0.001	38.139	0.001
OQL4C	Lichens, Orlovka	9.8	37.6	5.5	18.114	0.001	15.555	0.001	38.148	0.001
OQL5B	Lichens, Orlovka	13.3	76.3	7.1	18.128	0.001	15.548	0.001	38.134	0.002
SML7	Lichens, Orlovka	19.7	87.9	8.9	18.140	0.001	15.574	0.001	38.139	0.002
LBL1	Lichens, lake Baikal	4.2	63.8	8.5	18.152	0.001	15.561	0.001	38.321	0.001

2.4. CONCLUSIONS

The study demonstrated that:

(a) microwave-assisted acid decomposition of NIST 1515 (Apple Leaves), NIST 1547 (Peach Leaves) and CRM 482 #10 *Pseudovernia furfura* (Lichens) standards using 6ml HNO_3+2 ml H_2O_2+2 ml H_2O+ 0.8 ml HF resulted in quantitative recovery of Pb, Zn and Cu;

(b) 0.8 ml of HF in 10 ml of acid mixture was found to be sufficient and effective for the complete dissolution of lichen matrix independently from the degree of the lichens "contamination" with siliceous airborne particulates;

(c) addition of more than 0.8ml of HF in 10ml of acid mixture used for the lichen digestion resulted in fluoride formation;

(d) increase of pressure from 200 to 350 psi proved to be effective in achieving quantitative recovery of Pb, Zn and Cu;

(e) good agreement was achieved between ICP-AES and EMMA-XRF techniques for lichen samples digested using the developed method.

The developed closed-vessel microwave digestion method offers an easy and reliable method for the complete dissolution of lichens and leaves matrices prior to determination of trace elements and stable Pb isotope ratios. The method was successfully used in the development study of a peat reference material for the determination of elemental concentrations [32] and for the digestion of lichens from the polluted smelter town of Karabash, Russia [33].

Accurate and precise Pb isotope analyses of lichens from the mining site allow assessment of sources of lead contamination.

ACKNOWLEDGEMENTS

The authors would like to thank Paul Schofield for the XRD analysis of fluorides and John Spratt and Terry Greenwood for the assistance with SEM analysis of lichens. Andy Fleet and Terry Williams (Natural History Museum) and Mike Warner (Imperial College London) are thanked for support. Financial support from NERC, Imperial College London and The Natural History Museum is gratefully acknowledged. AD appreciates support through Albert Julius Bursary (Imperial College London), ORS Award, INTAS Young Scientist Award and research funds of the Department of Mineralogy (Natural History Museum, London). British Airways are thanked for providing London-Moscow return flights for DW and CJS under their Communities and Conservation Programme.

2.5. REFERENCES

[1] O.W. Purvis, *Science Progress*, 79 (4), 283-309 (1996).

[2] J.R. Haas, E.H. Bailey and O.W. Purvis, *American Mineralogist*, **83**, 1494-1502 (1998).

[3] R. Bargagli, F. Monaci, F. Bravi and C. Agnorelli, Environmental *Contamination*, **116**, 279-287 (2002).

[4] R. Scerbo, L. Possenti, L. Lampugnani, T. Ristori, R. Barale and C. Barghigiani, *The Science of the Total Environment*, **241**, 91-106 (1999).

[5] S.R. Getty, D.S. Gutzler, Y. Asmerom, C.K. Shearer and S.J. Free, *Atmospheric Environment*, **33**, 5095-5104 (1999).

[6] T. Zschau, S. Getty, C. Gries, Y. Ameron, A. Zambrano and T.H. Nash III, *Environmental Contamination*, **125**, 21-30 (2003).

[7] A. Simonetti, C. Gariepy and J. Carignan, *Atmospheric Environment*, **37 (20)**, 2853-2865 (2003).

[8] C. Baffi, M. Bettinelli, G.M. Beone and S. Spezia, *Chemosphere*, **48**, 299-306 (2002).

[9] M. Bettinelli, P. Maurizio, S. Spezia, C. Baffi, G.M. Beone, F. Alberici, S. Bergonzi, C. Bettinelli, P. Cantarini and L. Mascetti, *Microchemical Journal*, **73**, 131-152 (2002).

[10] H.M. Kingston and L.B. Jassie, *Analytical Chemistry*, **58**, 2534-2541 (1986).

[11] J.C.B. Rhoades, *Journal of Analytical Atomic Spectrometry*, **11**, 751-757 (1996).

[12] J.S. Alvarado, T.J. Neal, T.J. Smith and M.D. Erickson, *Analytica Chimica Acta*, 322, 11-20 (1996).

[13] A. Agazzi and C. Pirola, *Microchemical Journal,* 67, 337-341 (2000).

[14] M. Bettinelli, U. Baroni and N. Pastorelli, *Analytica Chimica Acta*, **225**, 159-174 (1989).

[15] J.E. Rechcigl and G.G. Payne, *Abstract at the Annual Meeting of American Society of Agronomy for the Crop Science Society of America and Soil Science Society of America*, Las Vegas Nevada, October 15-20 (1989).

[16] I. Rodushkin, T. Ruth and A. Huhtassari, *Analytica Chimica Acta*, **378**, 191-200 (1999).

[17] J. Sastre, A. Sahuquillo, M. Vidal and G. Rauret, *Analytica Chimica Acta,* **462**, 59-72 (2002).

[18] B. Madeddu and A. Rivoldini, *Atomic Spectroscopy*, **17 (4)**, 148-154 (1996).

[19] I. Kubrakova, *Spectrochimica Acta*, 52, 1469-1492 (1997).

[20] D. Weiss, W. Shotyk, H. Schaefer and U. Loyall, *Fresenius Journal of Analytical Chemistry*, **363**, 300-305 (1999).

[21] S. Wu, X. Feng and A. Wittmeier, *Journal of Analytical Atomic Spectrometry,* **12**, 797-806 (1997).

[22] T.T. Gorsuch, *The destruction of organic matter,* Pergamon Press (1970).

[23] A.K. Cheburkin and W. Shotyk, *Fresenius Journal of Analytical Chemistry*, **354**, 688- 691 (1996).

[24] D. Weiss, A.K. Cheburkin, W. Shotyk and M. Gloor, *The Analyst,* **123**, 2097-2102 (1998).

[25] D. Weiss, B. Kober, A. Dolgopolova, K. Gallagher, G. Le Roux, T.F.D. Mason, M. Kylander, B. Spiro, B.J. Coles, *International Journal of Mass Spectrometry*, **232**, 205-215 (2004).

[26] P.F. Schofield, K.S. Knight, S.J. Covey-Crump, G. Cressey and I.C. Stretton, *Mineralogical Magazine,* **66**, 189-200 (2002).

[27] A. Dolgopolova, R. Seltmann, B, Kober, D. Weiss, P. Dulski and C. Stanley, *IMM Transactions: Section B: Applied Earth Sciences,* (in press).

[28] D.J. Weiss, B. Kober, T.F.D. Mason, A. Dolgopolova, B.J. Coles, K. Gallagher, G. LeRoux, B. Spiro and R. Seltmann, *EGS-AGU-EUG Joint Assembly, Nice, France,* **5 (03521)**, (April 2003).

[29] T. Yokoyama, A. Makishima and E. Nakamura, *Chemical Geology*, **157**, 175-187 (1999).

[30] M. Krachler, C. Mohl, H. Emons and W. Shotyk, *Spectrochimica Acta*, **57**, 1277-1289 (2002).

[31] K.E. Levine, J.D. Batchelor, C.B. Rhoades, J. and B. T. Jones, *Journal of Analytical Atomic Spectrometry*, **14**, 49-59 (1998).

[32] C. Yafa, J. G. Farmer, M. C. Graham, J. R. Bacon, C. Barbante, W. R. L. Cairns, R. Bindler, I. Renberg, A. Cheburkin, H. Emons, M. J. Handley, S. A. Norton, M. Krachler, W. Shotyk, X. D. Li, A. Martinez-Cortizas, D. Pulford, V. MacIver, J. Schweyer, E. Steinnes, T. E. Sjøbakk, D. Weiss, A. Dolgopolova and M. Kylander, *Journal of Environmental Monitoring*, (accepted).

[33] O.W. Purvis, P.J. Chimonides, G.C. Jones, I.N. Mikhailova, B. Spiro, D.J. Weiss and B.J. Williamson, *Proceedings of the Royal Society London B,* DOI 10.1098/rspb.2003.2616, (2004).

CHAPTER 3. RAPID AND HIGH–PRECISION LEAD ISOTOPE MEASUREMENTS IN ENVIRONMENTAL SAMPLES BY MC-ICP-MS.

ABSTRACT

Analytical protocols for rapid and high precision Pb isotope ratio determinations in peat, lichen, vegetable, chimney dust and granites using MC-ICP-MS and its application to environmental studies are presented. Acid dissolution of various matrix types was achieved using high temperature/high pressure microwave digestion procedures for biological samples (peat, lichen, vegetable) and hot plate digestion for granites and other mineral and chimney dust samples. The digests were passed through a column packed with EiChrom Sr-resin employing only hydrochloric acid and one column passage. This simplified column chemistry allowed high sample throughput (*c.* 24 samples/day) and resulted in stable ion beam signals. Typically, internal precisions were below 100 ppm (±2SE) on all Pb ratios in all matrices. Tl was employed as an internal standard to correct for mass discrimination effects and to obtain accurate data for all ratios (below 80 ppm). This involved an optimization procedure using least squares for the Tl ratio relative to certified NIST SRM 981 Pb values. The measurement protocol used allowed to measure five unknown samples/1.5 hours. The long-term reproducibility (±2σ) for the NIST SRM 981 Pb standard over a five-month period (35 measurements) was better than 350 ppm for all ratios. Selected sample solutions were measured with TIMS and MC-ICP-MS and showed good correlation (r=0.9876 for $^{206}Pb/^{204}Pb$ ratios, slope=0.9474, n=13). The Tl mass bias and isotope intensities in natural and in synthetic samples did not differ significantly during a measurement session, indicating that the residual components of the complex peat and lichen matrix after one column step did not affect the mass bias behavior of the Tl spike and that matrix influences were negligible. Environmental samples with very different matrices were analyzed during two different studies: i) lichens, vegetables and chimney dust around a Cu smelter in the Urals in order to study local Pb dispersal during smelting activities, and ii) peat samples from an ombrotrophic bog in the Faroe Islands in order to assess large scale atmospheric Pb and Hg contamination in the sub-Arctic. The procedures of sample

preparation, mass spectrometry and data processing tools resulted in rapid and high precision Pb isotope data and allowed the reliable differentiation and identification of the respective Pb sources.

International Journal of Mass Spectrometry, 2004, 232, 205-215 (**APPENDIX 5.2**).

3.1. INTRODUCTION

The application of Pb isotopes in environmental geochemistry has had a tremendous effect on our understanding of the geochemical cycling of Pb in the environment and the anthropogenic impact (see [1] for a detailed review). Previous work used Pb isotopes for tracing contamination derived Pb in the atmosphere [2], oceans [3], ice and snow [4], marine sediments [5], soils [6] and peats [7] or as a transient tracer to study environmental processes and mechanisms such as ocean and atmosphere circulation [2, 8], trace element mobility in soils [9] and peats [10], Holocene climate change [11] and atmospheric deposition of Hg and other metals [12, 13].

Until recently, Pb isotopes in environmental samples, *i.e.,* soil, plant, sediment, peat, surface and subsurface waters, have mainly been measured with either thermal ionisation mass spectrometry (TIMS) or quadrupole based plasma source mass spectrometry (Q-ICP-MS). The advantage of TIMS is that ratios including the least abundant ^{204}Pb isotope (natural abundance of *c.* 1.4%) are measured with high reproducibility (down to 200 ppm) and good accuracy due to the small mass fractionation per atomic mass unit (frac/amu) during the measurements (typically below 0.1%). However, analytical procedures are time consuming and involve labour intensive sample preparation steps, *e.g.,* two column passages are needed to achieve stable emission for organic-rich samples [10] and long measurement times due to turret loading and filament heating occur, resulting in a low sample throughput (*c.* 6 samples/4 hours). This severely restricts the sample throughput. However, many environmental problems require a large sample number to infer statistically significant conclusions, which is due to inherent temporal and spatial variability in the environmental context. Consequently, most environmental investigations use quadrupole based plasma source mass spectrometry, where ion exchange steps are often omitted or at least reduced to one column passage [14]. ICP-MS based on quadrupole mass filters performs single measurements at the nominal mass value of

each peak using either scanning or peak hopping modes. This, in addition to plasma flicker, results in inherently poor peak shape and consequently in less precise measurements (typically 2000 ppm for $^{206}Pb/^{207}Pb$ ratios) and instrumental mass bias of over a percent [15]. The isotope ^{204}Pb with its small abundance (and additional Hg interference) is consequently rarely measured, which significantly limits the application of Pb isotopes for source assessment.

In recent years, multi collector plasma source mass spectrometry (MC-ICP-MS) has become a powerful alternative for studying Pb isotope ratios with high precision. This technique combines the high ionization efficiency of the Ar plasma (≥90%, [16]) with the precision attainable using multi collector array [17, 18]. Consequently, the MC-ICP-MS technique is of great interest for the environmental geochemist as it allows measurement of the ^{204}Pb and large sample throughput with less sample preparation and measurement time. This technique is still relatively new, however, and the complexities related to using an ICP ion source for high precision isotope measurements are only now becoming apparent. A number of papers have investigated high precision Pb isotope ratio measurements with MC-ICP-MS using different mass spectrometer designs, *i.e.*, double focussing instruments such as VG *P54*, Nu *Plasma*, VG *Axiom* and Finnigan *Neptune* [19-24] or single focussing type designs with collision cell such as the Micromass *IsoProbe* [25-28]. These papers showed that the external precision achieved are similar with TIMS. The main factors affecting precision and accuracy are mass discrimination, baseline corrections, instrument instability and matrix effects. The first three were discussed in several publications and various protocols have consequently been proposed and their respective advantages, pitfalls and problems were discussed [19, 20, 23, 26, 27]. Despite the growing numbers of methodological papers, the more instrumental aspects of Pb isotope measurement with plasma source mass spectrometry are still not well understood. In addition, to date, most investigations have been limited to synthetic and 'simple' silicate matrixes. This still warrants detailed investigations of matrix influences on high precision Pb isotope ratio measurements in environmental samples. Recent applications of MC-ICP-MS to environmental geochemistry included two papers on Pb isotope measurements in seawater matrices [21, 28].

The purpose of this contribution is: i) to present reliable, fast, and robust analytical (including sample preparation and mass spectrometry) and data processing protocols

for high precision and accurate Pb isotope measurements in environmental samples including biological (peat, lichen, vegetable) and inorganic (chimney dust, ore bearing granites) materials and ii) to assess its application to environmental geochemical studies.

3.2. EXPERIMENTAL

3.2.1 Materials and reagents

Environmental samples included peat from an ombrotrophic bog in the Faroe Islands [13], lichens, vegetables, and chimney dust collected around a Cu smelter in Karabash, Southern Urals [29], and ore bearing and barren granites from the Orlovka-Spokoinoe mining district in Eastern Transbaikalia [30, 31].

The acids were of ultra-pure (Merck and sub-boiling acid) or Aristar (Merck) quality. Dilute solutions of acids for mass spectrometry were prepared with purified water obtained from quartz still or an 18 MΩ -grade Millipore system (Bedford, MA).

Lead, Tl or mixed Pb-Tl standard solutions were made up from previously prepared stock solutions of NIST SRM 981 Pb (1.24 $\mu g\ ml^{-1}$ in 2% (v/v) HNO_3, from S. Bowring, MIT Cambridge) and NIST SRM 997 Tl (732 $mg\ l^{-1}$ in 2M HNO_3, from M. Rehkaemper, ETH Zürich). All solutions and samples were prepared and handled in laminar flow hoods.

3.2.2 Sample preparation of environmental samples

Peat samples were digested at the Institute for Environmental Geochemistry at the University of Heidelberg using a Milestone high pressure/high temperature microwave oven system and details are given elsewhere [32]. Lichens and vegetables samples from the Karabash smelter were digested at the Imperial College London/The Natural History Museum Joint Analytical Facility (ICL/NHM JAF) using a MARSX high pressure/high temperature microwave oven system and details are given elsewhere [29, 33]. Both of these microwave digestion methods have been recently developed and showed quantitative recovery for Pb. However, they have not been assessed before with respect to Pb isotope measurements. The barren and Ta-Nb-W bearing granites from the Orlovka-Spokoinoe mining district and the chimney dust samples were dissolved using standard HNO_3/HF acid mixtures on a hot plate in closed Teflon beakers [31].

After digestion, all solutions were dried and the residues redissolved in 2mls of 2.4M HCl prior to the passage through the column. After conversion to the chloride form, Pb was separated using the Pb selective extraction chromatographic Sr resin from EiChrom [34] and following the distribution factor dependencies for Pb as reported elsewhere [35]. The method uses only hydrochloric acid and one column passage. It consists of a cleaning step with 6M HCl, a pre-conditioning and a loading step, both with 2.4M HCl and an elution step using 6M HCl (see **Table 3.1**). The recovery of Pb from the column is quantitative from biological and silicate matrices.

3.2.3 Multicollector ICP-MS and TIMS Instrumentation

A Micromass *IsoProbe* multi-collector ICP-MS based at the ICL/NHM JAF was used during the study. The instrument is equipped with seven independently adjustable Faraday cups and a hexapole collision cell. A CETAC Aridus desolvating system (Omaha, NE, USA) with a T1H micro concentric nebulizer was used for sample introduction. The optimized data acquisition parameters selected for Pb isotope ratio measurements are summarized in **Table 3.2**.

For comparative purposes, additional Pb isotope analyses were conducted at Heidelberg using a FINNIGAN *MAT* 261 thermal ionization mass spectrometer (TIMS with multi-cup system for Pb isotopes) and standard sample preparation techniques. Raw TIMS data were normalized to NIST SRM 981 Pb international standard with reference values of Galer and Abouchami [36] and long-term reproducibility on the 95% confidence level was below 0.03% for ratios normalized to ^{204}Pb. Details of the TIMS procedure at Heidelberg have been described in detail before [37].

3.2.4 Measurement procedures

All isotopes measurements were performed by static multiple collection. The ion currents were measured using Faraday collectors at masses 200 (Hg), 203 (Tl), 204 (Pb), 205 (Tl), 206 (Pb), 207 (Pb) and 208 (Pb). The collector efficiencies were calibrated on a daily basis. Ion beam intensities of Pb and Tl were optimized adjusting accelerating voltage, lens system, torch settings and gas flows.

Table 3.1. Typical instrument operating conditions of the *IsoProbe* MC-ICP-MS and the CETAC nebulizer.

Instrument settings	
Accelerating voltage	~6,000 V
RF power	~1,375 W
(reflected power)	<2W
Coolant Ar flow	~14 l min^{-1}
Auxiliary Ar flow	1.0-1.2 l min^{-1}
Nebulizer flow	0.6-0.8 l min^{-1}
Ar collision gas flow	1-2 ml min^{-1}
Abundance sensitivity	~25 ppm
Analyser pressure	~4.8 x 10^{-8} mbar under full gas load
Sensitivity for Pb	~300 V ppm^{-1}
Cones (Skimmer and Sample)	Ni
Collector Positions	L2 - 200; Ax - 203; H1 - 204;
	H2 - 205; H3 - 206; H4 - 207; H5 - 208
Sample introduction	
Spray chamber temperature	75 °C
Desolvator temperature	160 °C
Ar sweep gas flow	~2.8-3.5 ml min^{-1}
Sample flow rate	~40-60µl min^{-1}

Table 3.2. Column chemistry procedure for separating Pb from sample matrix. Ion exchange columns were packed with 600µl of EiChrom Sr resin resulting in a bed height of about 0.5 cm. The columns used were made in house using Teflon tubing.

Stage	Acid strength of HCl (M) and volume (ml) used
1. Cleaning step	6M (6 x 1 ml)
2. Conditioning step	2.4M (2 x 0.5 ml)
3. Sample loading step	2.4M (1 x 1.5 ml)
4. Matrix elution step	2.4M (4 x 1 ml)
5. Pb elution step	6M (3 x 1 ml)
6. Cleaning step	6M (3 x 1 ml)

Data collection was carried out using two or three blocks with 25 measurements each when analyzing samples and using one block with 20 measurements when analyzing the acid blank before the sample for baseline correction (see below). Internal errors (±2SE) for synthetic solutions were below 50 ppm for all ratios. A 10 s integration and 50 s sample admission delay were allowed to guarantee a stable signal before measurement started. The rinse out time between samples and acid blank was approximately six minutes using a sequence of 2% and 0.2% (v/v) HNO_3 for cleaning. No memory effect was observed. Background scans were performed to assess possible interferences (ReO^+ and WO^+) but no significant background interference was detected even when measuring Ta-Nb-W bearing granites.

Samples were measured using an automated procedure. A typical measurement procedure included five samples taken up in 2% (v/v) HNO_3 and spiked with NIST SRM 977 Tl and one NIST SRM 981 Pb standard spiked with NIST SRM 977 Tl in 2% (v/v) HNO_3 to assess the reproducibility and to optimize the Tl ratio (see below). This set-up allowed measuring five real samples in 1.5 hours.

Analytical blanks at the ICL/NHM JAF for the total procedure, estimated from intensity data, were below 1000 pg. Although this is higher than typically published blanks in geochronology laboratories, it can be fully accounted for by Aristar grade acids used during sample preparation. However, the blank was always below 1% of the total Pb and mixing calculation showed that the contribution was insignificant at the level encountered at any time.

3.2.5 Data reduction and mass discrimination correction

All the data processing was carried out off-line using Microsoft® Excel 2001 spreadsheets.

To correct for Faraday cup offset, solvent blank and instrumental blank, averaged acid blank intensities were subtracted from individually measured raw isotope intensities and then the average was calculated. To account for the ^{204}Hg isobaric interference, the ^{200}Hg was measured on L2 and the intensity at *m/z* 204 was corrected using the equation: $I(^{204}Pb) = I(^{204}amu) - 0.2929 \times I(^{200}amu)$. Due to the low content of mercury, this correction was very small and accounted typically for $\leq 0.1\%$ of the ^{204}Pb level. Previous work assessing Pb isotope measurements on first generation *IsoProbe* MC-ICP-MS instruments highlighted the importance of

appropriate abundance sensitivity correction to achieve accurate Pb isotope data [25, 26, 28, 38]. Detailed work on *IsoProbe* instruments conducted at the MIT and Royal Holloway laboratories suggested that average abundance sensitivities are stable to approximately ±2 ppm (±2σ) under same vacuum conditions [28]. Abundance sensitivity correction during this study was achieved by fixing the Pb/Tl ratio and concentration matching.

The run intensities corrected for background and isobaric interference were used to calculate the raw ratios, which then were corrected for instrumental mass bias using Tl as external dopant and the Tl mass fractionation factor f_{Tl}. The $^{205}Tl/^{203}Tl$ ratio used to calculate the mass fractionation factor f_{Tl} was optimized each measurement session from repeated NIST SRM 981 Pb standard measurements (see below for details of this procedure). The exponential law proved to be the most accurate in our laboratory and this agrees with findings from other laboratories using the *IsoProbe* MC-ICP-MS [25, 28]. The mass fractionation coefficient for Tl was calculated using

$$f_{Tl} = \frac{\ln(R_{Tl} / r_{Tl})}{\ln(M_{205} / M_{203})} \qquad (1)$$

where R_{Tl} is the 'true' Tl ratio, r_{Tl} the measured ratio and M represents the atomic masses of Tl (202.9723 and 204.9745, respectively).

The Tl mass correction factor f_{Tl} was subsequently used to correct the calculated raw Pb isotope ratios (baseline, interference and abundance sensitivity corrected):

$$R_{Pb} = r_{Pb}\left(\frac{M_1}{M_2}\right)^{f_{Tl}} \qquad (2)$$

where R_{Pb} is the 'true' Pb ratio, r_{Pb} is the measured ratio, $M_{1,2}$ are the atomic masses of isotope 1 and 2, respectively, and f_{Tl} is the mass fractionation co-efficient derived from Eq. (1), assuming that $f_{Tl} \approx f_{Pb}$ (see discussion below).

The fractionation per atomic mass unit (frac/amu) was calculated using the relationship:

$$\text{frac / amu} = (\frac{r}{R} - 1) / (M_2 - M_1) \qquad (3)$$

3.3. RESULTS AND DISCUSSION

3.3.1 Tl optimization for mass bias correction

Mass fractionation in mass spectrometers is one of the major sources of error in isotope ratio measurements. With respect to Pb, the major draw back is that Pb has only one non-radiogenic isotope (^{204}Pb), and thus, mass fractionation cannot be corrected internally. One way to correct for mass bias is to spike the sample with an element of similar mass and with two stable isotopes. In the case of Pb with the isotopes 204, 206, 207 and 208, Tl with isotopes 203 and 205 is the preferred choice. This approach assumes that the mass fractionation behaviours of Tl and Pb are comparable. First experiments were conducted on quadrupole based plasma instruments [39] and Tl doping has consequently been adopted for multicollector plasma instruments [19, 24, 25]. However, ^{205}Tl/^{203}Tl normalising ratio had to be adjusted to higher ratios than the certified values to generate normalised values within error of values for NIST SRM 981 Pb determined using double and triple spikes. The latter vary significantly themselves from laboratory to laboratory, *i.e.* for the ^{206}Pb/^{204}Pb ratios with values of 16.9405±0.0015 [36], 16.9409±0.0022 [38] and 16.9356±0.0023 [40]. White et al. [19] assessed the graphical technique previously developed for Cu and Zn isotope analysis [41] which plots measured ratios of the Tl dopant vs. the Pb isotope pair of interest in a ln-ln space and the slope of the regression line is used for the calculations of f_{Pb} (f_{Pb} = f_{Tl} x $\ln[M_{205}/M_{203}]/\ln[M_{208}/M_{206}]$ x intercept). This approach yielded accurate results with around 600 ppm for ^{206}Pb/^{204}Pb ratio relative to the Todt values using the VG *P54* MC-ICP-MS instrument in Lyon [19]. However, this technique is not applicable on our first generation *IsoProbe* instrument due to the small mass bias variations using dry plasma conditions, which consequently results in poor linear fits with high errors and inaccurate isotope ratios. Similar observations were made at the Muenster *IsoProbe* instrument for Pb [25] and on our instrument for the Cu-Zn system [42].

Here, instrumental mass fractionation was determined during a measurement session by repeated analyses of the NIST SRM 981 Pb standard spiked with the NIST SRM 997 Tl using the same Pb/Tl ratio and concentrations as the samples. The Tl ratio was optimised against the ^{206}Pb/^{204}Pb value of Galer and Abouchami [36]. The optimisation was achieved using a least squares method described below. The

approach is based on the logarithmic law, which assumes that the 'true' Tl and Pb ratios are given by

$$R_i^{Tl} = r_i^{Tl}(c^{Tl})^f \text{ and } R_i^{Pb} = r_i^{Pb}(c^{Pb})^f \qquad (4) \text{ and } (5)$$

where f is the mass bias fractionation factor given by $f = \ln\left(\frac{R_i^x}{r_i^x}\right) / \ln(c^x)$ (with x = Pb or Tl), R^{Tl} and R^{Pb} are the 'true' ratios, i is a given number of measured NIST SRM 981 Pb standards, r^{Pb} and r^{Tl} are measured ratios of $^{205}Tl/^{203}Tl$ and $^{206}Pb/^{204}Pb$, respectively, $c^{Tl}=M_2/M_1=205/203=1.0088522167$, and $c^{Pb}= M_2/M_1=206/204=1.009803921$. Using the repeated NIST SRM 981 Pb measurements during a measurement session (typically between 6 to 12 standards), we define $\overline{R^{Pb}}$ (the mean value) as:

$$\overline{R^{Pb}} = \frac{1}{N}\sum_{i=1}^{N} R_i^{Pb}, \text{ with } R_i^{Pb} = r_i^{Pb}(c_{Pb})^{\frac{\ln(R^{Tl}/r_i^{Tl})}{\ln(c^{Tl})}} \qquad (6)$$

where N is the number of NIST SRM 981 Pb measurements during the measurement session.

Clearly, $\overline{R^{Pb}}$ is a function of the 'true' Tl ratio (R^{Tl}), which we do not know reliable. Given that we expect $\overline{R^{Pb}}$ to be equal to the certified value for Pb ($R^{Pb}_{cert.}$), then we want to adjust the unknown R^{Tl}, such that we minimize the prediction error for $\overline{R^{Pb}}$. Therefore, we choose an objective function

$$\varphi = \left(\frac{\overline{R^{Pb}}}{R^{Pb}_{cert.}} - 1\right)^2. \qquad (7)$$

which has a minimum (of zero) when $\overline{R^{Pb}} = R^{Pb}_{cert.}$ The value of R^{Tl} can be found by taking the denominator of φ with respect to R^{Tl} and setting this to zero ($\frac{\partial\varphi}{\partial R^{Tl}} = 0$). This leads to the final form:

$$R^{Tl} = \ln(c^{Tl}) \times \left(\frac{N R_i^{Pb}}{\sum_{i=1}^{N} r_i^{Pb}(c^{Pb})^{\ln(r_i^{Tl})/\ln(c^{Tl})}}\right)^{\ln(c^{Tl})/\ln(c^{Pb})} \qquad (8)$$

Figure 3.1a shows the optimized $^{205}Tl/^{203}Tl$ ratio (R^{Tl}) vs. the objective function for one measurement day (16.8.2002) using twelve individual measurements of NIST SRM 981 Pb standards doped with NIST SRM 997 Tl. Also shown are the estimated $\overline{R^{Pb}}$ and $R^{Pb}_{cert.}$ **Figure 3.1b** shows a frequency distribution histogram of optimized Tl ratios determined during 13 individual measurement sessions in a time period of one year (Aug. 02 – Aug. 03). No systematic trend or bias is visible in the frequency distribution of the 'optimized' Tl ratio.

The $^{205}Tl/^{203}Tl$ ranged between 2.3885 and 2.3907 with a mean value of 2.3897±0.0015 (±2σ). The mean value is slightly higher that the originally 'certified' ratio of 2.3875 [43].

Table 3.3 shows the average Pb isotope ratio of the NIST SRM 981 Pb standard from repeated measurements (n=35) during a six-month period using optimized $^{205}Tl/^{203}Tl$ ratios for mass bias correction (August to December 2002). Also shown are TIMS and multicollector ICP-MS data for the NIST SRM 981 Pb standard from other laboratories. Our average Pb ratios show average accuracy of 48, 70, 55, 41, and 77ppm for the ratios $^{206}Pb/^{204}Pb$, $^{207}Pb/^{204}Pb$, $^{208}Pb/^{204}Pb$, $^{207}Pb/^{206}Pb$, and $^{208}Pb/^{206}Pb$, relative to the Galer and Abouchami value. The ratios are slightly higher on our instrument, with *e.g.*, 2.16767±0.00063 or 16.9413±0.0039 for the ratios of $^{208}Pb/^{206}Pb$ and $^{206}Pb/^{204}Pb$ compared to the other data shown in Table 3.2. The error on our NIST SRM 981 Pb values is approx. a factor of two higher than the triple spike data of Galer and Abouchami [36].

3.3.2 Long term reproducibility on the IC/NHM JAF *IsoProbe* MC-ICP-MS

Figure 3.2 shows the long-term reproducibility of the *IsoProbe* MC-ICP-MS at the ICL/NHM JAF using repeated NIST SRM 981 Pb measurements over the same five-month period (August to December 2002). Errors are (expressed in ppm) 227 for $^{206}Pb/^{204}Pb$, 326 for $^{207}Pb/^{204}Pb$, 314 for $^{208}Pb/^{204}Pb$, 126 for $^{207}Pb/^{206}Pb$ and 292 for $^{208}Pb/^{206}Pb$. The errors estimated from long-term reproducibility are significantly higher than the ones estimated during a single measurement session, which was in general below 200 ppm for the $^{208}Pb/^{204}Pb$ ratio and below 150 ppm for all the other ratios. The long-term reproducibility of the London MC-ICP-MS is similar to the

Heidelberg TIMS and agrees with other laboratories using plasma source mass spectrometry instruments [19, 22-25, 44].

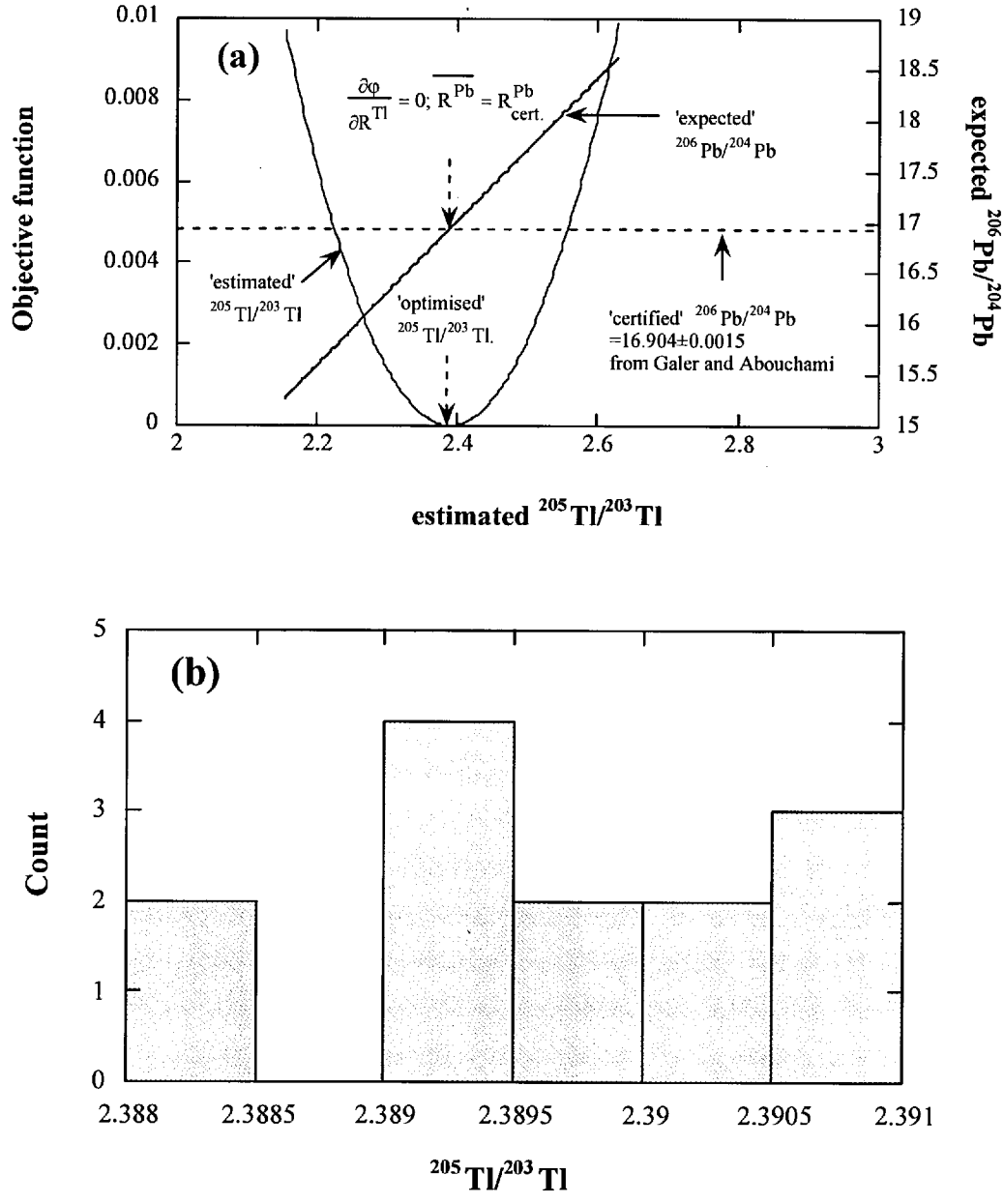

Figure 3.1. (a) Distribution of estimated $^{205}Tl/^{203}Tl$ (x-axes) as a function of the expected $^{206}Pb/^{204}Pb$ ratios ($\overline{R^{Pb}}$) and the objective function (φ). The optimized $^{205}Tl/^{203}Tl$ ratio of this measurement session (29.1.03) is given by 2.3905 and fulfills the conditions of $\frac{\partial\varphi}{\partial R^{Tl}} = 0$ and $\overline{R^{Pb}} = R^{Pb}_{cert.}$ (b) The distribution of optimized Tl ratios during 13 measurement sessions at the ICL/NHM JAF during one year (August 2002 to August 2003).

Table 3.3. Comparison of selected published Pb isotopic composition of NIST-SRM 981 Pb measured by TIMS and MC-ICP-MS. The Tl ratios used in this study were adjusted to the Galer and Abouchami value. The TIMS data are based on double and triple spike measurements. Errors shown refer to the least significant digits and are all given as $\pm 2\sigma$.

Authors	Mass Spectrometer	$^{208}Pb/^{206}Pb$	$^{207}Pb/^{206}Pb$	$^{206}Pb/^{204}Pb$	$^{207}Pb/^{204}Pb$	$^{208}Pb/^{204}Pb$
Todt et al. (1995)	TIMS	2.16701 (43)	0.914585 (132)	16.9356 (23)	15.4891 (30)	36.7006 (112)
Galer and Abouchami (1998)	TIMS	2.16771 (10)	0.914750 (35)	16.9405 (15)	15.4963 (16)	36.7219 (44)
Thirlwall (2000)	TIMS	2.16770 (21)	0.91469 (7)	16.9409 (22)	15.4956 (26)	36.7228 (80)
Hirata (1996)	MC-ICP-MS - *Plasma 54*	2.16636 (82)	0.914623 (37)	16.9311 (90)	15.4856	36.6800 (210)
Rehkaemper and Halliday (1995)	MC-ICP-MS - *Plasma 54*	2.16677 (14)	0.91469 (5)	16.9364 (55)	15.4912 (51)	36.7219 (44)
Belshaw et al. (1998)	MC-ICP-MS - Nu *Plasma*	2.1665 (2)	0.91463 (6)	16.932 (7)	15.487	36.683
White et al. (2000)	MC-ICP-MS - *Plasma 54*	2.1646 (8)	0.91404	16.9467 (76)	15.4899 (39)	36.6825 (78)
Rehkaemper and Metzger (2000)	MC-ICP-MS - *IsoProbe*	2.16691 (29)	0.91459 (13)	16.9366 (29)	15.4900 (17)	36.7000 (23)
Reuer et al. (2003)	MC-ICP-MS - *IsoProbe*	2.16639 (304)	0.91460 (18)			
This Study	MC-ICP-MS - *IsoProbe*	2.16767 (63)	0.914767 (120)	16.9413 (39)	15.4974 (51)	36.7239 (115)

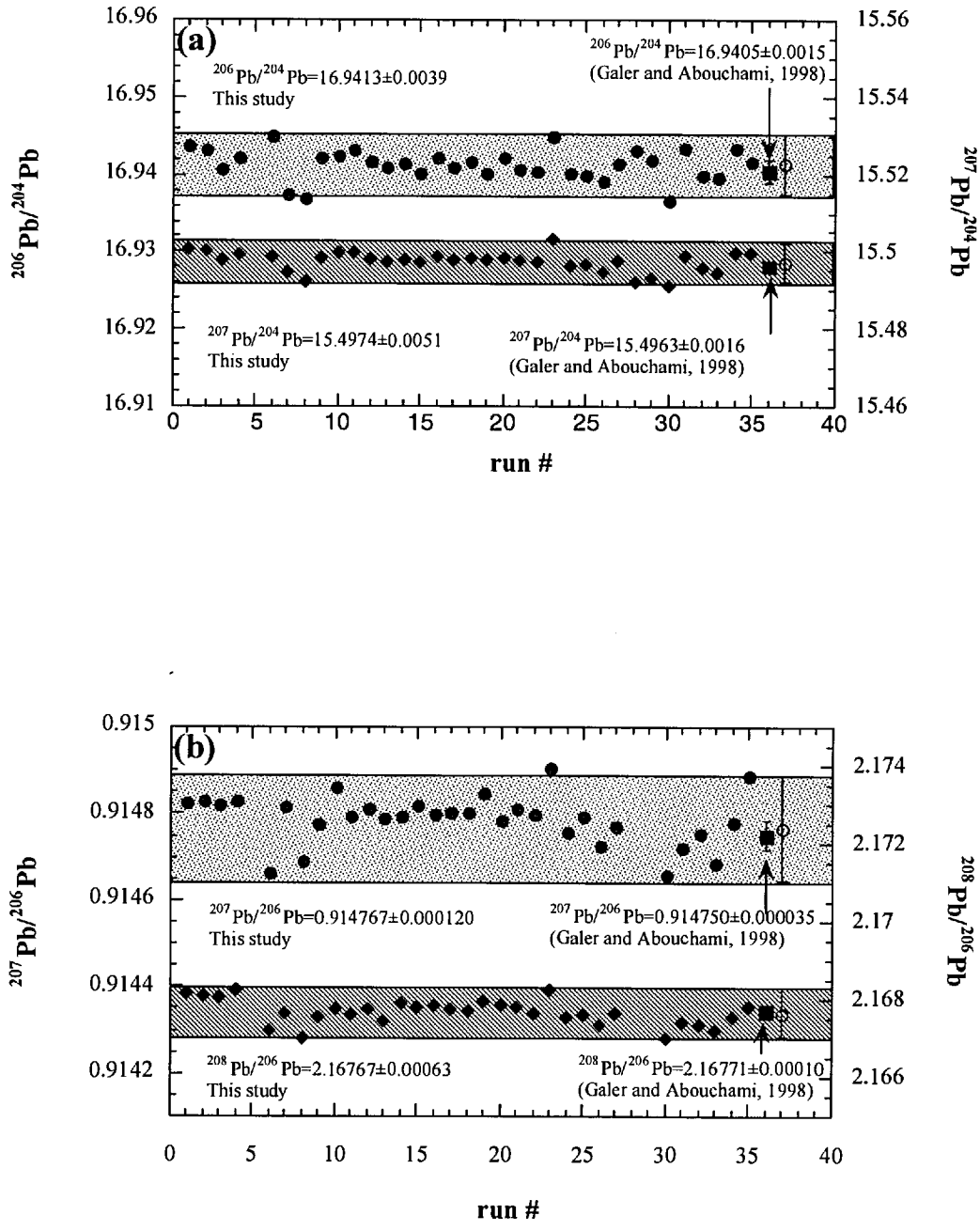

Figure 3.2. Typical long-term reproducibility achieved for the ratios (a) $^{208}Pb/^{206}Pb$ and $^{207}Pb/^{206}Pb$, and (b) $^{206}Pb/^{204}Pb$ and $^{207}Pb/^{204}Pb$ ratios on the Micromass *IsoProbe* MC-ICP-MS determined from repeated measurements of NIST-SRM 981 Pb standards spiked with NIST-SRM 997 Tl over the time period of five months (August to December 2002).

Figure 3.3 shows mass bias factors for Pb (f_{Pb}) and Tl (f_{Tl}) plotted against each other using data collected over three different measurement periods (16.8/19.8.02, 2./3.12.02 and 30.1/31.1.2003). The mass bias factors were calculated with the exponential law using the 'true' ratios for Pb taken from Galer and Abouchami and the optimized ratio for Tl after running our optimization program (Kevin).

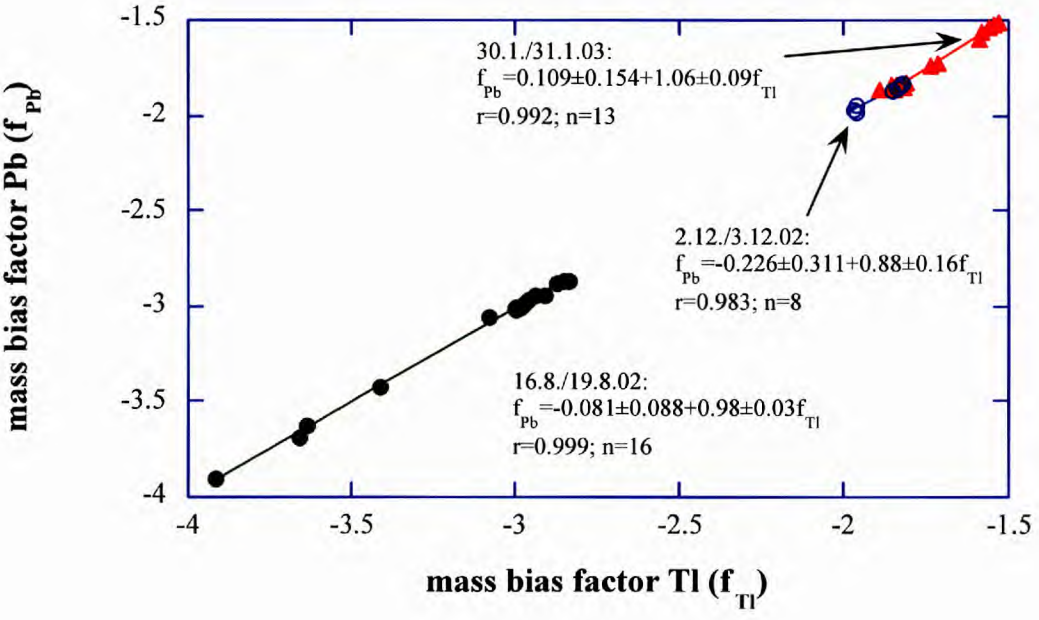

Figure 3.3. The mass bias factors of Pb and Tl (f_{Pb}, f_{Tl}) calculated using the Pb values published by Galer and Abouchami [17] and the optimized Tl ratio using our optimization procedure over a period of six months (August 2002 to January 2003). Shown are three measurement sessions (August 2002, December 2002 and January 2003).

As expected, given the boundary conditions for the Tl optimization procedure, all three measurement periods show the same mass bias factor for Pb and Tl on the 95% significance level, thus $f_{Tl}=f_{Pb}$, and all three data sets have an intercept at the origin within the error (calculated on the 95% significance level).

3.3.3 Matrix influence of peat and lichen samples

To minimize non-spectral and spectral influences from matrix components and to guarantee low internal errors during mass spectrometer measurements, ion exchange column chemistries are widely used to separate the analyte from the matrix. Analyzing Pb isotope ratios with TIMS in complex organic materials such as peat and plants, two column passages are required using conventional HCl/HBr anion exchange column chemistry [10, 11]. However, one of the great promises of plasma source mass spectrometry is to reduce sample preparation time by possibly omitting or reducing column chemistry steps [15]. Consequently, matrix effects of peat and lichen digests were assessed after only one single column passage.

Figure 3.4 shows the temporal variability of the Tl mass bias factor (f_{Tl}) during two measurement sessions: 16.8.02 (Figure 3.4a) when peat matrices were measured and 13.12.02 (Figure 3.4b) when lichen matrices were measured. Shown are the mass bias factors f_{Tl} calculated from $^{205}Tl/^{203}Tl$ ratios measured in spiked samples and in NIST SRM 981 Pb standard (measured between samples to assess the reproducibility and optimize the Tl ratio, shown as open symbols). Average f_{Tl} in peat (-3.359±0.427; n=18) or lichen (-1.742±0.277; n=23) matrix does not differ significantly from the f_{Tl} measured in the NIST SRM 981 Pb standards during the same measurement sessions (-3.456±0.359; n=8, and -1.769±0.222; n=11, respectively). The matrix seems not to affect the mass bias behavior of the Tl spike, suggesting that the column chemistry, the high plasma temperature and/or the sample dilution prior to the measurements remove any possible interferences. The intensities remain also the same (data not shown). The significantly different mass bias factors between peat and lichen measurement sessions reflects the effect of an instrument upgrade, which included a new line-of-sight (LOS) valve, a new hexapole and a shielded torch.

To further assess the matrix influence on data accuracy, selected ore bearing and barren granites (whole rock) from the Orlovka-Spokoinoe mining district were measured with the *IsoProbe* multi collector ICP-MS in London and with the FINNIGAN *MAT* 261 TIMS in Heidelberg.

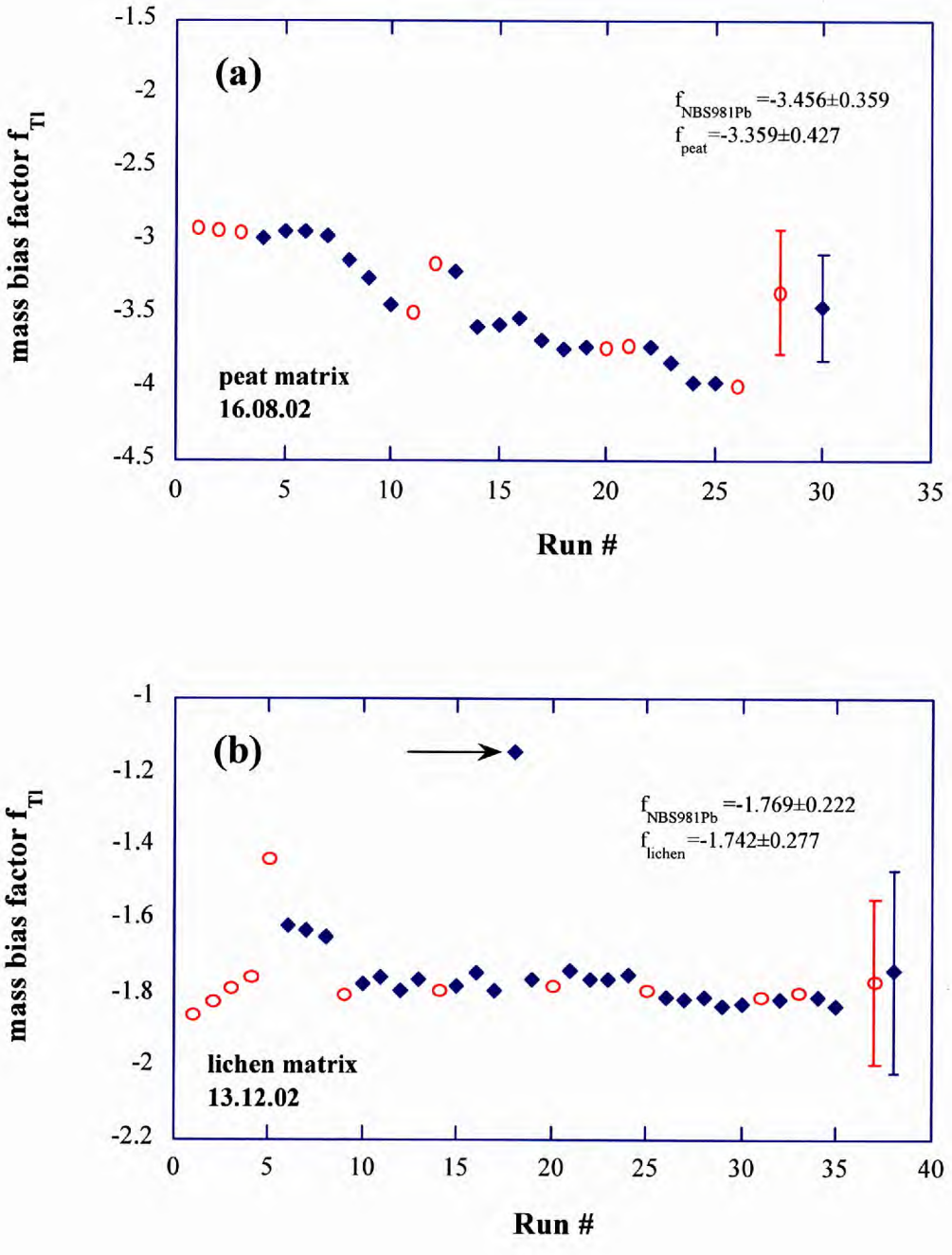

Figure 3.4. Changing mass bias factors (f_{Tl}) of the spiked Tl during two measurement sessions in samples and NIST SRM Pb 981: (a) measuring peat samples from the Faroe Islands, and (b) measuring lichens from the Karabash smelter. Open circles represent the NIST-SRM Pb 981 standard and the closed quadrangles represent the peat and lichen samples. The points with the error bars represent the mean value and the ±2σ standard deviation.

Figure 3.5 shows the $^{208}Pb/^{206}Pb$ and $^{207}Pb/^{206}Pb$ ratios measured in the same aliquots using the different instruments. The linear regressions ($[^{207}Pb/^{206}Pb]_{TIMS}=0.003+0.996[^{207}Pb/^{206}Pb]_{MC\text{-}ICPMS}$; r=0.999; n=13; $^{208}Pb/^{206}Pb]_{TIMS}=-0.018+1.009$ $[^{208}Pb/^{206}Pb]_{MC\text{-}ICPMS}$; r=0.998; n=17) and the theoretical 1:1 line are shown. A systematic offset between TIMS and multicollector-ICP-MS results exists, which has also been described before with the VG *Plasma54* double focusing instrument in Lyon [19]. **Table 3.4** shows the results, which agree on average within 0.08% for both $^{207}Pb/^{206}Pb$ and $^{208}Pb/^{206}Pb$ ratios. Similar agreement between multicollector plasma and TIMS data for 'real' samples were described for ferromanganese crust [23], volcanic rocks [19] and archeological samples [25].

3.3.4 Applications to environmental geochemical studies

Using the new analytical procedures (column chemistry, high temperature/high pressure microwave digestions) and modified data processing procedure ($^{205}Tl/^{203}Tl$ optimization, acid blank subtraction), we achieved high precision Pb isotope ratio measurements in peats, lichens, vegetables and chimney dust during two environmental geochemical projects conducted in London and Heidelberg. One study aimed to assess the local dispersal of Pb and other elements from a Cu smelter using lichen as biomonitors [29, 45], the second study aimed to characterize sources and pathways of Pb and Hg in the sub-Arctic region using a dated peat core in the Faroe Islands [13].

Table 3.5 shows the entire set of isotope ratios measured in the two studies with the internal precision expressed in ±2SE(%). The error of the internal isotope measurements is considerably better (in general below 200 ppm for all ratios) than the errors estimated from the long-term reproducibility (see section 3.2). Consequently, we used the long-term reproducibility based on repeated measurements of the NIST SRM Pb 981 from Table 3.3 as error estimates. Reproducibility estimated from 'true' sample (field samples) replicate measurements (different aliquots of same solution) showed very similar errors to the ones determined by the repeated measurements of NIST SRM 981 Pb.

Table 3.4. Comparison of $^{208}Pb/^{206}Pb$ and $^{207}Pb/^{206}Pb$ measurements from ore bearing granites at Orlovka (Russia) measured by TIMS and the Micromass *IsoProbe* at the NHM/IC JAF facility.

	$^{207}Pb/^{206}Pb$			$^{208}Pb/^{206}Pb$		
Sample ID	**ICP-MC-MS**	**TIMS**	Δ_{TIMS} (%)	**ICP-MC-MS**	**TIMS**	Δ_{TIMS} (%)
2068-Orlovka	0.8430	0.8418	0.14	2.0865	2.0844	0.10
2096-Orlovka	n.d.	n.d.		2.0361	2.0340	0.10
2128-Orlovka	0.8585	0.8580	0.06	2.0969	2.0962	0.03
2142-Orlovka	0.8364	0.8356	0.10	2.0628	2.0600	0.14
2147-Orlovka	0.8437	0.8428	0.11	2.0788	2.0762	0.13
2149-Orlovka	n.d.	n.d.		2.0484	2.0494	0.05
2164-Orlovka	0.7987	0.7980	0.09	1.9828	1.9816	0.06
2166-Orlovka	n.d.	n.d.		2.0359	2.0344	0.07
2068-Orlovka	n.d.	n.d.		2.0865	2.0844	0.10
2173-Orlovka	n.d.	n.d.		2.0326	2.0316	0.05
2182-Orlovka	0.8173	0.8170	0.04	2.0854	2.0852	0.01
2182-Orlovka	0.8265	0.8264	0.01	2.0840	2.0852	0.06
2169-Orlovka	0.8316	0.8314	0.02	2.0588	2.0578	0.05
2204-Orlovka	0.8430	0.8414	0.19	2.0835	2.0821	0.07
2213-Orlovka	0.8410	0.8416	0.07	2.0714	2.0733	0.09
2215-Orlovka	0.8459	0.8454	0.06	2.0824	2.0823	0.01
2220-Orlovka	0.8364	0.8356	0.10	2.0020	2.0003	0.08
2223-Orlovka	0.8414	0.8413	0.01	2.0685	2.0728	0.21

2σ errors externally derived using repeated NBS 981 measurements were all below 200 ppm

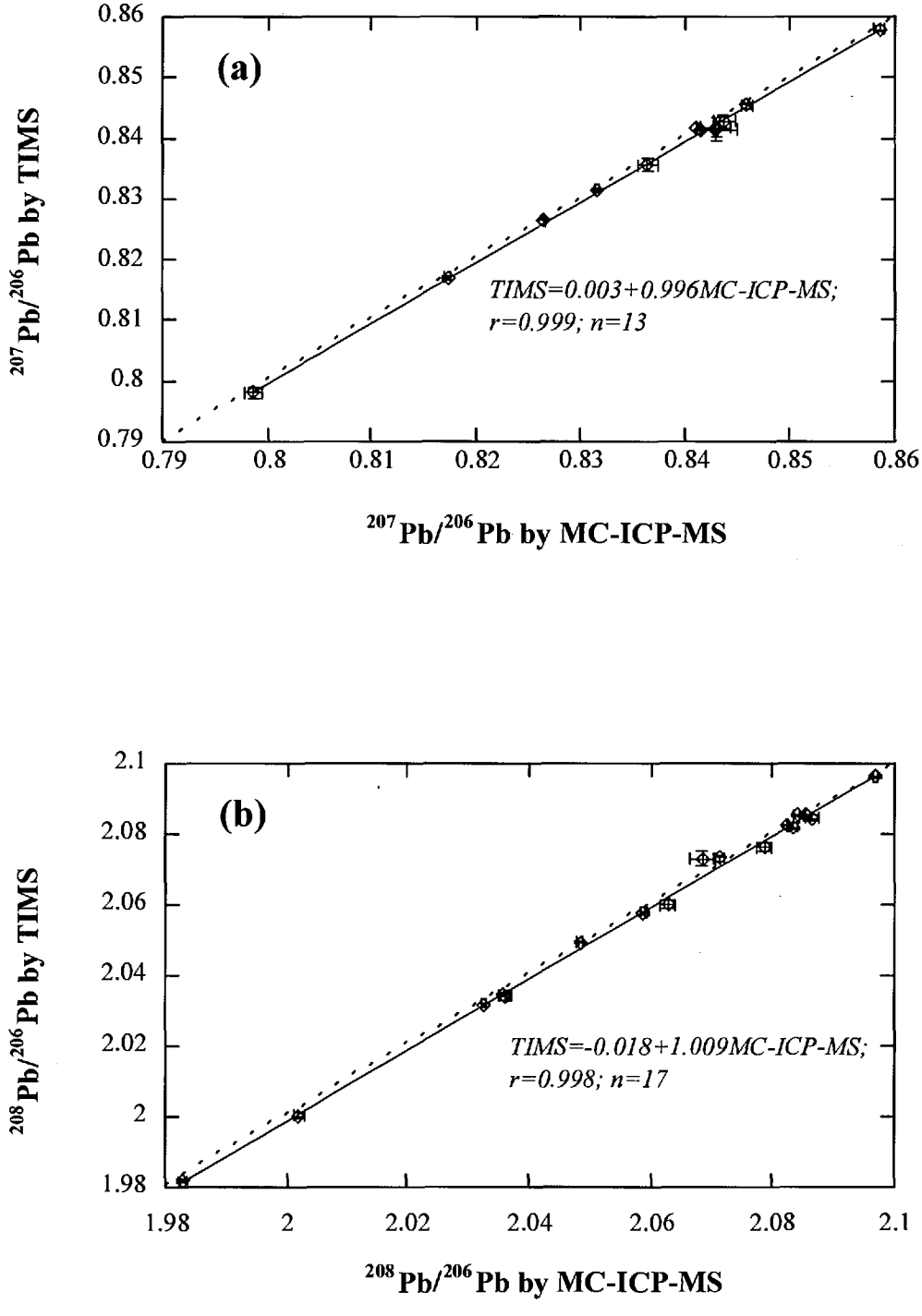

Figure 3.5. TIMS and MC-ICP-MS data from selected silicate samples (whole rock and mineral separates from Ta/W ore bearing granites). Shown is the best linear fit along with the theoretical (dashed) 1:1 line.

Table 3.5. Complete Pb isotope data set measured during the two environmental geochemical studies (see text for details).

Sample #	Sample ID	Sample Type	Pb (ppm)	$^{206}Pb/^{204}Pb$	±2SE (%)	$^{207}Pb/^{204}Pb$	±2SE (%)	$^{208}Pb/^{204}Pb$	±2SE (%)	$^{207}Pb/^{206}Pb$	±2SE (%)	$^{208}Pb/^{206}Pb$	±2SE (%)
Cu Smelter near Karabash													
1	I 15 3	Lichen	68.0	17.911	0.005	15.550	0.004	37.874	0.010	0.868	0.004	2.115	0.005
2	I 17 3	Lichen	120.0	17.897	0.015	15.535	0.013	37.847	0.033	0.868	0.004	2.115	0.006
5	I 19 3	Lichen	111.0	17.975	0.003	15.607	0.003	38.065	0.007	0.868	0.003	2.118	0.016
6	I 34 12 (1)	Lichen	213.0	17.916	0.003	15.571	0.002	37.856	0.005	0.869	0.003	2.113	0.016
7	I 35 12 (2)	Lichen	151.0	17.906	0.007	15.549	0.007	37.830	0.016	0.868	0.005	2.113	0.004
8	I 37/C	Lichen	n.d.	17.929	0.002	15.572	0.001	37.908	0.003	0.869	0.003	2.115	0.004
9	I 1K1	Lichen	112.8	17.935	0.004	15.557	0.003	37.840	0.007	0.867	0.003	2.110	0.007
10	I 2 K2	Lichen	64.0	17.801	0.027	15.457	0.023	37.635	0.056	0.868	0.007	2.114	0.004
11	I 4 K3	Lichen	118.2	17.896	0.004	15.545	0.004	37.788	0.009	0.869	0.003	2.112	0.004
12	II 5(D-2)	Vegetable	n.d.	17.831	0.013	15.506	0.011	37.684	0.027	0.870	0.004	2.113	0.009
13	II 40 3	Lichen	100.6	17.854	0.014	15.518	0.013	37.718	0.032	0.869	0.005	2.113	0.004
14	II 41/4	Lichen	446.5	17.899	0.003	15.553	0.002	37.798	0.006	0.869	0.003	2.112	0.006
15	II 42/5	Lichen	1199.9	17.824	0.014	15.505	0.013	37.708	0.031	0.869	0.005	2.116	0.008
16	II 43/6	Lichen	482.7	17.830	0.022	15.489	0.019	37.616	0.049	0.869	0.005	2.110	0.005
17	II 44(2)	Lichen	278.3	17.710	0.019	15.463	0.016	37.517	0.040	0.873	0.006	2.118	0.007
18	II C1 (D-9)	Chimney dust	n.d.	17.841	0.001	15.596	0.001	37.822	0.002	0.874	0.004	2.120	0.009
19	II C2 (D-10)	Chimney dust	n.d.	17.844	0.001	15.599	0.001	37.833	0.001	0.874	0.003	2.120	0.008
20	II C4	Chimney dust	n.d.	17.921	0.002	15.618	0.002	37.952	0.005	0.872	0.003	2.118	0.004
21	III 46	Lichen	n.d.	17.875	0.019	15.488	0.016	37.683	0.041	0.867	0.006	2.108	0.005
22	III 49 C/12	Vegetable	175.6	17.913	0.002	15.574	0.001	37.864	0.003	0.869	0.004	2.113	0.004

Sample #	Sample ID	Sample Type	Pb (ppm)	$^{206}Pb/^{204}Pb$	±2SE (%)	$^{207}Pb/^{204}Pb$	±2SE (%)	$^{208}Pb/^{204}Pb$	±2SE (%)	$^{207}Pb/^{206}Pb$	±2SE (%)	$^{208}Pb/^{206}Pb$	±2SE (%)
23	III 14/1	Vegetable	n.d.	18.044	0.001	15.727	0.001	38.342	0.001	0.872	0.002	2.125	0.004
24	III 14/2	Vegetable	n.d.	18.003	0.002	15.599	0.001	38.015	0.003	0.867	0.004	2.112	0.009
25	III KA 26/5	Vegetable	n.d.	17.813	0.007	15.533	0.006	37.689	0.014	0.872	0.005	2.116	0.005
26	III 26	Vegetable	n.d.	17.901	0.008	15.527	0.007	37.776	0.017	0.867	0.003	2.110	0.003
27	III KA 4/2	Vegetable	n.d.	17.961	0.002	15.570	0.001	37.899	0.003	0.867	0.003	2.110	0.005
Average					**0.008**		**0.007**		**0.017**		**0.004**		**0.006**
Myrarnar Peat Core													
1	Myr Neo 01	Peat	6	17.738	0.005	15.583	0.005	37.606	0.005	0.879	0.002	2.120	0.004
2	Myr Neo 02	Peat	14.8	17.688	0.004	15.582	0.005	37.577	0.005	0.881	0.002	2.124	0.005
3	Myr Neo 03	Peat	45.3	17.657	0.003	15.562	0.003	37.503	0.003	0.881	0.005	2.124	0.011
4	Myr Neo 04	Peat	65	17.774	0.006	15.567	0.005	37.651	0.005	0.876	0.002	2.118	0.004
5	Myr Neo 05	Peat	109.1	18.043	0.003	15.599	0.003	38.004	0.004	0.864	0.002	2.106	0.004
6	Myr Neo 07	Peat	107.1	18.307	0.008	15.621	0.009	38.326	0.009	0.853	0.002	2.094	0.005
7	Myr Neo 09	Peat	95.9	18.383	0.012	15.616	0.016	38.348	0.020	0.850	0.005	2.086	0.011
8	Myr Neo 15	Peat	28.1	18.404	0.002	15.637	0.002	38.443	0.002	0.850	0.001	2.089	0.003
9	Myr Neo 17	Peat	26	18.396	0.004	15.620	0.006	38.381	0.007	0.849	0.002	2.086	0.004
10	Myr Neo 19	Peat	6.2	18.470	0.007	15.629	0.006	38.505	0.006	0.846	0.002	2.085	0.006
11	Myr Neo 32	Peat	6.4	18.428	0.005	15.626	0.005	38.452	0.005	0.848	0.002	2.087	0.004
12	Myr Neo 42	Peat	5.4	18.557	0.005	15.614	0.005	38.600	0.006	0.841	0.002	2.080	0.004
Average					**0.005**		**0.006**		**0.007**		**0.002**		**0.005**

Figure 3.6 shows three isotope plots of ^{208}Pb, ^{207}Pb and ^{206}Pb measured during the two studies. In both studies, the differences in the isotope ratios among the individual samples are significant on the $\pm 2\sigma$ confidence level and the errors plot within the symbols, allowing consequently a very detailed source assessment. Figure 3.6a shows Pb isotope data measured in the Faroe Island peat bog profile (representing *c.* 2,500 yrs of atmospheric Pb deposition) with variations of $^{206}Pb/^{207}Pb$ (1.13-1.19) and $^{208}Pb/^{206}Pb$ ratios (2.07-2.12), which are significantly larger (5 and 2%, respectively) than the estimated long-term reproducibility for these isotope pairs (0.013 and 0.029%, respectively, Figure 3.2). The large variations of Pb isotope signatures in the peat samples are due to the different sources (gasoline, coal, soil dust, waste incineration, represented as gray fields in Figure 3.6a and estimated from data taken from [7]), which characterized the atmospheric Pb deposition in Europe during the last 2,500 years [1, 46]. The error bars plot well within the symbols and the individual samples are clearly discernible. The conclusions taken from this three-isotope plot agree well with other peat records in Europe covering the last 2,500 years of atmospheric Pb deposition [7, 47]. A detailed geochemical discussion of the peat profile is given elsewhere [13].

Figure 3.6b shows Pb isotope data measured in lichens, vegetables and chimney dust around the Cu smelter in Karabash, Southern Urals. The range of $^{206}Pb/^{207}Pb$ and of $^{208}Pb/^{206}Pb$ (1.14-1.15 and 2.11-2.12, respectively) is considerably smaller (0.9 and 0.7%, respectively) than in the peat study, but the variations are still an order of magnitude larger than the estimated errors of the individual data points using the long-term reproducibility. Most ratios of the lichens and vegetables plot on a mixing line between two end members - smelter dust (represented by the isotopic composition of the chimney dust) and natural background Pb, represented in this study by pre-anthropogenic aerosols [11]. However, there is a statistically significant scatter in the data and several samples are off the simple two component mixing line, which suggests that a third end member (most likely anthropogenic) with higher ^{208}Pb and higher ^{207}Pb concentrations remains unidentified. The data set shows that with the high precision achieved, even for local scale contamination having small variations, new end-members can be identified and hinting to additional sources. Such a detailed source assessment in a local contamination study has previously been achieved using TIMS [48] but not Q-ICP-MS [49].

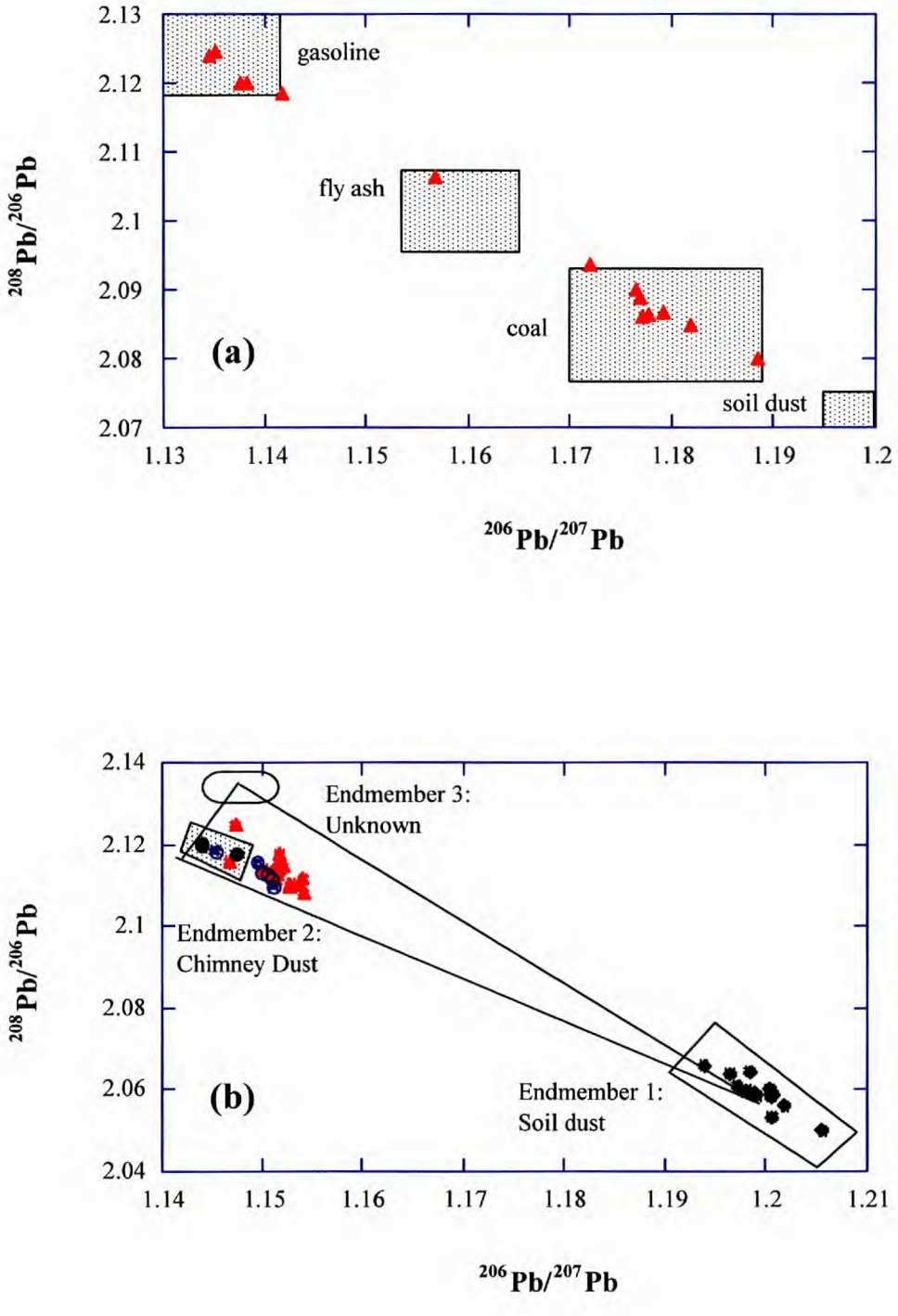

Figure 3.6. Three isotope plots including the isotopes ^{208}Pb, ^{207}Pb and ^{206}Pb of the two different environmental geochemical studies assessing Pb dispersal into the environment: (a) Pb isotope data from a peat core in the Faroe Islands (Shotyk et al., in print) and (b) Pb isotope data from chimney dust, vegetable and lichens within the vicinity of a Zn smelter in the Urals (Purvis et al., 2004).

3.4. CONCLUSIONS

A wide range of environmental samples was dissolved using the recently developed microwave assisted acid digestion methods for biological samples (peat, lichen, vegetable) at Imperial College London and the University of Heidelberg or conventional hot plate acid digestion for granites and chimney dust. After acid digestion, the solutions were passed through an exchange column packed with EiChrom Sr-resin applying a new simple monoacid elution procedure. The column chemistry yielded quantitative recoveries of Pb and allowed a high sample throughput (*c.* 24 samples/day).

Analysis of ^{204}Pb, ^{206}Pb, ^{207}Pb and ^{208}Pb on a Micromass *Isoprobe* MC-ICP-MS resulted typically in internal precisions of below 100 ppm ($\pm 2\sigma$) on all Pb isotope ratios in all matrices using 50 measurements. Mass bias correction using optimized $^{205}Tl/^{203}Tl$ ratios achieved accuracies below 80ppm for all ratios. The Tl optimization was achieved using a simple mathematical least square approximation. The 'certified' Tl ratio used for mass bias correction had to be adjusted for each measurement session up to 2.3907. The measurement protocol used during the study allowed the determination of the isotope ratios of 5 unknown samples/1.5 hours. This is a significant improvement to the sample throughput compared to TIMS. The long-term reproducibility (expressed as $\pm 2\sigma$) determined over a five month period using repeated measurements of the NIST SRM 981 Pb standard and optimized Tl values was below 350ppm for all ratios. Ore bearing granites samples passed through the columns and measured with TIMS and MC-ICP-MS showed excellent correlation (r=0.9876 for $^{206}Pb/^{204}Pb$ ratios, slope=0.9474, n=13). The mass bias of Tl spiked into natural and synthetic samples during a measurement session did not differ significantly, indicating that the complex peat and lichen matrix did not affect the mass bias behavior of the Tl spike.

3.5. REFERENCES

[1] M.K. Reuer and D.J. Weiss, Phil. Trans. R. Soc. Lond. A 360, 2889-2904, 2002.

[2] A.J. Véron and T.M. Church, J. Geophys. Res. 102(D23), 28,049-28,058, 1997.

[3] D.J. Weiss, E.A. Boyle, V. Chavagnac, J. Wu, A. Michel and M. Reuer, J. Geophys. Res., in press.

[4] K.J.R. Rosman, C. Ly, K. Van der Velde and C.F. Boutron, Earth Planet. Sci. Lett. 176(3-4), 413-424, 2000.

[5] A.J. Véron, C.E. Lambert, A. Isley, P. Linet and F.E. Grousset, Nature 326, 278-281, 1987.

[6] N. Teutsch, N. Erel, L. Halicz and A. Banin, Geochim. Cosmochim. Acta 65(17), 2853-2864, 2001.

[7] D. Weiss, W. Shotyk, P.G. Appleby, J.D. Kramers and A.K. Cheburkin, Environ. Sci. Technol. 33(9), 1340-1352, 1999.

[8] G.T. Shen and E.A. Boyle, J. Geophys. Res. 93, 15715-15732, 1988.

[9] W. Hansmann and V. Koeppel, Chem. Geol. 171, 123-144, 2000.

[10] D. Weiss, W. Shotyk, J.D. Kramers and M. Gloor, Atmos. Environ. 33(23), 3751-3763, 1999.

[11] W. Shotyk, D. Weiss, J.D. Kramers, R. Frei, A.K. Cheburkin, M. Gloor and S. Reese, Geochim. Cosmochim. Acta 65(14), 2337-2360, 2001.

[12] W. Shotyk, M.E. Goodsite, F. Roos-Barraclough, R. Frei, J. Heinemeier, G. Asmund, C. Lohse and T.S. Hansen, Geochim. Cosmochim. Acta 67(21), 3991-4011, 2003.

[13] W. Shotyk, M.E. Goodsite, F. Roos-Barraclough, N. Givelet, G. Le Roux, D.J. Weiss, A.K. Cheburkin, K. Knudsen, J. Heinemeier, W.O. Van der Knaap, S.A. Norton and C. Lohse, Geochim. Cosmochim. Acta, submitted.

[14] J.G. Farmer, L.J. Eades, A.B. MacKenzie, A. Kirika and T.E. Bailey-Watts, Environ. Sci. Technol. 30, 3080-3083, 1996.

[15] D. Weiss, V. Chavagnac, E.A. Boyle, J.F. Wu and M. Herwegh, Spectrochim. Acta, B 55(4), 363-374, 2000.

[16] K.E. Jarvis, Inductively coupled plasma-mass spectrometry, in: Modern Analytical Geochemistry, R. Gill, ed., pp. 171-187, Addison Wesley Longman, Singapore, 1997.

[17] A.J. Walder and P.A. Freedman, J. Anal. At. Spectr. 7, 571-575, 1992.

[18] A.N. Halliday, D.C. Lee, J.N. Christensen, M. Rehkaemper, W. Yi, X. Luo, C.M. Hall, C.J. Ballentine, T. Pettke and C. Stirling, Geochim. Cosmochim. Acta 62(6), 919-940, 1998.

[19] W.M. White, F. Albarède and P. Télouk, Chem. Geol. 167, 257-270, 2000.

[20] J.D. Woodhead, J. Anal. At. Spectrom. 17, 1381-1385, 2002.

[21] S. Ehrlich, Z. Karpas, L. Ben-Dor and L. Halicz, J. Anal. At. Spectrom. 16, 975-977, 2001.

[22] M. Rehkaemper and A.M. Halliday, Int. J. Mass. Spec. Ion. Proc. 58, 123-133, 1998.

[23] N.S. Belshaw, P.A. Freedman, K.A. O'Nions, M. Frank and Y. Guo, Int. J. Mass Spectrom. 181, 51-58, 1998.

[24] T. Hirata, Analyst 121, 1407-1411, 1996.

[25] M. Rehkaemper and K. Mezger, J. Anal. At. Spectrom. 15, 1451-1460, 2000.

[26] M. Thirlwall, J. Anal. At. Spectrom. 16, 1121-1125, 2001.

[27] M.F. Thirlwall, Chem. Geol., 2002.

[28] M.K. Reuer, E.A. Boyle and B.C. Grant, Chem. Geol. 200, 137-153, 2003.

[29] O.W. Purvis, P.J. Chimonides, G.C. Jones, I.N. Mikhailova, B. Spiro, D. Weiss and B.J. Williamson, Proc. R. Soc. London B 271, 221, 2004.

[30] F.G. Reyf, R. Seltmann and G.P. Zaraisky, Can. Mineral. 38(4), 1029-1051, 2000.

[31] A. Dolgopolova, R. Seltmann, B. Kober, D. Weiss, P. Dulski and C. Stanley, Trans. Inst. Min. Metall.: Section B: Applied Earth Sciences, 113, 83-99, 2004.

[32] M. Krachler, C. Mohl, H. Emons and W. Shotyk, J. Anal. Atom. Spectrom. 17(8), 844-851, 2002.

[33] A. Dolgopolova, D. Weiss, R. Seltmann and B. Coles, Intern. J. Environ. Anal. Chem., in press.

[34] E.P. Horwitz, M.L. Dietz, S. Rhoads, C. Felinto, N.H. Gale and J. Houghton, Anal. Chim. Acta 292, 263-273, 1994.

[35] E.P. Horwitz, Extraction chromatography of actinides and selected fission products: principles and achievement of selectivity, in: Intern. Workshop on the application of extraction chromatography in radionucleid measurements, IRMM, Geel 9-10, Belgium, 1998.

[36] S.J.G. Galer and W. Abouchami, Min. Mag. 62A, 491-492, 1998.

[37] B. Kober, M. Wessels, A. Bollhofer and A. Mangini, Geochim. Cosmochim. Acta 63(9), 1293-1303, 1999.

[38] M.F. Thirlwall, Chem. Geol. 163, 299-322, 2000.

[39] H.P. Longerich, B.J. Fryer and D.F. Strong, Spectrochim. Acta 42B, 39-48, 1987.

[40] W. Todt, R.A. Cliff, A. Hanser and A.W. Hofmann, Evaluation of a ^{202}Pb-^{205}Pb double spike for high precision lead isotope analysis, in: Earth Processes: Reading the Isotopic Code, S.R. Hart and A. Basu, eds. 95, pp. 429-437, American Geophysical Union, 1996.

[41] C.N. Maréchal, P. Télouk and F. Albarède, Chem. Geol. 156, 251-273, 1999.

[42] T.F.D. Mason, D.J. Weiss, M. Horstwood, R.R. Parrish, S.S. Russell, E. Mullane and B.J. Coles, J. Anal. Atom. Spectrom., submitted.

[43] L.P. Dunstan, J.W. Gramlich, I.L. Barnes and W.C. Purdy, J. Res. Nat. Bur. Stand. 85, 1-10, 1980.

[44] K.D. Collerson, B.S. Kamber and R. Schoenberg, Chem. Geol. 188, 65-83, 2002.

[45] B. Spiro, B.J. Williamson, V. Udachin, B. Coste and D.J. Weiss, Geophys. Res. Abstracts 5, 06775, 2003.

[46] D. Weiss, W. Shotyk and O. Kempf, Naturwissenschaften 86, 262-275, 1999.

[47] A. Martinez-Cortizas, E. Garcia-Rodeja Gayoso and D. Weiss, Sci. Total. Environ. 292(1-2), 1-5, 2002.

[48] C. Gobeil, W.K. Johnson, R.W. MacDonald and C.S. Wong, Environ. Sci. Technol. 28(1), 193-201, 1995.

[49] J.M. Blais, Water, Air, Soil Pollut. 92, 329-42, 1996.

CHAPTER 4. GEOCHEMICAL CHARACTERISTICS AND LEAD ISOTOPE SYSTEMATICS OF HIGHLY FRACTIONATED LI-F ENRICHED AMAZONITE GRANITES AND RELATED HOST ROCKS OF THE ORLOVKA-SPOKOINOE MINING DISTRICT, EASTERN TRANSBAIKALIA (RUSSIA)

ABSTRACT

Element concentrations and Pb isotope data are reported for the Khangilay, Orlovka and Spokoinoe granite massifs and their host rocks in the Orlovka-Spokoinoe mining district, Eastern Transbaikalia, Russia. The **aim** of the paper is to characterize the evolution trends and geochemical features of the Khangilay pluton and the Orlovka and Spokoinoe deposits and to study the genesis of the three granite massifs by examining fluid-rock and crust-mantle interaction in the evolution of granitoid magmatism. **Zr/Hf, Y/Ho, Rb/Sr, and Nb/U** demonstrate that all three granite bodies show a continuous fractionation history from parental biotite-muscovite granites of Khangilay to highly evolved ore-bearing amazonite granites of Orlovka. Khangilay and its derivates Spokoinoe and Orlovka represent different evolution stages. **REE patterns** of the amazonite granites of Orlovka show a stronger Eu anomaly and more apparent REE tetrad effects in comparison with the less evolved granites of Khangilay. **Pb isotope analyses** indicate one common Pb source for all three granite massifs reflecting a homogenous source melt from which all magmatic members generated. Based on Pb isotope systematics two possible scenarios for the source of Li-F granites are proposed: 1) a **crust-mantle source** where a mixture of MORB and continental-derived material were brought together in the orogenic environment; and 2) **type II enriched mantle source** where subducted continental material could have been strongly implicated in volcanic suites.

Revised version of the IMM Transactions section B: *Applied Earth Science*, 2004, 113, 83-89

4.1. INTRODUCTION

The rare-metal granite-related Orlovka tantalum deposit and the Spokoinoe tungsten vein quartz-greisen deposit are located in Eastern Transbaikalia 140 km and 148 km SE of Chita, respectively (**Figure 4.1**). Both deposits are hosted by the Khangilay granite pluton and are believed to be its satellites.[4,19,30] The appearance of two chemically contrasting rare-metal granites (tantalum vs. tungsten specialized) within a single pluton like Khangilay attracted a lot of scientific attention previously and is still a matter for debate. The anatomic uniqueness of the Orlovka deposit is caused by its vertically zoned internal structure. As a result of fractionation and alteration processes a complete petrographic range of rare-metal granites ranging from barren biotite granites to mineralized lepidolite-amazonite-albite granites, layered pegmatites-aplites and line rocks as well as greisens document a continuous transition from magmatic fractionation to hydrothermal mineralization processes. The Khangilay pluton with the Orlovka stock have been repeatedly used for studying A-type granite rock assemblages and their geochemistry, petrography and mineralogy.[2,4,28,39] The mechanisms that resulted in mineralized rare-metal granites and their evolution have also been addressed.[17,25,27,39] In recent years the research focus has been shifted towards the evolution of rare-metal granites, formation stages and relation to intraplate magmatism[2]. Specifically, the Rb-Sr and Sm-Nd isotopic systems have been used to reveal the sources of rare-metal granite melts from the study area [15,16,19-21,36,37] and results indicated that sources were likely to be either crustal, mantle or combined crustal-mantle. However, more isotopic and geochemical evidence is needed in order to better understand generation and formation mechanisms of such melts. Our study utilizes a complex approach in using indicative element concentrations, high field strength element (HFSE) ratios, rare earth element (REE) patterns and Pb isotopes for the granites of the Orlovka, Spokoinoe and Khangilay massifs and their host rocks. The aim of this approach is: i) to characterize the evolution trends and features of the Khangilay pluton and the Orlovka and Spokoinoe deposits (barren versus mineralized granites, ores, host rocks) and ii) to study the genesis and evolution of all three granite massifs by examining fluid-rock and crust-mantle interaction in the development of granitoid magmatism, the genetic relationship of the three massifs and controls of similarities and differences among them.

Pb isotope data presented here are the first obtained for the study area and are an important tool because Pb isotopic compositions in different kinds of rocks contain a record of the chemical environments in which Pb resided, including mantle and crustal rocks or Pb ores.[8] Specific questions for the application of Pb isotopes discussed in this paper are: 1) what can we conclude about the environment in which the Khangilay, Orlovka and Spokoinoe granite massifs and related deposits were formed; 2) is there a common Pb source for all three massifs and what controls Pb isotope variations; 3) can we distinguish between crustal and mantle sources in the formation of the massifs? This data supplement previous research available on the study area.

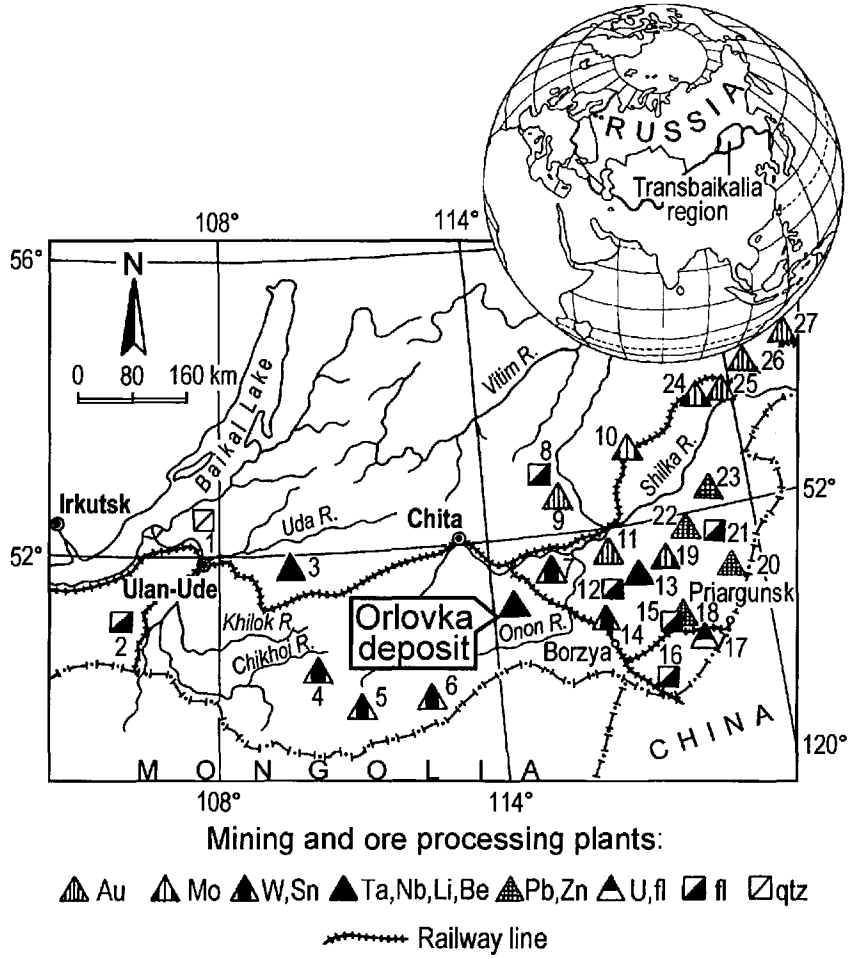

Figure 4.1. Location of the Orlovka mining area (after Kremenetsky et al., 1999).

4.2. GEOLOGICAL SETTING

4.2.1. Geodynamic-tectonic position

The Orlovka-Spokoinoe mining district belongs to the *Central Asian Orogenic Belt* (CAOB)[15] or *Transbaikal-Mongolian orogenic collage*[35] where several oroclinally bent magmatic arcs separated by accretionary complexes and ophiolitic sutures located between the major cratons.[35] Rare-metal Li-F enriched granites and pegmatites are widespread as products of continental crustal growth[15] and associated *intraplate magmatism*.[20] The long influence (Early Paleozoic - Early Cenozoic) of the *Asian superplume* on the territory of Siberia (including the Transbaikalia region) resulted in prolonged multistage magmatic activity.[19-21,36,37] As a result, series of intraplate magmatic areas of various ages were formed within Siberia controlling the size of rare-metal metallogenic provinces at different time intervals. The intraplate magmatism of the Late Mesozoic – Early Cenozoic epoch (180-170 Ma to 30 Ma) was concentrated in Transbaikalia, eastern Mongolia and a few other regions where rare-metal deposits related to Li-F enriched granites were formed.[20] The Orlovka and Spokoinoe deposits are representative examples of these within-plate rifting processes. The relation of rare-metal mineralization to intraplate magmatism resulting from separation of ore-bearing melts from parental magmas in the course of extensive crystal fractionation presumably due to mantle-triggered high heat flow, or the direct involvement of mantle melts.

4.2.2. Regional geology

The **Khangilay pluton** (**Figure 4.2**) is located in the central portion of the Paleozoic Aginskaya microplate that is made up of predominantly low-grade metamorphosed sandstone and shales.[4,27,30] The granitoids of the pluton cut metamorphosed Proterozoic to Carboniferous shales and volcanics, a Triassic terrigenous and volcano-sedimentary sequence, and gabbro-diorite, granodiorite, and lamprophyre bodies.[19] The microplate underwent dispersed magmatism during the Early Mesozoic. In its NE part it was intruded by granite plutons, the largest of which, from gravimetric data, is 24 km by 22 km in dimension at a depth of 500-2500 m and is exposed at surface as three separate granitic massifs (cupolas): central (Khangilay) of 8 km^2, eastern (Spokoinoe) of 0.06 km^2, and western (Orlovka) of about 2 km^2.[4,21]

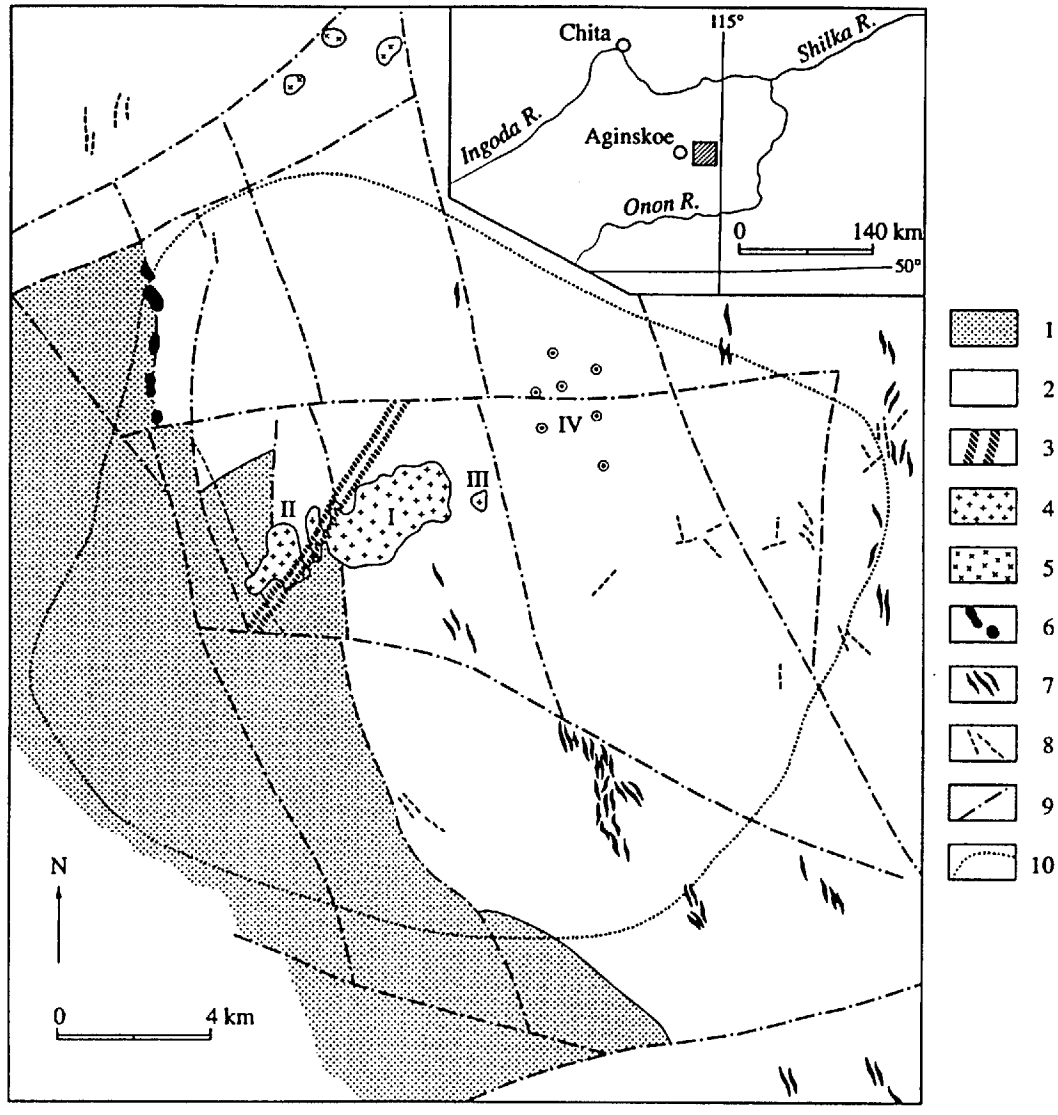

Figure 4.2. Schematic geological map of the Khangilay pluton (after Beskin et al., 1994). 1- Triassic terrigenous rocks and volcanoclastic sediments; 2 – Paleozoic metasedimentary rocks; 3 – Cenozoic diabase dikes; 4-6 – Mesozoic intrusives: 4 – granites, 5 – granodiorites, 6 – gabbro-diorites; 7 – granite-porphyry; 8 – pre-granite lamprophyres; 9 – faults; 10 – contour of a hidden granite pluton (based on gravity data). I - IV – Granite massifs and hosted deposits: I – Central Massif (Khangilay); II – Western Massif with Orlovka Ta deposit; III – Eastern Massif with Spokoinoe W deposit; IV – minor W and Sn deposits and showings.

The central Khangilay granite massif is composed of biotite granite and biotite-muscovite granites. The western Orlovka satellite is a highly differentiated Ta-(Nb-Sn-) bearing intrusion of lithionite-amazonite-albite granite; and the eastern Spokoinoe body is composed of muscovite-albite granite with W (Sn, Be) mineralization. For all the granites of the Khangilay-Orlovka-Spokoinoe massifs the most recent Rb-Sr age determination yielded a Jurassic age of 142.9 ± 1.8 Ma.[19]

The **Orlovka tantalum deposit (Figure 4.3)** is confined to the apical part of the Orlovka granite cupola.[30] The tantalum minerals are represented by finely-disseminated (0.01-1mm) tantalite, tantalite-columbite, microlite and pyrochlore accumulated in the endocontact rocks of the granite cupolas. There is a clear zonation observed in the Orlovka granite massif.[27] Outward from the deeper, central portion of the Orlovka cupola, that is composed of porphyritic biotite and two-mica granites, the Li-F granites become enriched in albite (29.5 to 44.6 vol.%), topaz (~0.1 to 2.8 vol.%), microlite (<10 up to 150 ppm), and columbite-tantalite (60 to 150-800 ppm). The Ta/Nb ratio in the latter increases from 0.57 to 2.36, Li-bearing muscovite gives way to lepidolite or zinnwaldite, and microcline turns into its variety amazonite.[4,20,40] The granite of the uppermost zone represents the actual ore body that has been partly open-pit mined for tantalum. It is now well-established that rare-metal granites like Orlovka are of magmatic origin[19] and were produced during the postorogenic stages of magmatic cycles.[16] The enrichment of the upper zone in Ta, Nb, Li, Rb, F has been significantly influenced by a redistribution of elements due to late to postmagmatic hydrothermal solutions.[4,17,40] Magmatic-hydrothermal transition processes are documented in the ore-bearing Li-F granite by fluid saturation textures such as miarolitic cavities, comb quartz, line rocks, layered pegmatite-aplites and "snowball" textured microgranites of variable grain size. These are alternating with mineralized irregular alteration bodies and subhorizontal layers of albitization, microclinization (amazonitization) and mainly muscovite and topaz-zinnwaldite dominated greisenization and are locally crosscut by mineralized amazonite aplite-pegmatite dikes and greisen zones representing younger fluid-magma pulses.

The presence of amazonite and specific rhythmically banded granitic rocks composed of quartz-albite, quartz-microcline (amazonite), and quartz-mica layers with an aplitic or pegmatitic texture is typical for the deposit.[3,30] The layered rocks form sub-horizontal layers or flat lenses in the massive rare-metal granites.

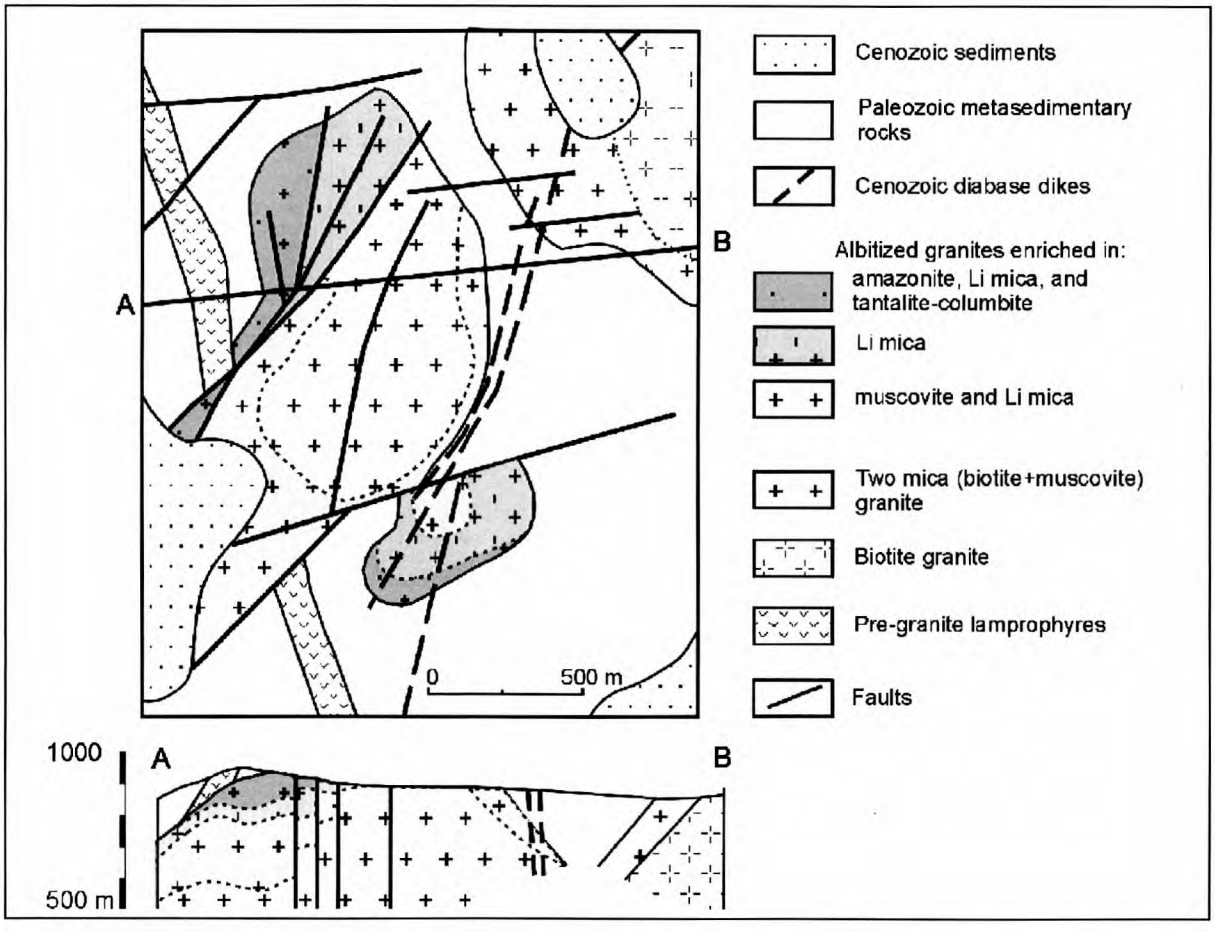

Figure 4.3. Schematic geological map of the Orlovka cupola and E-W cross-section derived from exploration-drilling data (simplified after Reyf et al., 2000). The SW end of the Khangilay cupola is shown at the top right of the map.

The thickness of the rhythmically layered bodies varies from 0.1m to 1-1.5m and they are up to several tens of meters across.[38] In addition to the prevailing horizontal layers, steeply dipping dike-like rhythmically banded bodies occur. Both rhythmically banded Li-F granites and tantalum mineralization are located in the granite cupola exclusively in the upper 30-50 m below the contact to the host rocks. Field evidence led to the conclusion that the Li-F granite, which is the most fractionated phase and represents the actual ore body, forms a separate sheet-like intrusion emplaced between the underlying biotite granite and the roof of the Orlovka cupola that has the characteristics of a quenched carapace. Because Ta-Nb minerals occur as interstitial crystals between the major silicate phases the crystallization of the ore minerals is seen as an integral part of the crystallization of the Li-F granite, whereas effects of postmagmatic alteration are limited to element redistribution and secondary enrichment in the endocontact.

The Orlovka deposit has Ta_2O_5 and Li_2O reserves estimated at 3,990 t and 760,102 t respectively, with 0.014 % Ta_2O_5 and 0.269 % Li_2O.[25] The ores also contain Rb_2O, Cs_2O and Nb_2O_5 with grades of economic interest. The average concentrations of accompanying components within the boundaries of the economic ore bodies are (in g/t): Rb_2O – 1200 (up to 2000), Cs_2O – 30 (up to 50), Nb_2O_5 – 220 (up to 800), F – 1500 (up to 35000), Be – 40 (up to 35000), U – 13 (up to 150), Th – 22 (up to 350), Pb – 50, MnO – 200 (up to 2800), Zn – 70 (up to 130), W – 50 (up to 300), Sn – 120 (up to 500).[4] The primary ores contain more than 70 minerals of which albite, microcline-amazonite, Li micas, quartz, topaz, microlite, tantalite-columbite group minerals and pyrochlore are predominant. Among common accessories are beryl, bertrandite, fluorite, cassiterite, scheelite, monazite, apatite and sulphides such as galena, pyrite, sphalerite, molybdenite, bismuthinite, arsenopyrite, chalcopyrite and tetrahedrite.

The **Spokoinoe tungsten deposit** characterized by tungsten (tin-beryl) vein quartz-greisens is situated 8 km from Orlovka. It is composed of albite-muscovite granites similar to the Khangilay massif, but predominantly alaskitic leucogranites. In the upper parts of the cupola the granites are albitized and greisenized with tungsten mineralization.[4] Wolframite, russellite, cassiterite, and beryl prevail. However, Spokoinoe is not the focus of this study.

4.3. SAMPLING AND ANALYTICAL TECHNIQUES

Representative whole-rock samples were collected in the field and from quarries representing the three granite massifs and host rocks with a special emphasis on the Orlovka deposit. In total 50 powdered rock samples were analyzed.

Major and minor element analyses were determined by wavelength-dispersive X-ray fluorescence spectrometry (XRF) and emission spectrophotometry (ES) at the laboratories of the All-Russia Geological Research Institute (VSEGEI) in St. Petersburg, Russia.

Fluorine was separated by pyrohydrolysis. 0.2g of rock powder was mixed with about 0.3g of vanadium pentaoxide flux and transferred the mixture to a ceramic boat. The boat was placed in the center of the combustion tube. The working temperature was about 900°C and nebulization time – 10 minutes. Samples were pyrohydrolised into plastic tubes containing H_2O_2 and $NaHCO_3$, were made up to 25 ml to achieve the concentration of eluent calibration solutions and then analyzed for fluorine by Dionex DX-300 ion chromatograph.

Trace elements Rb, Sr, Ba, Zr, Hf, Nb, Ta, Cs, Pb, U, Th, Y and REE were determined by inductively coupled plasma mass spectrometry (ICP-MS) at GFZ Potsdam. The analytical procedure is described in detail elsewhere.[6] Briefly, about 0.1 g of sample powder was dissolved using mixed acid digestion ($HF/HClO_4$) under pressure and finally filled up to 50 ml volume with 0.5 mol/l HCl (dilution factor 500). Prior to analysis, Ru, Re and Bi were added to aliquots of the solutions as internal standards for drift correction, and the mixtures were further diluted by a factor of ten. Solutions prepared following this procedure show a dilution factor of 5000 and are about 0.5 mol l^{-1} in HCl.

ICP-MS measurements have been performed using an ELAN 5000A quadrupole ICP mass spectrometer (Perkin-Elmer/SCIEX, Canada). Samples were measured in batches of five. Each batch was preceded by a 10 ng ml^{-1} calibration solution, two acid blanks and a procedure blank. Quantitative determination of element concentrations was performed applying external calibration using two calibration solutions, which bracketed each batch of samples.

To minimize the influence of drift effects on analytical precision relatively small batches of samples were analysed within one analytical run. Ru, Re and Bi were used as internal standards. Interference corrections are routinely applied to correct analyte

isotopes for molecular and isobaric interferences.[5] Analyses of most trace elements by different methods allowed the checking of dissolution procedures and inter-technique calibration for given elements within specified concentration ranges. Used methods yield accurate, high-precision element concentration values whose uncertainties (mainly below 5-10%) are significantly lower than uncertainties from other sources such as sampling.

32 geologic samples of the same sample suite have been analyzed for Pb isotopes by thermal ionization-mass spectrometer (TIMS, University of Heidelberg) and multi-collector ICP-MS (Imperial College, Natural History Museum London). Pb isotope analyses were carried out on whole rock samples. Lead was purified through an ion chromatography Sr resin in a hydrochloric acid medium. Raw TIMS data were normalized to NBS 981 Pb international standard with reference values of Galer and Abouchami[7] (reproducibility on the 95% confidence level: 0,03% for ratios normalized to ^{204}Pb). Raw MC-ICP-MS data were corrected for isobaric interferences on ^{204}Pb using ^{200}Hg. Mass discrimination correction was made using NBS 997 Tl as an internal standard. The Pb/Tl ratio was kept to 2:1 during the measurements. The $^{205}Tl/^{203}Tl$ ratio was optimized based on repeated measurements of a spiked NBS 981 Pb international standard. Long-term reproducibility of MC-ICP-MS for all ratios over five-month period was below 350 ppm. The error of the internal isotope measurements for all pairs of Pb isotopes was on average below 200 ppm. The reproducibility during the measurements ($\pm 2\sigma$) was 0.035% for $^{206}Pb/^{204}Pb$, 0.034% for $^{207}Pb/^{204}Pb$ and 0.05% for $^{208}Pb/^{204}Pb$.[33]

Samples measured with TIMS and MC-ICP-MS showed excellent correlation ($r=0.988$ for $^{206}Pb/^{204}Pb$ ratios, slope=0.947, n=13) (Weiss et al., 2004).

4.4. RESULTS

4.4.1. Whole rock geochemistry

The geochemical evolution trends of the Orlovka tantalum deposit were studied in order to achieve a better understanding of the relationships between different intrusive phases. Based on structural-textural characteristics of the deposit and according to the existing geological, petrological, and geochemical data of the district, the following rock groups were distinguished:[39] 1) barren biotite and biotite-muscovite granite - Khangilay pluton; 2) highly-evolved muscovite-albite and

amazonite granites - Orlovka stock; 3) ore-bearing amazonite granites represented by layered pegmatite-aplites, locally developed as line rocks, within the apical parts of the Orlovka stock. In addition, a gabbro-diorite presumably of Triassic age and belonging as subalkaline precursor intrusion to the Khangilay pluton has been included.

To assess possible magma – host-rock interactions of the Khangilay-Orlovka intrusions with the regional geochemical framework, greisenized granites from Spokoinoe and a representative suite of intruded host rocks (volcanics, hornfelses, metasediments, gabbro-diorite) were included in the study.

4.4.2. Major elements

Table 4.1 summarizes major, minor and trace element data for the Khangilay, Orlovka and Spokoinoe granites and their host rocks. The granite suites are characterized by high silica (70-87 wt. %), alumina (15-20 wt.%) and alkali contents (6-12 wt. % of Na_2O+K_2O) and low MgO, Fe_2O_3, CaO, and MnO contents. The Orlovka mineralized topaz-amazonite-albite granites exhibit high fluorine concentrations (up to 6 wt. %) whereas Khangilay and Spokoinoe granites have only 0.1-0.8 wt. % of this element.

4.4.3. Trace elements

The spidergrams (**Figures 4a-h**) compare primitive and evolved granites and their host rocks normalized to Continental Crust (CC). The element sequence has been organized according to decreasing concentrations in Khangilay biotite granite samples (average, n=3, thick black line on the graphs) to contrast relative element enrichment or, respectively, element depletion in other granites and host rocks. Remarkable for both Orlovka and Spokoinoe is the fractionation of Zr and Hf and enrichment of Sn and W (in mineralized granites). Orlovka granites show Ta and Zn enrichment; in contrast to Spokoinoe granites with low Ta concentrations but high W content. Both granites are enriched in Cs and Rb and depleted in Th, Ba, Eu, Sr, Cr and Nd. Spokoinoe granites also show strong depletion in La, Ce, Pr and Ga.

Table 4.1. Major and trace element concentrations and some indicative ratios for representative samples of Li-F granites and heir host rocks. Full data set and detection limits available from the corresponding author. Note: unless specified all concentrations are given in parts per million (ppm).

Sample type	Gabbro-diorite	Felsic volcanics	Metasediments	Hornfels	Amazonite granites	Biotite-muscovite granites	Hornfels	Greisenized granites	Shales
Location	Far from Khangilay pluton	Khila Formation	Onon Group	Orlovka open pit	Orlovka stock	Orlovka stock and Khangilay pluton	Spokoinoe open pit	Spokoinoe open pit	Orlovka stock
n	1	6	5	7	10	8	6	4	2
SiO_2, wt. %	60.8	47.2-77.5	63.5-72.2	58.9-74.2	64.8-73.8	71.6-87.2	46.5-72.1	75.3-96	N/A*
Al_2O_3, wt. %	14.8	12-16	14-15.7	13.3-16.5	14.9-20	7.5-16.6	9.6-18.8	1.9-15	N/A
Fe_2O_3, wt. %	7.6	0.5-9.5	0.9-6.7	2.4-12	0.1-4.3	0.3-1.7	3.4-17.9	0.1-1.1	N/A
MnO, wt. %	0.1	0.01-0.2	0.02-0.1	0.1-0.2	0.1-0.5	0.01-0.1	0.04-0.3	0.1-0.2	N/A
MgO, wt. %	3.9	0.4-8.1	1-2.2	0.7-3.9	< 0.1	0.2-0.6	1.6-4.7	<0.1	N/A
CaO, wt. %	1.9	<0.05-10.9	0.5-1.3	1.5-8	< 0.1-0.3	0.1-0.8	0.4-6.6	0.1-0.9	N/A
Na_2O, wt. %	4.2	0.7-5.7	2.1-5.6	1.6-5.6	2.3-6.8	0.5-4.1	0.1-6.7	<0.1-2.6	N/A
K_2O, wt. %	1.01	0.3-7.4	1.5-4.2	0.9-3.1	1.8-9.4	2.7-4.7	0.1-5.9	0.4-4.2	N/A
P_2O_5, wt. %	0.6	<0.1-0.2	0.1-0.14	<0.05-0.7	<0.05	<0.05-0.1	0.12-0.6	<0.05-0.7	N/A
LOI, wt. %	3.7	1.02-4.1	1.1-2.6	1.5-2.7	0.3-2.1	0.8-1.5	0.5-5.1	0.2-1.4	N/A
Ag	0.02	<0.02-0.05	<0.02-0.1	0.02-0.5	<0.02-0.04	<0.02-0.5	0.02-0.04	0.6-8	N/A
B	10	15-30	25-80	10-1000	10.0-50	20-50	10-1000	10-200	N/A
Ba	1827	147-688	326-833	44-436	1.8-9.5	70-294	29-870	4.8-35.8	68.8
Be	<1	<1-100	<1	<1-1000	1.5-30	<1 -10	<1-2	3-300	N/A
Bi	<1	<1-1	<1	<1-1000	1.2-400	1.5-3	<1.0-8.0	15-400	N/A
Ce	184	17-106	50-87	17-97	5.1-72	6.9-109	27-93	5.1-13	12.2
Co	25	<4-30	5.0-15	4-30	<4	<4-4	12.0-50	<4	N/A
Cr	300	3-80	30	1.5-100	2-5	3-12	60-150	2.5-3	N/A
Cs	2	0.13-25	0.52-4.4	14-142	22-108	11-65	5-457	5.4-58	43.5
Cu	30	25-50	25-60	20-30	12-30	20-40	25-40	15-30	N/A
Dy	5	2.6-9.6	2.5-4.7	3.6-12	2-12	2.7-11	3.5-8.6	1.1-7.2	1.8
Er	2	1.3-8.2	1.3-2.7	1.8-6.9	0.91-5.3	1.6-5	2-5.3	0.35-1.8	0.7
Eu	3.7	0.4-1.4	0.8-1.7	0.4-3.3	<0.02-0.04	0.1-0.5	0.96-2.1	0.06-0.67	0.2
F, wt. %	0.24	0.05-0.18	0.06-0.11	0.3-9.3	0.6-6.6	0.01-0.8	0.18-1.64	0.09-0.63	0.1
Ga	12	8-40	12-15	10-40	40-300	10-100	10-15	3-20	N/A
Gd	10	3.4-9.9	3.1-5.3	2.5-12	1.2-8.5	1.9-9.6	4.0-7.8	1.5-6.1	1.7
Ge	1	<1-1.2	<1-1.5	1.2-30	4.0-15	1-1.5	1.2-2	<1-1.5	N/A
Hf	9.4	2.6-9.2	4.2-6.3	2.4-12	1.5-21	2.7-7	3.9-6.4	0.3-2.2	2
Ho	0.82	0.45-2.7	0.4-0.9	0.6-2.4	0.3-1.9	0.5-1.8	0.7-1.8	0.15-0.9	0.3
La	86	7.2-49	20-44	5.5-46	4.8-21	3.1-55	16-46	1.8-4.1	5.5
Li	50	15-800	10-40	80-1000	500->3000	40-1000	20-800	<10-30	N/A
Lu	0.22	0.18-1.1	0.18-0.4	0.27-0.92	0.13-0.66	0.25-0.66	0.29-0.69	0.05-0.17	0.1

Sample type	Gabbro-diorite	Felsic volcanics	Metasediments	Hornfels	Amazonite granites	Biotite-muscovite granites	Hornfels	Greisenized granites	Shales
Location	Far from Khangilay pluton	Khila Formation	Onon Group	Orlovka open pit	Orlovka stock	Orlovka stock and Khangilay pluton	Spokoinoe open pit	Spokoinoe open pit	Orlovka stock
Mo	2	1.5-4	1-1.5	2-2.5	2-3	1.5-3	2-2.5	1-2.5	N/A
Nb	12	2.7-24	8.5-15	17-118	19-219	25-46	8-46	10-115	51.2
Nd	90	11-49	18-35	7.3-51	2.3-22	4.4-34	22-39	2.5-8.6	5.4
Ni	150	2-60	10-25	2-20	1-2	2-4	25-100	3-10	N/A
Pb	38	6.3-44	5.6-25	6.7-27	19-184	26-136	11-155	32-282	31.3
Pr	23	2.4-13	5.6-9.5	2.2-12	0.65-8.3	1.1-9.5	4.7-11	0.6-1.9	1.4
Rb	34	11-334	44-114	71-1272	1268-3239	235-1113	7.5-640	57-550	449
S, wt. %	<0.02	<0.02-0.13	<0.02-0.02	<0.02-0.79	<0.02-0.06	<0.02-0.021	<0.02-0.36	0.02-0.04	N/A
Sc	6	6-8	<6-6	6-8	6-8	<6-6	<6-10	6-8	N/A
Sm	16	3.2-10	4-6.1	2.9-12	1.2-8.6	1.8-7.3	4.5-7.1	1.3-4.6	1.66
Sn	2.5	1.2-100	1.5-5	6-100	8-300	3-150	2.5-30	5-250	N/A
Sr	425	15-112	146-226	28-122	1-7.6	42-141	73-502	14-69	49.9
Ta	0.7	0.3-1.9	0.54-2.8	1.1-114.9	20.5-429.8	4.06-22.6	0.6-3.4	0.5-39.5	24.2
Tb	1.1	0.5-1.9	0.44-0.8	0.58-2	0.3-0.75	0.4-1.8	0.6-1.3	0.3-1.4	0.3
Th	22	1-18	7.3-14	4.4-18	2-15	6.8-47	0.88-12	1.2-7.8	6.13
Tm	0.3	0.17-1.2	0.2-0.4	0.3-0.95	0.14-0.81	0.25-0.75	0.3-0.71	0.05-0.2	0.1
U	4.7	0.3-4.2	1.6-2.3	2.1-7.6	0.9-9.2	6.2-33	0.51-3.6	3.5-17	9.12
V	80	6-100	40-120	5-100	2-3	2-12	80-120	2-4	N/A
W	<3	<3-15	<3	<3-60	30->1000	<3-10	<3-10	200->1000	N/A
Y	22	8.8-76	12-25	14-63	5.3-44	15-50	19-52	4.9-27	8.79
Yb	1.5	1.3-7.5	1.2-2.7	2.2-6.2	1.1-5.3	1.8-5	1.9-4.7	0.36-1.2	0.64
Zn	60	15-100	40-120	60-120	60-800	60-150	60-150	30	N/A
Zr	400	106-336	167-245	64-578	6.9-45	41-214	151-240	5.4-17	28.3
Zr/Hf	42.5	24.4-36.6	37.5-40	6-46.3	2.34-5.97	14.86-32.9	37.2-39.6	9.2-23.6	13.9
Y/Ho	26.5	19.6-29.4	27.1-29.4	23.3-26.6	12.8-23	28.1-31.8	27-28.9	29.6-35.9	34.4
Rb/Sr	0.1	0.1-10.5	0.2-0.5	0.6-31.3	263-3218	2.1-15.9	0.01-8.7	2-17.7	9
Nb/U	2.6	2-8.8	5.3-7.7	6.2-15.6	6.1-27.2	1.2-7.5	3.3-54.6	0.8-21	5.6
Ce/Pb	4.8	1.5-11.3	2.3-15.2	2.5-5.4	0.1-1.5	0.3-2.5	0.6-7.2	0.04-0.2	0.4
(Ta+Nb)	12.9	3-26.2	9-15.6	17.7-174.1	34.7-648.8	29.6-65.5	8.6-49.9	13.4-153.7	75.4

*N/A – not analysed

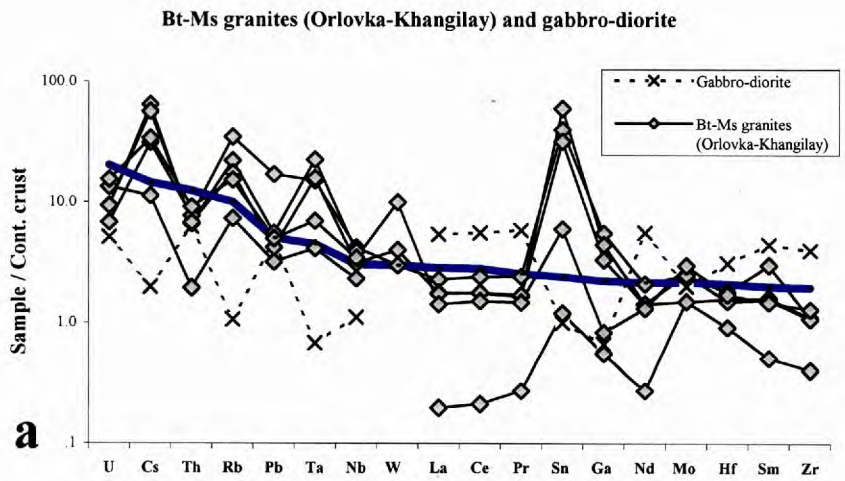
Bt-Ms granites (Orlovka-Khangilay) and gabbro-diorite
Gabbro-diorite
Bt-Ms granites (Orlovka-Khangilay)
Sample / Cont. crust
100.0
10.0
1.0
.1
a
U Cs Th Rb Pb Ta Nb W La Ce Pr Sn Ga Nd Mo Hf Sm Zr

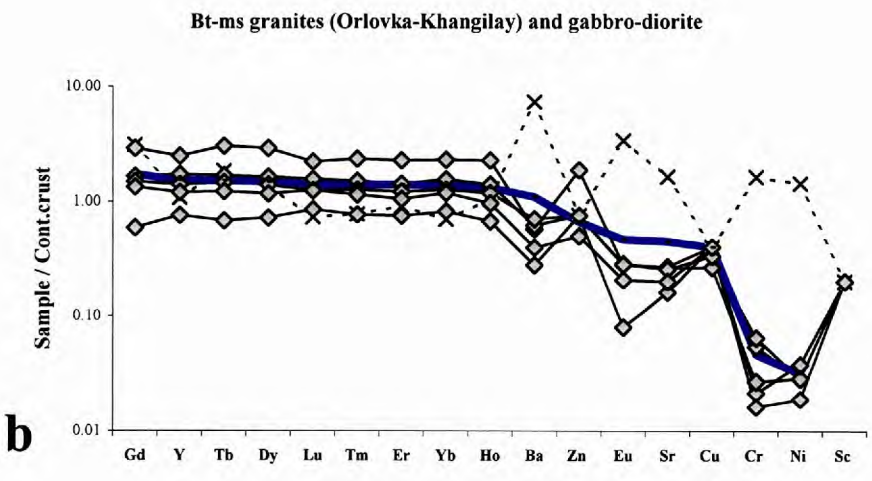
Bt-ms granites (Orlovka-Khangilay) and gabbro-diorite
Sample / Cont.crust
10.00
1.00
0.10
0.01
b
Gd Y Tb Dy Lu Tm Er Yb Ho Ba Zn Eu Sr Cu Cr Ni Sc

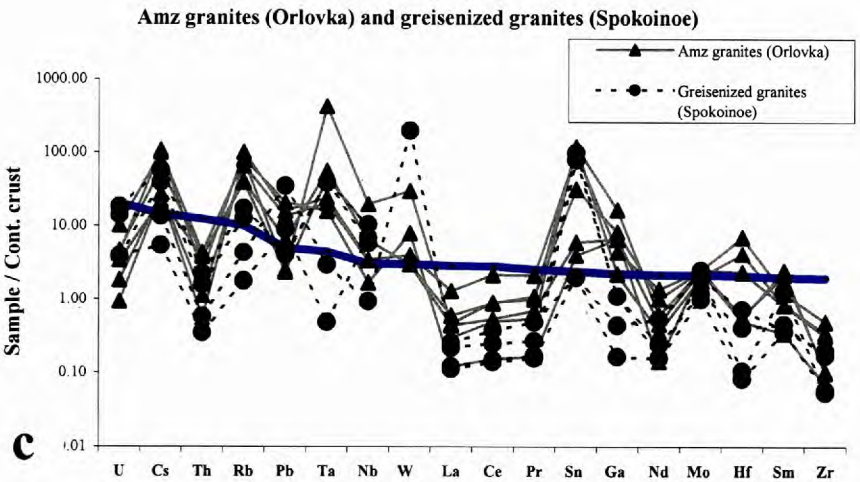
Amz granites (Orlovka) and greisenized granites (Spokoinoe)
Amz granites (Orlovka)
Greisenized granites (Spokoinoe)
Sample / Cont. crust
1000.00
100.00
10.00
1.00
0.10
.01
c
U Cs Th Rb Pb Ta Nb W La Ce Pr Sn Ga Nd Mo Hf Sm Zr

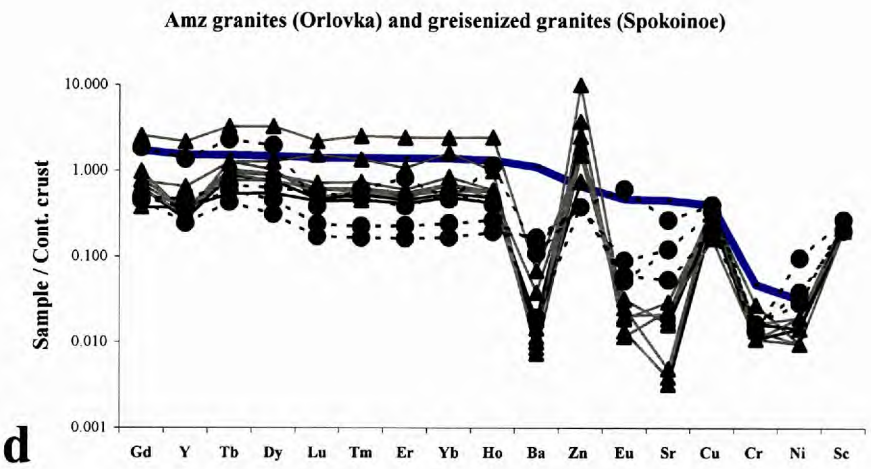
Amz granites (Orlovka) and greisenized granites (Spokoinoe)
Sample / Cont. crust
10.000
1.000
0.100
0.010
0.001
d
Gd Y Tb Dy Lu Tm Er Yb Ho Ba Zn Eu Sr Cu Cr Ni Sc

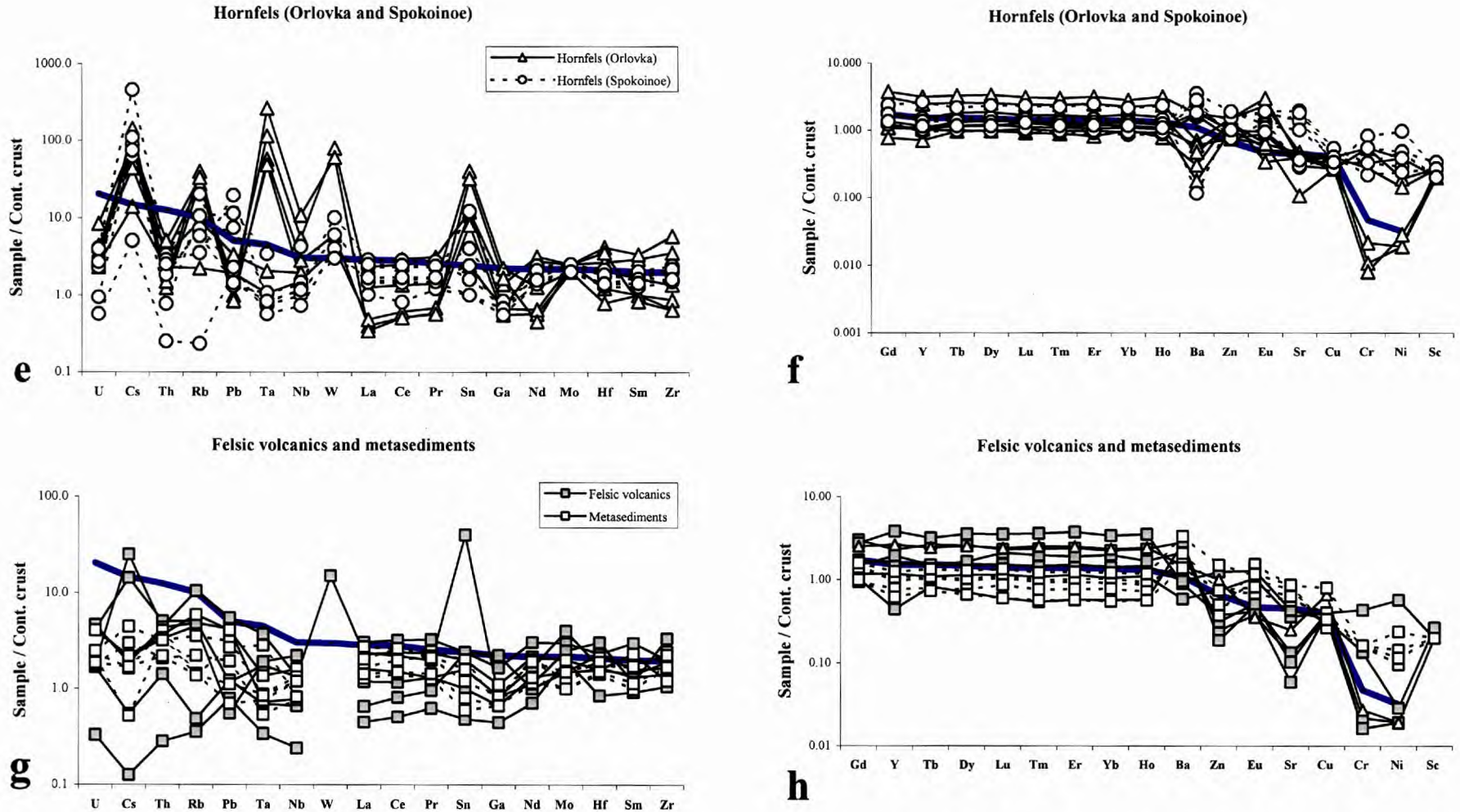

Figure 4.4. Spidergrams of primitive and evolved granites and host rocks normalized to Continental Crust. Element sequence is organized according to decreasing concentrations in Khangilay biotite granite samples (blue line, average, n=3) to contrast element enrichment/depletion in other granites and host rocks.

4.4.4. Use of Zr/Hf, Y/Ho, Rb/Sr, and Nb/U ratios as indicators of granite fractionation

Chemistry and modal composition, also intrusive contacts and spatial-temporal relationships between different granite groups within the Orlovka deposit allow distinction between groups according to their fractionation patterns. Petrogenetically indicative plots for the Orlovka-Spokoinoe mining district retrieved from the database show the characteristics of the most typical granite groups of the Orlovka and Spokoinoe stocks, the barren granites of the Khangilay pluton and their host rocks (**Figures 4.5-4.10**). Fractionation begins with biotite-muscovite and subsequent biotite granites of the Khangilay massif. More fractionated biotite-muscovite-lithionite granites develop into muscovite-albite high Li-F granites.

Zr/Hf is a good indicator of crystallization differentiation in magmatic rocks.[23,40,41] Zr/Hf regularly decreases in magmatic series in the process of magmatic evolution from basic (80) to alkaline (60) and acidic (40-30) rocks with the mean value for the continental crust of about 50.[39] For rare-metal granites with W-Mo and Sn-W mineralization types the differentiation up to leucogranite level (Zr/Hf = 20-25) is mostly favorable.[41] Zr/Hf together with Y/Ho, Nb/U, Ce/Pb, and Rb/Sr were used to geochemically characterize the most typical granites of the Orlovka-Spokoinoe mining district.

The less evolved barren Khangilay granites and the moderately evolved ore-bearing Spokoinoe granites are characterized by values of Y/Ho of 30-36. This is slightly higher than for the Continental Crust (CC) and Primitive Mantle (PM) values (26 and 28, respectively). Values for CC are calculated from Taylor and McLennan,[31] values for PM – from Hofmann et al.[11] Zr/Hf of the Khangilay parental granites are in the range of 25-33, that is comparable with continental crust and primitive mantle values (33 and 36 respectively) whereas Spokoinoe granites show depleted Zr/Hf (14-24) (**Figures 4.5, 4.6, 4.7**). The highly evolved amazonite granites and line rocks of the Orlovka deposit show strongly depleted ratios (Y/Ho 14-18 and Zr/Hf 2-6) compared to average crust and primitive mantle values. Less-evolved granites of the Orlovka stock show intermediate ratios for these element pairs. It should be noted that Zr/Hf and Y/Ho values are similar for continental crust and primitive mantle suggesting similar behavior of these element pairs during all the processes affecting the concentrations so that their ratios retained their original, primitive values.[10,12]

Nb/U shows an increase during granite fractionation coupled with metasomatic processes in the Orlovka cupola, the ratio varies from 1-7 for barren bt-ms granites of Khangilay reaching up to 27 for the highly evolved amazonite granites of Orlovka and greisenized granites of the Spokoinoe massif. An increase in Nb concentrations from 25 ppm in the bt-ms granites of Orlovka and Khangilay and up to >100 ppm in the amazonite granites of Orlovka was observed. The majority of ore-bearing amazonite granites of Orlovka and greisenized granites of Spokoinoe plot between continental crust and primitive mantle values.

The plot Rb/Sr vs. (Ta+Nb) (**Figure 4.8**) shows an increase in both Rb/Sr and (Ta+Nb) concentrations during granite evolution. Large change in Rb/Sr is mostly due to the sharply depleted Sr concentrations and high enrichment in Rb during the evolution of

granites. Rb/Sr and (Ta+Nb) concentrations are much higher than respective values of primitive mantle and are more comparable to continental crust values.

4.4.5. REE patterns

Rare earth elements (REE) were studied as a petrogenetically indicative tool to assess the evolution process of the most typical rock groups classified using their mineralogical characteristics. Analysis of the REE distribution within the mining area shows similar patterns for Khangilay granites and the bt-ms granites at the base of the Orlovka cupola. Therefore, they have been combined in one group (**Figure 4.10a**). Light REE (LREE) are more abundant than heavy REE (HREE), which forms a monazite-type pattern. The highly evolved amazonite granites of the Orlovka deposit show a stronger Eu anomaly and REE tetrad effects here become more apparent (**Figures 4.9a, b**). This is in agreement with the previous research on REE patterns that showed that a tetrad effect develops parallel to granite evolution, and significant tetrad effects are strictly confined to highly differentiated samples.[14] REE patterns of hornfelses, felsic volcanics and metasediments show flat patterns apart from a few samples of hornfelses from the Orlovka deposit and the felsic volcanics that developed a positive Eu anomaly (**Figures 4.9c, d**). Spokoinoe is characterized by relatively high Y contents and thus shows more flat REE patterns in contrast to REE patterns as typical of Khangilay and Orlovka that exhibit heavy REE (HREE) > light REE (LREE).

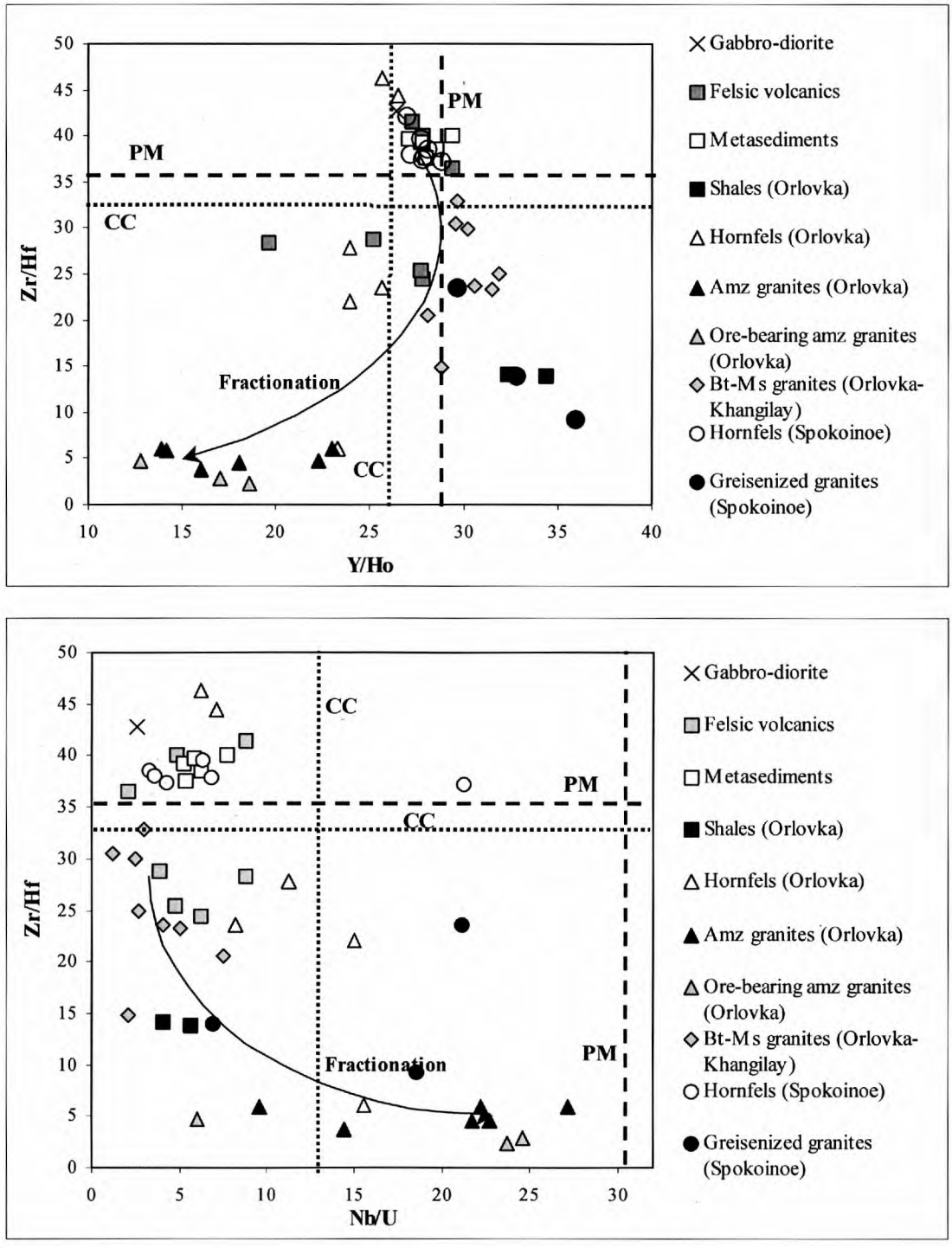

Figures 4.5 and 4.6. Zr/Hf vs. Y/Ho and Zr/Hf vs. Nb/U plots. Ore-bearing amazonite granites are defined here by (Ta+Nb) >100 ppm. **CC** corresponds to the bulk Continental Crust and **PM** – to the Primitive Mantle composition (from Taylor & McLennan, 1995). Fractionation trend is projected for Khangilay-Orlovka granites.

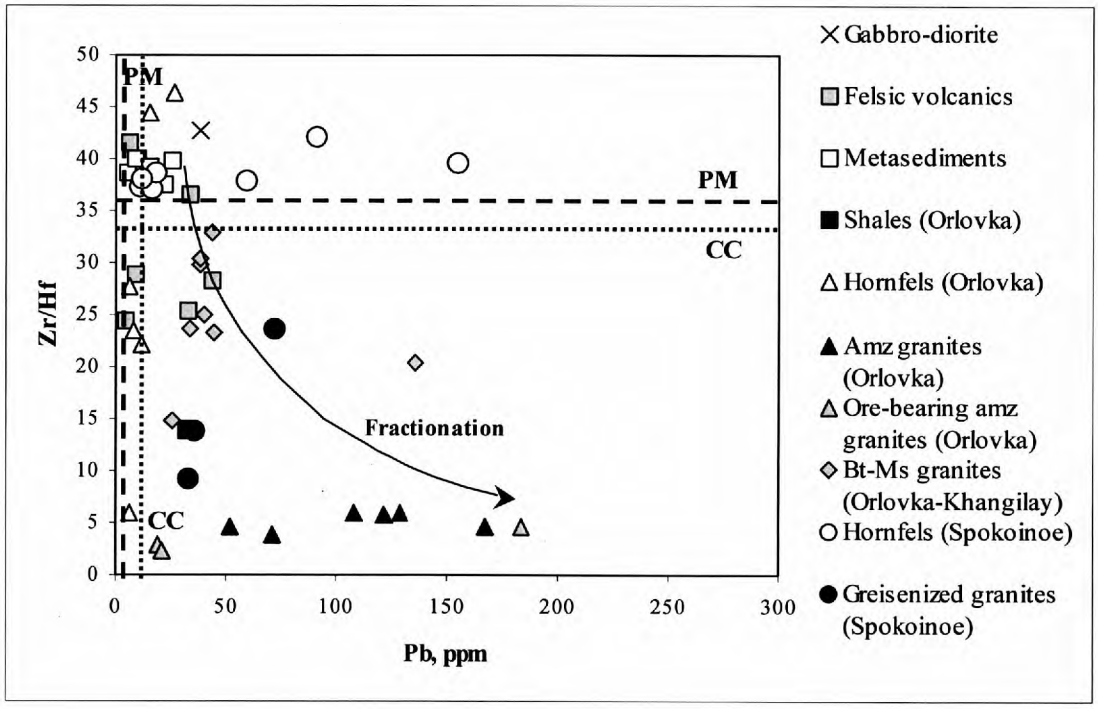

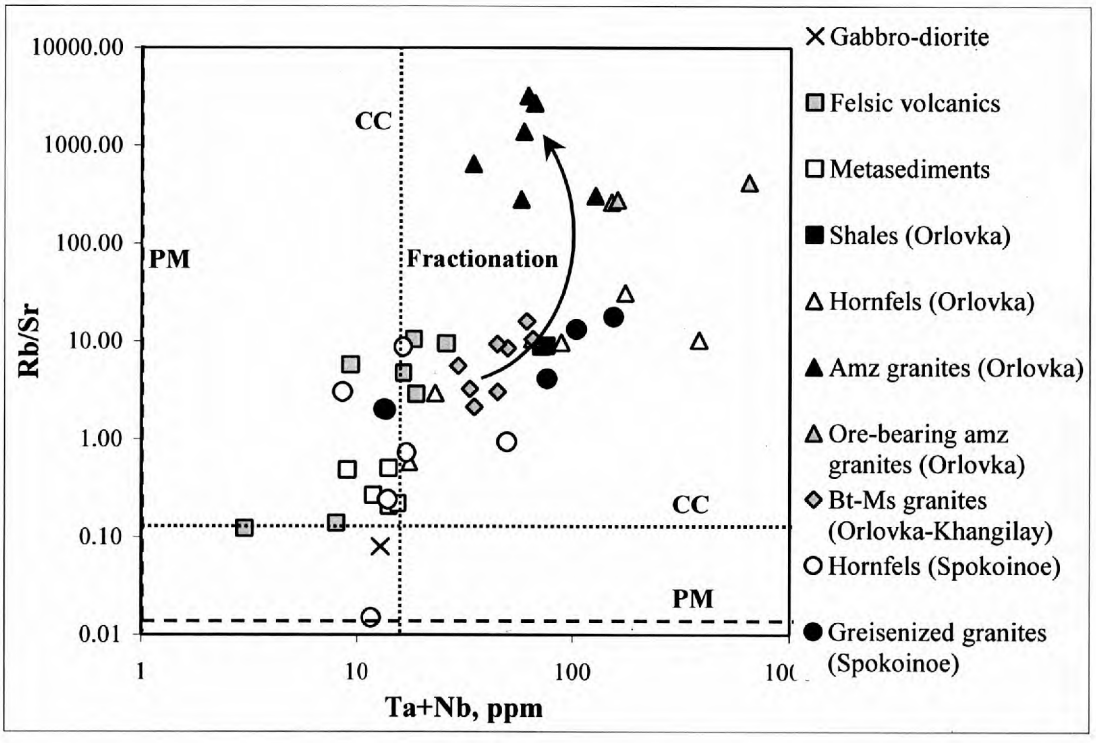

Figures 4.7 and 4.8. Zr/Hf vs. Pb and Rb/Sr vs. (Ta+Nb) plots. Ore-bearing amazonite granites are here defined by (Ta+Nb) >100 ppm. **CC** corresponds to the bulk Continental Crust and **PM** – to the Primitive Mantle composition (from Taylor and McLennan, 1995).

4.4.6. Pb isotope geochemistry

The mixing diagram (**Figure 4.10**) shows strong relationship between the barren parental granites of the Khangilay pluton and the ore-bearing granites of the Orlovka and Spokoinoe massifs. They all plot within a single line trend. Despite a wide range of Pb isotope compositions within each granite body, they do not differ significantly among all three granite massifs (**Table 4.2**). The following range of Pb isotopes characterizes the individual granite massifs: $^{206}Pb/^{204}Pb$ from 18.62 to 19.89; $^{207}Pb/^{204}Pb$ from 15.56 to 15.63 and $^{208}Pb/^{204}Pb$ from 38.35 to 38.79 for **Khangilay**; $^{206}Pb/^{204}Pb$ from 18.41 to 19.59; $^{207}Pb/^{204}Pb$ from 15.56 to 15.63 and $^{208}Pb/^{204}Pb$ from 38.29 to 38.82 for **Orlovka;** and $^{206}Pb/^{204}Pb$ from 18.50 to 19.20; $^{207}Pb/^{204}Pb$ from 15.57 to 15.61 and $^{208}Pb/^{204}Pb$ from 38.33 to 38.45 for **Spokoinoe (Figures 4.11a, b)**. Lead isotope signatures of the host rocks are more scattered than those of the granite rocks and are off the granites mixing line.

Pb isotopes for the three granite massifs spread near orogenic (OR) and upper crust (UC) curves.[42] At the same time Pb isotope data plot in the range between mid-ocean ridge basalts (MORB) and type II enriched mantle source (EM II)[43] (**Figure 4.12**) and will be discussed further below.

In order to assess sources of the granitic magmas, the initial Pb isotopic composition of the granite massifs was obtained by assuming a closed system whole rock Pb evolution, and by calculating the $\mu = {}^{238}U/^{204}Pb$ and $k = {}^{232}Th/^{204}Pb$ ratios from the measured U, Th and Pb concentrations for correction of the present Pb isotope ratios for radiogenic Pb, accumulated *in-situ* in the studied rocks since Jurassic times. The calculation of initial Pb ratios is complicated by the universally encountered mobility of U during surface weathering.[9] Therefore, granite data (Table 4.2) were only accepted for calculation of initial Pb compositions in case of compatibility with Jurassic reference isochrons in a $^{206}Pb/^{204}Pb$ versus μ diagram.

The initial Pb isotopic compositions calculated for the barren bt-ms granites of the Khangilay massif are very similar. The average values of $^{206}Pb/^{204}Pb = 18.49 \pm 0.05$; $^{207}Pb/^{204}Pb = 15.57 \pm 0.01$ and $^{208}Pb/^{204}Pb = 38.23 \pm 0.06$ represent a rather uniform Pb isotope composition of the parental granites.

The Orlovka ore-bearing amazonite granites with the highest Pb concentration have been used to identify the isotopic composition of the initial Pb component that was transferred to the ore-bearing rocks. Although Pb isotopes of a magma or

hydrothermal fluid can be changed due to interaction with country rocks,[32] ore-bearing amazonite granites in our case are well protected against such changes due to high Pb concentrations in these rocks (up to 190 ppm). They are characterized by the lowest rate of radiogenic Pb accumulation because of their very low $^{238}U/^{204}Pb$ ($\mu_{average}$ = 1.3). The calculated initial values for these "least sensitive" ore-bearing granites are very similar and their averages are: $^{206}Pb/^{204}Pb$ = 18.41 ± 0.02; $^{207}Pb/^{204}Pb$ = 15.562 ± 0.006 and $^{208}Pb/^{204}Pb$ = 38.30 ± 0.03. This is within the error limits identical to the average for initial Pb in the bt-ms granites of Khangilay. The Spokoinoe ore-bearing greisenized granites fit to the same trend as the Khangilay and Orlovka granites with the following initial Pb isotope composition: $^{206}Pb/^{204}Pb$ = 18.44 ± 0.01; $^{207}Pb/^{204}Pb$ = 15.56 ± 0.01 and $^{208}Pb/^{204}Pb$ = 38.33 ± 0.02.

4.5. DISCUSSION

4.5.1. The Khangilay – Spokoinoe – Orlovka sequence

Overall, for most of the geochemical characteristics, the geochemical trends are directed from Khangilay to Orlovka, with Spokoinoe in between. Some exceptional patterns for Spokoinoe hint to an autonomous evolution that may have different reasons such as magma-fluid interaction, magma – wall-rock interaction, and contrasting fractionation paths.

The Pb isotope data indicate a common source for the three massifs, Khangilay, Spokoinoe and Orlovka, and prove along with geological relationships and geochemical patterns that the Khangilay pluton can be considered as a barren parental intrusion for its hosted ore-bearing apical intrusions.

Zr/Hf shows a continuous fractionation history from the parental to the evolved granites, where Khangilay (Zr/Hf –25-33) and its derivates Spokoinoe (14-24) and Orlovka (2-6) represent different evolution stages. The mineralized Spokoinoe (W-Sn-Be) and Orlovka (Ta-Nb-Sn) cupolas exhibit different mineralization styles, which can be linked to the fractionation degree as expressed by the corresponding Zr/Hf values.

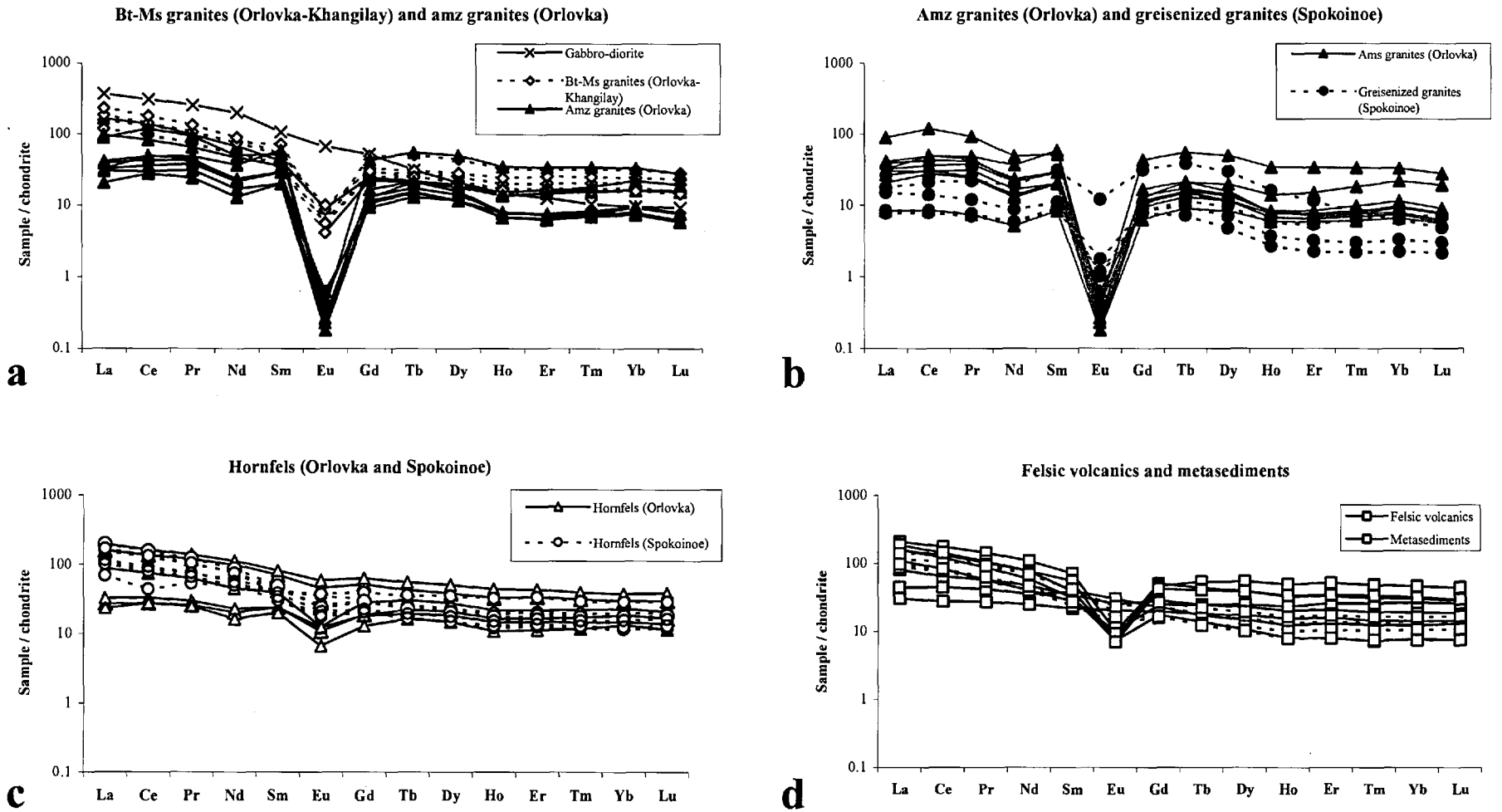

Figures 4.9a-d. REE patterns of less evolved bt-ms granites of Khangilay, Spokoinoe and Orlovka and highly evolved amz granites of Orlovka and their host rocks normalized to chondrite (Anders and Grevesse, 1989).

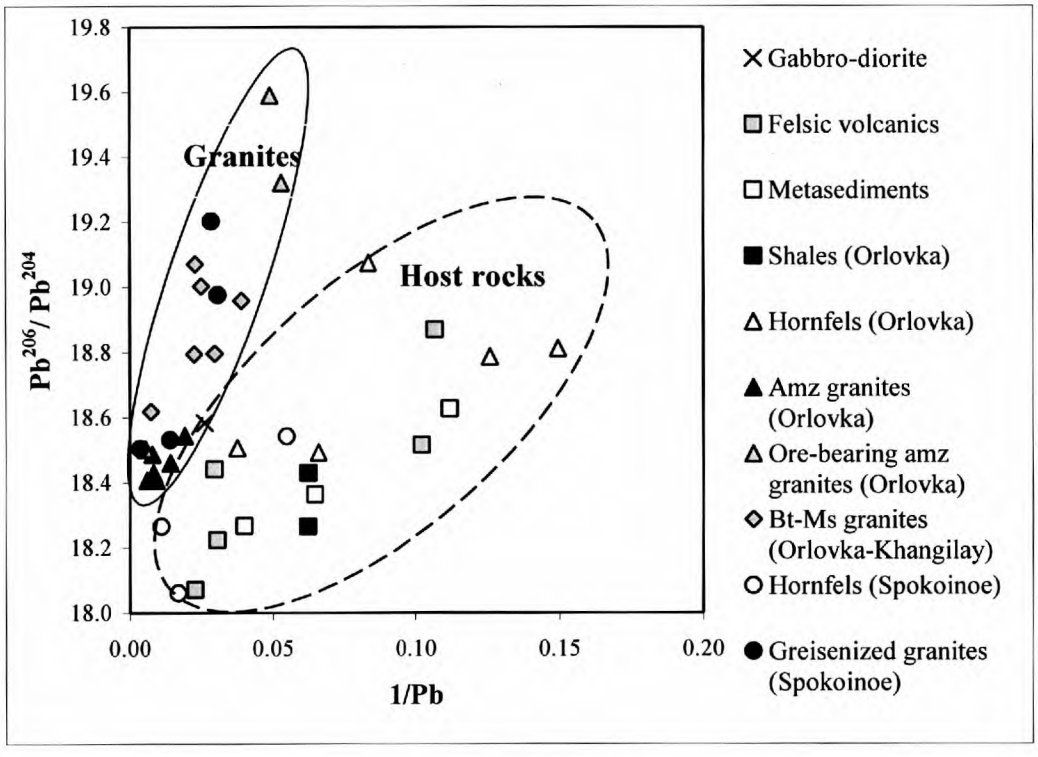

Figure 4.10. Pb^{206}/ Pb^{204} vs. 1/Pb mixing plot for Khangilay-Spokoinoe-Orlovka granites and their host rocks.

Table 4.2. Pb isotope data of Li-F granites and their host rocks from the Orlovka-Spokoinoe mining district.

Sample description	Location	Pb, ppm	Pb^{206}/Pb^{204}	±2σ	Pb^{207}/Pb^{204}	±2σ	Pb^{208}/Pb^{204}	±2σ
Gabbro-diorite	Far from Khangilay	38.2	18.583	0.004	15.652	0.007	38.689	0.008
Biotite / muscovite granite	Khangilay	25.7	18.958	0.003	15.598	0.002	38.360	0.009
Biotite granite	Khangilay	38.3	18.896	0.004	15.445	0.005	38.209	0.007
Biotite granite	Khangilay	38.4	19.893	0.001	15.633	0.001	38.691	0.001
Biotite / muscovite granite	Khangilay	40.1	19.003	0.001	15.597	0.001	38.604	0.001
Biotite granite	Khangilay	43.6	19.070	0.004	15.599	0.003	38.789	0.007
Biotite / muscovite granite	Orlovka	136.3	18.617	0.001	15.556	0.001	38.351	0.004
Biotite granite	Orlovka	44.3	18.794	0.002	15.596	0.002	38.558	0.006
Biotite / muscovite granite	Orlovka	33.7	18.796	0.001	15.581	0.001	38.481	0.001
Amazonite/muscovite granite	Orlovka	121.7	18.428	0.003	15.556	0.003	38.286	0.006
Amazonite pegmatite	Orlovka	128.6	18.486	0.001	15.572	0.001	38.359	0.004
Amazonite granite	Orlovka	70.8	18.460	0.002	15.559	0.001	38.326	0.005
Amazonite granite	Orlovka	52.1	18.544	0.006	15.610	0.008	38.503	0.010
Mineralized toz/amz/ab granite	Orlovka	167.3	18.407	0.001	15.565	0.001	38.332	0.002
Mineralized toz/amz/ab granite	Orlovka	18.9	19.320	0.004	15.596	0.003	38.599	0.009
Mineralized toz/amz/ab granite	Orlovka	20.4	19.589	0.006	15.631	0.006	38.817	0.012
Mineralized toz/amz/ab granite	Orlovka	184.1	18.502	0.004	15.571	0.003	38.360	0.008
Mineralized toz/amz/ab granite	Orlovka	107.7	18.407	0.001	15.562	0.001	38.328	0.004
Greisenized granite	Spokoinoe	35	19.202	0.004	15.608	0.004	38.445	0.010
Greisenized granite	Spokoinoe	24.1	19.289	0.009	15.631	0.008	38.507	0.008
Mineralized greisen with W	Spokoinoe	282	18.504	0.001	15.567	0.001	38.328	0.002
Mineralized greisen with W	Spokoinoe	71.4	18.531	0.001	15.581	0.001	38.363	0.001
Mineralized greisen with W	Spokoinoe	32.5	18.976	0.006	15.598	0.004	38.410	0.011
Hornfels	Orlovka	15.2	18.492	0.006	15.566	0.005	38.544	0.013
Hornfels	Orlovka	6.7	18.811	0.002	15.578	0.002	38.457	0.004
Hornfels	Orlovka	7.9	18.786	0.005	15.618	0.005	38.658	0.012
Hornfels	Orlovka	12	19.074	0.002	15.584	0.002	38.750	0.007
Hornfels	Orlovka	26.7	18.506	0.010	15.557	0.009	38.491	0.020
Hornfels	Spokoinoe	90.5	18.264	0.001	15.581	0.001	38.046	0.001
Hornfels	Spokoinoe	59	18.06	0.001	15.505	0.001	38.304	0.001
Hornfels	Spokoinoe	18.2	18.542	0.001	15.588	0.001	38.267	0.001
Hornfels	Spokoinoe	11.6	18.948	0.001	15.599	0.001	38.803	0.002
Rhyolite	Khangilay	43.6	18.071	0.001	15.501	0.001	38.376	0.001
Rhyolite	Exocontact of Orlovka stock	9.4	18.869	0.003	15.594	0.002	39.345	0.005
Andesitic dacite	Khangilay	9.8	18.515	0.003	15.578	0.003	38.550	0.008
Dacitic lava	Khangilay	33.8	18.441	0.001	15.544	0.001	38.541	0.001
Rhyodacitic lava	Khangilay	32.7	18.223	0.001	15.498	0.001	38.429	0.001
Metasandstone / graywacke	Khangilay	8.9	18.626	0.007	15.537	0.006	38.820	0.016
Metasandstone / graywacke	Khangilay	15.4	18.363	0.001	15.548	0.001	38.403	0.001
Mica schist	Khangilay	25	18.267	0.001	15.518	0.001	38.371	0.002
Mica schist	Khangilay	21.6	18.587	0.003	15.861	0.004	39.01	0.005
Shale	Orlovka	16	18.429	0.007	15.557	0.007	38.666	0.007
Shale	Orlovka	16	18.265	0.006	15.536	0.007	38.4	0.007

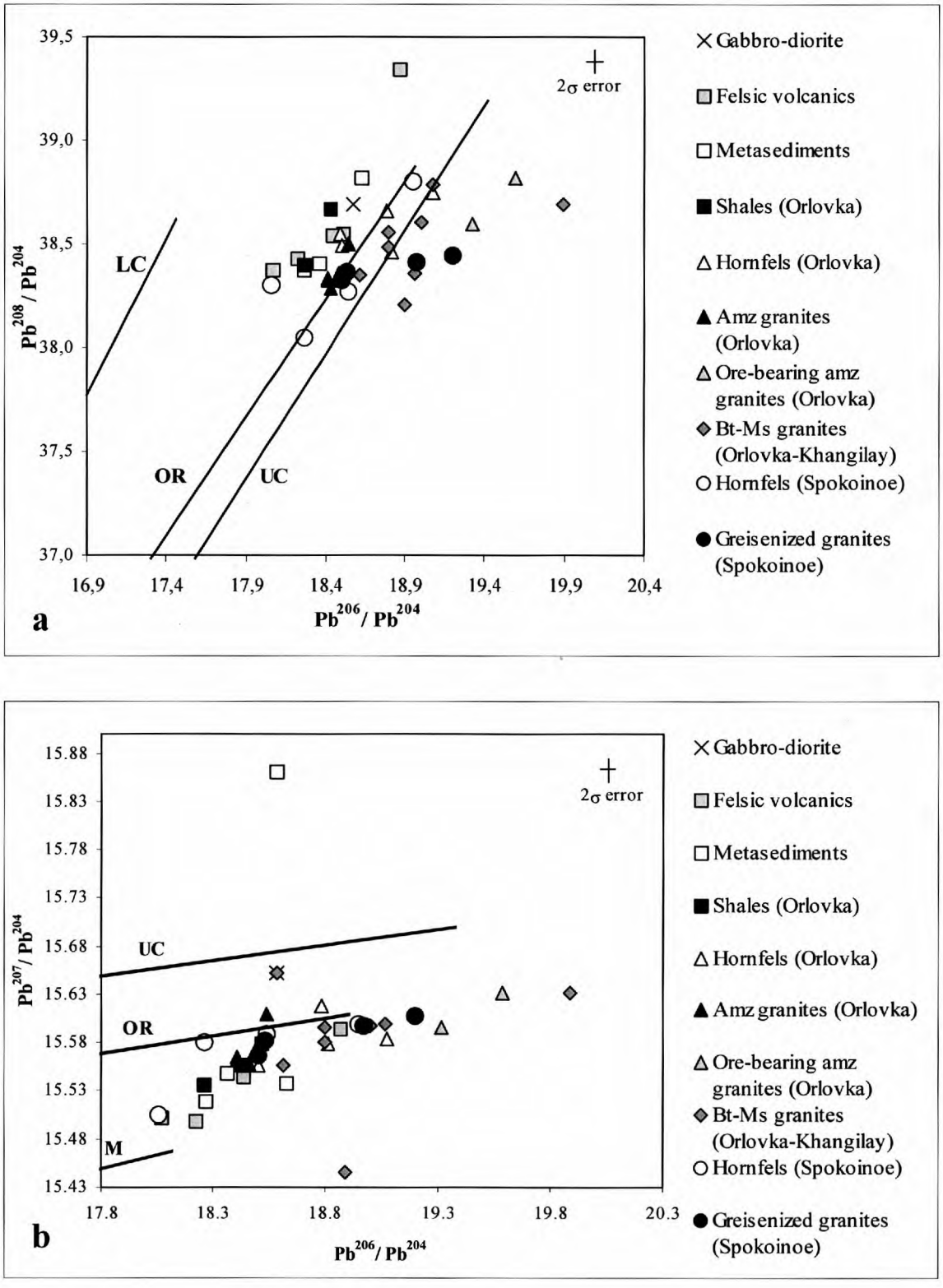

Figures 4.11a, b. Pb isotopes plots. LC – lower crust, CC – continental crust, UC – upper crust, OR – orogene, M - mantle (from Zartman and Doe, 1981).

Y/Ho complements Zr/Hf (and Nb/Ta) behavior and shows for Orlovka a similar trend towards lower ratios of these incompatible element pairs during the granite evolution. The elevated level of Y/Ho for Spokoinoe in contrast to Khangilay and Orlovka demonstrates autonomous evolution of its separated melts at a particular point of the parental magma during granite evolution. It hints to different mechanisms of element partitioning during melt-fluid processes that led to the relative enrichment of Y and explains the different REE patterns with the occurrence of more xenotime at Spokoinoe, while at Orlovka monazite prevails. Such fractionation of HFSE and (REE, Y) reflects the geochemical changes during granite evolution and explains the mineralogical diversity of the three massifs. Element partitioning during crystallization differentiation is typical of Li-F volatile-enriched granitic melts of high alkalinity associated with extreme fluid saturation that are favorable to separate ore-bearing melts and to control metal solubility, transport and precipitation. Evidence for the latter are the enrichment of fluorine and lithium by more than an order of magnitude (Table 4.1) and the dominance of amazonite and topaz at Orlovka in contrast to Spokoinoe, explaining the contrasting mineralization styles of both systems (Orlovka: Ta-Nb-Sn; Spokoinoe: W-Sn-Be).

Rb/Sr, in contrast to the above discussed element pairs, increases during granite evolution. This can be explained by the partitioning of large ion lithophile elements (LILE) that is controlled mainly by the Rb and Cs take-up through mica and feldspar at high fluid pressures (Li and F activity) in the Orlovka granites.[25] Fluid-rock interaction coupled with extreme fractionation in the Orlovka and Spokoinoe cupolas also explains the alteration of accessories like uraninite, thorite, monazite, apatite, fluorite (depletion in Th, U, REE), and re-equilibration of feldspars (depletion in Ba, Sr).

Ta and Nb concentrations rise for Orlovka as well as Spokoinoe in contrast to Khangilay, while indicators of fractionation and ore-bearing capacity like Nb/Ta show the lowest ratio for Orlovka (because of Ta enrichment).

Pb enrichment correlates with mineralogical observations on feldspar re-equilibration. Microprobe studies on K-feldspars show Pb enrichment from core to rim and in the perthite lamellae, allowing distinction between primary features and Pb-enriched secondary patterns, the latter related to late- and postmagmatic

redistribution processes. Pb redistribution is associated with microclinization and further amazonite formation associated with K↔Pb isomorphic replacement.[27] The Khangilay and Orlovka granites are slightly enriched in Pb, while highest Pb abundances occur in the Orlovka cupola. The Khangilay granites have up to 40 ppm Pb at relatively higher primary modal feldspar contents (30 vol% K-feldspar as major Pb carrier). The highly fractionated Orlovka granites contain the highest Pb abundances (up to 184 ppm) due to fractionation and metasomatic replacement processes in the ore-bearing granites.

4.5.2. Pb isotope distribution in the Orlovka deposit

Along with Pb isotopes we see one common source of the three granite massifs (the same mantle component cannot be excluded) and a clear link between the bt-ms granites of Khangilay, and the evolved Spokoinoe and Orlovka granites (Figure 4.10). It hints on fractionation from a homogenous (or homogenized) source melt with uniform initial $^{206}Pb/^{204}Pb$ and $^{207}Pb/^{204}Pb$ ratios. The greisens generated by fluids that redistributed the metals and overprinted the ore-bearing granites carry Pb components identical to those from which all magmatic members were generated (one mixing line). There is a strong relation between the barren parental granites and the ore-bearing bodies. The overall data trend demonstrates a simple mixing of the uniform Pb composition with different radiogenic components in the rocks and a strong genetic relation of the barren parental rocks to the ore-bearing rocks. The few off-trend Pb isotope distributions in some of the granites can be explained by their low Pb concentrations and resulting sensitivity of the Pb isotope system (Figure 4.11, Table 4.2). A reason could be the interaction of the intrusion with its wall rocks that shifted those Pb isotope ratios. The volcanic rocks carry a Pb component that is significantly different from the uniform source described above. It is related to the mantle-derived source, and Pb isotope signatures of the volcanic rocks represent mixtures between the crustal Pb component(s) and mantle Pb.

Pb isotope characteristics of the granite massifs suggest several possible sources for the granite melts. Figure 4.11a (thorogenic plot) shows that some of the Khangilay pluton samples and some of the ore-bearing amazonite granites are enriched in uranogenic lead and therefore likely to bear an in-situ radiogenic component. Figure 4.11b (uranogenic plot) indicates that they plot between the mantle and orogene

curves indicating possible input from both sources. Based on Rb-Sr and Sm-Nd isotope data it was suggested that a mantle-derived source had a significant contribution to the formation of A-type granites.[24] As can be seen on **Figure 4.12**, Pb isotope systematics show the presence of a mantle source in the formation of the studied granites. A mantle-derived component is in a transitional field between mid-ocean ridge basalt (MORB) and type II enriched mantle (EM II) but closer to the latter. The MORB source material is normally present beneath all active ridges and is restricted to the upper most hundred or several hundred kilometers of the upper mantle.[43] Sr/Nd isotope data of type II enriched mantle showed a strong similarity between continental and oceanic arrays.[43]

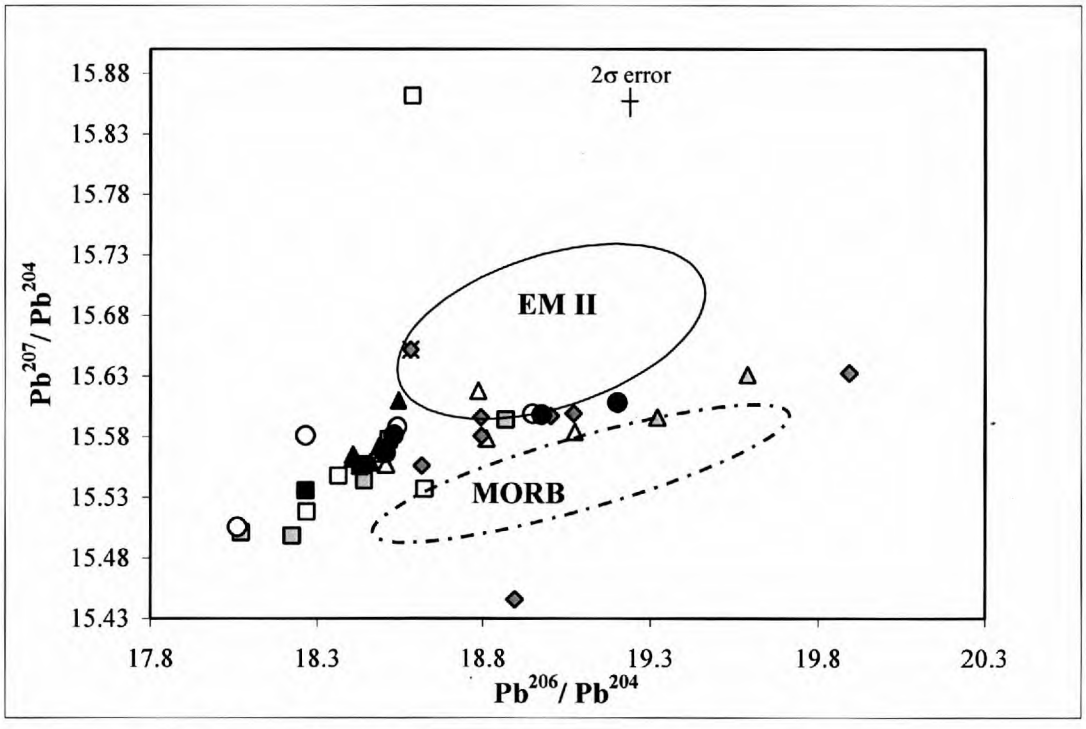

Figure 4.12. Pb^{206}/ Pb^{204} vs. Pb^{207}/ Pb^{204} diagram for Khangilay-Spokoinoe-Orlovka granites and their host rocks. All symbols are identical to those in Figures 4.10 and 4.11. EM II and MORB represent two types of mantle end members (Zindler and Hart, 1986). EM II = type II enriched mantle, MORB = mid-ocean ridge basalt.

It suggested similar styles of enrichment for the subcontinental and suboceanic mantle (although enrichment of the continental mantle is more extreme) as well as the possible involvement of the continental crust in the production of the enriched mantle. A type II enriched mantle source is commonly attributed to mixed metasomatism between mantle wedge material and crustal material introduced by

ancient subducted oceanic slab and sediments.[13] There is a mixture of different time episodes presented on Figure 4.12. The mantle arrays indicate present mantle Pb isotopes while granite data reflects "frozen" Jurassic Pb isotope compositions. If the mantle arrays are traced back to Jurassic age with less radiogenic EM II and MORB sources than the plotted arrays on Figure 4.12, they would slightly shift to the lower left part of the plot and therefore indicating EM II type input preferable.

Pb isotopic data suggest two possible sources contributed to the formation of the studied granites:

1) **crust-mantle source** where a mixture of MORB and upper crustal-derived material were brought together in the orogenic environment; and

2) **type II enriched mantle source** where subducted continental material could have been strongly implicated in several island-arc volcanic suites and the corresponding isotopic signatures, thus reflecting a strong similarity of EM II with upper continental crust or continentally derived sediment.

4.5.3. Regional evidence for the proposed model

Evidence from Sr, Nd and O isotope investigations[19-21,37] is consistent with the lead isotope data that exhibit two possible common sources for all granitic magmas of the Orlovka-Spokoinoe mining district. There is no unequivocal indication that would permit either a mixed upper crust-mantle source or a type II enriched mantle source to be favoured.

Regional studies of Transbaikalia granitoids consider geochemical, geophysical and geodynamic indications for both crustal and mantle input that trigger granitic melt generation of all petrochemical series.[15,18,25] The isotopic heterogeneity of these granites was predetermined by the isotopic heterogeneity of their sources.[18] Blocks of consolidated pre-Riphean crust were overthrusted during the accretionary collision of the foldbelts onto the younger crustal complexes of within-block oceanic basins contributing to an anomalous crustal thickness. The Riphean age of the crust in Caledonian structures most probably reflects the same average composition of a mixed source (basites + pelites) of the granitoid magmas; the source formed at 450-500 Ma. The isotopic evolution of this source resulted in $\varepsilon Nd_{(T)} \sim 0$ of the mixed source by 100-200 Ma. Some of the young (~120 Ma) granites show evidence of assimilation of the pre-Riphean crust.[18]

Some metaluminous and peralkaline syenite-granite suites and closely associated comendites of Transbaikalia constrain A-type granitoid magma generation emplaced at ca. 280 Ma as a result of fractional crystallization of syenite magmas. Alkali-rich silicic magma formed at a depth of 50-60 km (?) far exceeding the normal crust thickness. The Sr-Nd isotope data advocate the main role of mantle-derived material in the source region from which the alkali-rich syenitic and granitic magmas were produced.[24] Also, the alkali monzodiorite-syenite series that are widespread in Transbaikalia are explained by fractional crystallization from tephritic magma intrusions at ca. 130 Ma. In the $\varepsilon Nd_{(T)}$ vs. $(^{87}Sr/^{86}Sr)_i$ diagram the studied rock types fall in the enriched portion of the mantle array, suggesting their derivation from a metasomatized mantle source with a small crustal contamination during differentiation.[25]

In contrast to the calc-alkaline granite batholiths generated during continental crustal growths, subalkaline granites of Transbaikalia are often accompanied by basalt-trachyte-pantellerite-alkaline granite associations that mark rift structures of intraplate "hotspots".[18] The related Li-F and alkaline granites represent A-type granites with high heat production.

Sr, Nd and O isotope investigations of late Oligocene–Holocene volcanics from the adjacent area of the Southern Baikal region[37] showed that the isotopic signature of the magma source was formed by the contribution from moderately depleted mantle and enriched mantle reservoirs of types I and II enriched mantle (EM I and EM II).

EM II source has been reported to be one of the mantle sources that contributed to the formation of Early Mesozoic rocks of the Mongolia-Transbaikalia magmatic area[20] and has been listed among mantle sources for the CAOB as a whole.[20] The published data on Sr and Nd isotopes for the Orlovka massif with the values of $(^{87}Sr/^{86}Sr)_0 = 0.706 \pm 0.005$ and $\varepsilon Nd = 0.1$[19] favors EM II mantle input as well. It hints at the possibility that an EM II source controlled intraplate activity in Eastern Transbaikalia during late Mesozoic times when the Orlovka and Spokoinoe deposits were formed.

Sr, Nd and O isotope investigations of late Oligocene–Holocene volcanics from the adjacent area of the Southern Baikal region[37] showed that the isotopic signature of the magma source was formed by a contribution from moderately depleted mantle and enriched mantle reservoirs of types I and II enriched mantle (EM I and EM II). The EM II source has been reported to be one of the mantle sources that contributed to the

formation of Early Mesozoic rocks of the Mongolia-Transbaikalia magmatic area and has been listed among mantle sources for the CAOB as a whole.[20] Published data on Sr and Nd isotopes for the Orlovka massif with values of $(^{87}Sr/^{86}Sr)_0 = 0.706 \pm 0.005$ and $\varepsilon Nd = 0.1$[19] favours EM II mantle input and may suggest that an EM II source controlled intraplate activity in Eastern Transbaikalia during late Mesozoic times when the Orlovka and Spokoinoe deposits were formed.

4.6. CONCLUSIONS

(1) Zr/Hf, Y/Ho, Rb/Sr, and Nb/U show a continuous fractionation history from the parental to the evolved granites, where Khangilay and its derivates Spokoinoe and Orlovka represent different evolution stages. Geochemical trends are directed from Khangilay to Orlovka, commonly with Spokoinoe in between.

(2) The highly evolved amazonite granites of the Orlovka deposit show a stronger developed Eu anomaly and significant REE tetrad effects that developed parallel to granite evolution compared to parental granites of Khangilay.

(3) Pb isotope data indicate a strong genetic relationship between the barren biotite-muscovite granites of Khangilay, and the Spokoinoe and Orlovka ore-bearing granites suggesting a common source for the three massifs. Along with geological relationships and geochemical patterns the Pb isotope data confirm that the Khangilay pluton can be considered as the parental intrusion for its hosted mineralized apical intrusions.

(4) Pb isotope systematics outlines two possible scenarios for the sources of granitic melts: a mixed upper crust-mantle source, and a type II enriched mantle source.

Acknowledgements

The authors would like to thank AA Aksyuk, G.P. Zaraisky, A.V. Fedkin (IEM Chernogolovka), V.V. Shatov, G.B. Romanovsky (VSEGEI St. Petersburg), A.A Kremenetsky, L.I. Ginzburg, and V.F. Efimov (IMGRE Moscow) for inspiring discussions, assistance in field sampling and analytical support during the INTAS 97-0721 project. Continuous assistance of the EMMA laboratory at the Natural History Museum London and of Barry Coles (Imperial College London) with the analytical part of the project is acknowledged. AD appreciates support through Albert Julius Bursary (Imperial College London), ORS Award, INTAS Young Scientist Award and

research funds of the Department of Mineralogy (Natural History Museum, London). British Airways are thanked for providing London-Moscow return flights for DW and CJS under their Communities and Conservation Programme.

4.7. LIST OF SYMBOLS

toz – topaz

ab – albite

amz – amazonite

bt – biotite

ms –muscovite

REE – rare earth elements

HREE – heavy rare earth elements

LREE – light rare earth elements

HFSE – high field strength elements

CAOB – Central Asian Orogenic Belt

CC – continental crust

UC – upper crust

LC – lower crust

OR – orogene

M – mantle

PM – primitive mantle

MORB – mid-ocean ridge basalt

EM I – type I enriched mantle

EM II – type II enriched mantle

ppm – parts per million

4.8. REFERENCES

1. E. Anders and N. Grevesse: 'Abundances of the elements: Meteoritic and solar': *Geochimica et Cosmochimica Acta*, 1989, **53**, 197-214.
2. V.S. Antipin, E.A. Savina, M.A. Mitichkin and V.I. Perelyaev: 'Rare-metal lithium-fluorine granites, ongonites, and topazites of the Southern Baikal region': *Petrology*, 1999, **7 (2)**, 147-159.
3. V.N. Balashov, G.P. Zaraisky and R. Seltmann: 'Fluid-magma interaction and oscillatory phenomena during crystallization of granitic melt by accumulation and escape of water and fluorine', *Petrology*, 2000, **8**, *505-524.*
4. S.M. Beskin, A.M. Grebennikov, V.V. Matias: 'The Khangilai granite pluton and the related Orlovskoe tantalum deposit in the Transbaikal region', *Petrology*, 1994, **2**, 56-74.
5. P. Dulski: 'Interferences of oxide, hydroxide and chloride analyte species in the determination of rare earth elements in geological samples by inductively coupled plasma-mass spectrometry', *Journal of Analytical Chemistry*, 1994, **350**, 194-203.
6. P. Dulski: 'Reference materials for geochemical studies: New analytical data by ICP-MS and critical discussion of reference values', *Geostandard Newsletter: The Journal of Geostandards and Geoanalysis*, 2001, **25**, 87-125.
7. S.J.G. Galer and W. Abouchami: 'Practical application of lead triple spiking for correction of instrumental mass discrimination', *Mineral. Mag.*, 1998, **62A**, 491-492.
8. G. Faure: 'Principles of isotope geology', 2nd edition, 589, 1986, USA, John Wiley and Sons.
9. R.E. Harmer, J.M. Auret and B.M. Eglington: 'Lead isotope variations within the Bushveld complex, Southern Africa: a reconnaissance study', *Journal of African Earth Sciences*, 1995, **21 (4)**, 595-606.
10. A.W. Hofmann, K.P. Jochum, M. Seufert and W.M. White: 'Nb and Pb in oceanic basalts: new constraints on mantle evolution', *Earth and Planetary Science Letters*, 1986, **79**, 33-45.
11. A.W. Hofmann: 'Chemical differentiation of the Earth: the relationship between mantle, continental crust, and oceanic crust', *Earth and Planetary Science Letters*, 1988, **90**, 297-314.

12. A.W. Hofmann: 'Mantle geochemistry: the message from oceanic volcanism', *Nature*, 1997, **385**, 219-229.
13. Z. Hou, H. Ma, Z. Khin, Y. Zhang, M. Wang, Z. Wang, G. Pan and R. Tang: 'The Himalayan Yulong porphyry copper belt: product of large-scale strike-slip faulting in Eastern Tibet', *Economic Geology*, 2003, **98**, 125-145.
14. W. Irber: 'The lanthanide tetrad effect and its correlation with K/Rb, Eu/Eu*, Sr/Eu, Y/Ho and Zr/Hf of evolving peraluminous granite suites', *Geochimica et Cosmochimica Acta*, 1999, **63 (3/4)**, 489-508.
15. B. Jahn, F. Wu and B. Chen: 'Granitoids of the Central Asian Orogenic Belt and continental growth in the Phanerozoic', *Transactions of the Royal Society of Edinburgh,* 2000, **91**, 181-193
16. Yu.A. Kostitsyn: 'Sources of rare metals in peraluminous granites: a review of geochemical and isotopic data', *Geochemistry International,* 2001, **39 (1)**, 543-559.
17. P.V. Koval': 'Petrologiya I geokhimiya al'bitizirovannykh granitov (Petrology and Geochemistry of Albitized Granites)', 1975, Novosibirsk, Nauka.
18. V.I. Kovalenko, V.V. Yarmolyuk, V.P. Kovach, A.B. Kotov, L.K. Kozakov, E.B. Sal'nikova: 'Sources of Phanerozoic granitoids in Central Asia: Sm-Nd isotope data', *Geochemistry International,* 1996, **34(8)**, 628-640.
19. V.I. Kovalenko, Yu.A. Kostitsyn, V.V. Yarmolyuk, S.V. Budnikov, V.P. Kovach, A.B. Kotov, E.B. Sal'nikova and V.S. Antipin: 'Magma sources and the isotopic (Sr and Nd) evolution of Li-F rare-metal granites', *Petrology,* 1999, **7 (4)**, 383-409.
20. V.I. Kovalenko, V.V. Yarmolyuk, N.V. Vladykin, V.G. Ivanov, V.P. Kovach, A.M. Kozlovsky, Yu.A. Kostitsyn, A.B. Kotov and E.B. Sal'nikova: 'Epochs of formation, geodynamic setting, and sources of rare-metal magmatism in Central Asia', *Petrology,* 2002, **10 (3)**, 227-253.
21. V.I. Kovalenko, V.V. Yarmolyuk, E.B. Sal'nikova, S.V. Budnikov, V.P. Kovach, A.B. Kotov, V.A. Ponomarchuk, V.D. Kozlov, N.V. Vladykin and A.I. Khanchuk: 'Sources of igneous rocks and genesis of the Early Mesozoic tectonomagmatic area of the Mongolia-Transbaikalia magmatic region: 2. Petrology and geochemistry', *Petrology,* 2003, **11 (3)**, 227-254.

22. A.A. Kremenetsky, L.N. Ginsburg, V.V. Matias, V.V. Shatov, A.M. Aksyuk, G.P. Zaraisky, R. Seltmann, C.J. Stanley and L. Raimbault: 'Toxic element disposal in the Orlovka deposit area, Transbaikalia, Russia', in 'Mineral Deposits: Processes to Processing' (eds. C.J. Stanley *et al.*), 1191-1194; 1999, Rotterdam, A.A. Balkema.
23. R.L. Linnen and H. Keppler: 'Melt composition control of Zr/Hf fractionation in magmatic processes', *Geochimica et Cosmochimica Acta*, 2002, **66 (18)**, 3293-3301.
24. B.A. Litvinovsky, Bor-ming Jahn, A.N. Zanvilevich, A. Saunders, S. Poulain, D.V. Kuzmin, M.K. Reichow and A.V. Titov: 'Petrogenesis of syenite-granite suites from Bryansky Complex (Transbaikalia, Russia): implications for the origin of A-type granitoid magmas', *Chemical Geology,* 2002, **189**, 105-133.
25. B.A. Litvinovsky, Bor-ming Jahn, A.N. Zanvilevich, M.G. Shadaev: 'Crystal fractionation in the petrogenesis of an alkali monzodiorite-syenite series: the Oshurkovo plutonic sheeted complex, Transbaikalia, Russia', *Lithos,* 2002, **64**, 97-130.
26. F.A. Letnikov: 'Layered igneous bodies as a consequence of self-organization processes', *Petrology,* 2001, **9 (3)**, 204-213.
27. F.G. Reyf, R. Seltmann and G.P. Zaraisky: 'The role of magmatic processes in the formation of banded Li, F-enriched granites from the Orlovka tantalum deposit, Transbaikalia, Russia: microthermometric evidence', 2000, *The Canadian Mineralogist*, 2000, **38**, 915-936.
28. R. Seltmann, R., B. Taylor, A. Aksyuk, A. Fedkin, F. Reyf, V. Shatov and G. Zaraisky: 'Line Rock Formation in the Orlovka and Etyka Tantalum Deposits, Eastern Transbaikalia', Abstr. IMA Toronto, August 1998, A148.
29. R. Seltmann, G.P. Zaraisky, A.M. Aksyuk, V.V. Shatov and A.V. Fedkin: 'Amazonite in layered granites of the Orlovka and Etyka Ta deposits and its relation to magmatic-hydrothermal ore deposition', International symposium on 'Physico-chemical aspects of endogenic geological processes', Moscow-Chernogolovka, Russia, September 1999, 136-138.
30. L.F. Syritso, E.V. Tabuns, E.V. Volkova, E.V. Badanina and Yu.A. Vysotskii: 'Model for the genesis of Li-F granites in the Orlovka massif, Eastern Transbaikalia', *Petrology*, 2001, **9 (3)**, 268-289.

31. S.R. Taylor and S.M. McLennan: 'The geochemical evolution of the continental crust', *Reviews of Geophysics: application of radiogenic isotopes to ore deposit research and exploration,* 1995, **33 (2)**, 241-265.
32. R.M. Tosdal, J.L.Wooden and R.M. Bouse: 'Pb isotopes, ore deposits, and metallogenic terranes', *Reviews in Economic Geology*, 1999, **12**, 1-28.
33. D.J. Weiss, B. Kober, T.F.D. Mason, A. Dolgopolova, B.J. Cols, K. Gallagher, G. LeRoux, B. Spiro and R. Seltmann: EGS-AGU-EUG Joint Assembly, Nice, France, April 2003, **5**, Paper 03521.
34. D. Weiss, B. Kober, A. Dolgopolova, K. Gallagher, B. Spiro, G. Le Roux, T.F.D. Mason, M. Kylander and B.J. Coles: 'Accurate and precise Pb isotope ratio measurements in environmental samples by Mc-ICP-MS', *International Journal of Mass Spectrometry*, 2004, **232**, 205-215.
35. A. Yakubchuk: 'The Baikalide-Altaid, Transbaikal-Mongolian and North Pacific orogenic collages: similarity and diversity of structural patterns and metallogenic zoning', in 'The timing and location of major ore deposits in an evolving orogen', Geological Society, London, Special publication, (ed. D.J. Blundell, F. Neubauer and A. von Quadt), Vol. 204, 273-297, 2002, The Geological Society of London.
36. V.V. Yarmolyuk, B.A. Litvinovsky, V.I. Kovalenko, Bor-Ming Jahn, A.N. Zanvilevich, A.A. Vorontsov, D.Z. Zhuravlev, V.F. Posokhov, D.V. Kuz'min and G.P. Sandimirova: 'Formation stages and sources of the peralkaline granitoid magmatism of the Northern Mongolia-Transbaikalia Rift Belt during Permian and Triassic' *Petrology,* 2001, **9 (4)**, 350-380.
37. V.V. Yarmolyuk, V.G. Ivanov, V.I. Kovalenko and B.G. Pokrovskii: 'Magmatism and geodynamics of the Southern Baikal volcanic region (mantle hot spot): results of geochtonological, geochemical and isotopic (Sr, Nd and O) investigations', *Petrology,* 2003, **11 (1)**, 1-30.
38. N.E. Zalashkova: 'Zoning of metasomatically altered tantalum-bearing granites', in Mineralogical, geochemical and genetic characteristics of rare-metal apogranites, Moscow, 1969, 5-29.
39. G.P Zaraisky, A.M. Aksyuk, Yu.B. Shapovalov, V.Yu. Chevychelov, R. Seltmann and V.V. Shatov: 'Petrography and geochemistry of Li-F granites and pegmatite-aplite banded rocks from the Orlovka and Etyka tantalum deposits in

Eastern Transbaikalia, Russia', in 'Mineral Deposits', (ed. H. Papunen), 695-698, 1997, Rotterdam, Balkema.

40. Zaraisky, G.; Aksyuk, A.; Seltmann, R.; Shatov, V.; Fedkin, A.: 'Phosphorus in granites associated with W-Mo, W-Sn, and Ta-Nb mineralization', *Acta Universitatis Carolinae Geologica.* Special Issue on „Genetic significance of phosphorus in fractionated granites" (eds. Reiter & Janousek), 1998, **42(1),** 194-199.
41. G.P Zaraisky, A.M. Aksyuk, R. Seltmann and A.V. Fedkin: 'Evolution of rare-metal granites and Zr/Hf ratio as an indicator of their crystallization differentiation', N.P. Yushkin (ed.) Petrography at the Boundary of the XXI Century: Results and Perspectives. Proceed. 2nd Russian Petrography Meeting, 47-50, 2000, Syktyvkar, Geoprint III (in Russian).
42. R.E. Zartman and B.R. Doe: 'Plumbotectonics – the model', *Tectonophysics,* 1981, **75**, 135-162.
43. A. Zindler and S. Hart: 'Chemical geodynamics', *Ann. Rev. Earth Planet. Sci,* 1986, **14**, 493-571.

CHAPTER 5. TRACING DUST AND Pb DISPERSAL AT THE ORLOVKA Ta-Nb MINING AND ORE PROCESSING SITE: INSIGHTS FROM REE PATTERNS AND ELEMENTAL RATIOS.

ABSTRACT

Different geological, technogenic and environmental samples from around a Ta-W mining and ore crushing complex in Eastern Transbaikalia were analysed for Pb, Y, Zr and rare earth elements (REE) to trace the sources of dust and Pb within the mining site. Potential source material analyzed included ore bearing and barren granites, host rocks, tailing pond sediments, and ore concentrates. Lichens and birch leaves were used as receptor samples. Comparing the relative enrichment to chondritic values, the extent of the Eu anomalies, or the enrichments of heavy REE (HREE), we suggest that tailings and/or metasedimentary host rocks are the main source of dust in the studied mining environment. Lead concentrations, Pb/Zr ratios, and lead enrichment (relative to host rocks) show further that the environment is slightly polluted with metals but exclude the ore deposit (ore bearing granites, barren granites) or the processing plant (concentrates) as the potential source. Using the Zr/Y ratio, we propose tentatively the metasedimetary host rock as the main source of the Pb. Our results clearly demonstrate the potential of REE patterns and elemental ratios as a reliable technique to trace dust and metals sources and dispersal within a confined mining area offering a new tool for environmental assessment studies.

Keywords: REE patterns, elemental ratios, enrichment factors, dust, metals dispersal, Ta-W mining, Orlovka, Transbaikalia, Russia.

Journal of Hazardous Substance, submitted.

Date of submission: 14 May 2004.

5.1. INTRODUCTION

Abandoned hard-rock metal mines have left a heavy legacy for potential environmental contamination across the world. Mined quarries, mine dumps and tailings (the material left over from the ore processing) as well as associated mineral processing and smelting plants, can contaminate the surrounding water shed and ecosystem by the release of metals into the environment through wind blown dust particles [1-3], representing a serious threat to human health and local ecosystems, *e.g.* through accumulation of metals in food chains [4].

Dust dispersal represents a very important health hazard – due to both the small particle sizes and their effects on the respiratory system and to the dust's ability to carry potentially toxic trace elements such as Pb [5]. Dust carried away from the mine has a large surface area and is very susceptible to chemical weathering. When sulphide minerals contained in dust from mine tailings are exposed to oxygen and water, they oxidise and dissolve [6].

If contamination during mining or mineral processing is suspected, a thorough monitoring and source assessment is crucial to plan a cost efficient and targeted clean- up of the site. This, however, is often difficult given the many potential sources around a mining complex. Various microchemical, geochemical and mineralogical investigations of dust emitted by smelters have been conducted [7, 8] and showed that precise and accurate source characterisation and thus assessments are possible. However, these methods are all very labour intensive and do not allow rapid screening of dust dispersal and characterisation on a large scale [7].

Rare earth elements (REE) patterns have been used extensively in igneous, sedimentary and metamorphic petrology to trace sources of rocks and minerals during crustal and mantle evolution [9]. Due to its indicative and similar geochemical behaviour Y, with an ionic radius similar to that of Ho, is sometimes included along with REE. The low atomic number members of the series are termed the light rare earths (LREE) and those with higher atomic numbers the heavy rare earth elements (HREE). A number of properties of the REE suggest that they should also be useful in the study of environmental processes as: 1) they are among the least soluble trace elements, and 2) they are relatively immobile during low-grade metamorphism, weathering and hydrothermal alterations [9]. There have been environmental geochemical studies using the REE patterns in the environment e.g.,

in surface waters [10] and sewage water [11, 12] to assess acid mine drainages, in oceanic waters to assess riverine inputs [13] or in peat bogs to assess sources of dust [14]. For biomonitoring environmental contamination around smelters and mining sites lichens have proofed to be invaluable tools [15, 16]. Lichens receive dust and pollutants from atmospheric deposition and consequently are regarded as suitable tools for monitoring levels of atmospheric contamination. However, despite these previous findings, studies using REE patterns in lichens to assess the impact of mining on the environment are very limited [17-19].

The aim of this investigation was to assess the potential of REE patterns, elemental ratios and enrichment factors in lichens to trace dust and metal sources within the environment of an abandoned mining area. To achieve this, we undertook REE, Y, Pb and Zr analysis of potential sources and receptors of the Ta-W Orlovka-Spokoinoe mining site in Transbaikalia, Russia. The selected samples included ore-bearing and barren granites from the magmatic intrusion, host rocks, tailings, ore concentrates and lichens and birch leaves. This work was conducted in the framework of the INTAS project 97-0721, which determined the geologic controls on the distribution of potentially toxic concentrations of elements and assess most of the environmental situation in the abandoned Orlovka-Spokoinoe mining site [20].

The Orlovka-Spokoinoe mining site is situated within a previously closed territory and provided strategic metal resources (Ta, Nb, W, Li, Be) for the former Soviet Union defense industries. The Orlovka plant had processed rare-metal ores from Orlovka deposit since the early sixties. In 1993, the mining was temporarily stopped. However, significant reserves of unsold potentially economic products, as well as low-grade, metal-bearing waste tailings are stored. Ores of the Orlovka deposit are enriched in Ta, Nb, Li, and F, whereas ores from the adjacent Spokoinoe deposit are also rich in W, Sn and Be. The list of associated toxic elements includes Pb, As, Cd, U, Th, Se, Bi, Hg, Sb, Zn, Mo, and Be. Two towns, Novoorlovsky and Staroorlovsky, with 40,000 inhabitants in total are situated near the ore processing plant.

5.2. MATERIALS AND METHODS

5.2.1 Orlovka-Spokoinoe mining site and geological setting

The Orlovka-Spokoinoe mining site is located in Eastern Transbaikalia 140 km SE of Chita, Russia. It consists of two major quarries (Orlovka and Spokoinoe) situated ~8 km from each other. Adjacent to the quarries is an ore crushing and processing facility that provides Ta-Nb ore concentrate, which was then transported for further high temperature treatment outside of Orlovka. The tailings from the mining activities were deposited in a large pond next to the ore-processing complex.

The geology and the evolution of the ore-bearing granites of the Orlovka tantalum deposit and the Spokoinoe tungsten vein quartz-greisen deposit within the Orlovka-Spokoinoe mining site have been discussed in all detail elsewhere [21-23]. In summary, both deposits formed from magmatic intrusions into the host rocks (felsic volcanics, metasediments and hornfels) during the late Jurassic. The Orlovka tantalum deposit is confined to the apical part of the Orlovka granite cupola. The tantalum minerals are represented by finely-disseminated (0.01-1 mm) tantalite, tantalite-columbite, microlite and pyrochlore accumulated in the endocontact rocks of the granite cupolas. The Spokoinoe tin-tungsten deposit is characterized by tungsten (tin-beryl) vein quartz-greisens and is composed of albite-muscovite granites similar to the Khangilay massif, but alaskitic leucogranites prevail. In the upper parts of the cupola the granites are albitized and greisenized with tungsten mineralization, major minerals being wolframite, russellite, cassiterite, and beryl.

5.2.2 Ore processing plant and tailing pond

The ore processing plant produced high grade Ta-Nb and Sn-W concentrates from the ore-bearing granites through several low temperature physical and chemical separation steps. Firstly, the ore was crushed and milled to a particle size of 2 mm; then a further reduction of the particle size (down to 0.05 mm) was achieved using gravity concentration. The production of the raw Ta-Nb concentrate consisted of further gravity concentration, magnetic separation and sulphide flotation (Figure 5.1). The tailings from the ore mining, ore crushing and extraction processes were deposited next to the complex in a shallow pond.

5.2.3 Sampling of representative source and receptor material

Whole-rock samples were collected in the field and from the quarries representing the granite intrusions of Orlovka and Spokoinoe (ore-bearing (OB) and barren granites (BG), classified according to the mineralogy (see details in [21, 23]) and the host rocks. Samples from different stages of ore processing (gravitation (SM4), magnetic separation (SM5), flotation (SM3) and the final Ta-Nb concentrate) were collected in the plant and tailings were collected from the tailing pond.

Lichens (*Xanthoparmelia*) and birch leaves were collected from *Pinus betula* trees growing around the quarries, tailing pond, ore processing plant and in the Novoorlovsky settlement.

In the laboratory, ore processing plant samples, tailings, lichens and leaves were placed into previously cleaned ceramic beakers and dried at 40°C overnight. Lichens and leaf samples were ground in an agate mortar using liquid nitrogen. Samples were sieved through 100 μm stainless steel sieve, placed in ceramic beakers and dried overnight at 40°C prior to analysis. Whole rock samples, tailings and ore concentrates samples were prepared by milling them in a Tema agate mill. Samples were then homogenised, and transferred into the acid cleaned plastic bottles for further use. Table 5.1 summarizes the type of samples used and sampling location.

Lichens and birch leaves were digested using a MARSX high pressure/high temperature microwave oven system and a $HNO_3/HF/H_2O_2$ acid mixture [24]. The barren and ore bearing granites, host rocks, tailing pond sediments and ore concentrates were dissolved using hot plate digestion with a standard HNO_3/HF acid mixture in closed Teflon beakers [23].

Lead, Y, Zr and the REE were determined by quadrupole based inductively coupled plasma mass spectrometry (ICP-MS) at the GFZ Potsdam using an ELAN 5000A ICP MS (Perkin-Elmer/SCIEX, Canada). Detailed description of the instrumental parameters and method and the analytical precision and accuracy of the measurements are given elsewhere [25].

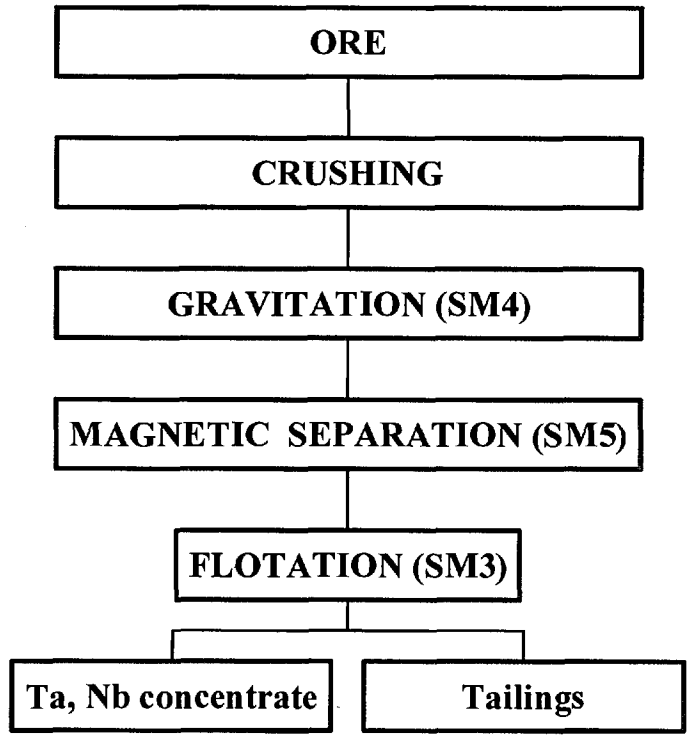

Figure 5.1. Processing stages of the Ta-Nb ore from the Orlovka deposit.

Table 5.1. Source/receptor description indicating the sample type, amount of samples analysed and sampling location within the Orlovka-Spokoinoe mining district (see text for details).

Source / Receptor	Sample Type	N	Sampling Location
Barren granites (BG)	Biotite and biotite/muscovite granites	7	Khangilay pluton, Orlovka stock
Ore bearing granites (OG)	Mineralized topaz/amazonite/albite granites	5	Orlovka open pit
Host rocks (HR)	Hornfels, metasediments, felsic volcanics	13	Orlovka open pit, Spokoinoe open pit
Concentrates	After crushing (SM), gravitation (SM4), magnetic separation (SM5), flotation (SM3)	14	Ore processing plant
Tailings	Surface sediments	5	Tailing pond
Lichens	Lichens	13	Orlovka quarry, Spokoinoe quarry, tailing pond, settlement, ore processing plant

5.3. RESULTS AND DISCUSSION

5.3.1. Pb concentrations, Pb/Zr and Pb enrichment – tracing the metal dispersal

Figure 5.2 shows the Pb concentrations (plot a), Pb/Zr ratios (plot b) and Pb enrichment (EF_{Pb}, plot c) from the granites (ore bearing – OG, barren – BG), the host rocks (HR), the concentrates, tailings and the lichens and leaves. The Pb enrichment (EF_{Pb}) was calculated using the equation:

$$EF_{Pb} = (Pb/Zr)_{sample} / (Pb/Zr)_{background},$$

where $(Pb/Zr)_{sample}$ is the ratio of the sample and $(Pb/Zr)_{background}$ is the ratio of the host rocks representing the local background value (0.152±0.123, n=13).

The Pb concentrations are on average lowest in the host rocks (30.2 μg/g including two high values of 155 and 90 μg/g), tailings (26.0 μg/g) and lichens and leaves (13.7 μg/g) but are higher in the barren and ore bearing granites (50.8 and 100.1 μg/g, respectively) due to the presence of amazonite. The range of Pb concentrations in the different ore concentrates is large, with highest values of 0.35% in concentrates after the gravitation stage, correlating with high Ta and W concentrations.

The Pb/Zr ratios are the highest in the ore bearing granites (up to 24.2) and ore concentrates (up to 7.7 after gravitation) but low (below 1) in all host rocks, barren granites and lichens. The tailings have slightly higher Pb/Zr ratios, ranging between 0.7 and 1.3.

As seen in Figure 5.2a, the Pb concentrations in lichens and leaves do not suggest any Pb contamination of the environment despite the high concentrations of potential sources such as ore concentrates and ore bearing granites. However, calculated Pb enrichment relative to host rocks Pb/Zr shows slight Pb enrichment in the tailings (between 5 and 8 times) and the lichens (between 2 and 5 times), suggesting a small but significant Pb enrichment despite the low Pb concentrations.

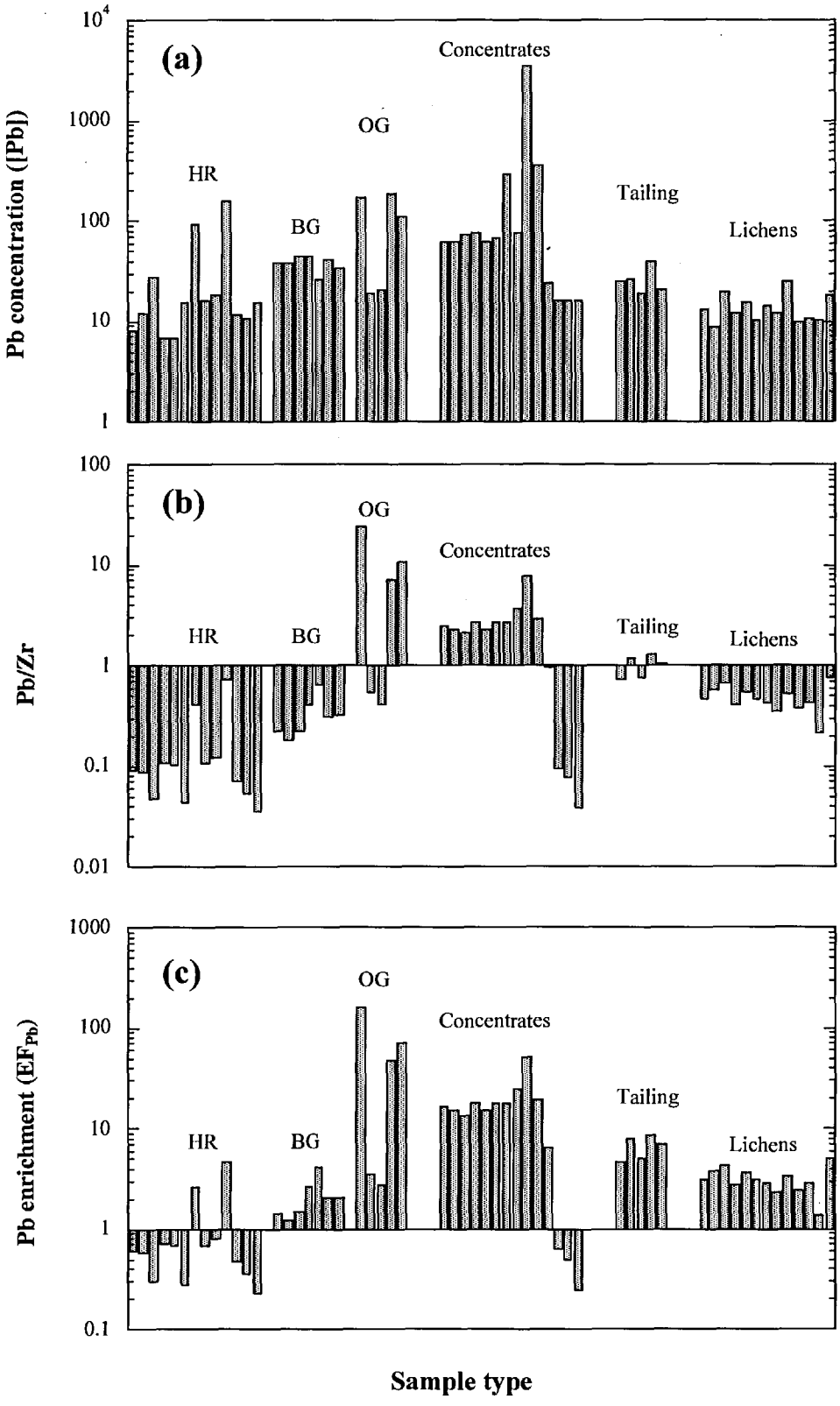

Figure 5.2. Lead concentrations [Pb], ppm (plot a), Pb/Zr ratios (plot b) and Pb enrichment factors EF_{Pb} (plot c) of the different potential sources (host rocks, HR, barren granites, BG, ore bearing granites, OG, concentrates, tailings) and receptors (lichens and birch leaves) within the Orlovka-Spokoinoe mining site.

5.3.2 REE patterns – tracing the dust sources

Figure 5.3 shows the REE patterns from the granites (ore bearing and barren) and the host rocks (plot a), the ore concentrates (plot b) and tailings (plot c). The REE concentrations were normalised relative to the average chondritic value taken from Boyton [26]. The REE patterns of all samples (Figure 5.3) form a monazite-type pattern, where the light REE (LREE) are more abundant than the heavy REE (HREE). Within the geological samples suite, the ore bearing granites, represented by highly evolved amazonite granites [23, 27], show the strongest developed Eu anomaly and REE tetrad effects (i.e. rounded segments or tetrads of the pattern) become more apparent (Figure 5.3a). This is in agreement with previous work showing that the tetrad effect develops parallel to granite evolution, and significant tetrad effects are strictly confined to highly differentiated samples. The REE patterns of the host rocks, represented by hornfelses, felsic volcanics and metasediments, show in general flat patterns apart from a few samples of hornfelses from the Orlovka deposit.

The REE patterns of ore concentrates inherit the general pattern of the ore bearing granites – including the tetrad effect, negative Eu anomaly and [LREE]>[HREE], even though after the concentration steps of gravitation, magnetic separation and flotation, the Eu anomaly has become significantly larger and most importantly, the REE are strongly enriched up to two orders of magnitude (Figure 5.3b) relative to the original granites.

The REE patterns of the tailing pond sediments (Figure 5.3c) strongly resemble the barren granites – no large variations in REE enrichment (all less than 40 times average chondrite values) and slightly developed Eu anomalies. The REE trends in the different ore concentrates fractions are in agreement with granites from the site. This allows the ore concentrates to be linked to their original geologic source, i.e. ore-bearing granites. Although tailing pond sediments plot within the ore samples reflecting some of the naturally inherited characteristics of the latter, they show a specific REE pattern, which can be used as their identification tool.

Among lichen species the average total concentrations of REE range from 9 to 32 μg/g with the highest concentrations found in lichens sampled around the ore processing plant (17-32 μg/g) and lowest around the settlement, quarry and the tailing pond (9 to 22 μg/g).

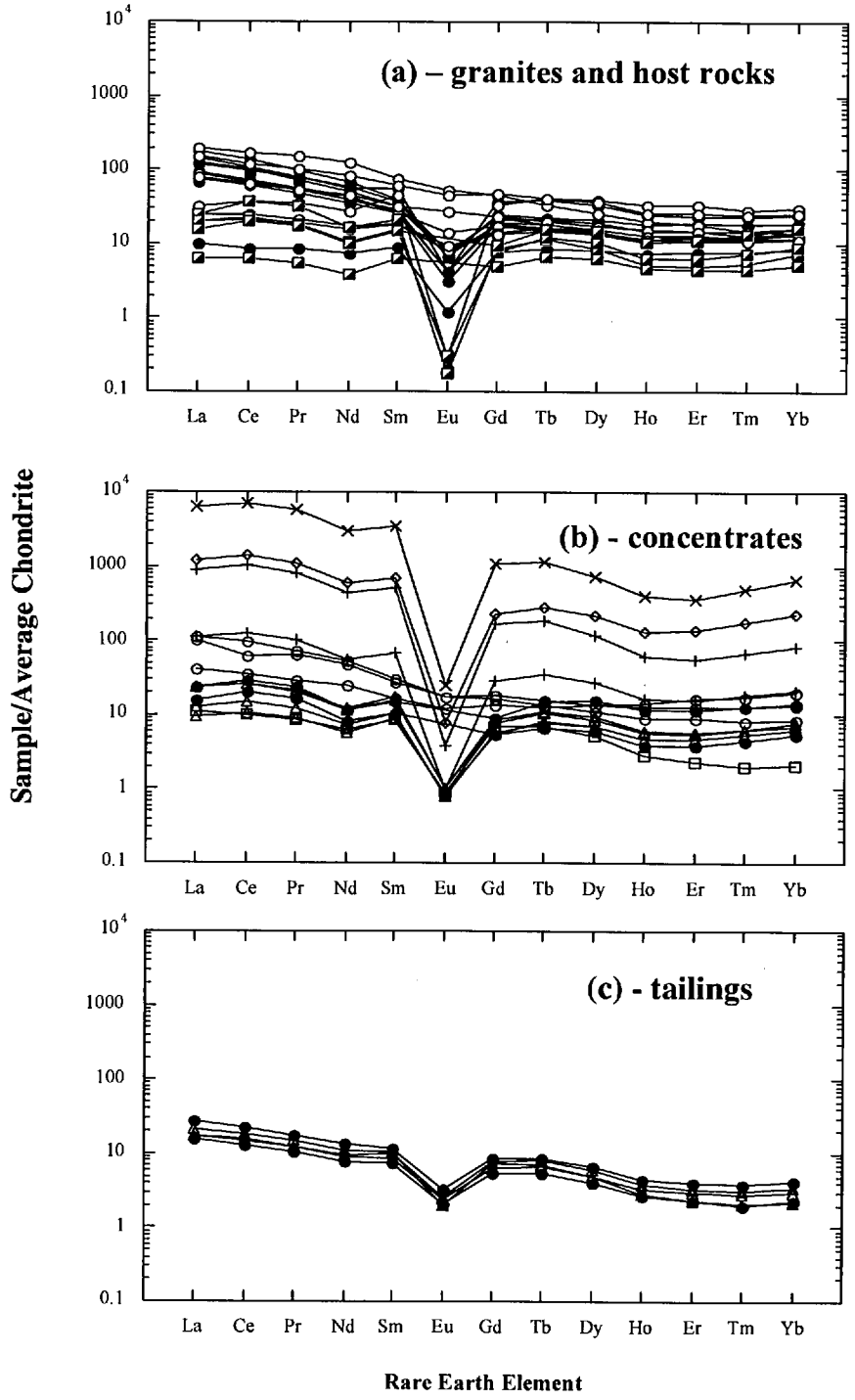

Figure 5.3. The REE patterns of possible pollutant sources including geologic suites with host rocks (open circles), barren granites (closed circles) and ore-bearing granites (quadrangles) (plot a); ore concentrates after crushing (SM, open squares, closed diamonds), gravitation (SM4, diagonal crosses), magnetic separation (SM5, open diamonds) and flotation (SM3, vertical crosses) (plot b); and tailing pond sediments (plot c).

These concentrations are of a similar range reported for the lichens earlier [19]. All lichen samples included in the study are depleted in REE with respect to average crustal REE abundances [28]; some by more than 20 times.

Assuming that REE patterns are congruent or parallel if linked to each other, we plotted the REE pattern of lichens with the REE patterns of the potential sources (Figures 5.4 and 5.5). As seen in Figure 5.4, the lichen's pattern is very similar to the REE patterns of the tailing pond sediments, showing similar slopes and shallower Eu anomaly compared to ore-bearing granites and ore concentrates described above. Comparison between REE patterns of lichens and host rocks (felsic volcanics, metasediments and hornfels) are shown in Figure 5.5. Beside the depletion of REE contents in lichens (likely reflecting dilution effects due to the organic matter), the HREE show stronger depletion (fractionation?) relative to the volcanic and hornfels host rock groups resulting in a more inclined REE pattern in lichens. However, the REE patterns of the lichens and leaves are very similar to the metasediments and consequently, this host rock cannot be excluded as a potential dust source.

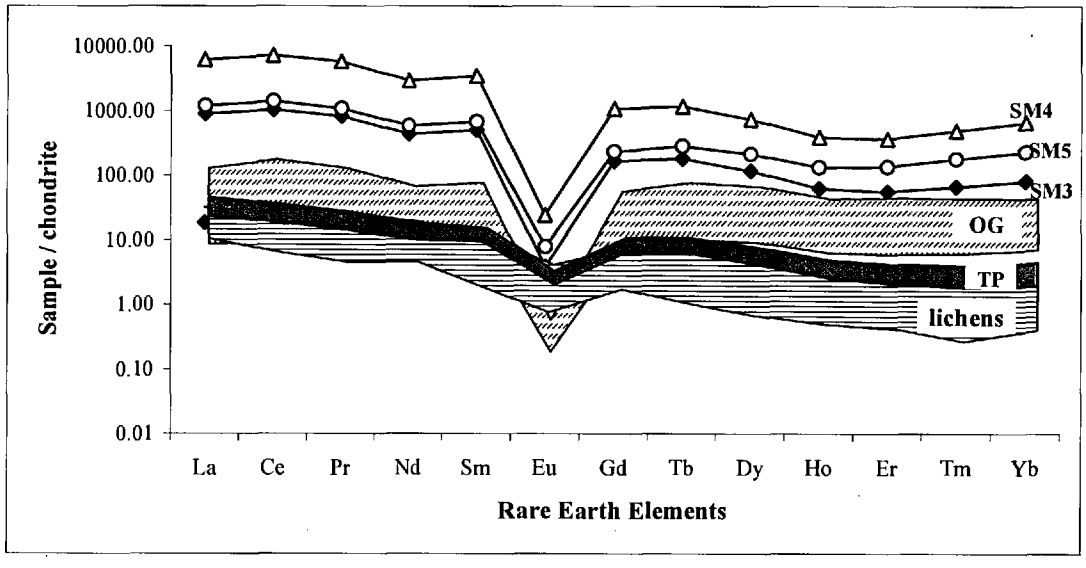

Figure 5.4. The REE patterns of lichens (horizontal shading) compared to the REE patterns of granitic intrusions (OG, oblique shading), tailing pond sediments (TP, grey shading) and ore concentrates (SM4, after gravitation; SM5, after magnetic separation; and SM3, after flotation).

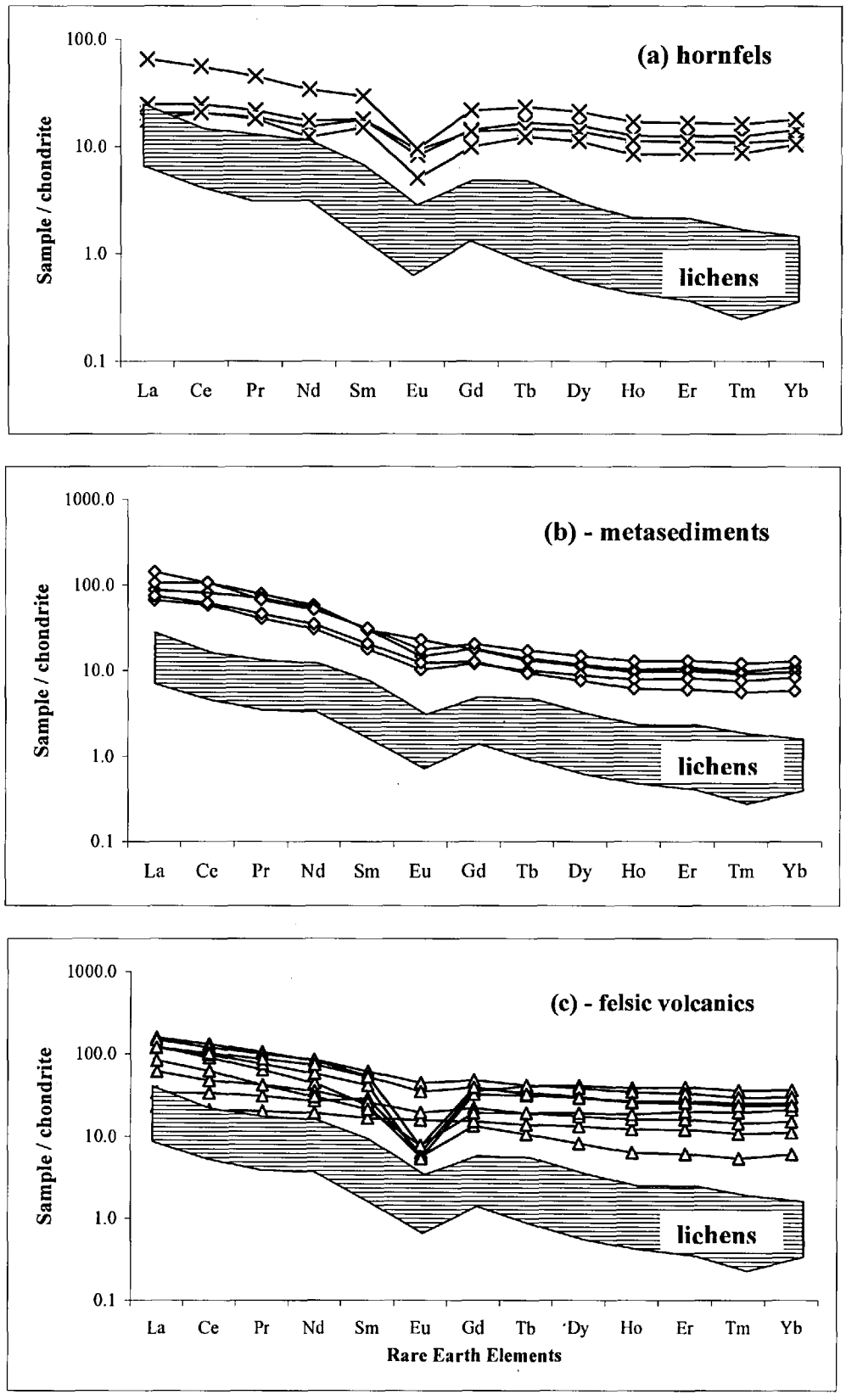

Figure 5.5. The REE patterns of lichens (horizontal shading) versus host rocks: hornfels (a), metasediments (b) and felsic volcanics (c) to assess the influence of the geological background on dust deposition.

5.3.3. Combining Pb, Zr and Y – additional insights into the dust and Pb sources

As discussed above, Pb enrichments relative to host rock using Pb/Zr ratio suggest a slight but significant Pb contamination despite the low Pb concentrations in the lichens. Other work has suggested [19, 29] that such overestimation might occur due to low Pb concentrations in the local bedrock and rather might represent an artefact, warranting further geochemical assessment. Consequently we plotted Pb/Y vs. Zr/Y (Figure 5.6a) and a mixing plot of 1/Pb vs. Pb/Y (Figure 5.6b). The Zr/Hf ratio has been used previously during the study of the geochemical evolution of the deposit as a very diagnostic ratio to assess the evolution of the granite intrusion [23]. In this study we apply the Zr/Y ratio to discriminate sample groups. The Zr/Y ratio reflects the influence of the mineral zircon and Y-containing phosphates such as xenotime. A close inspection of Figure 5.6a shows that the field of Zr/Y ratios in tailings is around 3, and is significantly lower than the field representing the lichens and leaves. 1/Pb vs. Pb/Y plot (Figure 5.6b) suggests that Pb dispersal within the mining site could be explained by contributions from tailings and host rocks – some with high Pb concentrations and some with low Pb concentrations.

5.4. SUMMARY

An environmental geochemical study has been conducted in the Orlovka-Spokoinoe mining site in Transbaikalia, Russia, to assess the sources of dust and metals in the environment and the impact of the mining and ore processing activities. Measurements of REE, Pb, Y and Zr in possible sources (host rocks, tailings, ore bearing and barren granites) and receptors (lichens and leaves) were conducted. REE patterns normalised to average chondritic values, Pb enrichment relative to host rocks, and Pb/Zr and Pb/Y ratios were used as geochemical tools to trace Pb sources within the mining site. We have shown that even though Pb concentrations are not elevated, Pb in lichens is slightly enriched relative to the host rocks. Ore concentrates with the highest Pb concentrations and ore bearing granites could be excluded as Pb sources using two component mixing plots and Pb/Y vs. Pb/Zr ratios. Host rocks and tailings are likely sources of Pb in the studied mining environment; however, an unidentified source could also be responsible, suggesting further work could include Pb isotope measurements. REE patterns were successfully used to link natural geological sources (Orlovka amazonite granites) to their anthropogenic products (ore

concentrates from different processing stages and tailings). This allowed identification of natural (geologic) and anthropogenic (ore concentrates, tailings) sources for particles dispersed within the mining area. Comparison between REE patterns of lichens and those of geological and anthropogenic origin showed that the tailing pond sediments and metasedimentary host rock can be considered also as the main source for the dust dispersion in the studied mining environment.

ACKNOWLEDGEMENTS

We wish to thank Barry Coles for help in the laboratories. We also thank Andy Fleet and Mike Warner for support with the running of the laboratories. AD appreciates support through Albert Julius Bursary (Imperial College London), ORS Award, INTAS Young Scientist Award and research funds of the Department of Mineralogy (Natural History Museum, London). Carlos and Camilla are thanked for indispensable support throughout the study.

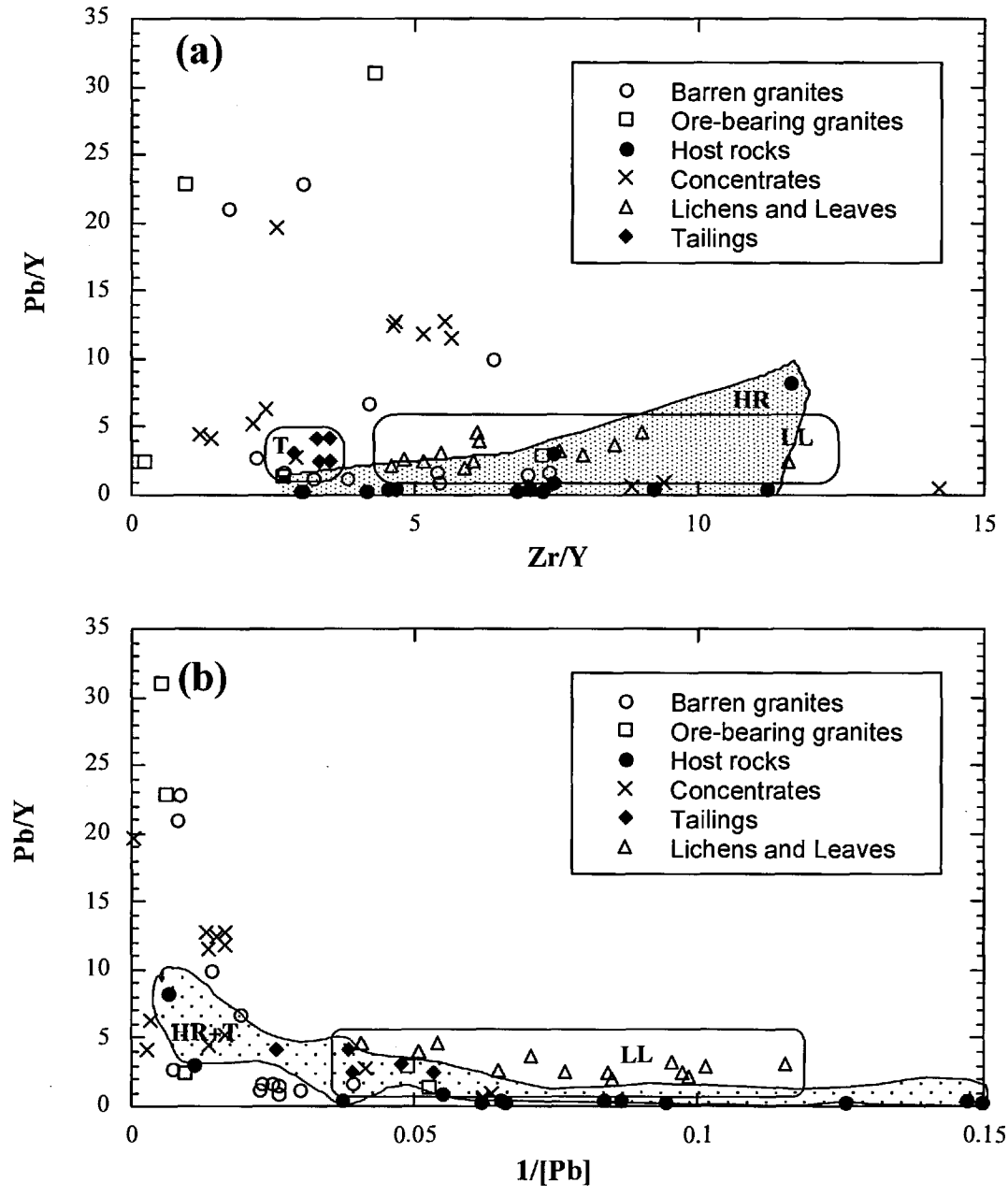

Figure 5.6. Plots of Pb/Y vs. Zr/Y (a) and 1/Pb vs. Pb/Y (b) for barren granites (open circle), ore bearing granites (open quadrangle), host rocks (closed circle), concentrates (cross), tailing pond sediments (closed diamond) and lichens and leaves (open triangle). The lichen and leaves field is characterised by low Pb/Y and higher Zr/Y ratios, agreeing well with the host rocks and tailing pond sediments but excluding most of ore concentrates, barren granites and ore bearing granites as possible sources.
T – tailings, **HR** – host rocks, **LL** – lichens and leaves.

5.5. REFERENCES

1. Dold, B. and L. Fontboté, *A mineralogical and geochemical study of element mobility in sulfide mine tailings of Fe oxide Cu-Au deposits from the Punta del Cobre belt, northern Chile.* Chem. Geol., 2002. **189**: p. 135-163.
2. Hudson-Edwards, K.A., et al., *The impact of tailings dam spills and clean-up operations on sediment and water quality in river systems: the Rios Agrio-Guadiamar, Aznalcollar, Spain.* Appl. Geochem., 2003. **18**: p. 221-239.
3. Antunes, I.M.H.R., A.M.R. Neiva, and M.M.V.G. Silva, *The mineralised veins and the impact of old mine workings on the environment at Segura, central Portugal.* Chem. Geol., 2002. **190**: p. 417-431.
4. Adriano, D.C., *Trace elements in the terrestrial environment.* 1986, Heidelberg - New York: Springer-Verlag.
5. Williamson, B., *Mineralogical composition of atmospheric airborne particulates.* Geol. Today, 2001. **17**(1): p. 32-35.
6. Jurjovec, J., C.J. Ptacek, and D.W. Blowers, *Acid neutralisation mechanisms and metal release in mine tailings: A laboratory column experiment.* Geochim. Cosmochim. Acta, 2002. **66**(9): p. 1511-1523.
7. Sobanska, S., et al., *Microchemical investigations of dust emitted by a lead smelter.* Environ. Sci. Technol., 1999. **33**: p. 1334-1339.
8. Sonke, J.E., et al., *A chemical and mineralogical reconstruction of Zn-smelter emissions in the Kempten region (Belgium), based on organic pool sediment cores.* Sci. Total. Environ., 2002. **292**: p. 101-119.
9. Rollinson, H.R., *Using geochemical data: evaluation, presentation, interpretation,* 1993: Longman Scientific, 352 pp.
10. Dinelli, E., et al., *REE mobility associated to acid mine drainage: Investigations in the Libiola area, northern Italy,* in *Geochemistry of the Earth's surface,* Armannsson, Editor. 1999, Balkema: Rotterdam. p. 173-176.
11. Knappe, A., et al., *Gadolinium in aquatic systems as indicator for sewage water contamination,* in *Geochemistry of the Earth's surface,* Armannsson, Editor. 1999, Balkema: Rotterdam. p. 187-190.
12. Bau, M. and P. Dulski, *Anthropogenic origin of positive gadolinium anomalies in river waters.* Earth Planet. Sci. Lett., 1996. **143**: p. 245-255.

13. Elderfield, H., *The oceanic chemistry of the rare earth elements.* Phil. Trans. R. Soc. London, 1988. **A325**: p. 105-126.
14. Krachler, M., et al., *Two thousand years of atmospheric rare earth element (REE) deposition as revealed by an ombrotrophic peat bog profile, Jura Mountains, Switzerland.* J. Environ. Monit., 2002. **5**: p. 111-121.
15. Purvis, O.W., et al., *Bioaccumulation of lead by the lichen Acarospora smaragdula from smelter emissions.* New Phytol., 2000. **147**: p. 591-599.
16. Purvis, O.W., et al., *Lichen biomonitoring in one of the most polluted areas in the world.* Proc. R. Soc. London B, 2004. **272**: p. 277-285.
17. Rossbach, M., et al., *Large scale air monitoring: lichens vs. air particulate analysis.* Sci. Total. Environ., 1999. **232**(1-2): p. 59-66.
18. Arne, D.C., J.E. Stott, and H.M. Waldron, *Biogeochemistry of the Ballarat East Goldfield, Victoria, Australia.* J. Geochem. Explor., 1999. **67**(1-3): p. 1-14.
19. Chiarenzelli, J., et al., *Multi-element and rare earth element composition of lichens, mosses, and vascular plants from the Central Barrenlands, Nunavut, Canada.* Appl. Geochem., 2001. **16**(2): p. 245-270.
20. Kremenetsky, A.A., et al., *Toxic element dispersal in the Orlovka deposit area, Transbaikalia, Russia*, in *Mineral Deposits*, C.J. Stanley, Editor. 1999, Balkema: Rotterdam. p. 1191-1194.
21. Zaraisky, G.P., et al., *Petrography and geochemistry of Li-F granites and pegmatite-aplite banded rocks from the Orlovka and Etyka tantalum deposits in eastern Transbaikalia, Russia*, in *Mineral Deposits*, H.P. Papunen, Editor. 1997, Balkema: Rotterdam. p. 695-698.
22. Reyf, F.G., R. Seltmann, and G.P. Zaraisky, *The role of magmatic processes in the formation of banded Li,F-enriched granites from the Orlovka tantalum deposit, Transbaikalia, Russia: Microthermometric evidence.* Can. Mineral., 2000. **38**(4): p. 1029-1051.
23. Dolgopolova, A., et al., *Geochemical characteristics and Pb isotope systematics of highly fractionated Li-F enriched amazonite granites and related host rocks of the Orlovka-Spokoinoe mining district, Eastern Transbaikalia (Russia).* Trans. Inst. Min. Metall.: Section B: Applied Earth Sciences, in press.

24. Dolgopolova, A., et al., *Closed-vessel microwave digestion technique for lichens and leaves prior to determination of trace elements (Pb, Zn, Cu) and stable Pb isotope ratios.* Intern. J. Environ. Anal. Chem., in press.
25. Dulski, P., *Interferences of oxide, hydroxide and chloride analyte species in the determination of rare elements in geological samples by inductive coupled plasma-mass spectrometry.* Fresenius J. Anal. Chem., 1994. **350**: p. 194-203.
26. Boynton, W.V., *Geochemistry of the rare earth elements: meteorite studies*, in *Geochemistry of the rare earth elements*, P. Henderson, Editor. 1984, Elsevier. p. 63-114.
27. W. Irber, *The lanthanide tetrad effect and its correlation with K/Rb, Eu/Eu*, Sr/Eu, Y/Ho and Zr/Hf of evolving peraluminous granite suites*, Geochimica et Cosmochimica Acta, 1999, **63** (3/4): p. 489-508.
28. Taylor and S.M. McLennan, *The geochemical evolution of the continental crust.* Reviews of Geophysics: application of radiogenic isotopes to ore deposit research and exploration, 1995, **33** (2): p. 241-265.
29. Reimann, C. and P. de Caritat, *Intrinsic flaws of element enrichment factors (EFs) in environmental geochemistry.* Environ. Sci. Technol., 2000. **34**(24): p. 5084-5091.

CHAPTER 6. USE OF ELEMENT AND ISOTOPE RATIOS TO ASSESS SOURCES AND PATHWAYS OF Pb AND Zn DISPERSED IN THE ENVIRONMENT DURING MINING AND ORE PROCESSING WITHIN THE ORLOVKA-SPOKOINOE MINING SITE (RUSSIA).

ABSTRACT

Element concentrations, element ratios and Pb and Zn isotope data are reported for different geologic samples (barren and ore-bearing granites and host rocks), technogenic products (ore concentrates and tailings) and environmental samples (lichens and birch leaves) from the Orlovka-Spokoinoe mining district, Eastern Transbaikalia, Russia, with the aim to trace the sources of Pb and Zn at a local level within the remote mining site. Lichens and birch leaves were used as receptors of contamination within the mining site. Pb/Zr and Zn/Zr values exhibit Pb and Zn enrichment relative to host rocks. Pb and Zn concentrations, Zr/Hf, Pb/Hf, Zn/Hf, Yb/Y, Pb/Y, Zn/Y, Yb/La, Pb/La, Zn/La ratios and Pb and Zn isotopes indicate that tailings, barren granites, host rocks and multi-source long-range aerosols are the main sources of Pb and Zn dispersed within the mining site. Zn isotope data of 15 geologic and 11 lichen samples showed a distinction between their Zn isotopic signature with the total range for the geologic suite of -0.4 to +1.1 ‰ and for lichens of +0.3 to +1.3 ‰ in δ^{66}Zn relative to the in-house Zn standard. We conclude that the source of isotopically heavy Zn within the Orlovka-Spokoinoe mining site could be potentially associated with long-range atmospheric aerosols that also contributed a significant amount of Pb to the studied mining site. Our results clearly demonstrate that a combination of independent geochemical tools such as element concentrations, elemental ratios and isotopes is vital for the comprehensive assessment of metal sources within the environment.

Keywords: elemental ratios; metals dispersal; Pb, Zn isotopes; Ta-Nb-Sn-W mining; Orlovka-Spokoinoe; Transbaikalia; Russia

Applied Geochemistry, submitted. Date of submission: 11 October 2004.

6.1. INTRODUCTION

Metals are transferred to the atmosphere, soils, vegetation, water reservoirs and sediments from local industries, mining and smelting, sewage sludge, gasoline and coal combustion, and waste incineration. At present fluxes of these metals due to anthropogenic activities exceed those linked to natural erosion, even in areas remote from cities and industries (Nriagu and Pacyna, 1988). The mining of metalliferous mineral deposits and associated metal processing activities has lead to severe perturbations in the cycling of metals in the surface environment (Thornton, 1996). Where ore deposits were mined, local geochemical anomalies were created, which significantly intensified metal and potentially toxic element supply into the environment. Information about contamination can be gathered from analyses of metal concentrations alone, but a lot of uncertainties remain concerning metal sources. Metal sources can be assessed using different geochemical tools. Trace element ratios are sensitive indicators to identify fractionation processes and fluid-rock interaction (Bau, 1996), and thus to serve as a tool to discriminate groups of different origin and genesis. In previous research Zr/Hf, Y/Ho and Rb/Sr were used as very diagnostic ratios for the investigation of the geochemical evolution of the deposit, i.e. to assess the evolution of the Orlovka granite intrusion (Zaraisky et al., 2000; Dolgopolova et al., 2004); Nb/U and Ce/Pb allowed constraining of crust-mantle input during the formation of the Orlovka-Spokoinoe ore-bearing granites (Dolgopolova et al., 2004). Use of Pb/Zr and Pb/Y resulted in identification of host rocks and tailing pond sediments as the main Pb sources within the mining environment (Dolgopolova et al., submitted); Pb/Zr was used in the same study to define Pb enrichment within different sample groups. Whereas the concentrations of metals can vary greatly as they move through the environment, metals often preserve their isotopic composition of the source(s), permitting conclusions as to their origin.

The use of Pb isotopes to identify and to distinguish between natural and anthropogenic sources of contamination became a routine fingerprinting tool in the last few decades (Rosman et al., 1993, 1994, 1999; Chiaradia et al., 1997; Kober et al., 1999; Luck et al., 2002). Pb isotope ratios are variable in natural materials and environments due to radioactive decay of U- and Th-nuclides. They are, however, not affected by industrial

or biological processes (Ault et al., 1970) and do not fractionate during transport and deposition processes and therefore retain the isotopic composition of their sources with great potential as source tracers. The use of a multi-collector ICP-MS allows collection of high-precision Pb isotope data and a large sample throughput at the same time. Although thermal ionisation mass spectrometry (TIMS) can also provide Pb isotope data of similar quality, its disadvantages are time-consuming analytical procedures and low sample throughput (Weiss et al., 2004). The precise isotope ratios including ^{204}Pb now allow the identification of multiple natural and anthropogenic sources of Pb contamination within even a small area, for example in the vicinity of a Cu smelter (Urals, Russia) as reported by Spiro et al., (in print). However, a reliable routine identification of potentially toxic element sources at a local level still remains poorly constrained.

Although development of Zn isotope measurements is still at an early stage, the first successful studies showed Zn isotopic variability in a variety of geological (carbonates and sulphides) and biological (lobster liver, mussel tissue, phytoplankton and plants) samples (Maréchal et al., 1999; Maréchal et al., 2000; Maréchal et al., 2002; Archer and Vance, 2002; Albarède, 2004; Mason et al., 2003a). This permits interpretations of the geochemistry and biochemistry of Zn in the natural environment. Zn is a biologically essential element and its isotopes potentially offer a powerful tool for studying geosphere-biosphere interactions. Zn isotopes studied in higher plants indicated that two or more processes control the isotopic composition of Zn in the plant material, some (e.g. kinetic precipitation) favoring isotopically lighter Zn while the others (e.g. adsorption) favor heavier Zn (Mason et al., 2003b). Some studies used Zn isotopes in rainwater, aerosols and loesses to constrain atmospheric pollutants (Luck et al., 1999; Ben Othman et al., 2001). Zn isotope variations in rainwater showed two different ranges of variations, i.e. $\delta^{66}Zn$ of -0.25‰ to 0‰ and 0‰ to 0.15‰ (see Chapter 3.2.3. for $\delta^{66}Zn$ quotation details) that corresponded to two different sources of Zn: the source with heavier Zn isotopes corresponded to a chemical product used in the catchment area ($\delta^{66}Zn$ of 0.05-0.55‰), whilst the source of lighter Zn isotopes remained undetermined. Another study observed large mass-dependent variations in commercially available Zn

metal standards compared to its natural isotopic variations (Mason et al., 2004). This was suggested to relate to the distillation process during metal purification and could potentially provide a marker to distinguish between anthropogenic and natural Zn contaminants within the environment. Zn has five stable isotopes, ^{64}Zn, ^{66}Zn, ^{67}Zn, ^{68}Zn and ^{70}Zn, with average atomic abundances of 49.19 %, 27.79 %, 4.04 %, 18.39 % and 0.60 % respectively (Tanimizu et al., 2002).

The main aim of this study is to use elemental ratios (Zr/Hf, Pb/Hf, Zn/Hf, Yb/Y, Pb/Y, Zn/Y, Yb/La, Pb/La, Zn/La) and high-precision measurements of Pb and Zn isotopes to identify sources and pathways of Pb and Zn within a remote and "closed" geochemical cycle of the Orlovka-Spokoinoe mining site (Eastern Transbaikalia, Russia) (Figure 6.1). To constrain a source-receptor model the following sample groups were distinguished and are discussed in the present paper: (a) geological samples (barren and ore-bearing granites and host rocks as sources); (b) anthropogenic products (gasoline, ore concentrates and tailings as sources) and (c) environmental samples (lichens and birch leaves as receptors). The main objectives of the paper are: 1) to distinguish between geologic sources, anthropogenic products and environmental samples; 2) to discriminate between natural and anthropogenic sources of Pb and Zn within the mining environment, and 3) to assess multi-component mixing. The novelty of our approach is in using a combination of several geochemical tools, including high-precision Pb and Zn isotopes to assess sources and migration pathways of Pb and Zn within the studied mining site.

6.2. Materials and Methods

6.2.1. Site description

The Orlovka-Spokoinoe mining district is located in Eastern Transbaikalia 140 km SE of Chita, Russia, within a previously closed territory and provided strategic metal resources (Ta, Nb, W, Li, Be) for the former Soviet Union defense industries. It consists of two major quarries (Orlovka and Spokoinoe) situated ~8 km apart. Close to the quarries is an ore processing plant that produces Ta-Nb and Sn-W ore concentrates, which are then transported for further smelting outside of the district. The tailings from the mining activities are deposited in a large pond next to the ore-processing complex. Significant reserves of unsold potentially economic products, as well as low-grade, metal-bearing

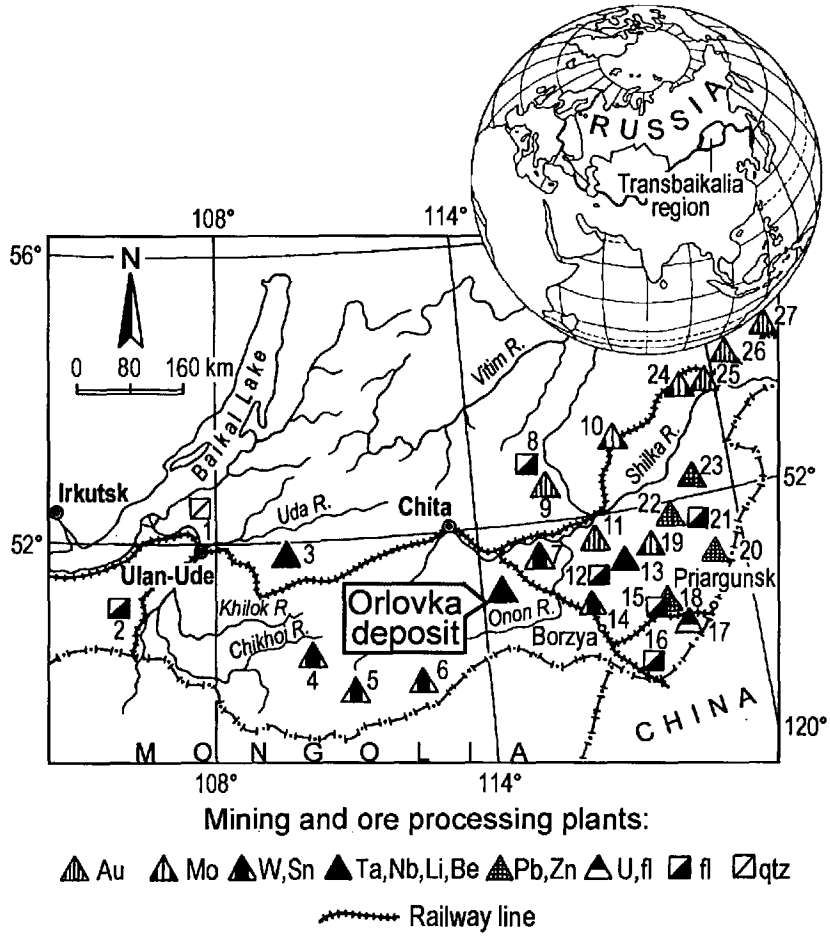

Figure 6.1. Location of the Orlovka-Spokoinoe mining site (after Kremenetsky et al., 1999).

tailings are stored. The Orlovka plant processed rare-metal ores from the Orlovka deposit since the early sixties. In 1993, mining was temporarily stopped and only in recent years has work at the processing plant restarted sporadically. Ores of the Orlovka deposit are enriched in Ta, Nb, Li, and F, whereas ores from the adjacent Spokoinoe deposit are also rich in W, Sn and Be. The list of associated toxic elements includes Pb, As, Cd, U, Th, Se, Bi, Hg, Sb, Zn, Mo, and Be (Ginsburg et al, 2000). Two towns, Novoorlovsky and Staroorlovsky, with 40,000 inhabitants in total are situated near the ore processing plant (Figure 6.2).

The geology and the evolution of the ore-bearing granites of the Orlovka tantalum deposit and the Spokoinoe tungsten deposit within the Orlovka-Spokoinoe mining district have been discussed in detail elsewhere (Zaraisky et al., 1997; Reyf et al., 2000; Dolgopolova et al., 2004; Badanina et al., 2004). In summary, both deposits formed from magmatic intrusions into the host rocks (felsic volcanics, metasediments and hornfels) during the late Jurassic. Both deposits are hosted by satellite intrusions of the Khangilay granite pluton (Beskin et al., 1994; Kovalenko et al., 1999; Syritso et al., 2001). The Orlovka tantalum deposit is confined to the apical part of the Orlovka granite cupola. The tantalum minerals are represented by ferrocolumbite, ferrocolumbite-ferrotantalite, microlite and pyrochlore accumulated in the endocontact rocks of the granite cupolas. The Spokoinoe tungsten deposit is characterized by tungsten (tin-beryl) vein quartz-greisens and is composed of albite-muscovite granites. Major minerals are wolframite, russellite, cassiterite, and beryl.

6.2.2 Ore processing plant and tailing pond

The ore processing plant produced high-grade Ta-Nb and Sn-W concentrates from the ore-bearing granites of the Orlovka and Spokoinoe deposits through several low temperature physical and chemical separation stages. Firstly, the ore is crushed and milled to a particle size of 2 mm and then to a size down to 0.05 mm. The production of the raw Ta-Nb and Sn-W concentrates consists of further gravity concentration, magnetic separation and sulphide flotation. The tailings from the ore processing plant are deposited next to the ore processing plant in a shallow pond.

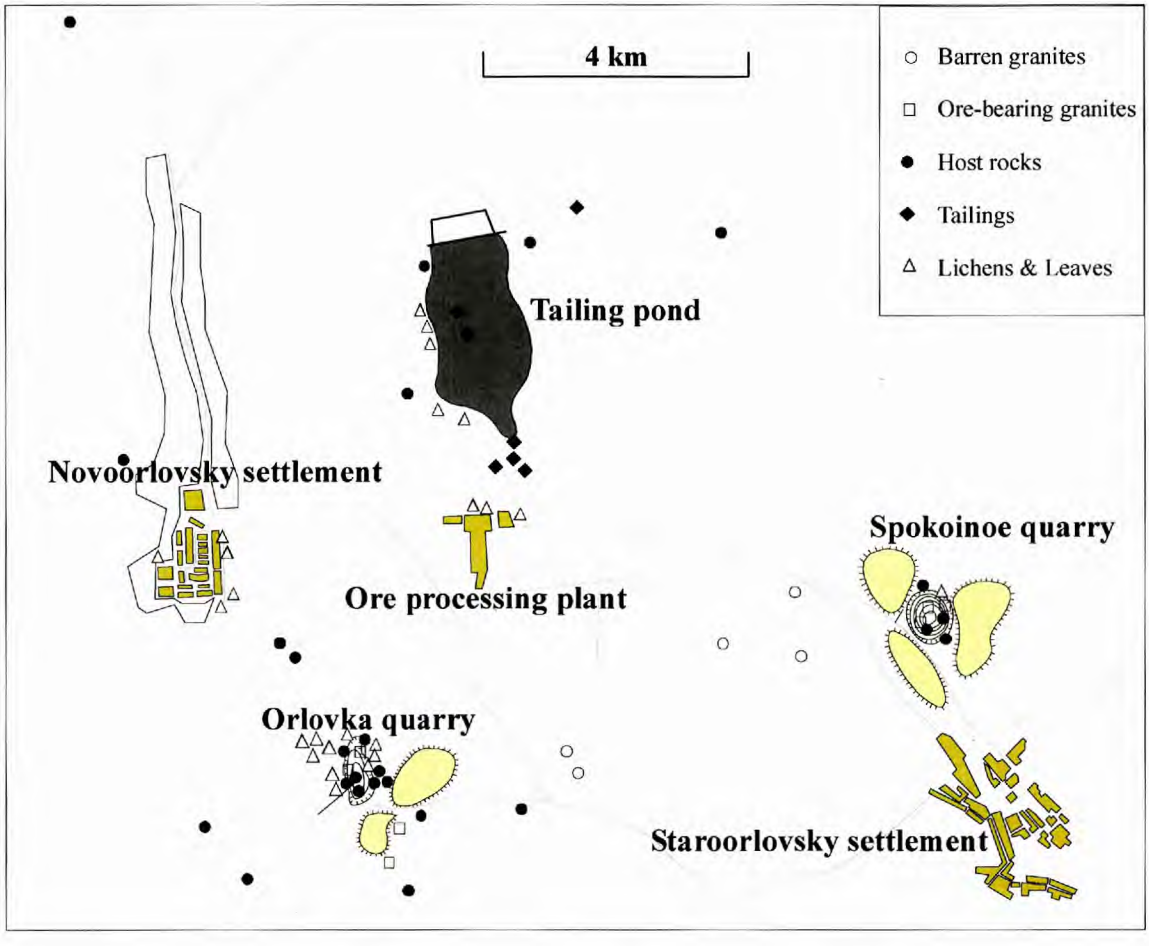

Figure 6.2. Location of the sampling sites within the Orlovka-Spokoinoe mining site. Samples of geologic (granites, host rocks), biologic (lichens and leaves) and anthropogenic (tailings) origins were collected around main infrastructure units within the site.

6.3. SAMPLING AND ANALYTICAL TECHNIQUES

6.3.1. Sampling of representative source and receptor material

Whole-rock samples were collected in the field and from the two quarries representing the granite intrusions of Orlovka and Spokoinoe, i.e. ore-bearing and barren granites, classified according to the mineralogy (see details in Zaraisky et al., 1997; Dolgopolova et al., 2004) and the host rocks represented by felsic volcanics, metasediments and hornfels. Samples from different stages of ore processing of the Orlovka ores such as (1) crushing, (2) gravitation, (3) magnetic separation and (4) flotation were collected from the ore processing plant, and tailings were collected from the tailing pond. Lichens (*Xanthoparmelia*) and birch leaves were sampled from *Pinus betula* trees growing around the quarries, the ore processing plant, the tailing pond and in the Novoorlovsky settlement. Gasoline samples were collected from the local petrol station.

In the laboratory, whole-rock samples, ore concentrates, tailings, lichens and leaves were placed into previously cleaned ceramic beakers and dried at 40°C overnight. Lichens and leaves were ground in an agate mortar using liquid nitrogen. Whole rock samples, tailings and ore concentrates were prepared by milling in a Tema agate mill. Samples were sieved through a 100μm stainless steel sieve, placed in ceramic beakers and dried overnight at 40°C prior to analysis. Samples were homogenized and transferred into acid–cleaned plastic bottles for further use.

6.3.2 Chemical analysis

6.3.2.1. Major and trace element analysis

Lichens and birch leaves were digested in $HNO_3/HF/H_2O_2$ acid mixture using a MARSX microwave oven system (Dolgopolova et al., in print). The barren and ore bearing granites, host rocks, tailing pond sediments and ore concentrates were dissolved using hot plate digestion with a standard HNO_3/HF acid mixture in closed Teflon beakers (Dolgopolova et al., in print). 0.2 ml of gasoline samples were at first evaporated until an oily dark brown drop was left. Then a mixture of concentrated 2 ml HNO_3 and 0.2 ml HF was added to fume down the residue. Aliquots were used for measurements of element concentrations and isotope analyses.

Zn concentrations were determined by inductively coupled plasma optical emission spectroscopy (ICP-OES) using an OPTIMA 4300 (Perkin Elmer) instrument at the laboratory of the All-Russia Geological Research Institute (VSEGEI) in St. Petersburg, Russia. 0.1g of samples were digested in HNO_3, HF and H_2SO_4 acids, evaporated and redissolved in HCl media for further analysis. The detection limit for Zn was 1ppm. Basalt BE-N (France) was used as the certified reference material for calibration. Precision and accuracy of measurements were within 10%.

Trace elements Zr, Hf, Pb, Y and Yb were determined by inductively coupled plasma mass spectrometry (ICP-MS) at GFZ Potsdam. The procedure and instrumental parameters of the measurements are described in detail elsewhere (Dulski et al., 2001). Briefly, about 0.1 g of sample powder was dissolved using mixed acid digestion ($HF/HClO_4$) under pressure and filled up with 0.5M HCl up to 50 ml of final volume. Prior to analysis, Ru, Re and Bi were added to aliquots of the solutions as internal standards for drift correction, and the mixtures were further diluted by a factor of ten. Measurements were made using an ELAN 5000A quadrupole inductively coupled plasma mass spectrometer (ICP-MS) (Perkin-Elmer/SCIEX, Canada). Samples were measured in batches of five. Each batch was preceded by a 10 ng/ml calibration solution, two acid blanks and a procedure blank. Quantitative determination of element concentrations was performed applying external calibration using two calibration solutions, which bracketed each batch of samples. To minimize the influence of drift effects on analytical precision relatively small batches of samples were analysed within one analytical run. Interference corrections were routinely applied to correct analyte isotopes for molecular and isobaric interferences (Dulski, 1994). Precision and accuracy were within 5-10%.

6.3.2.2. Pb isotopes analysis

The whole sample suite, including 48 geologic samples represented by barren and ore-bearing granites and host rocks, 12 anthropogenic products such as ore concentrates and tailings, 2 samples of local gasoline and 26 samples of lichens and birch leaves, was analyzed for Pb isotopes by thermal ionization-mass spectrometer (TIMS, University of Heidelberg) and GV *Isoprobe* multi-collector ICP-MS based at the Imperial College

London - Natural History Museum Joint Analytical Facility (ICL/NHM JAF). Pb was purified through an ion chromatography Sr-resin from EiChrom in a hydrochloric acid medium (see details of procedure in Weiss et al., 2004). TIMS raw data were normalized to NBS 981 Pb international standard with reference values of Galer and Abouchami (1998) (reproducibility on the 95% confidence level: 0.03% for ratios normalized to ^{204}Pb). MC-ICP-MS raw data were corrected for isobaric interferences on ^{204}Pb using ^{200}Hg. Mass discrimination correction was made using NBS 997 Tl as an internal standard. The Pb/Tl ratio was kept constant to 2:1 during the measurements. The $^{205}Tl/^{203}Tl$ ratio was optimized based on repeated measurements of a spiked NBS 981 Pb international standard. Long-term reproducibility of repeated NBS standards of MC-ICP-MS for all ratios during the time of investigation of five months was below 350 ppm. Analytical blanks for the procedure estimated from intensity data, were below 1ng and always below 1% of the total lead and mixing calculations showed that contributions were insignificant at any time at the level encountered. The error of the internal isotope measurements for all pairs of Pb isotopes was on average below 200 ppm. The reproducibility during the measurements ($\pm 2\sigma$) was 0.035% for $^{206}Pb/^{204}Pb$, 0.034% for $^{207}Pb/^{204}Pb$ and 0.05% for $^{208}Pb/^{204}Pb$.

Table 6.1 shows Pb, Zn, Zr, Hf, Y and Yb element concentrations and Pb isotope data for the Orlovka-Spokoinoe mining site.

6.3.2.3. Zn isotope measurements

15 geologic and 11 lichen samples from the same sample suite were also analyzed for Zn isotopes by multi-collector ICP-MS (ICL/NHM JAF) (Table 6.2). Zn was purified through ion chromatography AG MP-1 resin in hydrochloric medium. Isotopic measurements were made using 1 block of 25 integrations with an integration interval of 5 seconds. The "sample–standard bracketing" approach was used for Zn isotope measurements when an in-house IMP Zn standard was measured before and after each sample. Every sample was measured 4 times. All data were on-peak baseline corrected off-line using a 0.2% (v/v) ultra-pure HNO_3 acid blank run directly prior to each analysis. Zn isotope data are presented in δ notation relative to the in-house IMP Zn

standard (Imperial College London). A $\delta^{66}Zn$ was calculated for each unknown sample relative to the bracketing standards, using equation:

$$\delta^{66}Zn = ({}^{66}Zn/{}^{64}Zn_{sample} / {}^{66}Zn/{}^{64}Zn_{standard} - 1) \times 1000 \text{ (‰)}$$

The full description of the method, including the applied Cu correction, can be found in Mason et al. (2004). We measured the JMC Zn standard (Lyon) and the difference (2σ) between the in-house IMP Zn standard and the JMC Zn standard for $\delta^{66}Zn$ is -0.087 ± 0.070 (number of analysis n=10). No data were rejected during data processing. Acid blank analyses of one block of 25 measurements were taken before each analysis and used for an on-peak zero baseline subtraction (see details on procedure in Mason et al., 2004). The long-term reproducibility was obtained for repeat measurements of the difference between two Zn standards (IMP Zn and JMC Zn) for pure Zn reagents over a two-week period and was less than 0.07 ‰ (±2σ) for $^{66}Zn/^{64}Zn$ ratio. The typical average reproducibility determined as an average of four repeated measurements for each sample from the Orlovka-Spokoinoe site (±2σ) was 0.061‰ for $\delta^{66}Zn$ and 0.132‰ for $\delta^{68}Zn$.

6.4. RESULTS

6.4.1 Pb and Zn concentrations

The ore-bearing granites of Spokoinoe and Orlovka contain the highest Pb concentrations (up to 282 ppm in Spokoinoe and up to 184 ppm in Orlovka) (Table 6.1). High Pb concentrations in Orlovka can be explained by fractionation and metasomatic replacement processes in the ore-bearing granites as was previously discussed in Dolgopolova et al. (2004). Pb enrichment here correlates with mineralogical observations on feldspar re-equilibration. Pb redistribution is associated with microclinization and further amazonite formation associated with K↔Pb isomorphic replacement (Seltmann et al., 1999). Galena (PbS) plays a subordinate role and is found only in hydrothermal veinlets and occasionally in the host rocks. Barren granites have up to 40 ppm of Pb and host rocks up to 27 ppm (Table 6.2). Tailing pond sediments have similar Pb concentrations (up to 25 ppm) to the average Pb content of the host rocks.

Table 6.1. Pb, Zn, Zr, Hf, Y, Yb concentration values (μg/g) and Pb isotope ratios in geologic, anthropogenic and botanical samples from the Orlovka-Spokoinoe mining district, Eastern Transbaikalia, Russia. "T" next to the sample ID corresponds to samples that were measured by TIMS.

	Sample description	Sampling location	Pb	Zn	Zr	Hf	Y	Yb	$^{206}Pb/^{204}Pb$	±2σ	$^{207}Pb/^{204}Pb$	±2σ	$^{208}Pb/^{204}Pb$	±2σ
ID	**Barren granites:**													
2050-T	Biotite/muscovite granite	Khangilay pluton	26	60	41	2.7	15	1.8	18.958	*0.003*	15.598	*0.002*	38.360	*0.008*
2079	Biotite granite	Khangilay pluton	38	60	175	5.9	25	2.6	18.896	*0.004*	15.446	*0.005*	38.209	*0.007*
2080	Biotite granite	Khangilay pluton	38	40	214	7.0	39	3.9	19.893	*0.001*	15.633	*0.001*	38.691	*0.001*
2084	Biotite/muscovite granite	Khangilay pluton	40	40	129	5.2	24	2.6	19.003	*0.001*	15.597	*0.001*	38.604	*0.001*
2096-T	Biotite granite	Khangilay pluton	44	60	198	6.0	27	2.5	19.070	*0.004*	15.599	*0.003*	38.789	*0.007*
2142-T	Biotite/muscovite granite	Orlovka stock	136	150	109	5.3	50	5.0	18.617	*0.001*	15.556	*0.001*	38.351	*0.004*
2149-T	Biotite granite	Orlovka stock	44	60	110	4.7	35	3.4	18.794	*0.002*	15.596	*0.002*	38.558	*0.006*
2151	Biotite/muscovite granite	Orlovka stock	34	60	107	4.5	28	2.8	18.796	*0.001*	15.581	*0.001*	38.481	*0.001*
	Ore-bearing granites:													
2143-T	Amazonite/muscovite granite	Orlovka stock	122	200	16	2.8	5.3	1.2	18.428	*0.003*	15.556	*0.003*	38.286	*0.006*
2144-T	Amazonite pegmatite	Orlovka stock	129	300	10	1.8	6.1	1.3	18.486	*0.001*	15.572	*0.001*	38.359	*0.004*
2147-T	Strongly weathered amz granite	Orlovka stock	71	150	45	12	7.1	1.5	18.460	*0.002*	15.559	*0.001*	38.326	*0.005*
2148	Intensely weathered amz granite	Orlovka stock	52	120	32	7.0	7.7	1.5	18.544	*0.006*	15.610	*0.008*	38.503	*0.010*
2162-T	Mineralized toz/amz/ab* granite	Orlovka quarry	167	60	6.9	1.5	7.3	1.1	18.407	*0.001*	15.565	*0.001*	38.332	*0.002*
2215-T	Mineralized toz/amz/ab granite	Orlovka quarry	108	120	10	1.7	44	5.3	19.320	*0.004*	15.596	*0.003*	38.599	*0.009*
2163-T	Mineralized toz/amz/ab granite	Orlovka quarry	19	120	35	13	13	3.5	19.589	*0.006*	15.631	*0.006*	38.817	*0.012*
2164-T	Mineralized toz/amz/ab granite	Orlovka quarry	20	300	50	21	6.9	1.5	18.502	*0.004*	15.571	*0.003*	38.360	*0.008*
2213-T	Mineralized toz/amz/ab granite	Orlovka quarry	184	800	26	5.5	5.9	1.8	18.407	*0.001*	15.562	*0.001*	38.328	*0.004*
2220-T	Greisenized granite	Spokoinoe quarry	35	30	17	1.2	4.9	0.36	19.202	*0.004*	15.608	*0.004*	38.445	*0.010*
2223	Mineralized greisen with wolframite	Spokoinoe quarry	282	30	5.4	0.32	27	1.0	18.504	*0.001*	15.567	*0.001*	38.328	*0.002*
2224	Mineralized greisen with wolframite	Spokoinoe quarry	71	30	5.8	0.25	9.3	1.2	18.531	*0.001*	15.581	*0.001*	38.363	*0.001*
2056-T	Mineralized greisen with wolframite	Spokoinoe quarry	32	30	20	2.2	7.3	0.53	18.976	*0.006*	15.598	*0.004*	38.410	*0.011*
	Host rocks:													
2068-T	Hornfels	Khangilay pluton	15	120	355	8.0	49	4.9	18.492	*0.006*	15.566	*0.005*	38.544	*0.013*
2166	Hornfels	Orlovka quarry	6.7	80	66	2.4	22	3.0	18.811	*0.002*	15.578	*0.002*	38.457	*0.004*

	Sample description	Sampling location	Pb	Zn	Zr	Hf	Y	Yb	$^{206/204}$Pb	± 2σ	$^{207/204}$Pb	± 2σ	$^{208/204}$Pb	± 2σ
2169-T	Hornfels	Orlovka quarry	7.9	60	86	3.7	21	2.4	18.786	*0.005*	15.618	*0.005*	38.658	*0.012*
2173-T	Hornfels	Orlovka quarry	12	100	137	6.2	29	3.7	19.074	*0.002*	15.584	*0.002*	38.750	*0.007*
2174-T	Hornfels	Orlovka quarry	27	120	578	12	63	6.2	18.506	*0.010*	15.557	*0.009*	38.491	*0.020*
2177	Hornfels	Orlovka quarry	6.8	120	64	11	14	2.2	N/A*	N/A	N/A	N/A	N/A	N/A
2132	Hornfels	Spokoinoe quarry	11	60	197	5.3	29	3.2	N/A	N/A	N/A	N/A	N/A	N/A
2138	Hornfels	Spokoinoe quarry	90	120	224	5.3	30	2.8	18.264	*0.001*	15.581	*0.001*	38.046	*0.001*
2140	Hornfels	Spokoinoe quarry	16	120	155	4.2	52	4.7	N/A	N/A	N/A	N/A	N/A	N/A
2125	Hornfels	Spokoinoe quarry	59	150	240	6.4	27	2.8	18.060	*0.001*	15.505	*0.001*	38.304	*0.001*
2128	Hornfels	Spokoinoe quarry	155	60	217	5.5	19	1.9	N/A	N/A	N/A	N/A	N/A	N/A
2060	Hornfels	Spokoinoe quarry	18	60	151	3.9	20	2.0	18.542	*0.001*	15.588	*0.001*	38.267	*0.001*
2129	Hornfels	Onon group	12	80	161	4.2	23	2.6	18.948	*0.001*	15.599	*0.001*	38.803	*0.002*
2150	Rhyolite	Orlovka stock	44	20	143	5.0	8.8	1.3	18.071	*0.001*	15.501	*0.001*	38.376	*0.001*
2182	Rhyolite	Orlovka stock	9.4	15	201	7.0	46	4.9	18.869	*0.003*	15.594	*0.002*	39.345	*0.005*
2183	Rhyolite	Orlovka stock	4.4	30	167	6.8	76	7.5	N/A	N/A	N/A	N/A	N/A	N/A
2187	Andesitic dacite	Orlovka stock	6.3	60	106	2.6	24	2.3	N/A	N/A	N/A	N/A	N/A	N/A
2204	Andesitic dacite	Orlovka stock	10	100	190	4.8	32	3.1	18.515	*0.003*	15.578	*0.003*	38.550	*0.008*
2121	Dacitic lava	Orlovka stock	34	25	336	9.2	39	4.3	18.441	*0.001*	15.544	*0.001*	38.541	*0.001*
2101	Rhyodacitic lava	Orlovka stock	33	80	121	4.8	53	5.2	18.223	*0.001*	15.498	*0.001*	38.429	*0.001*
2010	Metasandstone	Orlovka stock	5.6	30	245	6.3	20	2.0	N/A	N/A	N/A	N/A	N/A	N/A
2011	Metasandstone	Orlovka stock	8.9	40	215	5.4	21	2.3	18.626	*0.007*	15.537	*0.006*	38.820	*0.016*
2028	Metasandstone	Orlovka stock	15	60	167	4.2	16	1.7	18.363	*0.001*	15.548	*0.001*	38.403	*0.001*
2029	Mica schist	Orlovka stock	25	120	226	5.7	25	2.7	18.267	*0.001*	15.518	*0.001*	38.371	*0.002*
2032	Chlorite/mica schist	Orlovka stock	22	60	170	4.5	12	1.2	18.587	*0.003*	15.861	*0.004*	39.010	*0.005*
SH2	Shale	Tailing pond	31.3	N/A	28.3	2.04	8.79	0.6	18.429	*0.007*	15.557	*0.007*	38.666	*0.007*
SH3	Shale	Tailing pond	32.8	N/A	31.9	2.26	12.5	1.0	18.265	*0.006*	15.536	*0.006*	38.400	*0.007*
	Tailings, ore concentrates and local gasoline:													
TP 3	Tailings	Tailing pond	25.4	59.6	35.6	1.91	10.2	0.86	N/A	N/A	N/A	N/A	N/A	N/A
TP 4	Tailings	Tailing pond	21.59	50.9	21.7	1.46	6.19	0.48	18.306	*0.005*	15.573	*0.006*	38.207	*0.007*

	Sample description	Sampling location	Pb	Zn	Zr	Hf	Y	Yb	$^{206/204}Pb$	±2σ	$^{207/204}Pb$	±2σ	$^{208/204}Pb$	±2σ
TP 5	Tailings	Tailing pond	17.85	113	24.5	1.68	7.39	0.62	19.182	*0.003*	15.612	*0.003*	38.563	*0.007*
TP 6	Tailings	Tailing pond	38.95	101	30.4	1.79	9.25	0.73	18.117	*0.003*	15.562	*0.003*	37.764	*0.003*
TP 7	Tailings	Tailing pond	20.83	37.8	19.8	1.28	6.93	0.45	19.032	*0.004*	15.611	*0.004*	38.487	*0.004*
SM1	Ore concentrate (after crushing)	Ore processing plant	60.23	83.5	24.7	9.04	11.4	3.02	18.802	*0.001*	15.618	*0.001*	38.551	*0.001*
SM2A	Ore concentrate (after crushing)	Ore processing plant	73.78	324	36.1	9.36	6.36	1.65	18.548	*0.004*	15.573	*0.004*	38.380	*0.004*
SM2B	Ore concentrate (after crushing)	Ore processing plant	60.39	259	26.4	6.47	5.11	1.34	18.564	*0.004*	15.578	*0.004*	38.383	*0.004*
SM3A	Ore concentrate (after flotation)	Ore processing plant	294.77	900	111	30.5	47	17.1	19.096	*0.005*	15.603	*0.005*	38.739	*0.006*
SM3B	Ore concentrate (after flotation)	Ore processing plant	74.2	416	20.2	4.37	16.5	4.48	18.962	*0.001*	15.679	*0.001*	38.816	*0.002*
SM4	Ore concentrate (after gravitation)	Ore processing plant	3514.08	3370	456	125	179	138	19.052	*0.005*	15.599	*0.005*	38.612	*0.006*
SM5	Ore concentrate (after magnetic separation)	Ore processing plant	359.16	851	122	25.3	86.4	48	19.101	*0.007*	15.598	*0.007*	38.762	*0.008*
G1	Gasoline	Orlovka settlement	N/A	N/A	N/A	N/A	N/A	N/A	18.650	*0.004*	15.665	*0.004*	38.307	*0.009*
G2	Gasoline	Orlovka settlement	N/A	N/A	N/A	N/A	N/A	N/A	18.653	*0.003*	15.655	*0.003*	38.306	*0.007*
	Lichens and birch leaves:													
LBL	Lichens	Lake Baikal	4.19	63.8	0.71	0.016	0.814	0.07	18.152	*0.001*	15.561	*0.001*	38.321	*0.001*
SEL 2	Lichens	Orlovka settlement	19.47	85.3	1.64	0.033	2.596	0.2	18.158	*0.006*	15.565	*0.005*	38.131	*0.012*
SEL 3	Lichens	Orlovka settlement	8.23	90.6	0.89	0.025	1.123	0.09	18.131	*0.001*	15.565	*0.001*	38.149	*0.002*
SEL 5	Lichens	Orlovka settlement	22.99	93.2	1.51	0.039	2.511	0.22	18.077	*0.001*	15.572	*0.001*	38.093	*0.001*
SEL 6	Lichens	Orlovka settlement	9.53	92.1	1.06	0.025	1.664	0.14	18.114	N/A	N/A	N/A	N/A	N/A
SEL 8	Lichens	Orlovka settlement	10.78	94.3	1.49	0.026	2.581	0.16	N/A	N/A	N/A	N/A	N/A	N/A
TPL 2	Lichens	Tailing pond	10.07	83.6	0.99	0.018	1.43	0.09	18.255	*0.001*	15.563	*0.001*	38.185	*0.001*
TPL 4	Lichens	Tailing pond	32.57	102.6	2.56	0.13	2.235	0.17	18.806	*0.001*	15.611	*0.001*	38.430	*0.002*
TPL1	Lichens	Tailing pond	10.5	N/A	N/A	N/A	N/A	N/A	18.300	*0.001*	15.567	*0.001*	38.180	*0.001*
TPL3	Lichens	Tailing pond	10.3	N/A	N/A	N/A	N/A	N/A	18.457	*0.001*	15.591	*0.001*	38.330	*0.002*
TPL4 ED	Lichens	Tailing pond	30.56	N/A	N/A	N/A	N/A	N/A	18.892	*0.001*	15.606	*0.001*	38.410	*0.001*
QBL	Birch leaves	Orlovka quarry	0.79	395.8	0.02	0.001	0.141	0.02	17.949	*0.003*	15.540	*0.002*	37.899	*0.006*
BGEBL	Birch leaves	2km east of Orlovka settlement	0.16	27.8	0.01	< 0.001	0.01	< 0.01	18.319	*0.002*	15.546	*0.002*	38.177	*0.004*
L1 C	Lichens	Orlovka quarry	13.62	45.5	0.87	0.035	3.578	0.2	18.113	*0.001*	15.560	*0.001*	38.159	*0.001*

	Sample description	Sampling location	Pb	Zn	Zr	Hf	Y	Yb	$^{206/204}$Pb	± 2σ	$^{207/204}$Pb	± 2σ	$^{208/204}$Pb	± 2σ
L1 ED	Lichens	Orlovka quarry	10.57	48.6	0.53	0.022	2.255	0.14	18.053	*0.001*	15.544	*0.001*	38.077	*0.002*
L2	Lichens	Orlovka quarry	21.68	41.7	1.37	0.038	2.944	0.22	18.100	*0.001*	15.555	*0.001*	38.113	*0.001*
OQL 2	Lichens	Orlovka quarry	13.37	49	1.11	0.039	3.278	0.2	18.127	*0.001*	15.564	*0.001*	38.170	*0.001*
OQL 3	Lichens	Orlovka quarry	17.88	50.3	1.29	0.052	3.869	0.31	18.089	*0.001*	15.562	*0.001*	38.139	*0.001*
OQL 4A	Lichens	Orlovka quarry	16.81	92.1	0.99	0.029	2.412	0.2	18.103	*0.001*	15.561	*0.001*	38.133	*0.002*
OQL 4C	Lichens	Orlovka quarry	11.57	43.4	0.89	0.033	2.977	0.2	18.114	*0.001*	15.555	*0.001*	38.148	*0.001*
OQL 5A	Lichens	Orlovka quarry	17.22	89.4	1.08	0.035	1.999	0.14	18.102	*0.001*	15.560	*0.001*	35.054	*0.042*
OQL 5B	Lichens	Orlovka quarry	14.59	50.3	0.9	0.036	3.817	0.22	18.128	*0.001*	15.548	*0.001*	38.134	*0.002*
SML 5	Lichens	Ore processing plant	17.7	107.5	1.66	0.037	2.645	0.2	18.216	*0.001*	15.560	*0.001*	38.194	*0.003*
SML 6	Lichens	Ore processing plant	32.52	83.7	2.57	0.072	4.004	0.26	18.212	*0.001*	15.567	*0.001*	38.118	*0.002*
SML 7	Lichens	Ore processing plant	19.73	87.9	1.67	0.037	2.276	0.18	18.140	*0.001*	15.574	*0.001*	38.139	*0.002*
SQL 4	Lichens	Spokoinoe quarry	29.26	94	2.71	0.094	6.195	0.38	18.459	*0.001*	15.565	*0.001*	38.290	*0.002*

* topaz-amazonite-albite

N/A – not analyzed

Table 6.2. Zn isotopes data for lichens and geologic samples from the Orlovka-Spokoinoe mining site. $\delta^{66}Zn$ values are given relative to in-house IMP Zn standard.

Sample ID	Sample description	Sampling location	$\delta^{66}Zn$	$\pm 2\sigma$*	$\delta^{68}Zn$	$\pm 2\sigma$
LBL	Lichens	Lake Baikal	1.270	*0.097*	2.504	*0.149*
SEL3	Lichens	Settlement	0.334	*0.021*	0.681	*0.030*
SEL6	Lichens	Settlement	0.812	*0.018*	1.612	*0.026*
TPL4	Lichens	Tailing pond	0.886	*0.044*	1.770	*0.083*
TPL1C	Lichens	Tailing pond	1.297	*0.025*	2.528	*0.029*
OQL2	Lichens	Quarry	1.163	*0.008*	2.225	*0.012*
OQL3	Lichens	Quarry	0.786	*0.015*	1.553	*0.058*
OQL4C	Lichens	Quarry	0.754	*0.016*	1.638	*0.049*
L2	Lichens	Quarry	0.890	*0.024*	1.788	*0.035*
SML6	Lichens	Processing plant	0.887	*0.044*	1.734	*0.075*
SML7	Lichens	Processing plant	1.096	*0.009*	2.143	*0.026*
2142	Biotite/muscovite granite	Orlovka stock	0.261	*0.065*	0.496	*0.072*
2151	Biotite/muscovite granite	Orlovka stock	-0.331	*0.124*	-0.734	*0.178*
2163	Mineralized toz/amz/ab** granite	Orlovka stock	1.110	*0.043*	2.164	*0.022*
2164	Mineralized toz/amz/ab granite	Orlovka stock	0.743	*0.008*	1.506	*0.015*
2213	Mineralized toz/amz/ab granite	Orlovka stock	-0.130	*0.057*	-0.153	*0.067*
2215	Mineralized toz/amz/ab granite	Orlovka open pit	0.210	*0.069*	0.446	*0.232*
2144	Amazonite pegmatite	Orlovka stock	0.704	*0.110*	1.310	*0.246*
2148	Intensely weathered amz granite	Orlovka stock	-0.241	*0.155*	-0.643	*0.630*
2173	Hornfels	Orlovka stock	-0.479	*0.024*	-0.768	*0.214*
2068	Hornfels	Khangilay pluton	0.094	*0.022*	0.095	*0.023*
2166	Hornfels	Orlovka open pit	-0.426	*0.129*	-1.074	*0.334*
2174	Hornfels	Orlovka open pit	0.174	*0.056*	0.266	*0.118*
2220	Greisenized granite	Spokoinoe open pit	-0.433	*0.126*	-0.949	*0.296*
2060	Biotite hornfels	Spokoinoe open pit	-0.479	*0.134*	-1.093	*0.137*
2125	Mineralized hornfels	Spokoinoe open pit	-0.356	*0.131*	-0.763	*0.283*

*2σ – reproducibility (n=6)

** topaz-amazonite-albite

Remarkable is the Pb enrichment during all stages of the ore processing, reaching up to 0.35% of Pb in the concentrate after gravity concentration, 359 ppm – after magnetic separation and up to 295 ppm after the sulphide flotation, final stage of the ore processing. Average Pb concentrations of lichens and leaves are lower than those of geological background represented by host rocks (16 ppm versus 24 ppm).

Ore-bearing granites of Orlovka are enriched in Zn with concentrations up to 800 ppm, whereas Zn abundances in Spokoinoe ore-bearing granites are up to 30ppm. There are two possible mechanisms that may lead to Zn accumulation in granites. The first is related to country rock – granite magma interaction processes, when fragments of Zn enriched wall rock sink into the magma. The second can refer to the hydrothermal alteration of granites and in this case Zn may be incorporated as a diadochic element in potassium feldspar and micas. Sphalerite (ZnS) can be found in hydrothermal veinlets in the greisens and host rocks contributing to elevated Zn values. Zn concentrations are on average lowest in the barren granites (66 ppm), host rocks (76 ppm including one high value of 150 ppm), and tailings (72 ppm) but are higher in the lichens and leaves (88 ppm) and ore bearing granites (176 ppm, including one high value of 800 ppm). Ore concentrates contain on average 886 ppm of Zn, with 84-324 ppm of this element found in the concentrate after the crushing stage, 3370 ppm after the gravitation stage, 851 ppm after magnetic separation and up to 900 ppm after flotation stage.

Zn is an essential element for plant metabolism and is accumulated by lichens throughout their lifetime (Takala et al., 1998). This explains the relatively high natural Zn concentrations in lichens and leaves.

6.4.2. Elemental ratios (Zr/Hf, Pb/Hf, Zn/Hf, Yb/Y, Pb/Y, Zn/Y, Yb/La, Pb/La, Zn/La)

In contrast to their behavior in common magmatic rocks, the ratios of pairs of chemically coherent elements such as Hf/Zr, Ta/Nb and heavy REE/light REE (rare earth elements) are found to increase in minerals of granitic pegmatites (Möller, 1989) typical of the Orlovka system. Extreme differentiation of melts is required to achieve changes of these ratios because of the nearly identical chemical behavior of the related elements, which is largely the result of their correspondence in ionic radii and valence. Such patterns permit the application of trace element ratios to discriminate groups of different origin and genesis.

Pb/Hf vs. **Zr/Hf** plot (Figure 6.3a) shows well-defined clusters of groups corresponding to representative groups of geologic (barren and ore-bearing granites and host rocks), anthropogenic (ore concentrates and tailings) and environmental (lichens and leaves) samples mentioned previously. Notably, lichens form a distinctive group that partially overlaps with the group of tailings. There is a wide range of Zr/Hf values for lichens and leaves ranging between 20 and 60.

On the **Zn/Hf** vs. **Zr/Hf** plot (Figure 6.3b) lichens form a separate cluster well above all sample groups. Ore-bearing granites and ore concentrates form one group whereas barren granites, host rocks and tailings are within another group.

Pb/Y vs. **Yb/Y** plot (Figure 6.3c) shows that the Pb/Y ratio of ore-bearing granites and ore concentrates is 10-100 times higher than that of the host rocks. Ore concentrates reflect features of the ore-bearing granites by forming one group with them. A group of lichens and leaves overlaps with the tailings and barren granites group. The Yb/Y ratio discriminates all samples into well-defined groups. However, ore concentrates that include products of ore processing after gravitation, magnetic separation and flotation stages do not show a distinct group but are rather scattered.

Zn/Y vs. **Yb/Y** plot (Figure 6.3d) is another suitable group discrimination diagram. There are four well-defined groups representing: 1) host rocks and barren granites which overlap at a moderate Yb/Y ratio and Zn/Y values are about 10 times lower than the other groups; 2) ore concentrates with a large range of Yb/Y and links to the ore-bearing granites, and 3) a lichens and leaves group that shows the closest overlap with the tailings, less close with other sample groups.

Pb/La vs. **Yb/La** plot (Figure 6.3e) shows that host rocks have Pb/La 10 times lower than all other groups. Ore-bearing granites are characterized by a broad range of Yb/La ratio. Lichens and leaves show the closest relationship with the tailings by plotting nearest to them.

Zn/La vs. **Yb/La** plot is shown on Figure 6.3f. Lower Zn/La levels and higher Yb/La are characteristic of host rocks and barren granites with Zn/La 10 times lower relative to other sample groups. Lichens and leaves as a cluster exhibit the lowest Yb/La ratio overlapping with tailings, ore concentrates and ore-bearing granites.

6.4.3. Pb and Zn isotopes

6.4.3.1. Pb isotopes

The following range of Pb isotope values characterizes the anthropogenic and biological samples: $^{206}Pb/^{204}Pb$ from 18.55 to 19.10; $^{207}Pb/^{204}Pb$ from 15.57 to 15.68 and $^{208}Pb/^{204}Pb$ from 38.38 to 38.82 for ore concentrates; $^{206}Pb/^{204}Pb$ from 18.12 to 19.18; $^{207}Pb/^{204}Pb$ from 15.56 to 15.61 and $^{208}Pb/^{204}Pb$ from 37.76 to 38.56 for tailings; and $^{206}Pb/^{204}Pb$ from 17.95 to 18.89; $^{207}Pb/^{204}Pb$ from 15.54 to 15.61 and $^{208}Pb/^{204}Pb$ from 37.9 to 38.43 for lichens and birch leaves (Table 6.1, Figure 6.4). Granites and ore concentrates exhibit the most radiogenic Pb isotope values of the analyzed sample suite while the majority of lichens and leaves exhibit the least radiogenic range of Pb isotopes and show a significantly different $^{206}Pb/^{204}Pb$ composition than the rest of the groups. Host rocks and tailings show intermediate values of Pb isotopes between the two groups described above.

6.4.3.2. Zn isotopes

The isotopic composition of Zn varies within the Orlovka-Spokoinoe mining district with the total range for geologic samples of -0.5 to +1.1‰ and for lichens of +0.3 to +1.3‰ in $\delta^{66}Zn$ (Figure 6.5). These deviations are significant compared to the analytical uncertainties associated with individual analyses of 0.06‰.

Mass-dependent fractionation of $\delta^{66}Zn$ and $\delta^{68}Zn$ is shown on Figure 6.6. Geological samples from the Orlovka and Spokoinoe deposits form a trend, where Orlovka ore-bearing granites are located at the isotopically heavier end ($\delta^{66}Zn$ of up to +1.1‰) and Orlovka barren granites, hornfels and Spokoinoe ore-bearing granites at the end with the lightest Zn isotopes ($\delta^{66}Zn$ of -0.1 to -0.4‰). Hornfels, barren granites and Spokoinoe ore-bearing (Sn-W) granite show a rather narrow range of Zn isotopes ($\delta^{66}Zn$ of –0.5 to +0.3‰) compared to the Orlovka ore-bearing (Ta-Nb) granites with larger and much heavier isotopic variability ($\delta^{66}Zn$ of -0.1 to +1.1‰). Among ore-bearing Orlovka granites only one sample showed a heavy Zn isotopic composition of +1.1‰ whereas the most common isotopic composition of these granites is in the range between –0.1 to +0.7‰. Other data on terrestrial geologic materials, i.e. USGS terrestrial basalt BCR-1 showed small fractionations of $\delta^{66}Zn$ of 0.2±0.06‰, whereas black shales exhibited a positive fractionation of Zn isotopes with large variations in $\delta^{66}Zn$ of +0.3 to +1.1‰ (Archer and Vance, 2002).

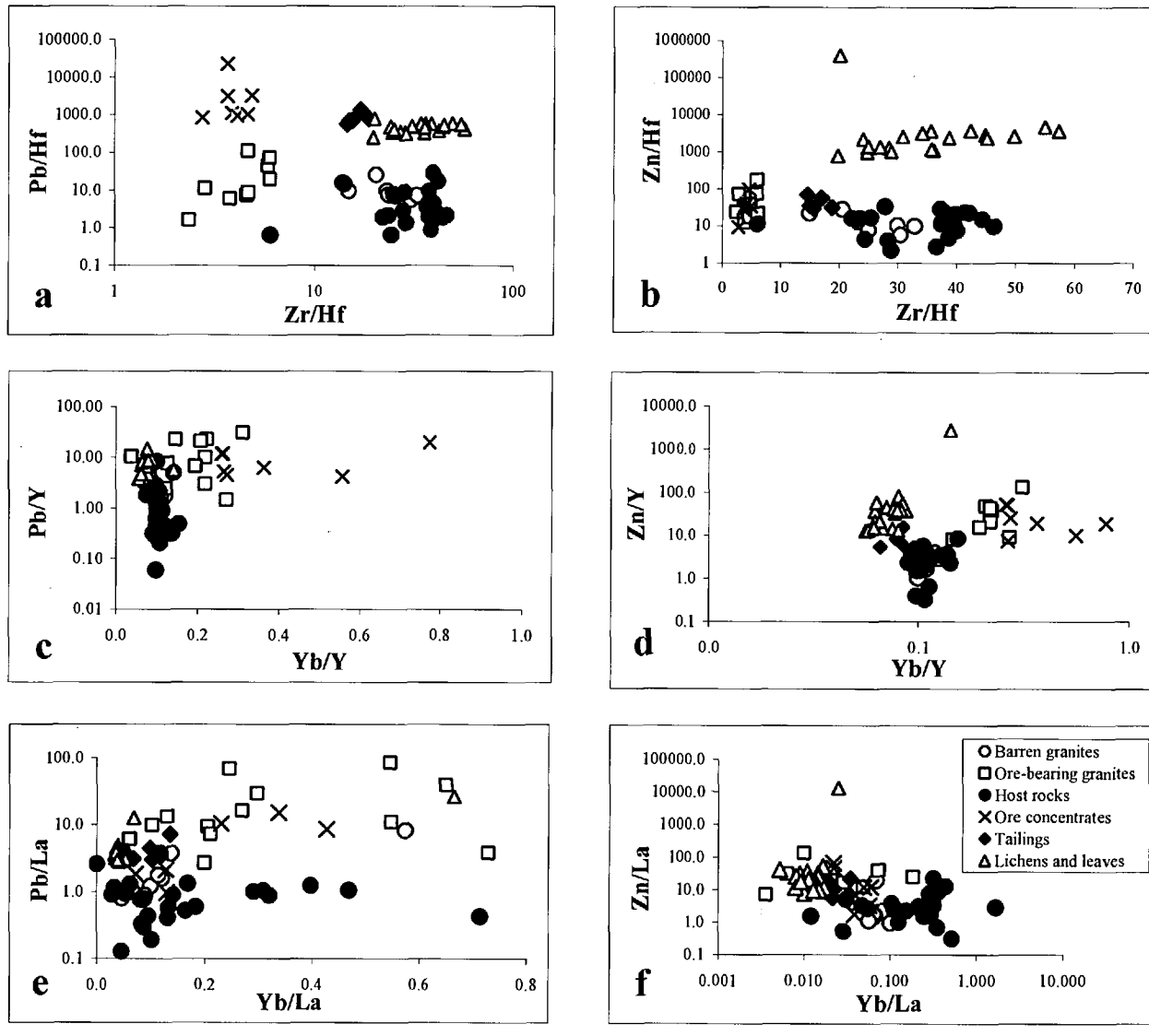

Figure 6.3. Plots of Zr/Hf vs. Pb/Hf (a), Zr/Hf vs. Zn/Hf (b), Yb/Y vs. Pb/Y (c), Yb/Y vs. Zn/Y (d), Yb/La vs. Pb/La (e) and Yb/La vs. Zn/La (f) for different potential sources (barren and ore-bearing granites, host rocks, ore concentrates and tailings) and receptors (lichens and birch leaves) from the Orlovka-Spokoinoe mining site.

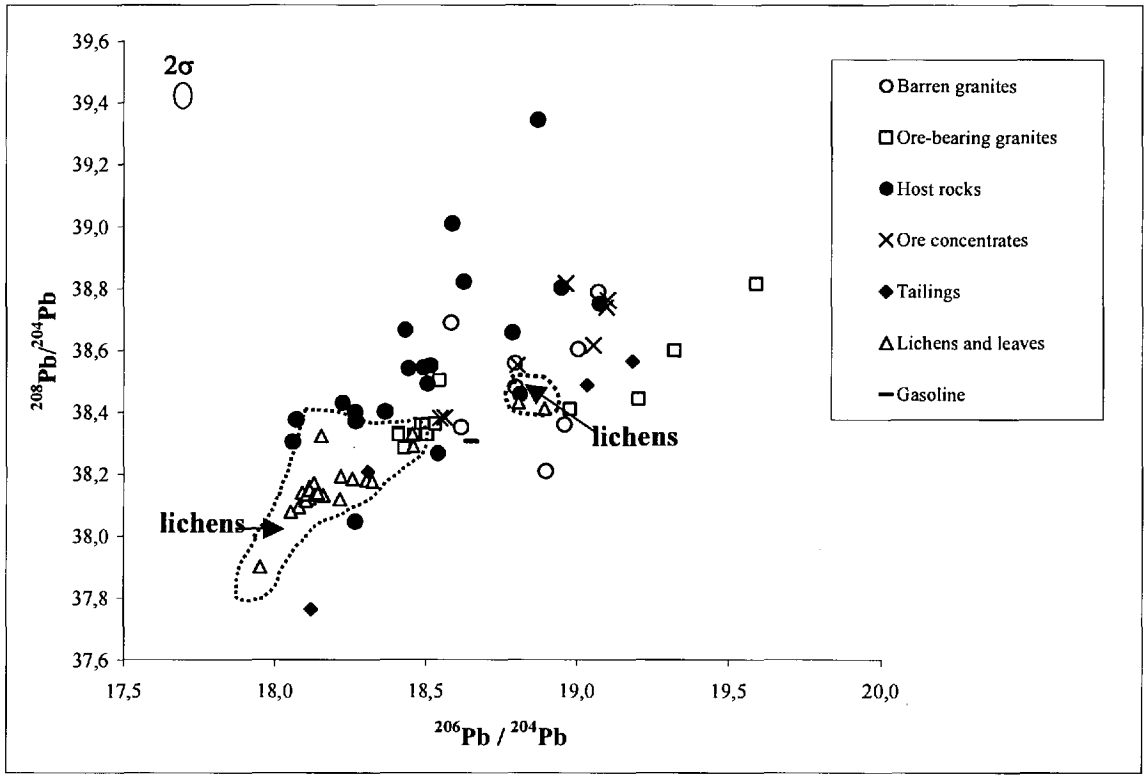

Figure 6.4. $^{206}Pb/^{204}Pb$ vs. $^{208}Pb/^{204}Pb$ for different potential sources (barren and ore-bearing granites, host rocks, ore concentrates, tailings, gasoline and Pb aerosols) and receptors (lichens and birch leaves) from the Orlovka-Spokoinoe mining site.

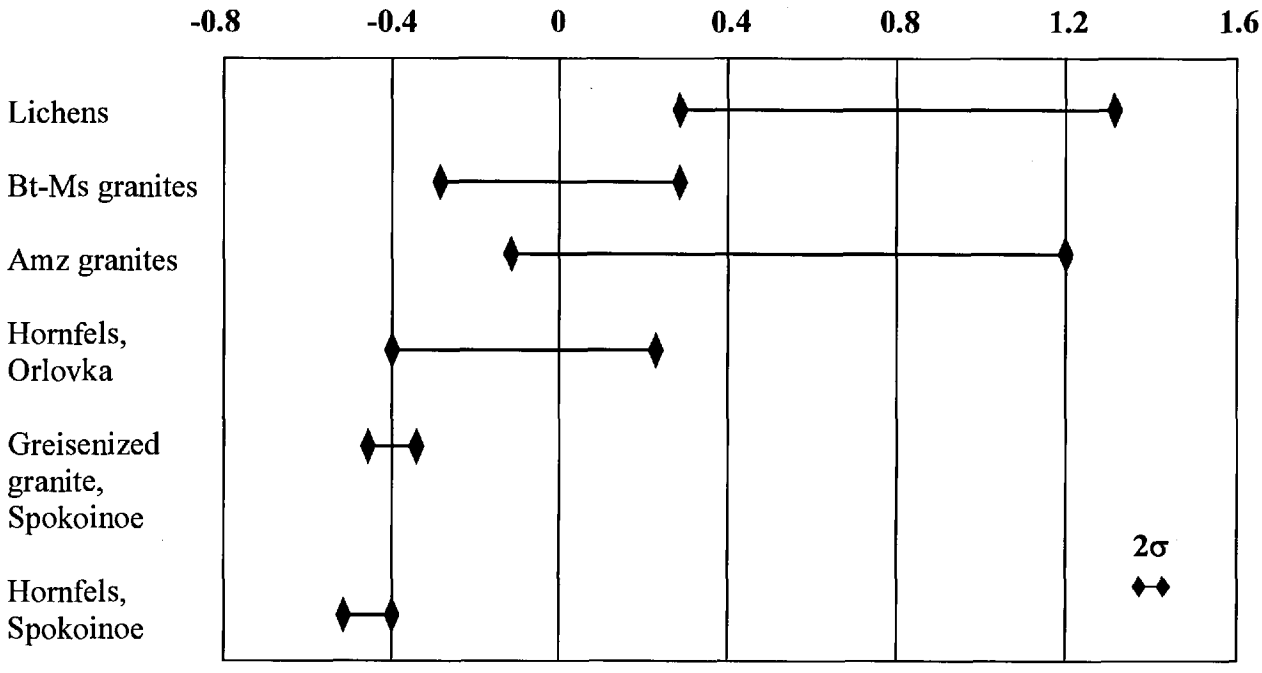

Figure 6.5. Summary of $\delta^{66}Zn$ data for geologic samples and lichens from the Orlovka-Spokoinoe mining site. All data are given relative to in-house IMP Zn standard. The number of replicates used for each samples is 4.

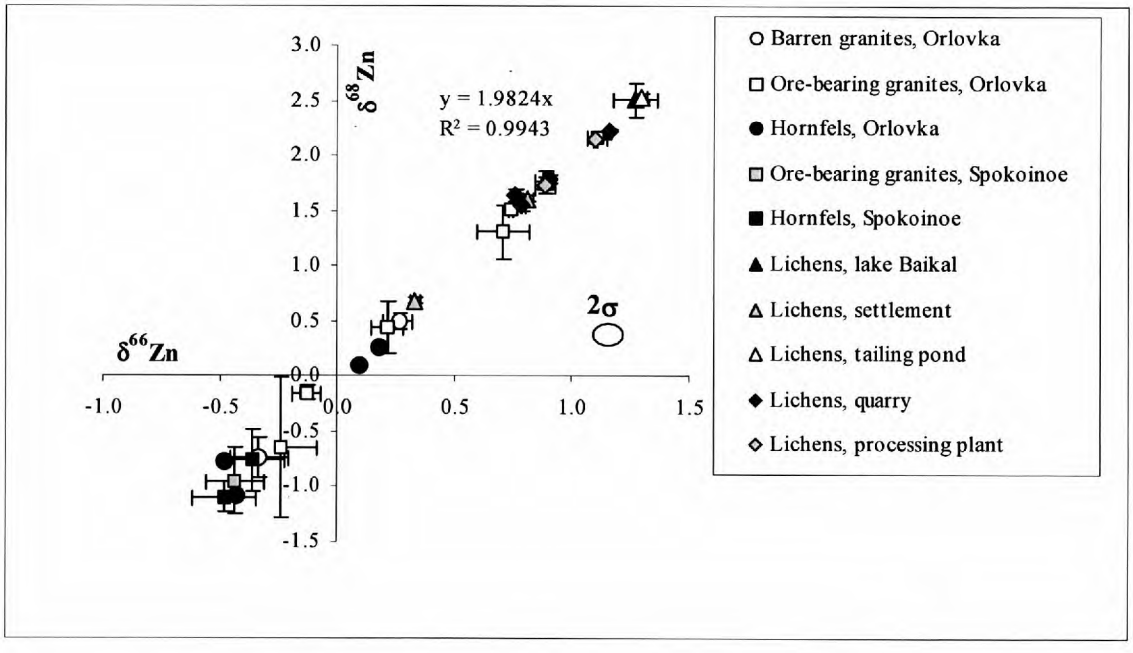

Figure 6.6. $\delta^{66}Zn$ versus $\delta^{68}Zn$ for 26 geologic and lichens samples from the Orlovka-Spokoinoe mining site. Error bars represent 2 × the combined errors (95% confidence level) for each determination. The gradient and intercept (within error of the origin) of this regression line are consistent with mass dependent Zn isotopic variability.

Both basalts and shales fall within the expanded range of Zn isotope variations typical for the Orlovka-Spokoinoe mining site. These variations are also similar to the reported Zn isotope composition of sphalerite in carbonate-hosted Zn-Pb deposits of the Irish ore field (δ^{66}Zn of -0.3 to +1.2‰) (Wilkinson et al., 2003).

Lichens show a positive and rather expanded range of Zn isotopes with δ^{66}Zn of +0.3 to1.3‰. Compared to geologic samples, lichens have the heaviest values of Zn isotopes. Possible explanations for this observation are discussed below.

6.5. DISCUSSION

6.5.1. Pb and Zn enrichment

Although the absolute enrichment value was shown to be of questionable value when calculated relative to average crustal abundances (Reimann and Caritat, 2000), in this paper we calculate Pb and Zn enrichment relative to local geologic background. Pb and Zn enrichments were calculated using the following equation:

$EF_X = (X/Zr)_{sample} / (X/Zr)_{host\ rocks}$,

where X – element of interest (Pb or Zn here), $(X/Zr)_{sample}$ – ratio of the sample and $(X/Zr)_{host\ rocks}$ – ratio of the host rocks representing the local background value. The used background values were: Pb/Zr = 0.152±0.123 and Zn/Zr = 0.398±0.277 (n=13). These values of the local geological background are comparable with the upper crustal Pb/Zr and Zn/Zr values of 0.105 and 0.373 respectively (Taylor & McLennan, 1985).

Figure 6.7a shows the Pb enrichment ($EFPb$) for the barren granites (A), ore-bearing granites (B), tailings (C), ore concentrates (D) and lichens and birch leaves (E).

The Pb/Zr ratios are highest in the ore-bearing granites (up to 24.2) and ore concentrates (up to 7.7 after gravitation) but low (below 1) in all host rocks, barren granites and lichens. The tailings have slightly higher Pb/Zr ratios, ranging between 0.7 and 1.3. Zn/Zr values vary between different sample groups, reaching a maximum in lichens (61 in average) and a minimum in barren granites and host rocks (0.6 and 0.4 respectively).

Zn/Zr for ore-bearing granites and ore concentrates are of higher values (9.3 and 9.5), compared to tailing pond sediments where Zn/Zr is around 3. Overall, Pb and Zn concentrations in lichens and leaves do not suggest any Pb and Zn contamination of the environment despite the high concentrations of potential sources such as ore

concentrates and ore bearing granites. However, calculated Pb enrichment relative to host rock Pb/Zr shows slight Pb enrichment in the tailings (between 5 and 8 times) and in lichens (between 2 and 5 times), suggesting a notable Pb enrichment despite the low Pb concentrations. Similarly, Zn enrichment relative to the average host rocks is noted for all sample suites with enrichment reaching up to 7 times in barren granites and tailings, 23-24 times in ore-bearing granites and ore concentrates and up to 152 times for lichens and birch leaves (Figure 6.7b). This suggests significant Zn enrichment despite low Zn concentrations.

6.5.2. Zr/Hf, Pb/Hf, Zn/Hf, Yb/Y, Pb/Y, Zn/Y, Yb/La, Pb/La, Zn/La – tracing the metal dispersal

Use of these indicative ratios allows assessment of the relationship between the sample groups of different origins. For example, use of Zr/Hf as a good indicator of crystallization differentiation in magmatic rocks was previously mentioned. Here, this indicative ratio plotted against Pb/Hf permitted: 1) distinction between different sample groups such as (a) ore-bearing granites, (b) barren granites and host rocks, (c) ore concentrates, and (d) lichens, leaves and tailings (Figure 6.3a); and 2) identification of the main Pb source such as tailings with which lichens and leaves form a clearly distinguished group.

Y, commonly used as an analogue to the LREE is contained in xenotime, which plays a role in the magmatic fractionation of the Orlovka-Spokoinoe granite suite. Xenotime is known to be a stable accessory phase in the Khangilay pluton but was unstable in the F-enriched environment of the ore-bearing processes leading to the Orlovka Ta-Nb and Spokoinoe W-Sn deposits. This explains the change from immobility to mobility of Y from the low fractionated Khangilay pluton to the highly fractionated Orlovka-Spokoinoe ore-bearing granites and consequently their technogenic (anthropogenic) products, – the ore concentrates. Yb represents the HREE and La – the LREE. Therefore, the Yb/La ratio is used to normalize the whole REE spectrum, showing slightly different features in contrast to the Yb/Y ratio (Figures 6.3 c-f). Comparison between Yb/Y and Yb/La indicated that Y and La behaved similarly relative to Yb in all sample groups except ore concentrates reflecting the different behavior of Y and La during the ore processing.

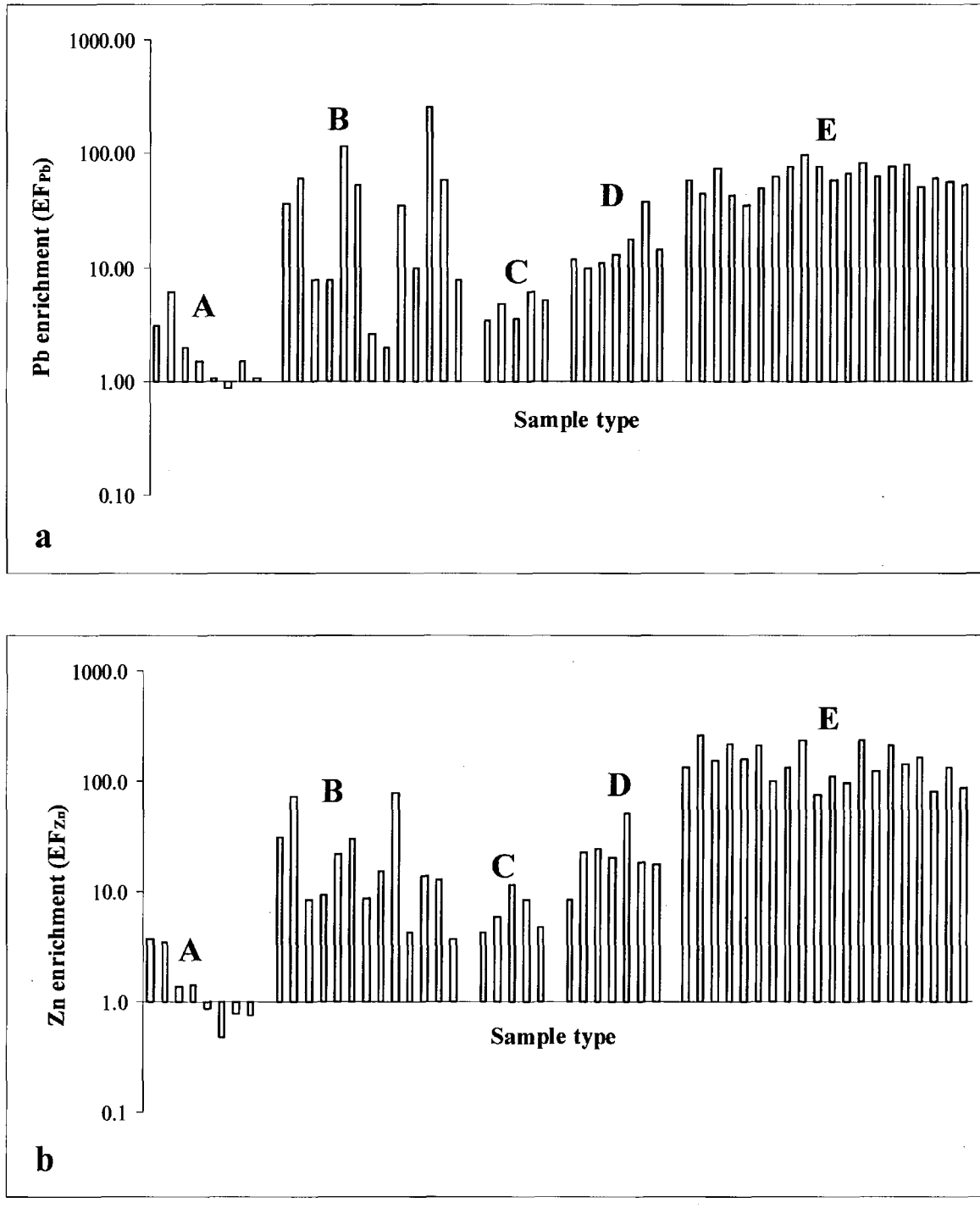

Figure 6.7 a,b. Pb and Zn enrichment factor EF_{Pb}, EF_{Zn} of the different potential sources (A – barren granites, B – ore-bearing granites, C – tailings and D – ore concentrates) and receptors (E – lichens and birch leaves) relative to the Pb/Zr and Zn/Zr background values of the host rocks (0.152±0.123 and 0.398±0.277, respectively, n=13).

Ore concentrates have the highest Yb/Y and moderate Yb/La values compared to other sample groups. The highest Yb/Y value can be explained by xenotime (as the Y carrier) removal during different stages of ore processing leading to the highest values. Plots of Pb/Y vs. Yb/Y, Zn/Y vs. Yb/Y, Pb/La vs. Yb/La and Zn/La vs. Yb/La (Figures 6.3 c-f) reflect different geologic and technogenic processes resulting in distinct sample groups. However, on all plots lichens and leaves always exhibit the closest link to the tailings and host rocks, in many cases forming a clearly defined group with them, whilst the relationship to the other sample groups is less clear.

6.5.3. Pb isotopes as contamination tracers

6.5.3.1. Mixing diagram

The mixing diagram ($^{206}Pb/^{204}Pb$ vs.1/Pb) was used previously to show a relationship between barren and ore-bearing granites of the Orlovka and Spokoinoe granite massifs (Dolgopolova et al., 2004). The Pb isotope signatures of the host rocks appeared to be more scattered than those of the granite rocks plotting off the granite mixing line. Although the Pb uptake phenomena of lichen is still poorly understood and may be the main reason for concentration variations and generally lower concentration levels found in the biological material compared to the geological samples, biological samples (lichens and leaves) and anthropogenic products (i.e. ore concentrates and tailings) are shown on the same plot together with the geologic suite (Figure 6.8). Ore concentrates and tailings are compatible with the basement sources and are plotted together with ore-bearing and barren granites as its end-members, thus reflecting their genetic relationship.

There is no clear relation of the isotope/concentration trend of most of the biological materials (lichens and leaves) to the trends of the mining district (e.g., to the radiogeneity of the ore concentrates and ore bearing granites, to the overall trend of the host rocks, to the barren granites and their higher radiogeneity, and to the tailing pond data, which are either oriented towards ore bearing granites or low-radiogenic host rocks). Taken as a whole, lichens and leaves from the Orlovka-Spokoinoe mining district form two groups. One, represented by three samples, fits the local mining district trends indicating response to local influence of mining and ore processing activities. The second (main) group (23 samples) is rather homogeneous and does not reflect the heterogeneous and rather radiogenic trends of the mining

district. This main lichen group requires Pb deposition from well-mixed air masses, which transfer only minor Pb contribution from the local sources to the biological materials. Lichens are effective as tracers of atmospheric contamination on a regional scale as several studies indicated (Keinonen, 1992; Carignan and Gariepy, 1995; Getty et al., 1999; Simonetti et al, 2003; Zschau et al., 2003). The group of lichens and leaves plot closest to the combined group of Pb aerosols from Eastern Europe, Russia and Mongolia (the reference Pb aerosols values were taken from Bollhoefer and Rosman, 2001, 2002) (Figure 6.9). A few tailings also show a contribution from such external source, these samples plot within the lichens and leaves group (Figure 6.4). Importantly, Pb isotope data of lichens sampled from the Lake Baikal area located ca. 500 km away from the mining site perfectly fits the average isotope composition of the main biological material data group. This favors the importance of Pb transfer from distant sources to the lichens.

6.5.3.2. Geogenic and aerosol Pb and fractional contribution calculations

Two main mixing lines, i.e. "geogenic Pb" defined by geologic samples and their anthropogenic products and "aerosol Pb" represented by atmospheric Pb aerosols are shown in Figure 6.9. The relative contribution of each source was calculated using a binary mixing model described in detail in Chiaradia et al. (2000). The following system of equations was used for the calculations:

$R^a = R^a_1 X_1 + R^a_2 X_2$

$X_1 + X_2 = 1,$

where X is a fractional contribution of: X_1 – geogenic Pb, X_2 – aerosol Pb; R^a refers to $^{206}Pb/^{204}Pb$ ratio of: R^a – measured in sample, R^a_1 – geogenic Pb, R^a_2 – aerosol Pb. Pb isotopic composition of lichens from the Lake Baikal area indicates air mass composition on a large scale, and the impact of this air mass composition on the airborne Pb deposition in the study area; therefore it was taken as "aerosol Pb" end-member in the calculations ($^{206}Pb/^{204}Pb$ = 18.152). The geogenic data distribution is rather heterogenic. An average Pb isotopic composition of the ore concentrates was taken as representative of the "geogenic Pb" with $^{206}Pb/^{204}Pb$ of 18.875. The calculated fractional contribution from both sources, aerosol Pb and geogenic Pb, to Pb isotopic signatures of lichens is shown in Figure 6.10.

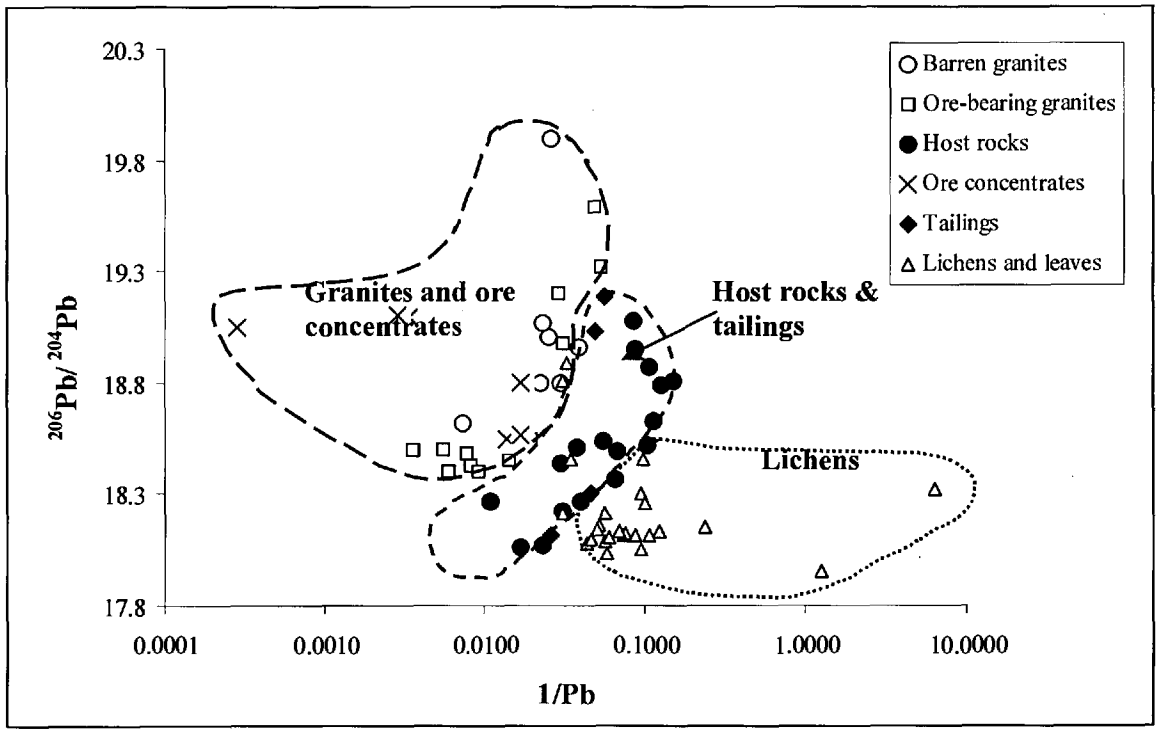

Figure 6.8. $Pb^{206}/Pb^{/204}$ vs.1/Pb mixing diagram for different potential sources (barren and ore-bearing granites, host rocks, ore concentrates and tailings) and receptors (lichens and birch leaves) from the Orlovka-Spokoinoe mining site.

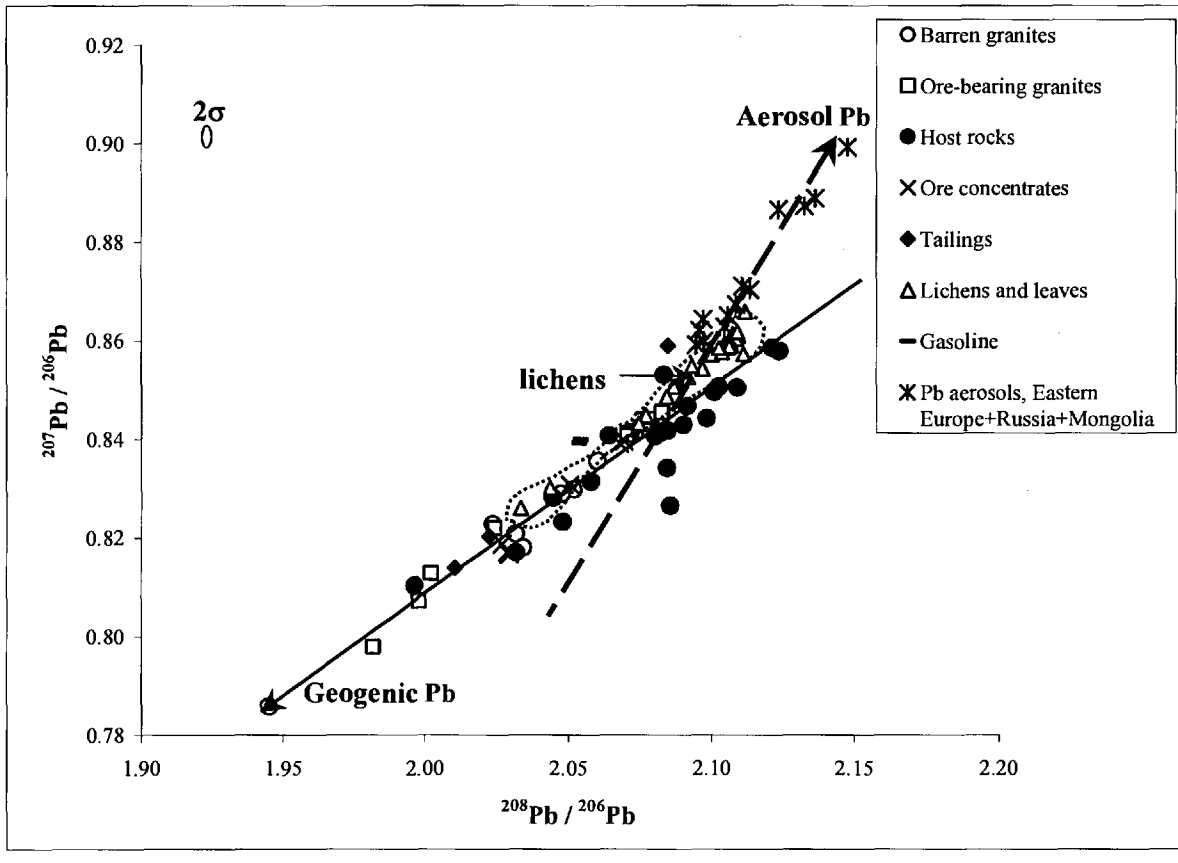

Figure 6.9. $^{208}Pb/^{206}Pb$ vs. $^{207}Pb/^{20b}Pb$ plot for different potential sources (barren and ore-bearing granites, host rocks, ore concentrates, tailings, gasoline and Pb aerosols) and receptors (lichens and birch leaves) from the Orlovka-Spokoinoe mining site. Pb input via two transport paths can interpret the data trends: atmospheric deposition of anthropogenic lead and non-atmospheric geogenic Pb.

The dominant impact of Pb aerosols on Pb isotopic signature of lichens is apparent. 86-100% of Pb aerosols contribution is observed on lichens sampled around the settlement, processing plant and quarry. The minimum impact of Pb aerosols is noted on lichens taken from the tailing pond vicinity, where 46% of Pb comes from Pb aerosols but the 54% of Pb originates from the geogenic source. In this location the wind-blown particles of the tailing pond accumulated in lichens (for details and SEM images of particles see Dolgopolova et al., in print), play a dominant role on their Pb isotopes signature and overprint the signature of long-range Pb aerosols.

One lichen sample that was taken from the Spokoinoe quarry located ~8 km away from the Orlovka quarry showed that 54% of Pb originated from the atmospheric aerosols and 46% - from the geogenic source in agreement with the trends of the Orlovka district.

6.5.4. Zn isotopes

Zn isotope variability in minerals, ore materials and environmental samples, including biological Zn isotopic discrimination remains poorly constrained. Isotopic variability of terrestrial Zn can provide unique opportunities for quantifying the sources and pathways of Zn within the terrestrial environment. Using Zn isotopic composition of sphalerites in carbonate-hosted Zn-Pb deposits of the Irish ore field, Wilkinson et al. (2003) suggested that Zn isotopes have a potential for distinguishing between fertile and barren geological systems, and for studying flow pathways utilised by hydrothermal fluids and processes of ore deposition. Distinctions between the Zn isotopic composition of host rocks, barren granites and Spokoinoe ore-bearing granite (Sn-W, one sample) and ore-bearing granites (Ta-Nb) of the Orlovka stock, may indicate yet unidentified processes controlling the formation of ore-bearing amazonite granites of Orlovka that resulted in selective accumulation of the isotopically heavier Zn. Another possibility may be two sources of Zn with contrasting isotopic composition found in the Spokoinoe Sn-W and in the Orlovka Ta-Nb deposits.

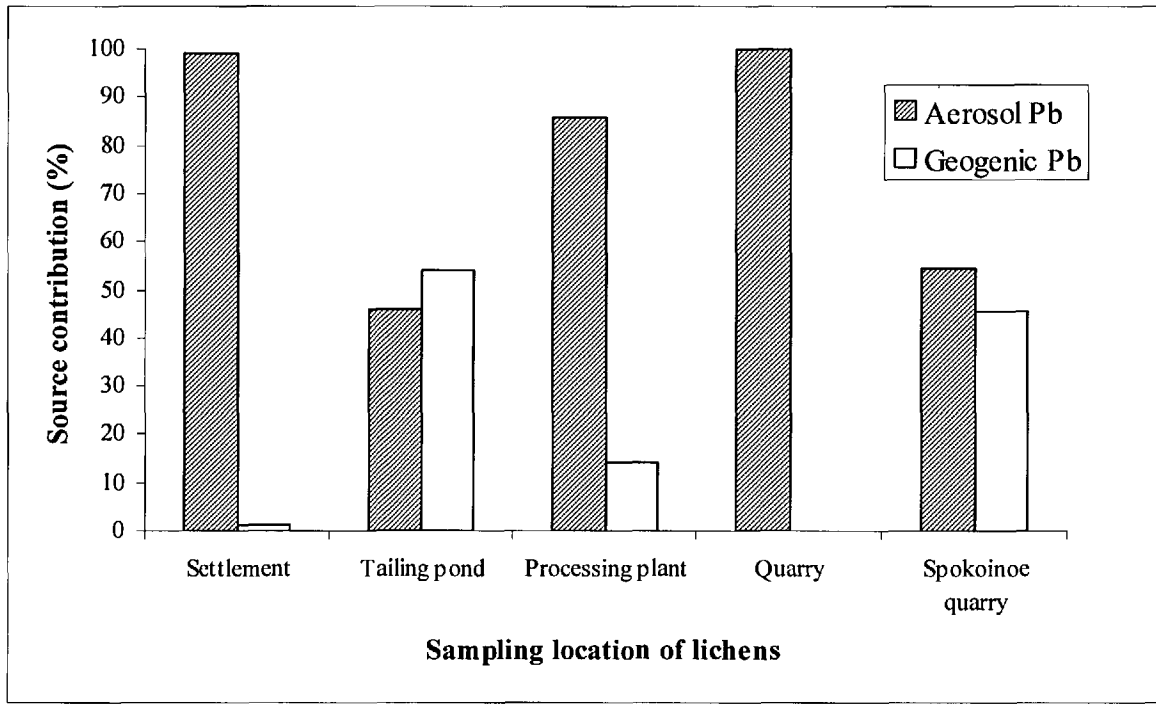

Figure 6.10. Source contribution to the Pb isotopic signature of lichens and birch leaves from the Orlovka-Spokoinoe mining site. Host rocks, barren granites and Pb aerosols contribution represent 3-component mixing model. The calculation for fractional source contribution is explained in section 4.3 of this paper.

A study on Zn isotope variations in deep-sea carbonates from the Pacific ocean showed that most of the Zn isotope variability in these rocks is a result of the selective entrapment of the light isotopes by organic matter in the surface water (Pichat et al., 2003). It was shown that biological activity fractionates isotopes and the biological processes prefer the light Zn isotopes. In a plant study Mason et al. (2003b) also showed evidence of preferential uptake of the lightest Zn isotopes in biochemical reactions (biological activity). Compared to geological material, lichens from the Orlovka-Spokoinoe mining site exhibit heavier Zn isotopic compositions that only partly overlap the positive variations of the extended Zn isotopic range of the geological samples. Interestingly, the isotopically heaviest Zn is found in lichens sampled from the tailing pond area within the Orlovka-Spokoinoe site and from the pristine environment of Lake Baikal situated about 500 km away from the mining area. Similarly to the Pb isotope data, Zn isotopes in lichens exhibit uniform Zn isotopic variations that are independent of the sampling locality. The presence of isotopically heavier Zn in lichens compared to the geologic samples from the mining area suggests three possibilities. These are: 1) it is related to the rather selective adsorption of Zn on the lichen surface; 2) it reflects the influence of regional aerosols characterized by a heavy Zn isotopic composition as a result of smelting or other industrial activities that lead to the distinctive Zn isotopic signature, and 3) the source of isotopically heavy Zn detected in lichens has not yet been found and still needs to be identified. Although there are no published Zn isotope data on plants and lichens, Zn isotopes have been shown to be fractionated during uptake and incorporation by higher plants and by more than one process during plant uptake (Mason, 2003b). The average δ^{66}Zn isotopic composition of roots and shoots of rice, lettuce and tomato were in the range from -0.08 to +0.19‰ and from +0.06 to a maximum of +0.72‰ of their seeds. These reported values are well below the Zn isotope data obtained for lichens from the studied mining site. An unidentified source of isotopically heavy Zn within the Orlovka-Spokoinoe mining site possibly reflects Zn contamination from a geographically remote high-temperature furnace or smelting complex; emissions from these industries may have an impact even on distant regions when transported by aerosols. Earlier studies demonstrated the hundred-fold enrichment for Zn and Pb in aerosols (Luck et al., 2002). Therefore the source of isotopically heavy Zn within the Orlovka-Spokoinoe mining site could be

potentially associated with earlier described long-range atmospheric aerosols that also contributed a significant amount of Pb to the studied mining site (see discussion on Pb isotopes).

6.6. CONCLUSIONS

A study using a combination of several powerful geochemical tools such as elemental concentrations, elemental ratios and Pb and Zn isotopic data provided a unique possibility to identify Pb and Zn sources within the studied mining site and resulted in the following conclusions:

1. Significant Pb and Zn enrichment relative to the host rocks was observed in all samples despite relatively low Pb and Zn concentrations;
2. Pb/Y vs. Yb/Y, Zn/Y vs. Yb/Y, Pb/La vs. Yb/La and Zn/La vs. Yb/La plots reflected different geologic and technogenic processes but all exhibited the closest link of lichens and leaves to the tailings and host rocks, suggesting these two sources to be the major geologic-anthropogenic contributors to the dispersal of Pb and Zn within the mining site using these indicators;
3. Pb isotopes allowed discrimination between four main sources of Pb dispersal within the Orlovka-Spokoinoe mining site, i.e. two geologic sources represented by granites and host rocks, an anthropogenic source such as tailings, and a long-range atmospheric Pb source. The influence of geologic and anthropogenic sources on Pb isotope signature of lichens accounts for only 11% of all lichen samples. Pb aerosols form a dominant source for Pb deposition on lichens within the mining site with 89% of lichens showing the influence of this source. This allows conclusion that Pb dispersal within the site is not mainly caused by human activities but rather reflects long-distance atmospheric aerosols input of Pb;
4. Zn isotope data enabled distinction to be made between isotopic signatures of lichens and the geological suite, where the isotopically heavier Zn is observed in lichens and lighter Zn in the geologic suite. Isotopically heavy Zn in lichens is likely to reflect Zn contamination from a geographically remote high-temperature furnace or smelting complex and could be potentially associated with earlier described long-range atmospheric aerosols that contributed a significant amount of Pb to the studied mining site.

5. Application of high-precision Pb, Zn isotope analyses allowed discrimination of important metal sources, which would have failed on the basis of the low Pb, Zn concentrations in the studied materials alone. Combined with Pb isotopes, Zn isotopes variations could establish new possibilities in assessing metal origins and processes in the environment.

Both elemental ratios and Pb isotopes identified host rocks and tailings as sources of Pb and Zn within the mining site whereas granites and a long-range atmospheric source of Pb were appointed in addition using Pb isotopes. Only a combination of different geochemical tools allowed a comprehensive appointment of Pb and Zn sources within the Orlovka-Spokoinoe mining site, where each of the methods brought additional insights on behavior of these elements in the studied mining environment.

ACKNOWLEDGEMENTS

The authors would like to acknowledge the assistance of staff of the EMMA laboratory at the Natural History Museum London with the analytical part of the project. AD appreciates support through Albert Julius Bursary (Imperial College London), ORS Award, INTAS Young Scientist Award and research funds of the Department of Mineralogy (Natural History Museum, London). British Airways are thanked for providing London-Moscow return flights for AD, DW and CJS under their Communities and Conservation Programme. Financial support from NERC, the Leverhulme Trust, Imperial College London and The Natural History Museum is gratefully acknowledged.

6.7. REFERENCES

Albarède F., 2004. The stable isotope geochemistry of copper and zinc. In: Johnson, M., Beard, B.L., and Albarède, F. (Eds.), Mineralogical Society of America. Reviews in Mineralogy and Geochemistry 55, 409-427.

Archer, K. and Vance, D., 2002. Large fractionations in Fe, Cu and Zn isotopes associated with Archean microbially-mediated sulphides. Geochimica et Cosmochimica Acta 66 (15A), A26 Suppl.

Ault, W.A., Senechal, R.G., Erlebach, W.E., 1970. Isotopic composition as a natural tracer of lead in the environment. Environmental Science and Technology 4, 305-311.

Badanina, E.V., Veksler, I.V., Thomas, R., Syritso, L.F., Trumbull, R.B., 2004. Magmatic evolution of Li-F, rare-metal granites: a case study of melt inclusions in the Khangilay complex, Eastern Transbaikalia (Russia). Chemical Geology 110(1-4), 113-133.

Bau, M., 1996. Controls on the fractionation of isovalent trace elements in magmatic and aqueous systems: evidence from Y/Ho, Zr/Hf, and lanthanide tetrad effect. Contributions to Mineralogy and Petrology 123, 323-333.

Ben Othman D., Luck J. M., Grousset F., Rousseau D., and Albarède F., 2001. Cu, Zn (and Pb) isotopes in aerosols and loesses. 11th European Union of Geosciences Conference, 688.

Beskin, S.M., Grebennikov, A.M., Matias, V.V., 1994. The Khangilai granite pluton and the related Orlovskoe tantalum deposit in the Transbaikal region. Petrology 2, 56-74.

Bollhoefer, A. and Rosman, K.J.R., 2001. Isotopic source signatures for atmospheric lead: The Northern Hemisphere. Geochimica et Cosmochimica Acta 65 (11), 1727-1740.

Bollhoefer, A. and Rosman, K.J.R., 2002. The temporal stability in lead isotopic signatures at selected sites in the Southern and Northern Hemispheres. Geochimica et Cosmochimica Acta 66 (8), 1375-1386.

Carignan, J. and Gariepy, C., 1995. Isotopic composition of epiphytic lichens as a tracer of the sources of atmospheric lead emissions in southern Quebec, Canada. Geochimica et Cosmochimica Acta 59 (21), 4427-4433.

Chiaradia, M. and Cupelin, F., 2000. Behavior of airborne lead and temporal variations of its source effects in Geneva (Switzerland): comparison of anthropogenic versus natural processes. Atmospheric Environment 34, 959-971.

Dolgopolova, A., Seltmann, R., Kober, B., Weiss, D., Stanley C., Dulski, P., 2004. Geochemical characteristics and Pb isotope systematics of highly fractionated Li-F enriched amazonite granites and related host rocks of the Orlovka-Spokoinoe mining district, Eastern Transbaikalia (Russia). IMM Transactions. Section B: Applied Earth Sciences, 113, 83-99.

Dolgopolova, A., Weiss, D., Seltmann, R., Stanley C., Coles, B., Cheburkin A.K. Closed-vessel microwave digestion technique for lichens and leaves prior to determination of trace elements (Pb, Zn, Cu) and stable Pb isotope ratios. International Journal of Environmental Analytical Chemistry, in print.

Dolgopolova, A., Weiss, D.J., Seltmann., R., Dulski, P. Tracing dust and Pb dispersal at the Orlovka Ta-W mining and ore processing site: insights from REE patterns and elemental ratios. Journal of Hazardous Materials, submitted.

Dulski, P., 1994. Interferences of oxide, hydroxide and chloride analyte species in the determination of rare elements in geological samples by inductive coupled plasma-mass spectrometry. Fresenius Journal of Analytical Chemistry 350, 194-203.

Dulski, P., 2001. Reference materials for geochemical studies: new analytical data by ICP-MS and critical discussion of reference values. Geostandard Newsletter. The Journal of Geostandards and Geoanalysis 25, 87-125.

Galer, S.J.G and Abouchami, W., 1998. Practical application of lead triple spiking for correction of instrumental mass discrimination, Mineralogical Magazine 62 (A), 491-492.

Getty, S.R., Gutzler, D.S., Asmerom, Y., Shearer, C.K., Free, S.J., 1999. Chemical signals of epiphytic lichens in southern North America; natural versus man-made sources for airborne particulates. Atmospheric Environment 33, 5095-5104.

Ginzburg, L., Mayorova, O., Shatov, V., 2000. In: INTAS 97-0721 project report on geological control of metal distribution and environmental consideration in the abandoned mine lands of Orlovka, Transbaikalia, Russia. Moscow, Russia.

Keinonen, M., 1992. The isotopic composition of lead in man and the environment in Finland 1966-1987: isotope ratios of lead as indicators of pollutant sources. The Science of the Total Environment 113, 251-268.

Kober, B., Wessels, M., Bollhoefer, A., Mangini, A., 1999. Pb isotopes in sediments of lake Constance, Central Europe constrain the metal pathways and the contamination history of the catchment, the lake and the regional atmosphere. Geochimica et Cosmochimica Acta 63 (9), 1293-1303.

Kovalenko, V.I., Kostitsyn, Yu.A., Yarmolyuk, V.V., Budnikov, S.V., Kovach, V.P., Kotov, A.B., Sal'nikova, E.B. and Antipin, V.S., 1999. Magma sources and the isotopic (Sr and Nd) evolution of Li-F rare-metal granites. Petrology 7 (4), 383-409.

Kremenetsky, A.A., Ginsburg, L.N., Matias, V.V., Shatov, V.V., Aksyuk, A.M., Zaraisky, G.P., Seltmann, R, Stanley, C.J., Raimbault, L., 1999. Toxic element dispersal in the Orlovka deposit area, Transbaikalia, Russia. In: Stanley, et al. (Ed.). Mineral Deposits. Joint SGA-IAGOD Symposium London, Balkema Rotterdam 1191-1194.

Luck, J.M., Othman D.B., Albarède F.A., Telouk P., 1999. Pb, Zn and Cu isotopic variations and trace elements in rain. In: Armannsson (Ed.), Geochemistry of the Earth's surface. Balkema, Rotterdam.

Luck, J.M. and Othman D.B., 2002. Trace element and Pb isotope variability during rainy events in the NW Mediterranean: constraints on anthropogenic and natural sources. Chemical Geology 182, 443-460.

Maréchal, C.N., Telouk, P., Albarède, F., 1999. Precise analysis of copper and Zn isotopes by plasma-source mass spectrometry. Chemical Geology 156, 251-274.

Maréchal, C. N., Nicolas, E., Douchet, C., Albarède, F., 2000. Abundance of Zn isotopes as a marine biogeochemical tracer. Geochemistry Geophysics Geosystems 1, GC000029.

Maréchal, C. N. and Albarède, F., 2002. Ion-exchange fractionation of copper and Zn isotopes. Geochimica et Cosmochimica Acta 66, 1499-1509.

Mason, T.F.D., Weiss, D.J., Coles B.J., Horstwood, M., Parrish, R.R., Zhao F.J., Kirk G.J.D., 2003a. Isotopic discrimination of Zn during root-uptake and cellular incorporation in higher plants. Geophysical Research Abstracts, Vol. 5, 02954.

Mason, T.F.D., 2003b. High precision transition metal isotope analysis by plasma-source mass spectrometry and implications for low temperature geochemistry. PhD thesis, Imperial College London.

Mason, T.F.D., Weiss, D.J., Horstwood, M., Parrish, R.R., Russell, S.S., Mullane, E., Coles, B.J., 2004. High-precision Cu and Zn isotope analysis by plasma source mass spectrometry. Part 2. Correcting for mass discrimination effects. Journal of Analytical Atomic Spectrometry 19, 218-226.

Möller, P., 1989. REE (Y), Nb, and Ta enrichment in pegmatites and carbonatite-alkalic rock complexes. In: Möller, P., Černý, P. and Saupé F. (Eds.), Lanthanides, tantalum and niobium. Special publication No.7 of the Society for Geology Applied to Mineral Deposits. Springer-Verlag Berlin Heidelberg.

Nriagu, J.O. and Pacyna, J.M., 1988. Quantitative assessment of worldwide contamination of air, water, and soils by trace metals. Nature 33, 134-139.

Pichat, S., Douchet, C., Albarède, F., 2003. Zinc isotope variations in deep-sea carbonates from the eastern equatorial Pacific over the last 175 ka. Earth and Planetary Science Letters 210, 167-178.

Reimann, C. and de Caritat, P., 2000. Intrinsic flaws of element enrichment factors (EFs) in environmental geochemistry. Environmental Science and Technology 34, 5084-5091.

Reyf, F.G., Seltmann, R., Zaraisky, G.P., 2000. The role of magmatic processes in the formation of banded Li,F-enriched granites from the Orlovka tantalum deposit, Transbaikalia, Russia: Microthermometric evidence. Canadian Mineralogist 38 (4), 1029-1051.

Rosman, K.J.R., Chisholm, W., Boutron, C.F., Candelone, J.P., Gorlach, U., 1993. Isotopic evidence for the source of lead in Greenland snow since the late 1960s. Nature 362, 333-334.

Rosman, K.J.R., Chisholm, W., Boutron, C.F., Candelone, J.P., Hong, S., 1994. Isotopic evidence to account for changes in the concentrations of lead in Greenland snow between 1960 and 1988. Geochimica et Cosmochimica Acta 58, 3265-3269.

Rosman, K.J.R., Ly, C., Steinnes, E., 1999. Spatial and temporal variations in isotopic composition of the atmospheric lead in Norwegian moss. Environmental Science and Technology 32, 2542-2548.

Seltmann, R., Zaraisky, G.P., Aksyuk, A.M., Shatov V.V., Fedkin A.V., 1999. Amazonite in layered granites of the Orlovka and Etyka Ta deposits and its relation to magmatic-hydrothermal ore deposition. In: Physico-chemical aspects of endogenic geological processes. Abstracts of international symposium, Moscow-Chernogolovka, Russia, Moscow, 136-138.

Simonetti, A., Gariepy C., Carignan, J., 2003. Tracing sources of atmospheric contamination in Western Canada using the Pb isotopic composition and metal abundances of epiphytic lichens. Atmospheric Environment 37 (20), 2853-2865.

Spiro, B., Weiss, D., Purvis, O.W., Mikhailova, I., Williamson, B., Udachin, V. Lead isotopes in lichen transplants around a Cu smelter in Russia determined by MC-ICP-MS reveal transient records of multiple sources. Environmental Science and Technology, in press.

Syritso, L.F., Tabuns, E.V., Volkova, E.V., Badanina, E.V., Vysotskii, Yu.A., 2001. Model for the genesis of Li-F granites in the Orlovka massif, Eastern Transbaikalia. Petrology 9 (3), 268-289.

Takala, K., Salminen, R., Olkkonen, H., 1998. Geogenic and anthropogenic Zn in epiphytic and terricolous lichens in Finland. Journal of Geochemical Exploration 63, 57-66.

Tanimizu, M., Asada, Y., Hirata, T., 2002. Absolute isotopic composition and atomic weight of commercial Zn using inductively coupled plasma mass spectrometry. Analytical Chemistry 74, 5814-5819.

Taylor, S.R. and McLennan, S.M., 1995. The geochemical evolution of the continental crust. Reviews of Geophysics 33 (2), 241-265.

Thornton I., 1996. Impact of mining on the environment; some local, regional and global issues. Applied Geochemistry 11, 355-361.

Weiss, D.J., Kober, B., Dolgopolova, A., Gallagher, K., Spiro, B., Le Roux, G., Mason, T.F.D., Kylander, M., Coles, B.J., 2004. Accurate and precise Pb isotope ratio measurements in environmental samples by MC-ICP-MS. International Journal of Mass Spectrometry 232, 205-215.

Wilkinson, J.J., Weiss D.J., Coles B., Mason T.F.D., 2003. Zn isotopes: applications to ore deposit studies. Annual Meeting of the Mineral Deposit Studied Group, University of Leicester, 5-7 January. B163, 73-74.

Zaraisky, G.P, Aksyuk, A.M., Shapovalov, Yu.B., Chevychelov, V.Yu., Seltmann, R., Shatov, V.V., 1997. Petrography and geochemistry of Li-F granites and pegmatite-aplite banded rocks from the Orlovka and Etyka tantalum deposits in Eastern Transbaikalia, Russia. In: Papunen, H. (Ed.), Mineral Deposits, Rotterdam, Balkema.

Zaraisky, G.; Aksyuk, A.; Seltmann, R.; Shatov, V., Fedkin, A., 1998. Phosphorus in granites associated with W-Mo, W-Sn, and Ta-Nb mineralization. Acta Universitatis Carolinae Geologica. In: Breiter & Janousek (Ed.), Special issue on genetic significance of phosphorus in fractionated granites 42 (1), 194-199.

Zaraisky, G.P, Aksyuk, A.M., Seltmann, R. and Fedkin, A.V., 2000. Evolution of rare-metal granites and Zr/Hf ratio as an indicator of their crystallization differentiation. In: Yushkin, N.P. (Ed.), Petrography at the Boundary of the XXI Century: Results and Perspectives. Proceed. 2nd Russian Petrography Meeting, Syktyvkar, Geoprint III (in Russian).

Zschau, T., Getty, S., Gries, C., Ameron, Y., Zambrano, A., Nash III, T.H., 2003. Historical and current atmospheric deposition to the epilithic lichen Xanthoparmelia in Maricopa County, Arizona. Environmental Contamination 125, 21-30.

CHAPTER 7. CONCLUSIONS AND RECOMMENDATIONS

The Orlovka-Spokoinoe mining site in Eastern Transbaikalia (Russia) was chosen for this investigation to apply a complex approach that used element ratios, REE patterns and Pb and Zn isotopes as innovative diagnostic tools to trace natural, anthropogenic and environmental sources of dust and Pb and Zn within the mining site. The study resulted in a number of findings that are summarised below.

7.1. ANALYTICAL DEVELOPMENT TECHNIQUES

7.1.1. Microwave digestion method

The newly developed method of microwave-assisted acid decomposition of the standards NIST 1515 (Apple Leaves), NIST 1547 (Peach Leaves) and CRM 482 #10 *Pseudovernia furfura* (Lichens) using 6ml HNO_3 + 2 ml H_2O_2 + 2 ml H_2O + 0.8 ml HF resulted in quantitative recovery of Pb, Zn and Cu. 0.8 ml of HF in 10 ml of acid mixture was found to be sufficient and effective for the complete dissolution of lichen matrix independently from the degree of the lichens "contamination" with siliceous airborne particulates. Addition of more than 0.8ml of HF in 10ml of acid mixture used for the lichen digestion resulted in fluoride formation. Increase of pressure from 200 to 350 psi proved to be effective in achieving quantitative recovery of Pb, Zn and Cu. Good agreement was achieved between ICP-AES and EMMA-XRF techniques for lichen samples digested using the developed method. The developed closed-vessel microwave digestion method offers an easy and reliable method for the complete dissolution of lichens and leaves matrices prior to determination of trace elements and high precision Pb, Zn isotope ratios. The method was successfully used in the development study of a peat reference material for the determination of elemental concentrations (see **Appendix 1** for full publication).

7.1.2. High-precision Pb isotopes measurements

Analysis of ^{204}Pb, ^{206}Pb, ^{207}Pb and ^{208}Pb on a Micromass *Isoprobe* MC-ICP-MS resulted in internal precisions of below 100 ppm ($\pm 2\sigma$) on all Pb isotope ratios measured in geologic and biologic matrices using 50 measurements. Mass bias correction using optimized $^{205}Tl/^{203}Tl$ ratios achieved accuracies below 80ppm for all ratios. The Tl optimization was achieved using a simple mathematical least square approximation. The 'certified' Tl ratio used for mass bias correction had to be

adjusted for each measurement session up to 2.391. The measurement protocol used during the study allowed determining the isotope ratios of 5 unknown samples/1.5 hours. This is a significant improvement to the sample throughput compared to TIMS. The long-term reproducibility (expressed as $\pm 2\sigma$) determined over a five month period using repeated measurements of the NIST SRM 981 Pb standard and optimized Tl values was below 350ppm for all ratios. Ore-bearing granite samples passed through the columns and measured with TIMS and MC-ICP-MS showed excellent correlation (r=0.9876 for $^{206}Pb/^{204}Pb$ ratios, slope=0.9474, n=13). The mass bias of Tl spiked into natural and synthetic samples during a measurement session did not differ significantly, indicating that the complex peat and lichen matrix did not affect the mass bias behavior of the Tl spike.

7.2. GEOCHEMICAL CHARACTERISATION OF THE ORLOVKA-SPOKOINOE MINING SITE USING ELEMENTAL RATIOS AND Pb ISOTOPES

Elemental ratios and Pb isotopes were used to characterize geologic sources of metals within the Orlovka-Spokoinoe mining site. Along with geological relationships and geochemical patterns, the Pb isotope data confirmed that the Khangilay pluton could be considered as the parental intrusion for its hosted mineralised apical intrusions of Orlovka and Spokoinoe. Zr/Hf, Y/Ho, Rb/Sr showed a continuous fractionation history from the parental to the evolved granites, where Khangilay and its derivates Spokoinoe and Orlovka represent different evolution stages. Geochemical trends are directed from Khangilay to Orlovka, commonly with Spokoinoe in between. The highly evolved amazonite granites of the Orlovka deposit showed a stronger developed Eu anomaly and significant REE tetrad effects that developed parallel to granite evolution compared to parental granites of Khangilay. Pb isotope data confirm a strong genetic relationship between the barren biotite–muscovite granites of Khangilay, and the Spokoinoe and Orlovka ore-bearing granites suggesting a common source for the three massifs. Pb isotope systematics outlined two possible scenarios for the sources of granitic melts: a mixed upper crust-mantle source, and a type II enriched mantle source.

7.3. TRACING DUST AND Pb DISPERSAL USING REE PATTERNS AND ELEMENTAL RATIOS

An environmental geochemical study was conducted to assess the sources of dust and metals in the environment within the Orlovka-Spokoinoe mining site as a result of mining and ore processing activities. REE patterns, Pb enrichment relative to host rocks, and Pb/Zr and Pb/Y ratios in possible sources (host rocks, tailings, ore bearing and barren granites) and receptors (lichens and leaves) were used as geochemical tools to trace pollutants within the mining site. It was shown that even though Pb concentrations are not elevated, Pb in lichens is slightly enriched relative to the host rocks. Ore concentrates with the highest Pb concentrations, barren and ore-bearing granites could be excluded as Pb sources using Pb/Y vs. Pb/Zr ratios. Host rocks and tailing pond sediments are likely sources of Pb in the studied mining environment; however, an unidentified source could also be responsible. REE patterns were successfully used to link natural geological sources (Orlovka barren and ore-bearing granites) to their anthropogenic products (ore concentrates from different ore processing stages and tailings). This allowed identification of natural (geologic) and anthropogenic (ore concentrates, tailings) sources for particles dispersed within the mining area. Comparison between REE patterns of lichens and those of geological and anthropogenic origin showed that the tailing pond sediments and metasedimentary host rocks can be considered also as the main sources for the dust dispersion in the studied mining environment.

7.4. TRACING SOURCES AND PATHWAYS OF Pb AND Zn USING ELEMENT AND ISOTOPE RATIOS

Use of a combination of several powerful geochemical tools such as elemental concentrations, elemental ratios and Pb and Zn isotopic data provided a unique possibility to identify Pb sources and to assess Zn sources within the studied mining site and resulted in the following findings.

Significant Pb and Zn enrichment relative to the host rocks was observed in all samples despite relatively low Pb and Zn concentrations. Pb and Zn normalised to lithogenic elements reflected different geologic and technogenic processes but all exhibited the closest link of lichens and leaves to the tailings and host rocks,

suggesting these two sources to be the major geologic-anthropogenic contributors to the dispersal of both elements within the mining site using these indicators.

Pb isotopes allowed discrimination between four main sources of Pb dispersal within the Orlovka-Spokoinoe mining site, i.e. two geologic sources represented by granites and host rocks, an anthropogenic source such as tailings, and a long-range atmospheric Pb source. The influence of geologic and anthropogenic sources on Pb isotope signature of lichens accounts for only 11% of all lichen samples. Pb aerosols form a dominant source for Pb deposition on lichens within the mining site with 89% of lichens showing the influence of this source. This allows conclusion that Pb dispersal within the site is not mainly caused by human activities but rather reflects long-distance atmospheric aerosols input of Pb.

Preliminary Zn isotopes data allowed distinction between isotopic signatures of lichens and the geological suite, where the isotopically heavier Zn is observed in lichens and lighter Zn in the geologic suite. Isotopically heavy Zn in lichens is likely to reflect Zn contamination from a geographically remote high-temperature furnace or smelting complex and could be potentially associated with earlier described long-range atmospheric aerosols that contributed a significant amount of Pb to the studied mining site.

Application of high-precision Pb and Zn isotope analyses allowed discrimination of important metal sources, which would have failed on the basis of the low Pb, Zn concentrations in the studied materials alone. Combined with Pb isotopes, Zn isotopes variations could establish new possibilities in assessing metal origins and processes in the environment.

Both elemental ratios and Pb isotopes identified host rocks and tailings as sources of Pb and Zn within the mining site whereas granites and a dominant long-range atmospheric source of Pb were appointed using Pb isotopes. Host rocks and tailings were also appointed as the main dust sources within the Orlovka-Spokoinoe district based on the comparison between REE patterns of lichens and samples of geological and anthropogenic origins. Only a combination of different geochemical tools allowed a comprehensive appointment of Pb and Zn sources within the Orlovka-Spokoinoe mining site, where each of the methods brought complementary insights on the behaviour of these elements in the studied mining environment.

7.5. RECOMMENDATIONS FOR FUTURE WORK

The listed above findings open up new possibilities for future research. The most novel and challenging ones can be outlined as follows.

REE patterns that were previously extensively used in igneous, sedimentary and metamorphic petrology to trace sources of rocks and minerals during crustal and mantle evolution, for the first time highlighted new possibilities to trace dust pollutants within the mining environment. The same is also relevant for **elemental ratios** that were unconventionally used in this research to assess sources and pathways of metals. More case studies are required to extend these application possibilities.

Pb isotopes as a powerful geochemical tool allowed identification of main Pb sources within the mining site. It was found that Pb dispersal within the site is not caused by human activities but rather reflects naturally occurring Pb sources and long-distance atmospheric aerosols input of Pb. It is therefore recommended that every environmental assessment targeting identification of Pb sources shall include Pb isotopes as a reliable fingerprinting tool of contamination sources. In relation to this investigation an additional study that focuses on Pb isotopes of aerosols from the Orlovka-Spokoinoe mining site and within the Eastern Transbaikalia region could be beneficial in bringing a new evidence on the role of Pb aerosols to Pb distribution within the mining site and the Transbaikalia region as a whole.

Zn isotopes measured in lichens and geologic suite from the Orlovka-Spokoinoe mining site exhibited a clear distinction between Zn isotopic variations of geologic and biologic materials. To realize the potential for using Zn isotopes as a geochemical tracer it is vital to understand biotic and abiotic processes that fractionate Zn isotopes within biological and terrestrial materials. This offers challenging possibilities for further investigation of Zn isotope variability and fractionation within the natural environment.

The developed approach is not limited to the given mining district and could be potentially applied to any other industrial site where a comprehensive assessment of metal sources is required.

APPENDICES

APPENDIX I.

ORLOVKA-SPOKOINOE MINING DISTRICT

1.1. Photos of the mining site

A. Novoorlovsky settlement (overview)

B. Orlovka quarry

C. Ore processing plant

D. Tailing pond

1.2. Map of the main infrastructure units

1.1. PHOTOS OF THE MINING SITE

A. Overview of the Novoorlovsky settlement

B. Overview of the Orlovka quarry

C. Ore processing plant

D. View from the ore processing plant to the tailing pond

1.2. MAP OF THE MAIN INFRACTRUCTURE UNITS

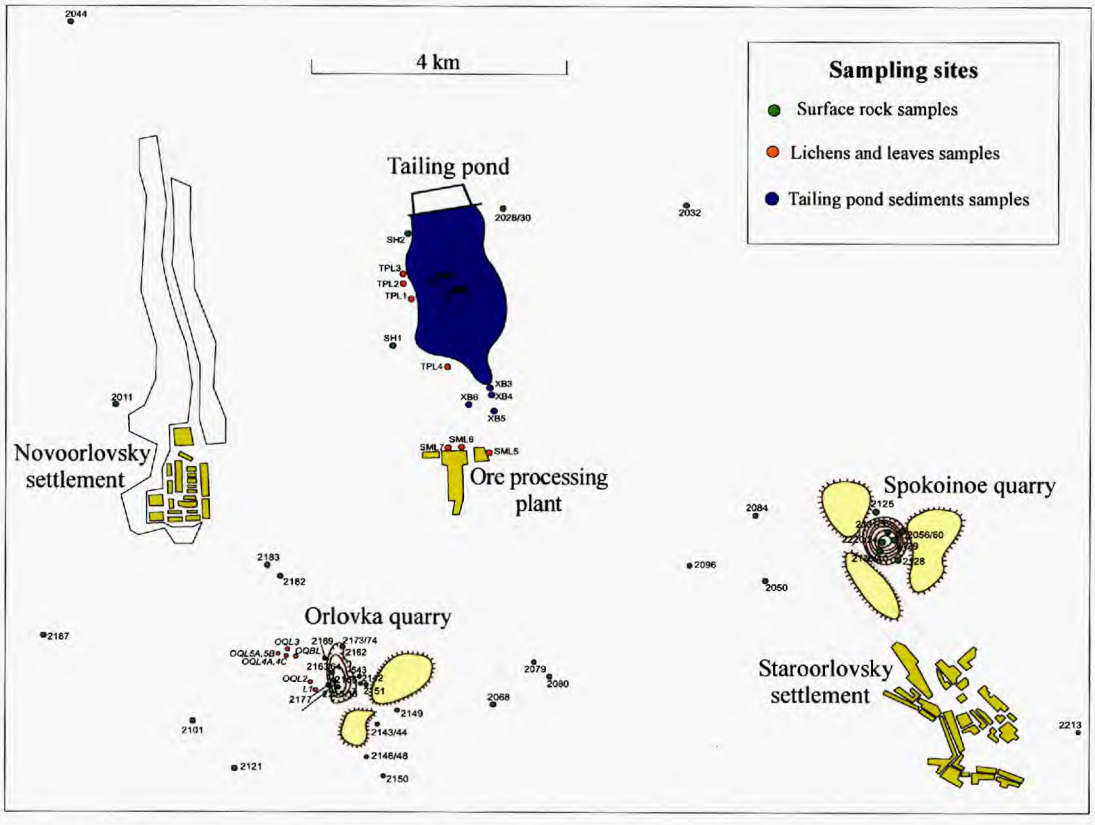

Orlovka-Spokoinoe mining site: main infrastructure units and sampling points

APPENDIX II.

A SELECTION OF LICHENS FOR THE ENVIRONMENTAL STUDY

2.1. Photos of *Xanthoparmelia* lichens

2.2. Images of particles on the lichen surface and typical spectrum of the particle analyses (analytical SEM).

2.1. Photos of *Xanthoparmelia* lichens

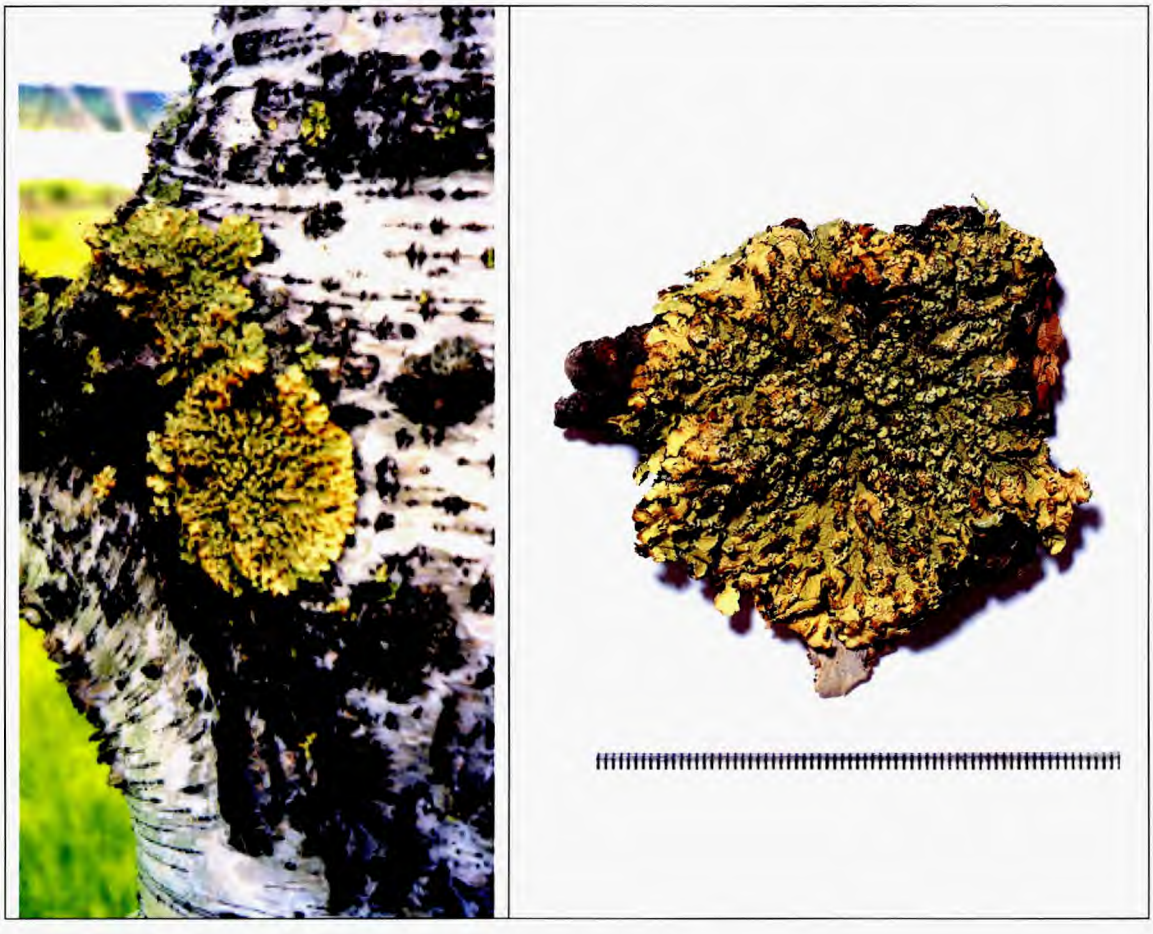

Xanthoparmelia lichens were sampled from the birch tree in the vicinity of the tailing pond. A yellow rim indicates "unhealthy" condition of the lichen.

2.2. Images of particles on the lichen surface and the typical spectrum of the particle analysis (analytical SEM).

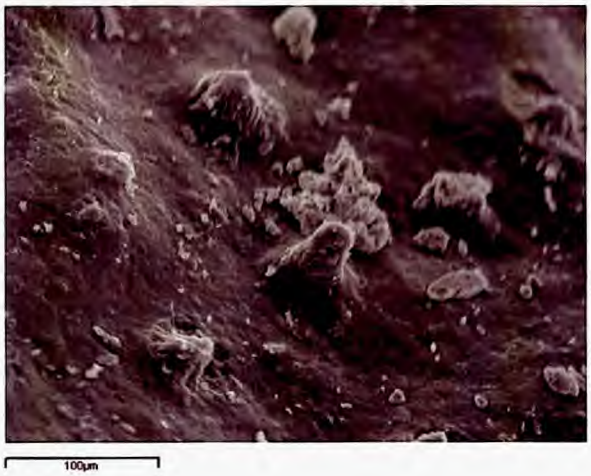

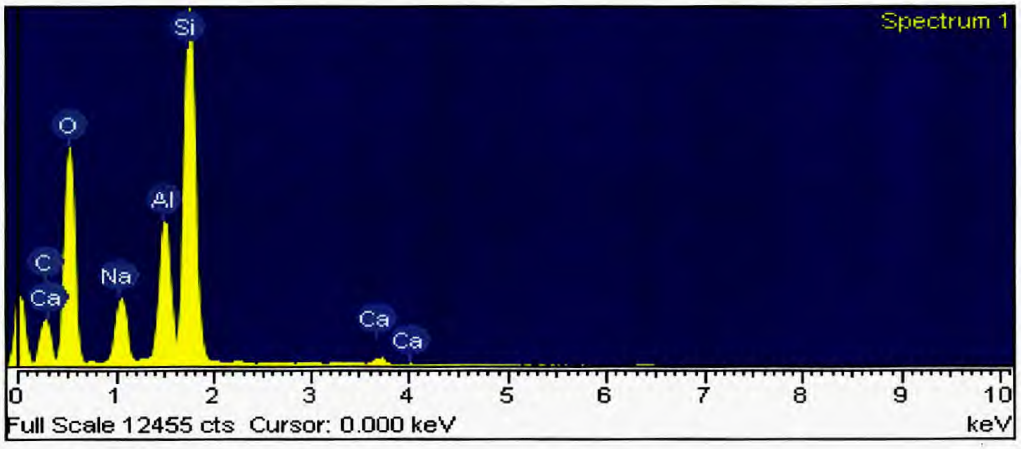

SEM analysis of the particle on the lichen surface shows its silicate composition.

APPENDIX III.

COLUMN CHEMISTRY SEPARATION OF Zn PRIOR HIGH-PRECISION Zn ISOTOPIC MEASUREMENTS BY MC-ICP-MS

Determination of high-precision Zn isotope ratios by MC ICP-MS requires separation of zinc fraction from the sample matrices. A separation procedure is required to (1) remove the majority of major element matrix components from the isolated analyte fractions, (2) eliminate elemental species known to cause spectral interferences with the species of interest, and (3) separate the analyte from elements used to monitor mass discrimination fluctuations during isotope measurements (Mason, 2003). Use of anion exchange AG MP-1 resin reported to be an effective way for zinc separation (Marechal et al., 1999). Zn column chemistry procedure, which was used in the research, is provided below. The procedure is based on Marechal et al. (1999) and is well established in the laboratory of the Natural History Museum providing 100% recovery of Zn.

The column chemistry procedure was used for rock (granites and host rocks) and lichen samples from the Orlovka-Spokoinoe mining site. Prior to procedure all samples were dissolved using the following acid mixtures. Rock sample powder was dissolved using mixed acid digestion ($HF/HClO_4$) (see more details in **CHAPTER 5**). Lichens were digested using $HNO_3/H_2O_2/HF$ mixture using the developed microwave digestion method as was outlined earlier in **CHAPTER 2**. After digestion, all samples were evaporated and further re-dissolved in 2ml of 7M HCl before loading on the ion exchange columns.

A standard procedure of Zn column chemistry separation is provided in **Table 3.1**. Before loading the sample on the column, the resin was thoroughly washed with 10ml 0.5M HNO_3 and several backwashes of the resin with Milli-Q H_2O. All working solutions were prepared in Aristar grade acids with deionised water (>18.2 MΩ cm) from a Milli-Q water system (Millipore Corporation, Bedford, MA, USA). **Figure 3.1** shows the typical elution curve for the separation of Cu, Fe and Zn from the synthetic solution.

Table 3.1. Column procedure for Zn separation (adapted from Marechal et al., 1999)

Elution steps
1. Pre-treat column with 7ml 7M HCl
2. Load 1ml of sample in 7M HCl
3. Wash with 6ml 7M HCl.
4. Elute 24ml of 7M HCl and collect the Cu fraction
5. Elute 12ml 2M HCl and collect the Fe fraction
6. Elute 10ml 0.1M HCl and collect the Zn fraction

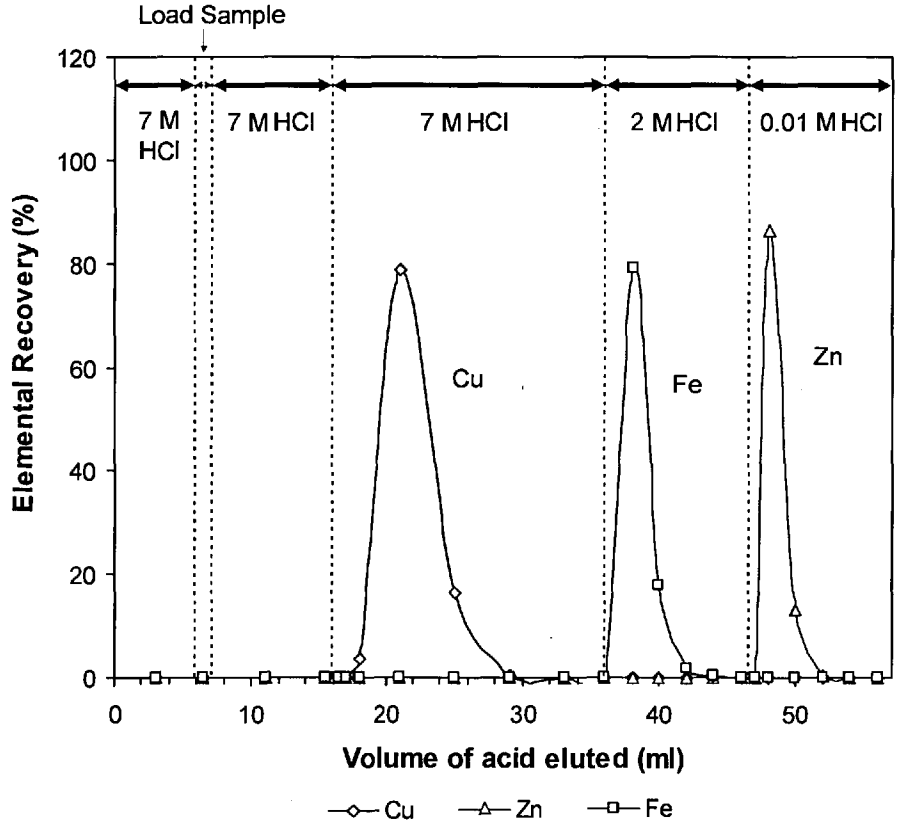

Figure 3.1. Typical elution curve for the separation of Cu, Fe and Zn from the synthetic (single element ICP-MS standards) solution. Elution curves for geologic and biologic matrices showed identical patterns and elemental recoveries and are not shown here. The data have been normalized to an aliquot of the initial sample solution. All elements exhibited quantitative recoveries that are within error of the ICP-AES measurements. The separation of Zn (element of main interest) appeared to be unaffected by the presence of matrix components as earlier studies indicated (Mason, 2003).

REFERENCES

Marechal C.N., Telouk P., Albarede F. Precise analysis of copper and zinc isotopes by plasma-source mass spectrometry. Chemical Geology, Vol. 156 (1999) 251-274.

Mason, T.F.D., 2003. High precision transition metal isotope analysis by plasma-source mass spectrometry and implications for low temperature geochemistry. PhD thesis, Imperial College London.

APPENDIX IV.

TABLES

Table 4.1. Bulk rock analysis of representative rock suites.

Rock type	Place of sampling	Sample ID	SiO_2	TiO_2
			2	*2*
Metasandstone / graywacke	Onon group	*2010*	66.19	0.837
Metasandstone / graywacke	Onon group	*2011*	72.24	0.578
Metasandstone / graywacke	Onon group	*2028*	72.06	0.466
Mica schist	Onon group	*2029*	63.45	0.948
Chlorite/mica schist	Onon group	*2032*	71.16	0.458
Fyllic altered gabbro-diorite of T_3 age	Far from Khangilay pluton	***2044***	60.83	1.396
Biotite/muscovite granite	Khangilay pluton	***2050***	87.23	<0.02
Mineralised greisen with W	Spokoinoe open pit	***2056***	79.21	<0.02
Biotite hornfels formed over Onon mica schist	Spokoinoe open pit	***2060***	72.13	0.755
Hornfels formed over lamprophyre dyke	Exocontact zone of Khangilay pluton	***2068***	58.89	1.524
Biotite granite	Khangilay pluton	***2079***	72.08	0.296
Biotite granite	Khangilay pluton	***2080***	72.82	0.298
Biotite/muscovite granite	Khangilay pluton	***2084***	73.85	0.140
Biotite granite	Khangilay pluton	***2096***	72.56	0.318
Rhyodacitic lava	Khila Formation	***2101***	72.77	0.092
Dacitic lava	Khila Formation	***2121***	72.19	0.311
Mineralised hornfels formed over mica Onon schist	Spokoinoe open pit	***2125***	60.94	0.954
Biotite hornfels formed over Onon mica schist	Spokoinoe open pit	***2128***	68.84	0.754
Biotite hornfels formed over mica schist	Onon Group	***2129***	61.61	1.042
Gabbro-diorite of T_3 age	Far from Khangilay pluton	***2131***	72.68	<0.02
Biotite hornfels formed over Onon mica schist	Spokoinoe open pit	***2132***	58.46	0.996
Amphibole hornfels formed over Onon mica schist	Spokoinoe open pit	***2138***	46.49	2.472
Amphibole hornfels formed over Onon mica schist	Spokoinoe open pit	***2140***	48.58	2.482
Biotite/muscovite granite	Orlovka stock	***2142***	72.32	0.139
Amazonite/muscovite granite	Orlovka stock	***2143***	72.83	<0.02
Amazonite pegmatite	Orlovka stock	***2144***	73.82	<0.02
Strongly weathered amz granite	Orlovka stock	***2147***	71.27	<0.02
Intensely weathered amz granite	Orlovka stock	***2148***	69.62	<0.02
Biotite granite	Orlovka stock	***2149***	73.16	0.124
Biotite/muscovite granite	Khangilay pluton	***2150***	77.48	0.090
Biotite/muscovite granite	Orlovka stock	***2151***	71.58	0.146
Mineralised toz/amz/ab granite	Orlovka open pit	***2162***	69.94	<0.02
Mineralised toz/amz/ab granite	Orlovka open pit	***2163***	74.00	<0.02
Mineralised toz/amz/ab granite	Orlovka open pit	***2164***	64.84	<0.02
Hornfels formed from lamprophyre dyke	Orlovka open pit	***2166***	62.14	0.933
Hornfels formed from lamprophyre dyke	Orlovka open pit	***2169***	60.99	0.729
Hornfels formed from Khila dacite	Orlovka open pit	***2173***	74.24	0.168
Hornfels formed from Khila tuffite	Orlovka open pit	***2174***	51.07	1.098
Hornfels formed from lamprophyre dyke	Orlovka open pit	***2177***	67.12	0.600
Rhyolite	Exocontact of Orlovka stock	***2182***	76.22	0.136
Rhyolite	Exocontact of Orlovka stock	***2183***	75.61	0.062
Andesitic dacite	Khila Formation	***2187***	47.23	1.047
Andesitic dacite	Khila Formation	***2204***	55.77	1.184
Mineralised toz/amz/ab granite	Orlovka open pit	***2213***	70.06	<0.02
Mineralised toz/amz/ab granite	Orlovka open pit	***2215***	72.84	<0.02
Greisenized granite	Spokoinoe open pit	***2220***	75.30	0.048
Mineralised greisen with W	Spokoinoe open pit	***2223***	90.95	<0.02
Mineralised greisen with W	Spokoinoe open pit	***2224***	95.95	<0.02
Sand from tailing pond	Novoorlovka tailing pond (surface)	***XB1***	n. a.	n. a.
Sand from tailing pond	Novoorlovka tailing pond (40 cm depth)	***XB2***	n. a.	n. a.
		unit	wt.%	wt.%

Methods: *0* – XRF (1); 1 – ES; 2 - XRF (2); *3* - ICP MS

	Al_2O_3	Fe_2O_3	MnO	MgO	CaO	Na_2O	K_2O	P_2O_5
	2	*2*	*2*	*2*	*2*	*2*	*2*	*2*
2010	15.35	6.677	0.121	2.237	1.305	3.925	1.497	0.143
2011	14.88	0.936	0.020	1.354	1.307	5.640	1.670	0.108
2028	13.97	4.066	0.050	1.224	0.528	3.191	2.600	0.098
2029	17.83	6.005	0.068	1.687	1.158	2.138	4.172	0.105
2032	15.70	2.762	0.053	0.996	0.167	5.245	1.560	0.131
2044	14.80	7.619	0.096	3.942	1.846	4.223	1.007	0.622
2050	7.471	0.275	<0.005	0.177	<0.050	0.459	2.722	<0.05
2056	12.78	0.595	0.115	<0.100	0.377	1.686	3.560	0.116
2060	9.586	3.368	0.265	2.516	3.236	0.143	2.782	0.201
2068	13.32	11.96	0.140	3.903	2.442	4.253	0.929	0.666
2079	15.75	1.282	0.014	0.320	0.320	3.850	4.686	<0.05
2080	15.32	1.143	0.009	0.281	0.425	3.888	4.304	0.062
2084	14.78	1.231	0.018	0.403	0.160	3.736	4.777	0.054
2096	14.44	1.743	0.023	0.604	0.838	3.725	4.396	0.087
2101	14.89	1.860	0.013	0.904	0.279	2.251	5.465	0.073
2121	13.45	2.913	0.006	0.413	<0.050	2.163	7.223	0.238
2125	18.72	5.955	0.043	1.678	0.715	2.966	3.927	0.120
2128	14.02	4.962	0.105	1.593	2.336	3.470	2.219	0.120
2129	15.97	7.875	0.052	3.588	2.307	0.292	3.532	0.129
2131	16.27	0.596	0.098	<0.100	0.658	3.953	4.060	0.190
2132	18.24	8.420	0.039	4.485	0.347	0.317	5.902	0.173
2138	18.82	12.25	0.231	4.653	6.578	3.671	3.587	0.593
2140	16.15	17.85	0.244	1.693	5.573	6.739	0.073	0.438
2142	15.91	1.571	0.098	0.252	0.310	3.738	4.563	<0.050
2143	16.12	0.140	0.166	<0.100	0.077	4.242	5.495	<0.050
2144	14.86	0.555	0.353	<0.100	<0.050	2.319	6.942	<0.050
2147	17.83	0.250	0.202	<0.100	<0.050	5.592	3.932	<0.050
2148	18.90	0.242	0.158	<0.100	<0.050	6.135	3.654	<0.050
2149	15.14	1.216	0.032	0.451	0.501	3.936	4.448	<0.050
2150	12.03	0.522	0.011	0.644	<0.050	0.736	7.344	<0.050
2151	16.62	1.315	0.030	0.307	0.0804	4.100	4.711	<0.050
2162	16.51	0.340	0.073	<0.100	0.115	3.000	9.350	<0.050
2163	15.80	2.151	0.260	<0.100	0.237	4.553	1.780	<0.050
2164	20.02	4.318	0.468	<0.100	0.256	4.480	3.495	<0.050
2166	13.82	5.487	0.095	3.911	7.967	1.763	1.990	0.079
2169	14.38	5.669	0.127	3.725	6.109	2.122	3.120	0.104
2173	14.15	2.402	0.077	0.684	1.445	2.860	2.372	<0.050
2174	16.54	13.95	0.175	3.996	1.786	5.555	2.774	0.494
2177	15.02	4.761	0.113	2.505	4.147	1.575	2.053	<0.050
2182	13.20	0.698	0.007	0.569	<0.050	2.037	6.030	<0.050
2183	13.86	1.126	0.009	0.752	<0.050	2.162	5.019	<0.050
2187	16.04	9.486	0.147	8.045	10.87	2.693	0.306	0.125
2204	15.80	8.040	0.161	4.493	3.064	5.720	0.695	0.161
2213	18.14	0.433	0.310	<0.100	0.292	6.832	2.832	<0.050
2215	15.41	0.802	0.162	<0.100	0.301	2.557	7.098	<0.050
2220	14.97	1.143	0.116	<0.100	0.0875	2.596	4.152	<0.050
2223	4.838	0.237	0.060	<0.100	0.875	<0.100	1.297	0.649
2224	1.907	0.136	0.211	<0.100	0.186	0.384	0.355	0.114
XB1	n. a.	n. a.	n. a.	n. a.	n. a.	n. a.	n. a.	n. a.
XB2	n. a.	n. a.	n. a.	n. a.	n. a.	n. a.	n. a.	n. a.
unit	wt.%	wt.%	wt.%	wt.%	wt.%	wt.%	wt.%	wt.%

	LOI	Total	Ag	As	B	Ba	Ba	Ba
	2	*2*	*1*	*1*	*1*	*3*	*1*	*2*
2010	2.010	100.3	<0.020	<80.0	25.0	403	0.050	0.044
2011	1.140	99.88	<0.020	<80.0	25.0	326	0.050	0.033
2028	1.570	99.82	0.10	<80.0	30.0	516	0.050	0.055
2029	2.550	100.1	0.040	<80.0	80.0	833	0.050	0.093
2032	1.770	100.0	<0.020	<80.0	30.0	349	0.040	0.039
2044	3.650	100.0	0.020	<80.0	10.0	1827	0.10	0.186
2050	1.470	99.87	0.060	<80.0	40.0	69.6	0.008	<0.010
2056	1.420	99.86	6.00	<80.0	200.0	35.8	0.030	<0.010
2060	5.130	100.1	0.030	80.0	800.0	413	0.050	0.042
2068	2.220	100.2	0.080	<80.0	10.0	174	0.040	0.024
2079	1.090	99.73	0.020	<80.0	20.0	278	0.030	0.027
2080	1.280	99.83	<0.020	<80.0	20.0	248	0.030	0.026
2084	0.860	100.0	0.020	<80.0	25.0	99.0	0.010	<0.010
2096	0.830	99.56	0.020	<80.0	20.0	294	0.040	0.029
2101	1.150	99.74	0.020	<80.0	30.0	370	0.030	0.039
2121	1.020	99.92	<0.020	<80.0	15.0	529	0.040	0.052
2125	4.040	100.1	0.040	300.0	50.0	870	0.060	0.088
2128	1.670	100.1	0.020	<80.0	30.0	696	0.050	0.071
2129	4.230	100.6	0.020	<80.0	800.0	451	0.050	0.048
2131	1.300	99.81	6.00	<80.0	80.0	1163	0.020	<0.010
2132	2.620	99.99	0.020	<80.0	1000	608	0.060	0.071
2138	0.670	100.0	0.030	<80.0	10.0	391	0.050	0.046
2140	0.510	100.3	0.030	<80.0	10.0	29.0	0.008	0.010
2142	1.100	100.0	0.50	<80.0	50.0	144	0.020	0.015
2143	0.680	99.75	0.020	<80.0	20.0	4.51	0.005	<0.010
2144	1.040	99.92	0.020	<80.0	30.0	2.5	0.003	<0.010
2147	0.950	100.0	0.020	<80.0	50.0	2.9	0.005	<0.010
2148	1.220	99.97	0.030	<80.0	15.0	9.5	0.005	<0.010
2149	0.950	100.0	0.030	<80.0	40.0	154	0.030	0.016
2150	1.050	99.91	0.050	<80.0	25.0	688	0.060	0.068
2151	1.120	100.1	0.020	<80.0	40.0	175	0.030	0.018
2162	0.270	99.60	0.020	<80.0	10.0	3.6	0.005	<0.010
2163	1.260	100.0	0.030	<80.0	10.0	1.8	0.005	<0.010
2164	2.090	99.96	<0.020	<80.0	10.0	2.56	0.003	<0.010
2166	1.920	100.1	0.020	<80.0	10.0	44.4	0.020	<0.010
2169	2.480	99.56	0.50	<80.0	60.0	148	0.030	0.015
2173	1.480	99.92	0.080	<80.0	30.0	119	0.020	0.013
2174	2.670	100.1	0.030	150.0	1000	436	0.050	0.054
2177	2.160	100.1	0.030	5000	30.0	75.7	0.020	<0.010
2182	1.100	100.1	0.040	<80.0	30.0	710	0.050	0.068
2183	1.200	99.84	0.040	<80.0	30.0	224	0.040	0.023
2187	3.930	99.92	<0.020	<80.0	15.0	147	0.040	0.024
2204	4.130	99.22	<0.020	<80.0	20.0	242	0.030	0.029
2213	0.970	99.88	1.00	<80.0	10.0	2.14	0.003	<0.010
2215	0.830	100.00	0.040	<80.0	30.0	16.9	0.008	<0.010
2220	1.320	99.77	0.60	150.0	60.0	41.5	0.010	<0.010
2223	0.700	99.62	0.60	<80.0	50.0	26.9	0.020	<0.010
2224	0.240	99.48	8.00	<80.0	10.0	4.82	0.005	<0.010
XB1	n. a.	n. a.	n. a.	n. a.	n. a.	66.6	n. a.	n. a.
XB2	n. a.	n. a.	n. a.	n. a.	n. a.	75.45	n. a.	n. a.
unit	wt.%	wt.%	ppm	ppm	ppm	ppm	wt.%	wt.%

	Be	Bi	Cd	Ce	Ce	Co	Cr	Cr
	1	*1*	*1*	*3*	*1*	*1*	*2*	*1*
2010	<1.00	<1.00	<8.00	85.2	<80.0	12.0	<0.005	30.0
2011	<1.00	<1.00	<8.00	65.4	<80.0	5.00	<0.005	30.0
2028	<1.00	<1.00	<8.00	47.1	<80.0	8.00	<0.005	30.0
2029	<1.00	<1.00	<8.00	86.8	<80.0	15.0	<0.005	30.0
2032	<1.00	<1.00	<8.00	49.7	<80.0	8.00	<0.005	30.0
2044	<1.00	<1.00	<8.00	184	<80.0	25.0	0.037	300.0
2050	1.50	3.00	<8.00	6.94	<80.0	<4.00	<0.005	4.00
2056	300.0	100.0	<8.00	5.05	<80.0	<4.00	<0.005	3.00
2060	2.00	1.00	<8.00	47.8	<80.0	25.0	0.008	100.0
2068	<1.00	<1.00	<8.00	81.7	<80.0	30.0	<0.005	2.00
2079	1.20	2.00	<8.00	83.5	100.0	4.00	<0.005	8.00
2080	1.00	3.00	<8.00	85.9	80.0	4.00	<0.005	10.0
2084	1.20	1.50	<8.00	49.8	<80.0	<4.00	<0.005	3.00
2096	<1.00	1.50	<8.00	109	120.0	4.00	<0.005	8.00
2101	1.20	1.00	<8.00	78.9	<80.0	<4.00	<0.005	5.00
2121	<1.00	<1.00	<8.00	49.8	<80.0	<4.00	<0.005	3.00
2125	<1.00	<1.00	<8.00	92.5	<80.0	12.0	0.005	60.0
2128	<1.00	8.00	<8.00	80.0	<80.0	15.0	<0.005	40.0
2129	1.20	<1.00	<8.00	55.5	<80.0	20.0	0.008	60.0
2131	150.0	30.0	<8.00	137	<80.0	<4.00	<0.005	2.00
2132	2.00	1.00	<8.00	76.0	<80.0	20.0	0.012	100.0
2138	1.00	2.00	<8.00	51.7	<80.0	40.0	0.018	150.0
2140	<1.00	<1.00	<8.00	26.5	<80.0	50.0	0.016	60.0
2142	1.50	3.00	<8.00	79.1	<80.0	<4.00	<0.005	10.0
2143	30.0	3.00	<8.00	26.0	<80.0	<4.00	<0.005	2.00
2144	30.0	3.00	<8.00	71.6	<80.0	<4.00	<0.005	2.00
2147	30.0	3.00	<8.00	21.6	<80.0	<4.00	<0.005	2.00
2148	1.50	3.00	<8.00	17.8	<80.0	<4.00	<0.005	5.00
2149	1.50	1.50	<8.00	57.9	80.0	4.00	<0.005	5.00
2150	100.0	<1.00	<8.00	72.6	80.0	<4.00	<0.005	4.00
2151	10.0	3.00	<8.00	58.6	<80.0	<4.00	<0.005	12.0
2162	1.50	1.20	<8.00	5.13	<80.0	<4.00	<0.005	3.00
2163	1.50	400.0	<8.00	16.6	<80.0	<4.00	<0.005	2.00
2164	50.0	5.00	<8.00	30.1	<80.0	<4.00	<0.005	2.00
2166	1000	10.0	<8.00	16.7	<80.0	12.0	0.008	100.0
2169	300.0	1000	<8.00	20.1	<80.0	15.0	0.008	100.0
2173	25.0	500.0	<8.00	44.8	<80.0	4.00	<0.005	4.00
2174	1.00	<1.00	<8.00	96.9	<80.0	12.0	<0.005	1.50
2177	600.0	300.0	<8.00	16.8	<80.0	12.0	<0.005	50.0
2182	<1.00	<1.00	<8.00	106	<80.0	<4.00	<0.005	3.00
2183	<1.00	1.00	<8.00	26.9	<80.0	<4.00	<0.005	3.00
2187	<1.00	<1.00	<8.00	16.7	<80.0	30.0	0.026	80.0
2204	<1.00	<1.00	<8.00	38.4	<80.0	15.0	<0.005	25.0
2213	15.0	30.0	<8.00	18.4	<80.0	<4.00	<0.005	2.50
2215	3.00	1.50	<8.00	29.4	<80.0	<4.00	<0.005	3.00
2220	15.0	15.0	<8.00	8.36	<80.0	<4.00	<0.005	3.00
2223	3.00	400.0	<8.00	12.5	<80.0	<4.00	<0.005	3.00
2224	50.0	300.0	<8.00	4.6	<80.0	<4.00	<0.005	2.50
XB1	n. a.	n. a.	n. a.	9.5	n. a.	n. a.	n. a.	n. a.
XB2	n. a.	n. a.	n. a.	13.1	n. a.	n. a.	n. a.	n. a.
unit	ppm	ppm	ppm	ppm	ppm	ppm	wt.%	ppm

	Cs	Cu	Dy	Er	Eu	Ga	Gd	Ge
	3	*1*	*3*	*3*	*3*	*1*	*3*	*1*
2010	1.63	20.0	3.62	2.07	1.69	12.0	4.55	1.20
2011	0.523	20.0	3.78	2.24	1.08	15.0	4.66	1.00
2028	3.00	30.0	2.84	1.69	0.754	12.0	3.11	<1.0
2029	4.45	60.0	4.75	2.73	1.29	15.0	5.26	1.50
2032	1.68	25.0	2.46	1.26	0.906	12.0	3.27	<1.0
2044	1.98	30.0	4.98	1.99	3.72	12.0	10.2	1.00
2050	11.3	30.0	2.66	1.65	0.088	10.0	1.95	1.00
2056	39.2	25.0	1.67	0.500	0.098	20.0	1.62	1.50
2060	109	20.0	3.62	2.16	0.960	10.0	4.01	1.50
2068	13.8	30.0	9.35	5.42	2.55	12.0	10.2	1.20
2079	13.9	40.0	4.60	2.58	0.503	40.0	4.77	1.20
2080	12.2	30.0	6.79	4.02	0.482	40.0	6.39	1.00
2084	33.9	30.0	4.30	2.30	0.228	15.0	4.39	1.20
2096	17.4	20.0	5.04	2.57	0.556	40.0	5.87	1.00
2101	2.18	50.0	9.43	5.52	0.390	20.0	8.32	1.20
2121	1.88	30.0	6.11	4.16	0.565	15.0	4.92	1.00
2125	62.7	30.0	4.86	2.85	1.31	15.0	5.716	1.20
2128	73.7	30.0	3.53	1.98	1.18	12.0	4.33	1.20
2129	74.1	25.0	4.27	2.59	1.03	10.0	4.42	1.20
2131	4.73	40.0	8.19	3.74	3.94	30.0	11.8	1.50
2132	457	30.0	5.39	3.26	1.45	15.0	5.83	1.50
2138	88.6	25.0	5.67	3.17	1.99	15.0	6.13	2.00
2140	5.01	40.0	8.57	5.34	2.09	12.0	7.80	2.00
2142	31.1	30.0	10.7	5.00	0.309	100.0	9.58	1.50
2143	52.0	20.0	2.84	0.987	< 0.009	100.0	2.10	10.0
2144	108	30.0	3.76	1.13	0.015	80.0	3.25	8.00
2147	68.9	30.0	3.39	1.19	0.028	100.0	2.63	10.0
2148	22.1	25.0	2.82	1.17	0.035	120.0	1.83	1.50
2149	64.6	20.0	6.06	3.13	0.315	60.0	5.48	1.50
2150	25.1	30.0	2.61	1.27	0.413	15.0	3.416	<1.0
2151	56.7	25.0	5.15	2.66	0.309	80.0	4.91	1.50
2162	26.8	20.0	2.00	0.907	< 0.01	120.0	1.24	4.00
2163	60.6	25.0	4.72	2.34	< 0.01	40.0	2.49	15.0
2164	102	12.0	2.81	1.03	0.013	300.0	2.26	15.0
2166	97.1	30.0	5.07	2.61	0.605	10.0	3.683	10.0
2169	142	20.0	4.45	2.33	0.681	12.0	3.56	10.0
2173	43.4	20.0	6.80	3.49	0.695	40.0	5.61	20.0
2174	102	20.0	12.3	6.91	3.255	25.0	12.3	1.50
2177	88.37	30.0	3.59	1.80	0.372	30.0	2.54	30.0
2182	14.2	25.0	9.65	5.29	0.549	30.0	9.9	<1.0
2183	2.11	30.0	13.2	8.21	0.459	40.0	9.06	<1.0
2187	0.127	30.0	4.22	2.51	1.15	8.00	3.89	1.20
2204	0.550	25.0	5.61	3.34	1.42	12.0	5.63	1.20
2213	44.4	20.0	3.28	1.32	0.022	150.0	2.04	15.0
2215	27.8	25.0	12.07	5.31	0.021	150.0	8.47	4.00
2220	58.2	25.0	1.14	0.353	0.057	20.0	1.48	1.50
2223	13.5	30.0	7.23	1.80	0.670	8.00	6.08	1.00
2224	5.42	15.0	2.34	0.841	0.065	3.00	1.61	<1.0
XB1	40.7	n. a.	1.22	0.46	0.104	n. a.	1.22	n. a.
XB2	40.14	n. a.	1.86	0.744	0.110	n. a.	1.56	n. a.
unit	ppm	ppm	ppm	ppm	ppm	ppm	ppm	ppm

	Hf	Ho	La	La	Li	Lu	Mn	Mo
	3	*3*	*3*	*1*	*1*	*3*	*1*	*1*
2010	6.34	0.685	43.8	<15.0	25.0	0.314	0.080	1.20
2011	5.37	0.726	26.8	<15.0	10.0	0.335	0.008	1.20
2028	4.25	0.564	20.5	<15.0	30.0	0.260	0.020	1.00
2029	5.69	0.920	32.6	<15.0	40.0	0.402	0.040	1.50
2032	4.53	0.441	22.9	<15.0	20.0	0.180	0.050	1.00
2044	9.36	0.816	86.3	<15.0	50.0	0.219	0.050	2.00
2050	2.74	0.524	3.14	<15.0	40.0	0.255	0.008	1.50
2056	2.19	0.205	1.97	<15.0	20.0	0.071	0.12	2.00
2060	3.92	0.722	23.3	<15.0	200.0	0.311	0.40	2.00
2068	8.01	1.85	37.0	<15.0	120.0	0.720	0.060	2.50
2079	5.86	0.832	38.6	30.0	100.0	0.363	0.020	2.50
2080	7.02	1.33	43.7	30.0	80.0	0.545	0.020	2.00
2084	5.15	0.751	22.8	15.0	150.0	0.372	0.010	3.00
2096	6.02	0.908	54.6	40.0	120.0	0.347	0.010	2.00
2101	4.76	1.90	36.5	<15.0	20.0	0.717	0.020	2.00
2121	9.18	1.31	25.8	<15.0	20.0	0.629	0.006	2.50
2125	6.36	0.963	45.6	<15.0	80.0	0.431	0.040	2.50
2128	5.48	0.676	39.6	<15.0	100.0	0.288	0.10	2.50
2129	4.23	0.841	26.8	<15.0	120.0	0.388	0.060	2.00
2131	8.99	1.41	60.3	<15.0	30.0	0.434	0.12	1.50
2132	5.28	1.04	36.3	<15.0	800.0	0.477	0.010	2.50
2138	5.33	1.11	24.0	<15.0	600.0	0.421	0.080	2.50
2140	4.16	1.81	16.1	<15.0	20.0	0.690	0.10	2.00
2142	5.33	1.77	36.4	<15.0	800.0	0.662	0.050	2.50
2143	2.76	0.375	9.08	<15.0	3000	0.138	0.12	2.50
2144	1.75	0.441	20.9	<15.0	>0.3%	0.146	0.20	2.50
2147	11.9	0.440	7.52	<15.0	2000	0.186	0.10	2.50
2148	7.01	0.425	7.10	<15.0	800.0	0.179	0.10	2.50
2149	4.72	1.09	28.2	40.0	1000	0.468	0.010	1.50
2150	5.04	0.451	38.0	30.0	800.0	0.180	0.006	4.00
2151	4.54	0.917	27.8	<15.0	600.0	0.370	0.020	2.50
2162	1.50	0.327	1.95	<15.0	500.0	0.132	0.080	2.50
2163	12.5	0.768	4.83	<15.0	3000	0.454	0.15	2.00
2164	21.1	0.369	7.53	<15.0	>0.3%	0.180	0.15	2.50
2166	2.36	0.906	6.35	<15.0	800.0	0.395	0.080	2.00
2169	3.68	0.810	7.68	<15.0	1000	0.332	0.080	2.50
2173	6.20	1.22	20.3	<15.0	1000	0.496	0.080	2.00
2174	12.5	2.45	46.1	<15.0	80.0	0.923	0.10	2.50
2177	10.7	0.61	5.47	<15.0	1000	0.274	0.10	2.50
2182	6.95	1.82	48.9	<15.0	15.0	0.692	0.002	3.00
2183	6.84	2.75	10.5	<15.0	15.0	1.06	0.002	1.50
2187	2.55	0.865	7.18	<15.0	20.0	0.342	0.10	2.00
2204	4.75	1.14	18.9	<15.0	20.0	0.456	0.080	1.50
2213	5.49	0.463	6.22	<15.0	2000	0.215	0.12	3.00
2215	1.68	1.90	9.70	<15.0	1000	0.657	0.10	2.50
2220	1.25	0.148	3.54	<15.0	30.0	0.051	0.10	1.20
2223	0.32	0.886	4.11	<15.0	<10.0	0.115	0.12	2.50
2224	0.25	0.314	1.80	<15.0	<10.0	0.165	1.00	1.00
XB1	2.09	0.180	4.42	n. a.	n. a.	0.066	n. a.	n. a.
XB2	2.37	0.263	5.98	n. a.	n. a.	0.105	n. a.	n. a.
unit	ppm	ppm	ppm	ppm	ppm	ppm	wt.%	ppm

	Nb	Nb	Nd	Ni	Pb	Pb	Pb	Pr
	0	*1*	*3*	*1*	*3*	*0*	*1*	*3*
2010	13.35	12.0	34.5	15.0	5.62	6.160	5.00	9.55
2011	14.69	10.0	32.4	10.0	8.93	10.06	20.0	8.56
2028	8.492	12.0	18.4	15.0	15.4	16.38	20.0	4.94
2029	13.20	15.0	30.8	25.0	25.0	27.71	40.0	8.20
2032	9.077	15.0	20.9	12.0	21.6	24.01	20.0	5.60
2044	12.19	12.0	89.8	150.0	38.2	37.25	40.0	22.8
2050	25.46	40.0	4.38	4.00	25.6	346.8	30.0	1.06
2056	64.30	150.0	2.62	4.00	32.5	30.38	20.0	0.678
2060	8.002	20.0	22.6	40.0	18.2	17.48	25.0	5.84
2068	16.60	15.0	44.1	2.00	15.2	16.77	20.0	10.6
2079	29.47	25.0	30.1	3.00	38.3	39.53	50.0	8.62
2080	40.59	30.0	34.0	3.00	38.4	36.81	50.0	9.49
2084	37.90	40.0	21.0	2.00	40.1	40.55	50.0	5.74
2096	30.32	40.0	40.0	4.00	43.6	41.85	50.0	11.8
2101	17.67	20.0	34.3	2.00	32.7	35.09	50.0	9.19
2121	8.563	15.0	18.1	2.00	33.82	38.82	40.0	5.09
2125	16.03	15.0	38.6	30.0	59.0	65.23	60.0	10.7
2128	13.13	15.0	33.5	25.0	155	119.5	200.0	9.24
2129	12.76	20.0	25.2	40.0	11.6	11.76	8.00	6.60
2131	64.10	80.0	75.9	1.50	15.3	41.49	30.0	18.2
2132	15.40	20.0	33.9	50.0	10.6	9.597	10.0	8.95
2138	46.47	15.0	26.9	100.0	90.5	97.60	60.0	6.49
2140	10.91	8.00	22.5	50.0	16.2	17.95	10.0	4.71
2142	46.31	30.0	33.6	3.00	136	140.6	200.0	9.43
2143	41.44	50.0	10.5	1.50	121.7	134.7	200.0	3.71
2144	37.94	30.0	22.1	1.00	129	138.5	150.0	8.26
2147	34.39	25.0	9.59	1.00	70.8	78.14	60.0	3.35
2148	70.38	40.0	7.47	1.00	52.0	50.78	60.0	2.75
2149	42.89	40.0	22.9	3.00	44.3	46.72	50.0	6.47
2150	14.81	30.0	26.3	2.00	43.6	39.22	60.0	7.76
2151	34.26	25.0	23.1	3.00	33.7	31.11	50.0	6.61
2162	18.72	25.0	2.30	1.50	167	184.8	300.0	0.654
2163	104.5	300.0	5.81	2.00	18.9	21.34	15.0	2.12
2164	219.0	150.0	9.77	2.00	20.4	19.66	20.0	3.91
2166	31.02	30.0	9.15	20.0	6.69	5.655	15.0	2.28
2169	17.13	15.0	10.4	20.0	7.94	8.202	12.0	2.64
2173	59.18	100.0	20.3	2.00	12.0	13.03	20.0	5.51
2174	21.29	10.0	50.6	3.00	26.7	22.85	30.0	12.2
2177	118.4	80.0	7.3	15.0	6.8	5.835	8.00	2.21
2182	14.73	30.0	49.0	2.00	9.37	13.08	20.0	12.8
2183	24.28	30.0	16.1	2.00	4.44	4.661	12.0	3.74
2187	2.660	8.00	11.4	60.0	6.32	5.728	8.00	2.44
2204	7.327	8.00	21.2	3.00	9.79	9.339	12.0	5.12
2213	52.55	50.0	6.21	1.00	184	169.7	300.0	2.22
2215	37.23	30.0	16.4	2.00	108	116.5	200.0	4.32
2220	115.0	100.0	3.92	3.00	34.9	27.61	25.0	1.06
2223	10.39	40.0	8.60	4.00	282	201.7	40.0	1.93
2224	75.79	500.0	2.54	10.0	71.4	63.89	25.0	0.621
XB1	n. a.	n. a.	4.11	n. a.	22	n. a.	n. a.	1.11
XB2	n. a.	n. a.	5.59	n. a.	17.8	n. a.	n. a.	1.575
unit	ppm	ppm	ppm	ppm	ppm	ppm	ppm	ppm

	Rb	Rb	S	Sb	Sc	Sm	Sn	Sr
	3	*0*	*2*	*1*	*1*	*3*	*1*	*3*
2010	46.1	44.74	<0.020	<30.0	6.00	5.77	5.00	222
2011	44.5	45.72	0.020	<30.0	<6.00	5.89	4.00	202
2028	70.7	68.71	0.020	<30.0	<6.00	3.47	1.50	146
2029	114	122.0	<0.020	<30.0	6.00	6.06	3.00	226
2032	43.9	42.92	<0.020	<30.0	6.00	4.01	2.00	164
2044	34.0	33.19	<0.020	<30.0	6.00	15.6	2.50	425
2050	235	2640	0.020	<30.0	6.00	1.78	3.00	42.0
2056	412	434.0	0.020	<30.0	6.00	1.34	200.0	31.3
2060	232	242.1	0.130	<30.0	6.00	4.48	2.50	76.6
2068	71.1	70.68	0.792	<30.0	8.00	10.3	6.00	122
2079	343	351.0	0.021	<30.0	<6.00	6.07	6.00	106
2080	318	322.8	0.020	<30.0	<6.00	7.27	6.00	105
2084	487	488.1	<0.020	<30.0	6.00	5.15	15.0	52.1
2096	300	315.4	0.021	<30.0	<6.00	7.51	6.00	141
2101	188	190.0	0.021	<30.0	6.00	8.10	5.00	65.3
2121	154	154.4	0.030	<30.0	6.00	4.11	4.00	26.8
2125	188	189.6	<0.020	<30.0	<6.00	7.06	4.00	260
2128	112	116.5	0.145	<30.0	8.00	5.66	6.00	466
2129	185	190.0	0.092	<30.0	6.00	5.03	6.00	93.4
2131	41.1	475.4	0.020	<30.0	6.00	14.7	200.0	998
2132	640	651.3	0.363	<30.0	6.00	6.51	10.0	73.5
2138	335	343.8	<0.020	<30.0	8.00	6.03	30.0	356
2140	7.49	8.240	<0.020	<30.0	10.0	6.11	2.50	502
2142	1113	1140	<0.020	<30.0	6.00	10.6	100.0	69.9
2143	2265	2360	0.021	<30.0	6.00	4.23	200.0	0.83
2144	3239	3440	0.020	<30.0	6.00	7.62	250.0	1.01
2147	1755	1810	<0.020	<30.0	6.00	4.20	20.0	1.27
2148	1294	1320	0.020	<30.0	6.00	2.91	15.0	4.23
2149	707	736.1	<0.020	<30.0	<6.00	5.63	80.0	67.8
2150	334	333.4	0.134	<30.0	6.00	4.63	100.0	31.8
2151	563	566.4	<0.020	<30.0	6.00	5.42	150.0	66.6
2162	2689	2880	0.061	<30.0	8.00	1.22	10.0	4.16
2163	1268	1390	<0.020	<30.0	8.00	2.92	300.0	4.82
2164	2546	2650	0.020	<30.0	6.00	4.23	300.0	6.03
2166	894	900.7	<0.020	<30.0	8.00	3.49	20.0	92.0
2169	1272	1290	0.021	<30.0	8.00	3.50	30.0	121
2173	868	894.6	0.034	<30.0	6.00	5.76	100.0	27.8
2174	291	302.4	0.715	<30.0	6.00	11.8	30.0	98.9
2177	1059	1120	0.148	<30.0	8.00	2.92	80.0	102.39
2182	162	168.1	<0.020	<30.0	6.00	10.5	6.00	34.2
2183	144	152.4	0.020	<30.0	6.00	5.60	6.00	15.2
2187	11.5	16.21	<0.020	<30.0	6.00	3.22	1.20	93.5
2204	15.5	16.02	0.022	<30.0	8.00	5.01	2.50	112
2213	1527	1600	0.020	<30.0	6.00	3.01	8.00	5.48
2215	2149	2270	0.020	<30.0	6.00	8.59	80.0	7.60
2220	550	564.8	0.038	<30.0	8.00	1.61	250.0	31.0
2223	140	142.3	0.021	<30.0	6.00	4.56	5.00	68.9
2224	57.0	63.31	0.021	<30.0	8.00	1.26	5.00	13.8
XB1	451	n. a.	n. a.	n. a.	n. a.	1.19	n. a.	43.2
XB2	499.1	n. a.	n. a.	n. a.	n. a.	1.67	n. a.	41.7
unit	ppm	ppm	wt.%	ppm	ppm	ppm	ppm	ppm

	Sr	Sr	Tb	Th	Th	Ti	Tm	U
	1	*0*	*3*	*3*	*0*	*1*	*3*	*3*
2010	0.010	204.7	0.62	14.0	12.56	0.60	0.298	2.14
2011	0.010	194.4	0.652	11.9	12.74	0.50	0.317	1.91
2028	0.010	140.2	0.471	7.27	9.179	0.50	0.246	1.61
2029	0.010	216.9	0.808	11.1	14.45	0.50	0.392	2.25
2032	0.010	164.1	0.442	7.64	9.794	0.50	0.181	1.70
2044	0.030	415.6	1.10	21.8	22.61	0.80	0.247	4.67
2050	<0.001	511.1	0.406	6.78	156.5	0.05	0.245	12.2
2056	0.015	30.45	0.347	5.57	11.13	0.06	0.071	3.45
2060	0.030	76.79	0.595	6.40	6.715	0.80	0.308	2.44
2068	0.010	116.3	1.53	8.00	8.487	0.80	0.758	2.33
2079	<0.001	107.5	0.772	40.7	40.61	0.40	0.379	11.9
2080	0.010	103.8	1.08	42.2	39.64	0.50	0.589	33.0
2084	<0.001	50.33	0.731	32.1	31.25	0.40	0.366	14.0
2096	0.010	140.2	0.881	47.0	42.30	0.40	0.370	10.4
2101	<0.001	63.64	1.46	12.9	13.56	0.10	0.810	3.70
2121	<0.001	25.61	0.900	15.1	16.46	0.50	0.627	4.19
2125	0.010	249.5	0.825	11.6	11.90	0.60	0.407	2.35
2128	0.030	468.1	0.600	10.0	13.06	0.60	0.286	2.09
2129	0.030	91.85	0.692	8.75	9.813	0.60	0.370	3.59
2131	0.015	51.22	1.56	2.54	13.07	0.06	0.485	0.741
2132	0.015	72.79	0.847	11.1	10.63	0.80	0.470	3.63
2138	0.015	357.2	0.937	2.69	4.053	0.80	0.423	0.852
2140	0.015	510.6	1.28	0.88	2.755	0.80	0.708	0.515
2142	<0.001	70.23	1.82	27.0	25.02	0.40	0.750	6.21
2143	<0.001	1.678	0.526	8.25	7.883	0.10	0.165	1.53
2144	<0.001	3.127	0.754	8.19	5.119	0.10	0.180	3.95
2147	<0.001	1.645	0.608	15.1	14.57	0.10	0.197	2.39
2148	<0.001	4.020	0.465	13.3	11.79	0.10	0.194	3.10
2149	<0.001	71.26	1.005	23.2	21.86	0.30	0.482	8.57
2150	<0.001	30.30	0.497	15.4	14.90	0.20	0.174	1.68
2151	<0.001	65.61	0.873	23.7	21.12	0.40	0.403	8.52
2162	<0.001	4.969	0.321	1.96	<2.00	0.08	0.144	0.861
2163	<0.001	7.524	0.741	14.0	<2.00	0.30	0.431	4.25
2164	<0.001	8.599	0.545	15.2	14.48	0.40	0.179	9.23
2166	<0.001	88.31	0.787	4.36	7.493	0.50	0.407	2.76
2169	0.010	117.1	0.693	5.29	<2.00	0.50	0.350	2.08
2173	<0.001	26.79	1.10	12.0	<2.00	0.30	0.529	3.95
2174	0.012	100.4	1.97	11.2	12.39	0.80	0.950	3.43
2177	0.010	101.1	0.580	17.6	25.13	0.60	0.282	7.6
2182	<0.001	35.04	1.58	17.6	17.39	0.40	0.753	3.78
2183	<0.001	14.26	1.92	11.7	13.04	0.30	1.16	3.92
2187	<0.001	91.69	0.651	1.00	2.368	0.50	0.345	0.301
2204	0.025	108.2	0.897	4.97	5.695	0.50	0.462	1.53
2213	<0.001	6.244	0.564	13.1	<2.00	0.20	0.233	8.69
2215	<0.001	7.153	1.96	3.97	4.922	0.08	0.805	1.68
2220	<0.001	31.40	0.255	7.79	8.583	0.10	0.052	16.6
2223	0.015	61.66	1.38	2.04	<2.00	0.05	0.194	12.9
2224	<0.001	12.33	0.405	1.23	<2.00	0.05	0.151	3.59
XB1	n. a.	n. a.	0.22	6.07	n. a.	n. a.	0.067	7.1
XB2	n. a.	n. a.	0.320	8.01	n. a.	n. a.	0.113	7.57
unit	wt.%	ppm	ppm	ppm	ppm	wt.%	ppm	ppm

	U	V	V	W	Y	Y	Y	Yb
	0	*2*	*1*	*1*	*3*	*0*	*1*	*3*
2010	<2.00	0.00961	50.0	<3.00	19.6	20.37	<10.0	2.00
2011	<2.00	<0.0050	50.0	<3.00	21.4	19.04	<10.0	2.26
2028	<2.00	<0.0050	50.0	<3.00	15.7	16.66	<10.0	1.72
2029	2.545	0.0106	120.0	<3.00	24.9	29.53	10.0	2.66
2032	<2.00	<0.0050	40.0	<3.00	12.4	11.92	10.0	1.21
2044	4.889	0.0168	80.0	<3.00	21.6	23.05	10.0	1.54
2050	246.3	<0.0050	2.00	<3.00	15.1	369.4	20.0	1.80
2056	4.711	<0.0050	2.00	>0.1%	7.35	8.186	10.0	0.531
2060	3.077	0.00593	80.0	4.00	20.3	27.21	25.0	2.04
2068	2.199	0.0113	5.00	<3.00	49.1	55.19	20.0	4.89
2079	11.24	<0.0050	10.0	3.00	25.1	29.28	30.0	2.60
2080	40.74	<0.0050	10.0	3.00	39.3	37.70	50.0	3.91
2084	14.92	<0.0050	8.00	10.0	23.9	22.90	30.0	2.60
2096	10.72	<0.0050	15.0	<3.00	26.9	28.30	40.0	2.53
2101	2.568	<0.0050	8.00	<3.00	52.7	52.14	20.0	5.18
2121	5.056	<0.0050	15.0	<3.00	38.6	40.53	25.0	4.35
2125	2.208	0.00990	100.0	10.0	26.9	26.00	20.0	2.82
2128	<2.00	0.00763	80.0	3.00	18.7	19.60	10.0	1.88
2129	3.574	0.0132	100.0	3.00	22.9	24.66	12.0	2.55
2131	5.612	<0.0050	2.00	1000	39.1	14.37	15.0	2.99
2132	4.131	0.0222	100.0	6.00	29.1	27.84	12.0	3.17
2138	<2.00	0.0270	100.0	<3.00	30.1	31.53	<10.0	2.81
2140	<2.00	0.0336	120.0	<3.00	52.2	61.79	12.0	4.68
2142	4.590	<0.0050	12.0	3.00	49.8	53.25	60.0	5.04
2143	<2.00	<0.0050	2.00	3.00	5.32	8.719	25.0	1.18
2144	4.734	<0.0050	2.00	4.00	6.12	12.59	10.0	1.27
2147	2.434	<0.0050	3.00	3.00	7.06	9.905	10.0	1.54
2148	4.022	<0.0050	3.00	3.00	7.67	8.734	10.0	1.49
2149	9.348	<0.0050	10.0	<3.00	34.5	36.76	80.0	3.41
2150	2.441	<0.0050	6.00	15.0	8.83	11.31	15.0	1.25
2151	7.248	<0.0050	12.0	4.00	28.1	31.12	40.0	2.77
2162	2.718	<0.0050	2.00	8.00	7.28	10.51	30.0	1.06
2163	4.934	<0.0050	3.00	>0.1%	13.1	13.72	20.0	3.52
2164	7.533	<0.0050	2.00	30.0	6.87	6.155	20.0	1.50
2166	3.014	0.00935	100.0	6.00	21.7	25.30	80.0	2.98
2169	<2.00	0.0116	80.0	4.00	20.8	25.32	20.0	2.38
2173	4.065	<0.0050	10.0	80.0	29.2	31.29	30.0	3.72
2174	3.965	<0.0050	15.0	<3.00	62.8	73.12	15.0	6.16
2177	8.952	0.00581	50.0	60.0	14.1	20.33	15.0	2.18
2182	3.977	<0.0050	6.00	<3.00	46.0	51.79	25.0	4.93
2183	4.680	<0.0050	6.00	<3.00	76.5	87.41	40.0	7.51
2187	<2.00	0.0219	60.0	<3.00	23.5	23.60	10.0	2.30
2204	<2.00	0.0203	100.0	<3.00	31.8	32.28	10.0	3.12
2213	9.867	<0.0050	2.50	4.00	5.93	6.832	20.0	1.84
2215	3.152	<0.0050	2.50	3.00	43.7	47.96	100.0	5.31
2220	9.675	<0.0050	4.00	>0.1%	4.88	6.205	10.0	0.36
2223	11.01	<0.0050	2.50	200.0	27.0	25.43	15.0	1.01
2224	4.665	<0.0050	3.00	>0.1%	9.29	8.884	10.0	1.17
XB1	n. a.	n. a.	n. a.	n. a.	6.3	n. a.	n. a.	0.47
XB2	n. a.	n. a.	n. a.	n. a.	7.88	n. a.	n. a.	0.82
unit	ppm	wt.%	ppm	ppm	ppm	ppm	ppm	ppm

	Yb	Zn	Zr	Zr	Zr	Th/U	Zr/Hf	Y/Ho
	1	*1*	*3*	*0*	*1*			
2010	<3.00	30.0	245	324.1	80.0	6.57	38.6	28.6
2011	<3.00	40.0	215	280.0	80.0	6.22	40.0	29.4
2028	<3.00	60.0	167	212.7	60.0	4.52	39.2	27.8
2029	<3.00	120.0	226	245.6	80.0	4.94	39.7	27.1
2032	<3.00	60.0	170	199.1	60.0	4.50	37.5	28.0
2044	<3.00	60.0	400	383.4	150.0	4.67	42.7	26.5
2050	<3.00	60.0	40.7	894.3	60.0	0.56	14.9	28.9
2056	<3.00	30.0	20.1	21.27	<60.0	1.61	9.2	35.9
2060	<3.00	60.0	151	193.3	120.0	2.62	38.6	28.1
2068	<3.00	120.0	355	349.6	80.0	3.43	44.4	26.6
2079	3.00	60.0	175	174.8	150.0	3.44	29.9	30.2
2080	3.00	40.0	214	185.0	300.0	1.28	30.5	29.6
2084	3.00	40.0	129	125.9	80.0	2.28	25.0	31.8
2096	3.00	60.0	198	174.8	150.0	4.53	32.9	29.7
2101	<3.00	80.0	121	126.5	80.0	3.48	25.4	27.7
2121	<3.00	25.0	336	375.7	100.0	3.61	36.6	29.4
2125	<3.00	150.0	240	264.6	100.0	4.96	37.8	27.9
2128	<3.00	60.0	217	246.3	80.0	4.78	39.6	27.7
2129	<3.00	80.0	161	155.6	100.0	2.44	38.0	27.2
2131	<3.00	20.0	437	29.43	<60.0	3.43	48.6	27.7
2132	<3.00	60.0	197	207.4	80.0	3.06	37.3	27.9
2138	<3.00	120.0	224	222.6	100.0	3.16	42.1	27.0
2140	<3.00	120.0	155	165.8	80.0	1.70	37.2	28.8
2142	5.00	150.0	109	115.9	150.0	4.36	20.5	28.1
2143	<3.00	200.0	16.1	14.93	120.0	5.40	5.8	14.2
2144	<3.00	300.0	10.4	10.01	120.0	2.08	5.9	13.9
2147	<3.00	150.0	44.9	47.73	150.0	6.33	3.8	16.0
2148	<3.00	120.0	32.1	26.36	100.0	4.30	4.6	18.1
2149	8.00	60.0	110	113.0	120.0	2.71	23.3	31.6
2150	<3.00	20.0	143	148.3	80.0	9.17	28.3	19.6
2151	3.00	60.0	107	112.4	150.0	2.78	23.6	30.6
2162	3.00	60.0	6.95	10.37	80.0	2.27	4.6	22.2
2163	<3.00	120.0	35.2	37.43	<60.0	3.29	2.8	17.0
2164	<3.00	300.0	49.6	50.21	80.0	1.65	2.3	18.6
2166	<3.00	80.0	65.6	58.36	60.0	1.58	27.8	24.0
2169	<3.00	60.0	86.4	101.7	60.0	2.54	23.5	25.7
2173	3.00	100.0	137	178.3	80.0	3.04	22.1	24.0
2174	<3.00	120.0	578	556.6	100.0	3.26	46.3	25.7
2177	<3.00	120.0	64	63.56	60.0	2.32	6.0	23.3
2182	<3.00	15.0	201	203.6	150.0	4.65	28.8	25.2
2183	3.00	30.0	167	162.4	80.0	2.98	24.4	27.8
2187	<3.00	60.0	106	105.4	60.0	3.31	41.5	27.2
2204	<3.00	100.0	190	178.4	80.0	3.25	40.0	27.8
2213	<3.00	800.0	25.6	23.35	120.0	1.50	4.7	12.8
2215	10.0	120.0	10.0	12.39	100.0	2.37	6.0	23.0
2220	<3.00	30.0	17.3	13.13	<60.0	0.47	13.9	32.8
2223	<3.00	30.0	5.41	8.093	80.0	0.16	16.9	30.4
2224	<3.00	30.0	5.85	3.579	<60.0	0.34	23.6	29.6
XB1	n. a.	n. a.	33.99	n. a.	n. a.	0.85	16.2	35.3
XB2	n. a.	n. a.	34.08	n. a.	n. a.	1.06	14.4	30.0
unit	ppm	ppm	ppm	ppm	ppm			

Table 4.2. REE analysis of ore concentrates from the ore processing plant and tailings from the tailing pond (ppm).

Element	TP* 3	TP 4	TP 5	TP 6	TP 7	SM1 -1	SM1- 2	SM2 a-1	SM2 a-2	SM2 b-1	SM2b- 2	SM3 a	SM3 b	SM4	SM5
Rb	443	453	481	382	366	1484	1462	1455	1486	1448	1463	558	834	29.4	4361
Sr	59.2	49.0	45.8	49.6	47.2	4.01	3.81	12.0	11.9	11.6	11.1	22.2	14.1	51.4	35.9
Y	10.2	6.19	7.39	9.25	6.93	11.4	4.73	6.36	5.97	5.11	5.35	47.0	16.5	179	86.4
Zr	35.6	21.7	24.5	30.4	19.8	24.7	26.2	36.1	27.9	26.4	24.8	111	20.2	456	122
Nb	68.6	51.2	48.8	72.1	51.0	73.7	76.8	95.3	44.6	62.1	41.0	1025	118	14201	1209
Cs	47.5	43.3	38.1	38.6	36.3	33.4	31.9	36.8	37.0	37.4	38.7	14.4	22.0	2.22	107
Ba	93.4	71.3	67.6	59.8	59.4	9.75	9.32	8.77	9.09	8.02	8.17	6.68	6.74	12.0	35.4
La	8.39	4.87	5.27	5.38	6.67	7.08	4.95	7.15	7.24	3.97	2.92	277	34.9	1924	370
Ce	18.2	10.6	12.5	12.2	14.8	23.5	16.5	20.5	20.6	11.7	8.62	836	102	5794	1137
Pr	2.15	1.28	1.50	1.49	1.78	2.81	1.97	2.53	2.50	1.45	1.08	99.6	12.3	702	132
Nd	7.95	4.65	5.44	5.64	6.51	6.94	4.93	7.31	7.07	4.30	3.42	260	33.1	1749	349
Sm	2.23	1.42	1.71	1.91	1.99	2.94	2.09	3.35	3.10	2.02	1.75	98.1	13.4	673	132
Eu	0.24	0.15	0.18	0.19	0.14	< 0.01	< 0.01	0.07	0.08	0.06	0.06	0.28	0.07	1.78	0.57
Gd	2.17	1.42	1.61	2.02	1.87	2.28	1.37	2.25	2.03	1.48	1.42	43.3	7.28	279	60.0
Tb	0.40	0.26	0.31	0.39	0.33	0.71	0.32	0.53	0.49	0.36	0.38	8.62	1.68	55.1	13.4
Dy	2.13	1.30	1.60	1.94	1.55	4.94	1.92	2.99	2.72	2.20	2.24	37.7	8.70	238	69.3
Ho	0.32	0.19	0.24	0.27	0.20	0.82	0.28	0.43	0.40	0.33	0.34	4.47	1.20	27.9	9.51
Er	0.83	0.48	0.64	0.70	0.48	2.40	0.81	1.22	1.11	0.96	0.96	11.7	3.32	76.9	28.5
Tm	0.13	0.06	0.09	0.10	0.07	0.42	0.15	0.20	0.20	0.17	0.17	2.15	0.60	15.9	5.80
Yb	0.86	0.48	0.62	0.73	0.45	3.02	1.12	1.65	1.49	1.34	1.31	17.1	4.48	138	48.0
Lu	0.12	0.07	0.09	0.12	0.06	0.37	0.15	0.22	0.19	0.17	0.17	2.24	0.56	18.5	6.23
Hf	1.91	1.46	1.68	1.79	1.28	9.04	9.96	9.36	6.78	6.47	5.62	30.5	4.37	125	25.3
Ta	26.1	19.7	24.7	23.2	17.9	168	168	121	103	101	87.6	281	80.4	21641	151
Pb	25.4	26.1	18.7	39.0	20.8	60.2	60.4	73.8	75.8	60.4	66.4	295	74.2	3514	359
Th	6.03	3.85	4.22	3.55	5.14	10.6	8.81	11.7	11.2	8.04	7.72	231	26.0	1315	302
U	10.9	5.10	4.09	5.95	6.09	6.02	6.35	5.09	6.75	4.65	6.27	129	18.2	1561	140
Y/Ho	31.6	32.6	31.4	34.3	34.3	13.9	17.1	15.0	15.0	15.6	15.7	10.5	13.8	6.4	9.1
Nb/Ta	2.63	2.60	1.98	3.11	2.85	0.44	0.46	0.78	0.43	0.61	0.47	3.64	1.47	0.66	8.02
Zr/Hf	18.68	14.9	14.5	17.0	15.5	2.73	2.63	3.85	4.12	4.09	4.41	3.66	4.61	3.64	4.83
Th/U	0.56	0.75	1.03	0.60	0.84	1.75	1.39	2.31	1.66	1.73	1.23	1.79	1.42	0.84	2.15

*TP – tailing pond sediments, SM – ore concentrates

Table 4.3. Total element analysis of lichens and birch leaves.

Element	Sample description	Sampling location	Mo	Cu	Pb	Zn	Ag	Ni	Co	Mn	Fe	As	U	Au	Th	Sr	Cd	Sb
SAMPLES			ppm	ppm	ppm	ppm	ppb	ppm	ppm	ppm	%	ppm	ppm	ppb	ppm	ppm	ppm	ppm
LBL	Lichens	Lake Baikal	0.23	8.45	4.19	63.8	48	2.6	0.52	58	0.146	3.4	0.16	52.4	0.27	5.1	0.08	0.18
SEL 2	Lichens	Settlement	0.25	8.41	19.47	85.3	40	7.2	1.78	273	0.545	4.2	0.2	< 0.2	0.84	71.4	0.33	0.24
SEL 3	Lichens	Settlement	0.2	7.12	8.23	90.6	33	4.3	1.06	265	0.284	2.8	0.12	< 0.2	0.52	40.7	0.19	0.12
SEL 5	Lichens	Settlement	0.25	7.87	22.99	93.2	46	4.3	1.38	222	0.427	5.6	0.18	1.8	0.77	37.5	0.29	0.24
SEL 6	Lichens	Settlement	0.15	5.81	9.53	92.1	29	3.7	0.99	222	0.312	3.8	0.11	1	0.46	57.3	0.37	0.13
SEL 8	Lichens	Settlement	0.19	6.81	10.78	94.3	38	4.3	1.2	217	0.464	5.1	0.15	3.9	0.64	48	0.29	0.18
TPL 2	Lichens	Tailing pond	0.27	6.43	10.07	83.6	92	4.5	0.88	223	0.226	6	0.73	8	0.47	31.8	0.26	0.09
TPL 4	Lichens	Tailing pond	0.65	6.53	32.57	102.6	507	3	0.78	254	0.257	12.4	6.47	6.4	2.28	26.3	0.37	0.12
QBL	Birch Leaves	Orlovka quarry	0.04	4.97	0.79	395.8	2	1.3	0.86	1393	0.008	0.3	0.01	< 0.2	0.02	6.3	2.01	0.03
BGEBL	Birch Leaves	East	0.24	3.89	0.16	27.8	3	0.5	0.25	185	0.006	0.2	< .01	2.1	< 0.01	117.1	0.03	< 0.02
L1 c	Lichens	Orlovka quarry	0.33	5.56	13.62	45.5	63	2.8	1	120	0.421	6.1	0.22	< .2	0.58	32.7	0.28	0.11
L1ed	Lichens	Orlovka quarry	0.2	5.2	10.57	48.6	86	2	0.66	94	0.241	3.4	0.15	0.7	0.34	25.7	0.27	0.06
L2	Lichens	Orlovka quarry	0.42	6.7	21.68	41.7	90	4.4	1.44	107	0.42	3.4	0.67	2.4	0.93	61.5	0.38	0.13
OQL 2	Lichens	Orlovka quarry	0.38	6.84	13.37	49	61	4	1.54	155	0.488	6.6	0.26	1.6	0.71	47.4	0.27	0.15
OQL 3	Lichens	Orlovka quarry	0.34	7.54	17.88	50.3	61	4.6	1.43	133	0.419	5.3	0.27	1.1	0.77	46.3	0.42	0.15
OQL 4a	Lichens	Orlovka quarry	0.25	7.58	16.81	92.1	52	3.3	1.16	292	0.398	5.9	0.24	1.2	0.56	56.5	0.63	0.12
OQL 4c	Lichens	Orlovka quarry	0.34	5.43	11.57	43.4	82	3.1	0.98	123	0.385	4.7	0.22	0.8	0.57	36.2	0.26	0.12
OQL 5a	Lichens	Orlovka quarry	0.29	7.23	17.22	89.4	58	3.4	1.19	365	0.401	5.8	0.22	11.3	0.6	103	0.75	0.13
OQL 5b	Lichens	Orlovka quarry	0.46	7.12	14.59	50.3	77	3.7	1.47	154	0.626	7.7	0.27	< 0.2	0.87	34.9	0.29	0.16
SML 5	Lichens	Orlovka quarry	0.4	10.77	17.7	107.5	90	7.2	2.17	508	0.628	7.2	0.58	1.9	0.96	82.2	0.67	0.22
SML 6	Lichens	Orlovka quarry	0.61	11.62	32.52	83.7	117	8.1	2.5	449	0.686	12.2	1.42	1	1.44	104.9	0.4	0.32
SML 7	Lichens	Orlovka quarry	0.19	8.87	19.73	87.9	46	6.1	1.63	251	0.453	3.8	0.18	0.3	0.96	66.9	0.33	0.24
SQL 4	Lichens	Orlovka quarry	0.69	10.45	29.26	94	281	11.5	2.77	681	0.749	19.6	1.37	0.5	2.14	230.5	1.31	0.18

Element	Bi	V	Ca	P	La	Cr	Mg	Ba	Ti	B	Al	Na	K	W	Sc	Tl	S	Hg	Se	Te	Ga
SAMPLES	ppm	ppm	%	%	ppm	ppm	%	ppm	ppm	ppm	%	%	%	ppm	ppm	ppm	%	ppb	ppm	ppm	ppm
LBL	0.07	6	0.1	0.265	1.26	5.42	0.066	9.7	73	2	0.07	0.002	0.52	0.2	1	0.03	0.29	1823	0.2	< 0.02	0.5
SEL 2	0.11	10	2.86	0.188	5.7	6.26	0.128	46.1	75	2	0.39	0.006	0.41	0.4	1	0.03	0.23	231	0.2	< 0.02	1.3
SEL 3	0.08	6	1.14	0.195	2.59	4.25	0.107	38.7	55	2	0.19	0.007	0.49	0.3	0.7	0.02	0.2	202	0.2	< 0.02	0.7
SEL 5	0.14	7	1.57	0.22	5.59	5.19	0.105	30.5	74	2	0.25	0.006	0.42	1.2	0.8	0.03	0.15	86	0.2	< 0.02	0.9
SEL 6	0.09	5	1.83	0.203	2.96	4.12	0.086	28.2	52	1	0.16	0.006	0.44	0.5	0.6	0.02	0.13	70	0.1	< 0.02	0.6
SEL 8	0.13	6	1.5	0.194	3.83	4.97	0.096	30.2	61	2	0.23	0.005	0.43	0.6	0.9	0.02	0.13	1578	0.2	< 0.02	0.8
TPL 2	0.67	4	1.01	0.215	2.8	3.9	0.090	28.6	43	3	0.16	0.005	0.45	25.6	0.6	0.02	0.14	4174	0.3	< 0.02	0.5
TPL 4	6.77	3	0.67	0.16	2.54	4.63	0.078	20.6	36	2	0.16	0.005	0.35	328.5	0.7	0.04	< 0.01	1491	0.4	< 0.02	0.6
QBL	0.02	< 2	0.57	0.09	0.03	1.22	0.216	2.7	4	5	0.02	0.003	0.9	0.2	0.2	0.02	0.04	16	< 0.1	< 0.02	0.1
BGEBL	<0.02	< 2	0.96	0.152	0.02	1.49	0.384	28	6	24	< 0.01	0.003	0.74	< 0.1	0.3	< 0.02	0.13	27	0.1	< 0.02	< 0.1
L1 c	0.66	5	1.38	0.124	4.35	4.14	0.083	30.4	86	< 1	0.23	0.005	0.3	4.1	1	0.07	0.09	104	< .1	< 0.02	0.8
L1ed	0.35	3	1.07	0.168	2.53	3.38	0.066	19.6	52	1	0.14	0.003	0.37	1.9	0.7	0.04	0.18	110	< .1	0.02	0.5
L2	0.81	6	1.75	0.138	5.41	6.11	0.099	45.8	103	1	0.35	0.005	0.35	15.8	0.9	0.05	0.09	113	0.4	< 0.02	1.1
OQL 2	0.61	6	1.49	0.138	4.36	4.9	0.113	37.5	89	1	0.3	0.006	0.35	2.7	1.1	0.07	0.07	130	0.5	< 0.02	1.1
OQL 3	0.64	6	2.01	0.134	5.52	5.11	0.110	42.5	79	2	0.3	0.005	0.34	3.4	1.1	0.06	< 0.01	112	0.5	< 0.02	1.1
OQL 4a	0.45	6	2.68	0.211	4	4.32	0.112	42.3	86	1	0.22	0.006	0.44	3	0.9	0.06	0.1	350	0.4	0.04	0.9
OQL 4c	0.5	5	1.46	0.161	3.76	4.26	0.098	31	85	1	0.23	0.007	0.36	2.9	1	0.06	0.09	97	0.3	0.02	0.9
OQL 5a	0.51	5	3.76	0.16	3.55	4.4	0.106	50.4	85	1	0.21	0.007	0.41	3.3	0.9	0.06	0.06	125	0.3	<0.02	0.9
OQL 5b	0.79	8	1.34	0.139	5.15	5.12	0.112	35.2	131	1	0.34	0.006	0.35	4.1	1.4	0.08	< 0.01	134	0.4	0.02	1.2
SML 5	0.83	9	2.24	0.248	5.18	7.32	0.193	57	102	2	0.38	0.024	0.43	17.9	1	0.06	0.17	335	0.3	0.03	1.3
SML 6	1.45	9	2.13	0.167	7.26	7.84	0.169	85.4	119	4	0.43	0.019	0.36	50	1.1	0.07	0.09	361	0.4	< 0.02	1.5
SML 7	0.09	7	2.51	0.211	5.05	5.35	0.131	44.4	67	2	0.33	0.006	0.42	0.4	0.9	0.02	0.11	571	0.4	< 0.02	1.1
SQL 4	3.49	9	5.25	0.168	9.88	8.22	0.195	59.3	126	2	0.39	0.013	0.39	67	0.8	0.08	0.11	311	0.2	0.02	1.3

Table 4.4. REE analysis of lichens and birch leaves.

Element	Cs	Ge	Hf	Nb	Rb	Sc	Sn	S	Ta	Zr	Y	Ce	In	Re	Be	Li	Pr	Nd	Sm	Eu	Gd	Tb	Dy	Ho	Er	Tm	Yb	Lu
SAMPLES	ppm	ppm	ppm	ppm	ppm	ppm	ppm	%	ppm	ppm	ppm	ppm	ppm	ppb	ppm	ppm	ppm	ppm	ppm	ppm	ppm	ppm	ppm	ppm	ppm	ppm	ppm	ppm
LBL	0.108	0.09	0.016	0.242	5.1	0.9	0.31	0.26	0.005	0.71	0.814	2.17	< 0.02	< 2	< 0.1	0.48	0.25	1.11	0.21	0.03	0.27	0.02	0.18	0.03	0.07	0.01	0.07	< 0.02
SEL 2	0.571	0.03	0.033	0.461	11.4	0.9	0.32	0.21	0.004	1.64	2.596	9.72	<0.02	< 2	0.3	4.2	1.11	4.94	0.89	0.15	0.87	0.11	0.51	0.1	0.26	0.03	0.2	0.03
SEL 3	0.335	0.05	0.025	0.217	5.2	0.6	0.18	0.18	0.003	0.89	1.123	4.38	< 0.02	< 2	0.2	2.22	0.5	2.39	0.36	0.06	0.43	0.05	0.23	0.04	0.1	0.01	0.09	< 0.02
SEL 5	0.535	0.03	0.039	0.372	6.5	0.7	0.3	0.13	0.004	1.51	2.511	9.3	< 0.02	< 2	0.3	3.61	1.09	4.93	0.76	0.13	0.69	0.11	0.52	0.1	0.26	0.03	0.22	0.03
SEL 6	0.37	0.02	0.025	0.234	9.5	0.5	0.21	0.12	0.002	1.06	1.664	4.94	< 0.02	< 2	0.3	2.03	0.57	2.56	0.48	0.07	0.51	0.07	0.31	0.06	0.16	0.02	0.14	0.02
SEL 8	0.428	0.02	0.026	0.344	11	0.8	0.25	0.12	0.004	1.49	2.581	6.36	< 0.02	< 2	0.3	2.67	0.74	3.2	0.58	0.1	0.69	0.09	0.43	0.09	0.23	0.03	0.16	0.03
TPL 2	0.426	0.02	0.018	0.563	6	0.5	0.33	0.13	0.039	0.99	1.43	4.83	< 0.02	< 2	0.2	2.15	0.57	2.6	0.45	0.06	0.48	0.06	0.31	0.05	0.13	0.02	0.09	0.02
TPL 4	1.077	0.01	0.13	4.444	11.2	0.6	0.55	< 0.02	0.272	2.56	2.235	4.39	0.03	4	0.5	6.02	0.56	2.45	0.6	0.08	0.7	0.11	0.49	0.07	0.21	0.03	0.17	0.02
QBL	8.944	0.01	0.001	0.011	122.3	0.2	0.03	0.03	< 0.001	0.02	0.141	0.05	< 0.02	< 2	0.2	0.14	< .02	0.06	0.03	< 0.02	0.06	0.01	0.04	< 0.02	< 0.02	< 0.01	0.02	< 0.02
BGEBL	0.022	0.01	< 0.001	0.01	7.5	0.2	0.03	0.11	< 0.001	0.01	0.01	0.02	< 0.02	< 2	<0.1	< 0.01	< 0.02	< 0.02	< 0.02	< 0.02	< 0.02	< 0.01	< 0.02	< 0.02	< 0.02	< 0.01	< 0.01	< 0.02
L1 c	1.345	0.03	0.035	0.473	14.2	1	0.5	0.08	0.019	0.87	3.578	8.01	0.02	< 2	0.2	7.62	1	4.56	0.99	0.17	0.88	0.16	0.76	0.12	0.3	0.04	0.2	0.03
L1ed	0.723	0.04	0.022	0.245	10.8	0.6	0.24	0.16	0.009	0.53	2.255	4.64	< 0.02	< 2	0.1	3.88	0.56	2.53	0.51	0.11	0.64	0.09	0.44	0.08	0.19	0.03	0.14	0.02
L2	0.634	0.05	0.038	0.703	9.3	0.8	0.31	0.08	0.018	1.37	2.944	10.11	< 0.02	< 2	0.3	3.46	1.13	5.15	0.9	0.14	0.77	0.12	0.61	0.11	0.29	0.03	0.22	0.03
OQL 2	1.365	0.05	0.039	0.495	14.5	1.1	0.5	0.06	0.012	1.11	3.278	8.11	0.02	< 2	0.3	9	0.97	4.59	0.94	0.16	1.01	0.13	0.7	0.11	0.31	0.03	0.2	0.03
OQL 3	1.295	0.03	0.052	0.404	16.5	1	0.53	< .02	0.011	1.29	3.869	10.13	0.02	< 2	0.4	8.56	1.27	5.59	1.06	0.19	1.06	0.18	0.84	0.15	0.39	0.05	0.31	0.04
OQL 4a	1.143	0.03	0.029	0.37	12.9	0.9	0.4	0.09	0.008	0.99	2.412	7.15	0.02	< 2	0.2	6.31	0.83	3.79	0.69	0.12	0.81	0.11	0.48	0.09	0.25	0.03	0.2	0.02
OQL 4c	1.134	0.03	0.033	0.404	12.7	0.9	0.39	0.08	0.014	0.89	2.977	7.19	0.02	< 2	0.2	7.53	0.85	3.98	0.78	0.12	0.87	0.14	0.64	0.11	0.3	0.04	0.2	0.03
OQL 5a	1.225	0.04	0.035	0.402	15	0.9	0.36	0.05	0.014	1.08	1.999	6.1	0.02	< 2	0.1	7.43	0.74	3.21	0.59	0.1	0.68	0.09	0.46	0.08	0.2	0.02	0.14	0.02
OQL 5b	1.896	0.03	0.036	0.566	17	1.3	0.75	< .02	0.012	0.9	3.817	9.84	0.03	2	0.3	11.41	1.17	5.48	1.09	0.21	1.32	0.17	0.87	0.15	0.4	0.05	0.22	0.03
SML 5	1.141	0.02	0.037	0.986	13.5	0.9	0.42	0.15	0.019	1.66	2.645	9.56	0.02	< 2	0.2	6.82	1.13	5.06	1.01	0.15	0.88	0.12	0.59	0.1	0.26	0.03	0.2	0.03
SML 6	1.483	0.06	0.072	1.421	18.3	1	0.53	0.08	0.039	2.57	4.004	12.93	0.02	3	0.4	9.34	1.62	6.95	1.32	0.21	1.18	0.17	0.84	0.13	0.36	0.04	0.26	0.04
SML 7	0.486	0.04	0.037	0.38	9.9	0.9	0.24	0.1	0.003	1.67	2.276	8.74	< 0.02	< 2	0.2	3.7	1	4.3	0.72	0.12	0.62	0.11	0.49	0.08	0.24	0.03	0.18	0.02
SQL 4	2.914	0.04	0.094	1.831	21.5	0.8	0.52	0.1	0.056	2.71	6.195	15.35	<0.02	< 2	0.5	12.3	2.03	8.68	1.74	0.27	1.55	0.27	1.19	0.2	0.56	0.07	0.38	0.05

APPENDIX V.

ADDITIONAL PUBLICATIONS

5.1. "Development of an ombrotrophic peat bog (low ash) reference material for the determination of elemental concentrations"

The paper demonstrates an application of the developed method of the microwave assisted acid dissolution for plant material (see CHAPTER 2 for full details) to the acid decomposition of peat samples (the method is cited under "Laboratory 2" in the publication).

5.2. "Accurate and precise Pb isotope ratio measurements in environmental samples by MC-ICP-MS"

The paper summarises the findings of the CHAPTER 3.

PAPER

Development of an ombrotrophic peat bog (low ash) reference material for the determination of elemental concentrations†

C. Yafa,[a] J. G. Farmer,*[a] M. C. Graham,[a] J. R. Bacon,[b] C. Barbante,[c,d] W. R. L. Cairns,[d] R. Bindler,[e] I. Renberg,[e] A. Cheburkin,[f] H. Emons,[g,h] M. J. Handley,[i] S. A. Norton,[i] M. Krachler,[j] W. Shotyk,[j] X. D. Li,[k] A. Martinez-Cortizas,[l] I. D. Pulford,[m] V. MacIver,[m] J. Schweyer,[n] E. Steinnes,[o] T. E. Sjøbakk,[o] D. Weiss,[p,q] A. Dolgopolova[p,q] and M. Kylander[p,q]

[a]*School of GeoSciences, Joseph Black Building, University of Edinburgh, West Mains Road, Edinburgh, UK EH9 3JJ. E-mail: J.G.Farmer@ed.ac.uk; Fax: +44 (0)131 650 4757; Tel: +44 (0)131 650 4757*
[b]*Macaulay Institute, Craigiebuckler, Aberdeen, UK AB15 8QH*
[c]*Department of Environmental Sciences, University Ca' Foscari of Venice, Dorsoduro 2137, 30123 Venice, Italy*
[d]*Institute for the Dynamics of Environmental Processes, CNR, Dorsoduro 2137, 30123 Venice, Italy*
[e]*Department of Ecology and Environmental Science, Umeå University, SE-901 87 Umeå, Sweden*
[f]*Key Analytical, 267 Brebeuf Avenue, Sudbury, Ontario P3C 5H2, Canada*
[g]*Institute for Phytosphere Research, Research Centre Juelich, 52425 Juelich, Germany*
[h]*European Commission, Joint Research Centre, Institute for Reference Materials and Measurements, Retieseweg 2440 Geel, Belgium*
[i]*Department of Earth Sciences and The Climate Change Institute, 314 Bryand Global Sciences Center, University of Maine, Orono, ME, 04469-5790, USA*
[j]*Institute of Environmental Geochemistry, University of Heidelberg, Im Neuenheimer Feld 236, D-69120 Heidelberg, Germany*
[k]*Department of Civil and Structural Engineering, The Hong Kong Polytechnic University, Hung Hom, Kowloon, Hong Kong*
[l]*Department of Soil Science and Agricultural Chemistry, University of Santiago di Compostela, Campus Sur s/n, E-15782 Santiago di Compostela, Spain*
[m]*Department of Chemistry, University of Glasgow, Glasgow, UK G12 8QQ*
[n]*Geoscience Laboratories, 933 Ramsey Lake Road, Sudbury, Ontario, P3E 6B5, Canada*
[o]*Department of Chemistry, Norwegian University of Science and Technology, NO-7491 Trondheim, Norway*
[p]*Department of Earth Science and Engineering, Imperial College of London, London, UK SW7 2BP*
[q]*Department of Mineralogy, The Natural History Museum, London, UK SW7 5AZ*

Received 1st December 2003, Accepted 12th March 2004
First published as an Advance Article on the web 7th April 2004

Given the increasing interest in using peat bogs as archives of atmospheric metal deposition, the lack of validated sample preparation methods and suitable certified reference materials has hindered not only the quality assurance of the generated analytical data but also the interpretation and comparison of peat core metal profiles from different laboratories in the international community. Reference materials play an important role in the evaluation of the accuracy of analytical results and are essential parts of good laboratory practice. An ombrotrophic peat bog reference material has been developed by 14 laboratories from nine countries in an inter-laboratory comparison between February and October 2002. The material has been characterised for both acid-extractable and total concentrations of a range of elements, including Al, As, Ca, Cd, Cr, Cu, Fe, Hg, Mg, Mn, Na, Ni, P, Pb, Ti, V and Zn. The steps involved in the production of the reference material (*i.e.* collection and preparation, homogeneity and stability studies, and certification) are described in detail.

DOI: 10.1039/b315647h

Introduction

Environmental samples such as tree rings, mosses, aquatic sediments, snow, ice, and peat have been used as archives for the study of atmospheric metal deposition.[1–3] The surface layers in ombrotrophic raised bogs are isolated from the influence of local ground water and surface water, and receive their inorganic content by atmospheric deposition only.[4] Ombrotrophic peat that has accumulated during the past hundreds or thousands of years, therefore, can be used to study vegetation history, climate change, and, in principle, the historical trend of atmospheric metal deposition. Most recent

† Presented as part of the Archives of Environmental Contamination at the 6th International Symposium on Environmental Geochemistry, Edinburgh, Scotland, 7–11 September 2003.

relevant research results,[5–9] *e.g.* for Pb, have been consistent with information from other archives, including lake sediments and ice cores, and are compatible with known historical trends where available, *e.g.* the emission of Pb from different sources. Given the increase in this type of study, the lack of a common, validated sample preparation method and of a certified peat reference material has hindered not only the quality assurance of the generated analytical data but also the interpretation and comparison of peat core metal profiles from different laboratories in the international community. Instead of using an authentic peat reference material, quality control in this sort of study has long been referred to certified reference materials (CRMs) developed for plants and soils. Although an attempt, as yet uncompleted, was made to develop a peat reference material for quality control use by laboratories in the international peat bog community,[10] the material was of fen origin and had high ash content (~20%), uncharacteristic of ombrotrophic peat bogs. In addition, different laboratories in this field of research currently adopt a wide range of practices, including the determination of acid-extractable and of total elemental concentrations by various instrumental analytical techniques. To compare and standardise these different approaches, we developed a new candidate peat reference material, derived from an ombrotrophic bog, and subjected it to an international inter-laboratory study as part of the certification process.

The total concentrations of elements can be determined by using non-destructive analytical techniques (XRF, INAA, *etc.*) or destructive analytical techniques employing ashing procedures, such as mixtures of mineral acids with HF for wet ashing or dissolution after dry ashing, alkaline fusion *etc.*, followed by AAS, ICP-OES, ICP-MS *etc.* The acid-extractable concentrations of elements are conventionally defined by the procedures involving extraction with aqua regia, boiling 2 M HNO_3, or cold 2 M HNO_3.[11] Reference materials characterised for both acid-extractable and total concentrations of elements are of value to laboratories that cannot or do not employ HF to achieve total dissolution of aluminosilicate minerals in sample matrices.

Methods

Collection and preparation of the candidate ombrotrophic peat reference material

On 11 September, 2001, the starting material was collected from the ombrotrophic peat bog at Flanders Moss, near Stirling, Scotland. Vegetation on top of the bog was removed using a stainless steel knife and the peat sample dug up by a spade from a depth of ~30 cm in blocks of approximate size 20 cm × 20 cm × 30 cm. Seven blocks of peat of about the same size were collected, yielding a total wet weight of ~70 kg. The wet peat was wrapped up in a polyethylene bag and transported to the Macaulay Institute, Aberdeen, UK, the following day. It was then divided into sub-samples, from which root material was extracted by hand, and air-dried at 30 °C for 10 days on paper-lined aluminium trays. The dried peat was then broken into small aggregates with a wooden hammer and air-dried for a further week. Ten sub-samples were then randomly taken from the drying trays. The moisture content based on oven-drying at 105 °C was determined on each sub-sample, yielding a mean moisture content of ~10% in 30 °C air-dried peat. The air-dried peat was milled to less than 2 mm in particle size with a stainless steel hammer mill (Christie Hunt). Approximately 4.5 kg of peat material was obtained and transferred into a 20-litre glass jar, which was placed on a roller bed for two weeks.

Preliminary study of homogeneity

Ten sub-samples (~2 g each) were randomly taken from the jar and analysed for metal concentrations to make a preliminary assessment of the bulk homogeneity using a modified version of ASTM 826-85 "Standard practice for testing homogeneity of material for development of reference material".[12] This mainly involved the selection of test sub-samples from the bulk material, digestion and analysis of sub-samples (0.25 g), and statistical treatment of the measurement data using the ASTM 826-85 standard protocol. The total concentration for each element of interest was the variable we evaluated to assess homogeneity. The USEPA Method 3052 Protocol[13] was modified for the digestion of sub-samples, carried out by microwave-assisted HF–HNO_3 digestion of peat (total-total digestion method). This method consisted of a representative sample of up to 0.25 g (the initial weight) being ashed at 450 °C for 4 h prior to digestion in 9 ml of concentrated HNO_3 and 0.5 ml HF for about 15 minutes using microwave heating with a suitable laboratory microwave system. The sample and acid are placed in suitably inert polymeric microwave vessels. The vessel is sealed and heated in the microwave system. The temperature profile is specified to permit specific reactions and incorporates reaching 180 ± 5 °C in ~5.5 minutes and remaining at 180 ± 5 °C for 9.5 minutes for the completion of specific reactions. After cooling, the vessel contents are filtered, evaporated to ~1 ml, and then diluted to volume and analysed by FAAS, GFAAS, ICP-OES, or ICP-MS.

Following the preliminary homogeneity tests, the peat material was further homogenised by mixing in the jar on the roller bed for another week. The roller bed was then stopped, and peat material was taken from the jar to fill a series of five pre-cleaned amber glass bottles, each containing a minimum of 30 g. After that, they were promptly closed using polyethylene screwcaps. The glass jar was again rotated for another five minutes and the next five bottles were filled in the same way. The cycle was repeated until a total of 145 (29 × 5) bottles of candidate peat reference material were finally obtained. About ten percent of the bulk peat material that was left on the bottom of the jar was discarded, just in case it was less homogeneous.[14,15] Twenty-nine bottles (one from each series) were set aside for homogeneity and stability testing. The candidate ombrotrophic peat bog reference material was then named NIMT/UOE/FM/001. The ash content (450 °C) of this material was ~4–5% of the 30 °C air-dried weight.

Homogeneity testing

Homogeneity testing for total and acid-extractable concentrations of elements in the candidate ombrotrophic peat bog reference material was carried out by using the *F*-test and ANOVA statistical test. Sixteen (three times the cube root of n units)[16] bottles of candidate peat bog reference material were randomly selected from the 29 bottles that had been set aside earlier. As before, microwave-assisted HF–HNO_3 digestion of peat (total–total digestion method), a modification of the USEPA Method 3052 Protocol, was utilised for total element concentration, while microwave-assisted HNO_3 digestion of peat (total–extractable digestion method), a modification of the USEPA Method 3051 Protocol,[17] yielded acid-extractable element concentration. The latter digestion method employs 10 ml of HNO_3 as reagent instead of the HNO_3–HF mixture used in the former.

Stability study

The stability of the candidate peat bog reference material was tested by storing bottles of the candidate reference material at −20 °C, +4 °C, +20 °C, and +40 °C for a period of 12 months. After 1, 3, 6 and 12 months, the total and acid-extractable elemental concentrations were determined (in five replicates). The procedures were the same as those used in the homogeneity study. Instability would be detected by comparing the

measured element concentrations of samples stored at +4 °C, +20 °C, +40 °C with those of samples stored at −20 °C as determined at various times over 12 months. The samples stored at −20 °C were used as reference for the samples stored at +4 °C, +20 °C and +40 °C, respectively.

Certification of concentration

An international inter-laboratory comparison exercise was conducted to certify the reference material. Laboratories invited to take part in the certification exercise were those of experienced research groups in this field of study, considered to be well-equipped and employing quality control and quality assurance procedures. The 14 laboratories taking part were requested to verify the quality of their measurements, in particular, the validity of calibration (including calibration of balances, volumetric glasswares and other tools of relevance). Participants were free to choose analytical methods of which they had previous experience and could therefore be expected to give valid results when applied by an experienced analyst. They were also asked to make a minimum of five independent replicate determinations of each element in the candidate reference material, each laboratory being supplied with one bottle of prepared peat material.

On receipt of data from participants, an identification number (Laboratory ID) was assigned to each laboratory. Where there were two separate sets of data, *i.e.* one for total elemental concentration and another for acid-extractable element concentration, the Laboratory ID for the latter set is not necessarily the same as that for the former set. Nine laboratories reported data for total (HNO_3–HF, HNO_3–HBF_4, HNO_3–H_2O_2–H_2O–HF) concentrations, and ten laboratories for acid-extractable (HNO_3, HNO_3–HCl, HNO_3–$HClO_4$) concentrations, using a range of digestion conditions and a variety of analytical techniques (AAS, GFAAS, ICP-OES, ICP-MS), including, in the case of one laboratory, XRF analysis of the solid phase, and, in two others, thermal decomposition AAS for Hg. Table 1 lists the digestion methods and instrumental analytical techniques used by the participants.

Results and discussion

Preliminary study of homogeneity

Using Pb as an example, the measurement results (Table 2) were treated as follows:

T, B, t', and G were computed, where: T = sum of each column; B = sum of each row; t' = mean of each column; and G = sum of $B_1 \ldots B_n$; b = number of replicate measurements from different aliquots of the solid material (3); and t = number of sub-samples (10)

The degree of freedom at 95% confidence level was calculated from:

$v = (b - 1)(t - 1)$, where v = the number of degrees of freedom

$v = 18$

The value of symbol q corresponding to t and v was found from the reference table given in ASTM 826-85.[12]

$q = 5.07$

The sum of squares due to the sub-samples, S_t, was calculated from

$S_t = [(T_1^2 + T_2^2 + \ldots T_t^2)/b] - (G^2/tb) = 341$

The sum of squares due to runs, S_b, was calculated from

$S_b = [(B_1^2 + B_2^2 + \ldots B_t^2)/t] - (G^2/tb) = 69$

Table 1 Digestion methods and instrumental analytical techniques used by participants in the inter-laboratory comparison exercise for elemental concentrations in NIMT/UOE/FM/001

Methodologies	
Total concentration	**Acid-extractable concentration**
Lab1: HNO_3–HBF_4 high pressure microwave autoclave, ICP-MS	**Lab1**: HNO_3 microwave-assisted, ICP-OES
Lab2: HNO_3–H_2O_2–H_2O–HF microwave-assisted, ICP-OES	**Lab2**: HNO_3 microwave-assisted, HR-ICP-MS
Lab3: HNO_3–HF pressure digestion, ICP-MS	**Lab3**: HNO_3 high-pressure ashing, ICP-MS, HG-AAS (for As)
Lab4: XRF	**Lab4**: HNO_3 microwave-assisted (USEPA Method 3051 Protocol), ICP-OES, GFAAS
Lab5: HNO_3–HF total digestion, ICP-OES	**Lab5**: aqua regia reflux digestion, ICP-OES
Lab6: HNO_3–HF microwave-assisted (USEPA Method 3052 Protocol), ICP-OES, GFAAS	**Lab6**: HNO_3 microwave-assisted (USEPA Method 3051 Protocol), GFAAS, ICP-OES; HNO_3/H_2SO_4 digestion @60 °C, 2 h, CVAAS (for Hg only)
Lab7: HNO_3–HF microwave-assisted (USEPA Method 3052 Protocol), ICP-MS	**Lab7**: aqua regia digestion RT 24 h, 100 °C, 1 h, ICP-MS, ICP-OES
Lab8: thermal decomposition AAS (for Hg only)	**Lab8**: aqua regia digestion @125 °C, 3 h, FAAS
Lab9: thermal decomposition AAS (for Hg only)	**Lab9**: HNO_3–$HClO_4$, heating, ICP-OES
	Lab10: HNO_3 microwave-assisted (USEPA Method 3051 Protocol), ICP-MS

The laboratory ID numbers in the total concentration column (and in Figs. 1 and 2) do not necessarily correspond to those in the acid-extractable concentration column (and in Figs. 3 and 4).

Table 2 Data for total Pb concentration (mg kg^{-1}) (dry-weight (105 °C) basis, *i.e.* corrected for moisture content of the air-dried peat) in the preliminary homogeneity testing of the candidate ombrotrophic peat (low ash) reference material

	Sub-sample numbers										
Replicate	1	2	3	4	5	6	7	8	9	10	Total
1	154	172	168	164	164	170	165	174	164	175	$B_1 = 1672$
2	175	188	169	163	164	169	163	172	163	180	$B_2 = 1705$
3	173	168	169	165	172	162	178	164	185	166	$B_3 = 1703$
Total	$T_1 = 501$	$T_2 = 528$	$T_3 = 506$	$T_4 = 493$	$T_5 = 500$	$T_6 = 501$	$T_7 = 507$	$T_8 = 511$	$T_9 = 512$	$T_{10} = 521$	$G = 5080$
Mean	$t'_1 = 167$	$t'_2 = 176$	$t'_3 = 169$	$t'_4 = 164$	$t'_5 = 167$	$t'_6 = 167$	$t'_7 = 169$	$t'_8 = 170$	$t'_9 = 171$	$t'_{10} = 174$	

The sum of squares of all the measurements in Table 2, $S_{average}$, was defined and calculated from

$$S_{average} = \left(\sum_{i=1}^{t}\right)\left(\sum_{j=1}^{b}\right) Y_{ij}^2 - (G^2/tb)$$

where Y_{ij} = individual values in Table 2.

$S_{average}$ = 1491

The symbol s was defined and calculated from

$$s = \sqrt{(S_{average} - S_b - S_t)/(b-1)(t-1)} = 7.8$$

The symbol w was defined and calculated from

$$w = qs/\sqrt{b} = 23$$

The maximum and minimum of the mean t' values in Table 2 are 176 and 164, respectively, so the maximum difference between any of the mean t' values in Table 2 is 12. As the absolute difference between any two mean values does not exceed w (=23), then there is strong evidence, at 95% confidence level, that the bulk material is homogeneous for Pb. The same treatment was applied to Al, Ca, Co, Cu, Fe, Mg, Mn, Ti, V, and Zn for which similar satisfactory evidence of homogeneity was obtained in each case.

Homogeneity testing

Analytical results for total Pb concentration, expressed in mg kg^{-1} on a dry-weight (at 105 °C) basis, are given in Table 3. Using Microsoft Excel®, Table 4 displays the associated ANOVA calculation (one-way layout), in which *SS* provides the sum of squares, *df* represents the associated degrees of freedom, and *MS* expresses mean squares, which form the basis for the computation of variation. The *P-value* gives the level for which the calculated F (F_{cal}) equals $F_{critical}$. From Table 4, where it can be seen that F_{cal} does not exceed $F_{critical}$, there is strong evidence, at the 95% confidence level, that the candidate peat bog reference material is homogeneous for total Pb concentration. The same treatment was applied to other elements of interest, in each case demonstrating the homogeneity of the candidate material. On the basis of these results, the material was considered to be homogeneous at the level of 0.25 g, the typical 30 °C air-dried weight taken for analysis.

Stability study

The ratios (R_T) of the mean values ($\bar{X}_T$) of five replicate measurements made for samples stored at +4 °C, +20 °C and +40 °C and the mean value ($\bar{X}_{-20\,°C}$) from the five determinations at −20 °C were calculated as:

$$R_T = \bar{X}_T/\bar{X}_{-20\,°C}$$

Table 4 Analysis of variance (ANOVA) for homogeneity testing of total Pb concentration (mg kg^{-1}) in the candidate ombrotrophic peat (low ash) reference material

Source of variation	*SS*	*df*	*MS*	F_{cal}	*P-value*	$F_{critical}$
Between bottles	575	15	38	1.559	0.142	1.992
Within bottles	787	32	25			
Total	1362	47				

The uncertainty U_T was obtained from the coefficient of variation (CV) of five measurements obtained at each temperature: $U_T = \left(CV_T^2 + CV_{-20\,°C}^2\right)^{1/2} R_T$

The R_T ratio should be 1 in the case of ideal stability but, as slight instability might be expected during long storage times, the value 1 should lie between $R_T - U_T$ and $R_T + U_T$. For greater than 98% of the measurements made for samples stored at these conditions, the values fell within $R_T \pm U_T$. It was concluded that there was no instability for a storage time of one year under these conditions. As the candidate material is stable under the storage condition of +40 °C for one year, it can be assumed that the material may be stable for up to two or three years under the storage condition of +20 °C or below. As a result of the stability testing, all of the elements determined were considered to be suitable for certification, provided that the material is stored at typical room temperature or under refrigeration.

Certification of concentration

The sets of results submitted by participants were assumed to be normally distributed, and analysed statistically[16,18] using Grubbs and Cochran's tests to detect outlying values. The Grubbs test[16,18] was used to detect outlying values in the population of individual results and in the population of laboratory means, while Cochran's test[16,18] was used to identify outlying values in the laboratory variances. A summary of the statistical evaluation is given in the certification report.

Using the certification of the total Pb concentration as an example, seven laboratories (1, 2, 3, 4, 5, 6, 7) submitted data for total Pb concentration. The Laboratory Means, standard deviation, and 95% confidence interval of the data from each laboratory are shown in Fig. 1a. The individual replicate results from each laboratory were tested for outliers by using Grubbs 1, Grubbs 2, and Grubbs 3 tests. One replicate from

Table 3 Data for total Pb concentration (mg kg^{-1}) (dry-weight (105 °C) basis, *i.e.* corrected for moisture content of the air-dried peat) in the homogeneity testing of the candidate ombrotrophic peat (low ash) reference material

	Concentration/mg kg^{-1}					
Sample	Replicate #1	Replicate #2	Replicate #3	Mean	Variance	*n*
#1	163	162	157	160	10.1	3
#2	162	160	161	161	0.8	3
#3	165	159	166	164	12.8	3
#4	165	158	159	161	17.1	3
#5	152	159	166	159	48.3	3
#6	159	166	161	162	10.2	3
#7	164	165	164	164	0.3	3
#8	165	162	165	164	3.2	3
#9	157	156	169	161	47.2	3
#10	164	163	161	163	2.6	3
#11	160	152	147	153	41.4	3
#12	158	154	148	153	27.6	3
#13	168	161	166	165	12.0	3
#14	162	165	166	164	4.2	3
#15	169	170	154	164	79.9	3
#16	154	154	169	159	75.8	3

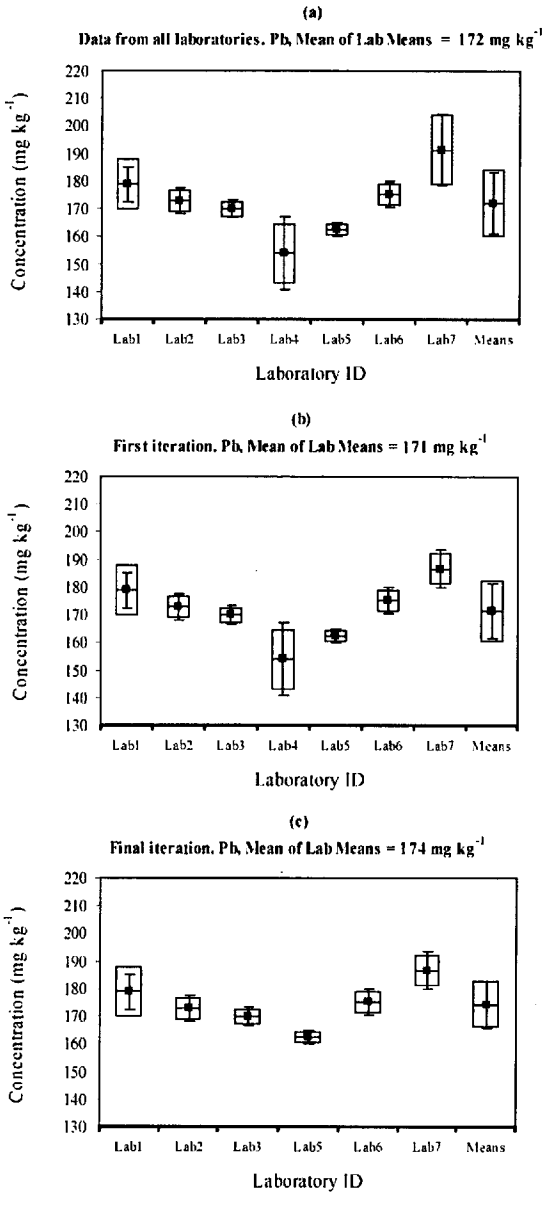

Fig. 1 Inter-laboratory comparison results for total Pb concentration (expressed as concentration, mg kg^{-1}, corrected for moisture content) of NIMT/UOE/FM/001: (a) data from all laboratories, (b) first iteration, (c) final iteration, along with the calculated mean (■), standard deviation (□) and 95% confidence interval (⊥⊥).

Laboratory 7 was identified as a Grubbs 1 outlier. The outlier was then removed, with the resulting outcome for Laboratory 7 shown in Fig. 1b. The Laboratory Means of data from each laboratory were then tested for possible Grubbs 1, Grubbs 2, Grubbs 3, and Cochran's outliers. No Grubbs outlier was identified but it was decided to reject the Laboratory Mean from Laboratory 4 as a Cochran's outlier (variance outlying), evaluation of the data at this stage being displayed in Fig. 1c. Although the Laboratory Mean from Laboratory 1 could perhaps have been rejected as a Cochran's outlier (variance outlying), it was decided to retain it as the spread of results from the six laboratories was considered acceptable. The data processing was therefore stopped at this stage, with a mean Pb concentration of 174 mg kg^{-1}.

The sets of results accepted on technical and statistical grounds are presented in Figs. 2–4. Fig. 2 displays the calculated mean, standard deviation and 95% confidence interval (CI) of the accepted inter-laboratory comparison results for total Cd, Co, Cr, Cu, Mn, Ni, Pb, V, and Zn concentrations (expressed as concentration, mg kg^{-1}, corrected for moisture content), after the final iteration. For acid-extractable concentrations (expressed as concentration, mg kg^{-1}, corrected for moisture content), the calculated mean, standard deviation and 95% confidence interval of the accepted inter-laboratory comparison results after the final iteration are shown for As, Cd, Co, Cr, Cu, Mn, Ni, Pb V, and Zn in Fig. 3 and for Al, Fe, Mg and P in Fig. 4.

Calculation of uncertainty

Again using Pb as the example, the uncertainty of the value assigned to the total Pb concentration (174 mg kg^{-1}) of the ombrotrophic peat bog certified reference material was calculated according to a modification of the Guide on the Expression of Uncertainty in Measurement[19–24] (GUM), using the equation: $U_{CRM} = k\sqrt{u_{char}^2 + u_{bb}^2}$ where U_{CRM} = expanded uncertainty of the total Pb concentration of the peat bog certified reference material; k = coverage factor; u_{char} = uncertainty of the certified metal concentration in the ombrotrophic peat bog reference material; u_{bb} = uncertainty of the between-bottle inhomogeneity. The uncertainty of the instability (u_{stab}) was not included in view of the previously demonstrated stability and in accordance with criteria for the production of a quality control reference material.[16]

As we do not have the full uncertainty budget from the participants in the inter-laboratory comparison exercise, u_{char} can be calculated from the equation: $u_{char} = \frac{s}{\sqrt{l}}$ where s = standard deviation of laboratory means, *i.e.* 8 mg kg^{-1}; l = number of laboratories, *i.e.* 6. Therefore, u_{char} = 3.27 mg kg^{-1}, *i.e.* 1.88% of 174.

The value of u_{bb} can be estimated from ANOVA of the data from homogeneity testing as: $u_{bb} = \sqrt{\frac{MS_{among} - MS_{within}}{n}}$ where MS_{among} = mean square among units, *i.e.* 38; MS_{within} = mean square within units, *i.e.* 25; n = number of subsamples per unit, *i.e.* 3. Therefore, u_{bb} = 2 mg kg^{-1}, *i.e.* 1.29% of 174.

The expanded uncertainty of the value assigned to the total Pb concentration (174 mg kg^{-1}) in the ombrotrophic peat bog certified reference material can be calculated from: $U_{CRM} = ku_c$ where $u_c = \sqrt{u_{char}^2 + u_{bb}^2}$, *i.e.* 2.28%. Therefore, U_{CRM} (k = 2) = 4.56% of 174.

Therefore the certified value for total Pb concentration in the ombrotrophic peat (low ash) reference material NIMT/UOE/FM/001 is 174 ± 8 mg kg^{-1}.

Certified and information-only values

By applying the same treatment as for Pb to the other inter-laboratory comparison results, the certified values (coverage factor of 2) for all inorganic elements determined in the ombrotrophic peat (low ash) reference material NIMT/UOE/FM/001 were calculated and are displayed in Table 5. Where concentration data were not sufficient and considered too variable, the arithmetic means (±1 SD) are given as information-only values for some elements.

The acid-extractable concentrations of Cd, Pb, and Zn are similar to their corresponding total concentrations (Table 5), whereas the acid-extractable concentration of Cr and of some major elements such as Al, Na, and Ti are clearly lower than their corresponding total concentrations. This suggests that Cr and these major elements occur in matrices that cannot

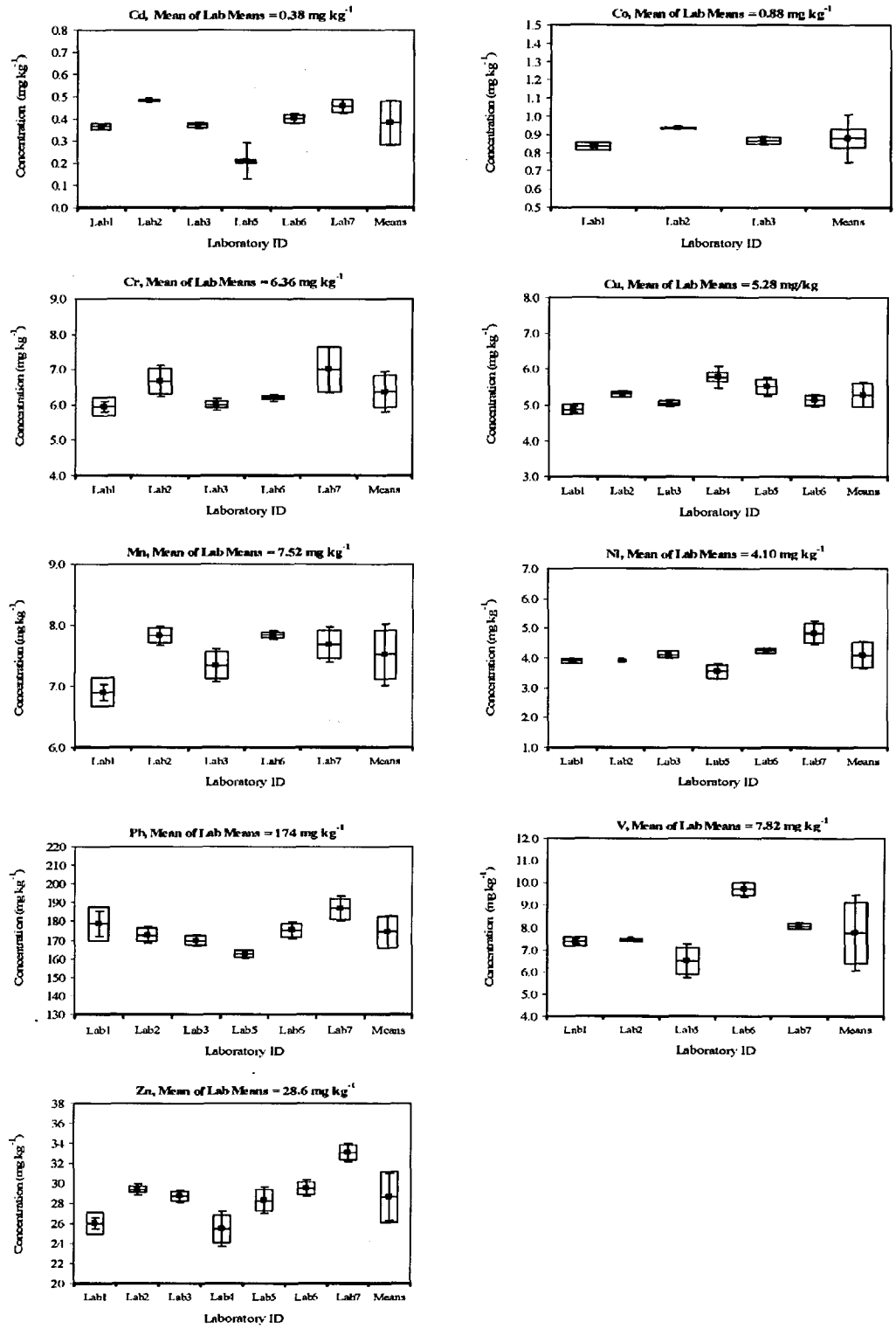

Fig. 2 Inter-laboratory comparison results for total Cd, Co, Cr, Cu, Mn, Ni, Pb, V, and Zn concentrations (expressed as concentration, mg kg^{-1}, corrected for moisture content) of NIMT/UOE/FM/001, after final iteration, along with the calculated mean (■), standard deviation (□) and 95% confidence interval (⊏⊐).

be dissolved by conventional acid digestion methods. The employment of HF for wet digestion is needed in the study of Cr and some major elements. The variation of the acid-extractable results for some elements such as Al is probably a consequence of the range of digestion methods used by the participants.

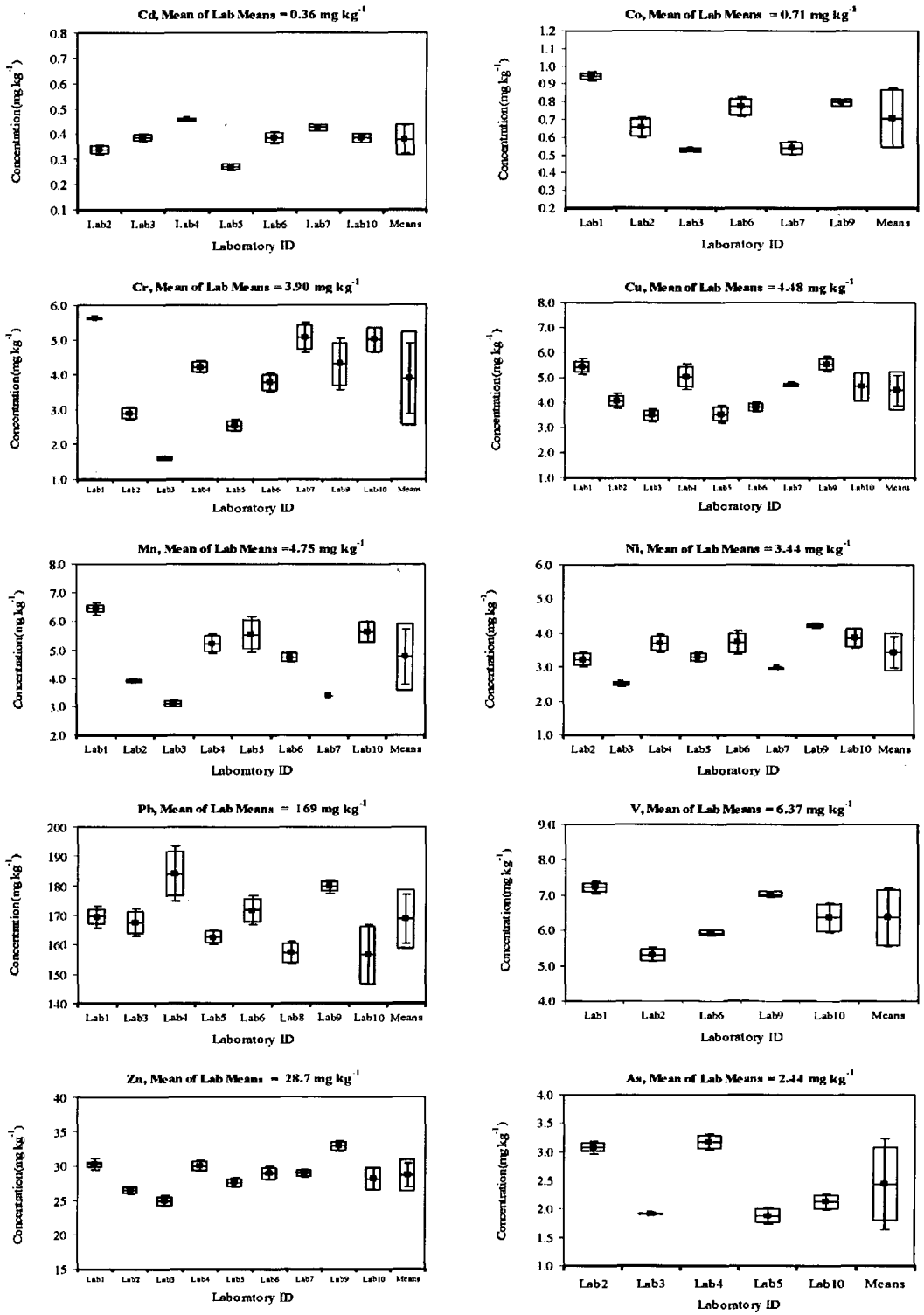

Fig. 3 Inter-laboratory comparison results for acid-extractable As, Cd, Co, Cr, Cu, Mn, Ni, Pb, V, and Zn concentrations (expressed as concentration, mg kg^{-1}, corrected for moisture content) of NIMT/UOE/FM/001, after final iteration, along with the calculated mean (■), standard deviation (□) and 95% confidence interval (⊏⊐).

In addition to elemental concentration data, information on Pb isotopic composition was provided by three laboratories. Reported mean values of 1.1766 ± 0.0008, 1.1759 ± 0.0006, and 1.1765 ± 0.0003 yielded an overall information value of 1.1763 ± 0.0004 (±1 SD) for the $^{206}Pb/^{207}Pb$ ratio.

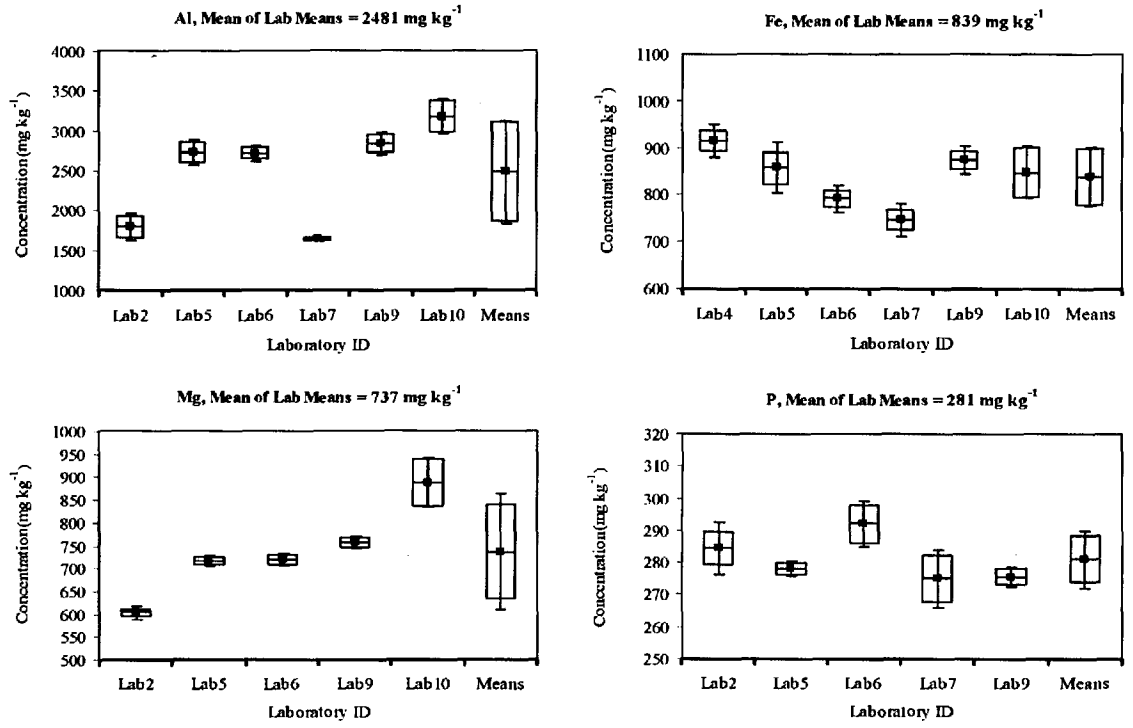

Fig. 4 Inter-laboratory comparison results for acid-extractable Al, Fe, Mg, and P concentrations (expressed as concentration, mg kg^{-1}, corrected for moisture content) of NIMT/UOE/FM/001, after final iteration, along with the calculated mean (■), standard deviation (□) and 95% confidence interval (⊥⊥).

Table 5 Certified values with uncertainties (coverage factor of 2) and information-only (italics) values [±1 SD ($n \leqslant 4$)] for the elemental concentration of the ombrotrophic peat (low ash) reference material NIMT/UOE/FM/001

	Certified values/mg kg^{-1}	
Element (x, y)[a]	Total concentration[b]	Acid-extractable concentration[b]
Cd (6, 8)	0.38 ± 0.08 (6)	0.36 ± 0.05 (7)
Co (4, 6)	0.88 ± 0.09 (3)	0.71 ± 0.13 (6)
Cr (6, 9)	6.36 ± 0.44 (5)	3.90 ± 0.90 (9)
Cu (7, 10)	5.28 ± 1.04 (6)	4.48 ± 0.73 (9)
Fe (4, 8)	*921 ± 84 (4)*	839 ± 54 (6)
Mn (6, 8)	7.52 ± 0.41 (5)	4.74 ± 0.87 (8)
Ni (7, 10)	4.10 ± 0.37 (6)	3.44 ± 0.40 (8)
Pb (7, 10)	174 ± 8 (6)	169 ± 8 (8)
V (5, 6)	7.82 ± 1.08 (5)	6.37 ± 0.73 (5)
Zn (7, 10)	28.6 ± 1.9 (7)	28.7 ± 1.6 (9)
As (4, 5)	*2.44 ± 0.55 (3)*	2.44 ± 0.58 (5)
Hg (2, 2)	*0.169 ± 0.007 (2)*	*0.164 ± 0.020 (2)*
Al (3, 6)	*3692 ± 347 (3)*	2481 ± 514 (6)
Ca (3, 4)	*683 ± 198 (3)*	*763 ± 172 (4)*
Mg (2, 5)	*582 ± 168 (2)*	737 ± 95 (5)
Na (3, 3)	*817 ± 307 (3)*	*229 ± 78 (3)*
P (2, 5)	*265 ± 8 (2)*	281 ± 7 (5)
Ti (3, 3)	*357 ± 18 (3)*	*110 ± 11(3)*

[a] x and y indicate the number of laboratories that submitted results for total and acid-extractable elemental concentrations, respectively. [b] Under total and acid-extractable concentration, the number in brackets indicates the number of accepted laboratory results used in the certification exercise for each element.

Applicability and availability

Although this ombrotrophic peat (low ash) reference material has been developed specifically for use in the analysis of ombrotrophic peat, it may also be of some value in the analysis of minerotrophic peat. Enquiries concerning the availability of the reference material NIMT/UOE/FM/001 for use by laboratories should be made to Dr. J. G. Farmer, University of Edinburgh, from whom instructions for use can also be obtained.

Acknowledgements

We gratefully acknowledge assistance from G. J. Patrick and R. P. Thomas, University of Edinburgh, in the collection of the starting material. L. J. Eades and P. Anderson with J. M. Cloy assisted in the determination of lead isotopic ratios and mercury, respectively, at the University of Edinburgh. At the University of Santiago de Compostela, X. Pontevedra-Pombal, J. C. Nóvoa-Muñoz, E. Peiteado-Varela and R. Pineiro-Rebolo assisted in the inter-laboratory comparison exercise. S. C. Wong helped in the production of data at the Hong Kong Polytechnic University, as did T. Wilson at the University of Maine. Charun Yafa thanks the Royal Thai Government for sponsorship of his PhD studentship *via* the National Institute of Metrology, Thailand (NIMT).

References

1 W. Shotyk, *Environ. Rev.*, 1996, **4**, 149.
2 A. Veysseyre, K. Moutard, C. Ferrari, K. Van de Velde, C. Barbante, G. Cozzi, G. Capodaglio and C. F. Boutron, *Atmos. Environ.*, 2001, **35**, 415.
3 M. L. Brannvall, R. Bindler, O. Enteryd, M. Nilson and I. Renberg, *Water Air Soil Pollut.*, 1997, **100**, 243.
4 R. Lindsay, *Bog: The Ecology, Classification and Conservation of Ombrotrophic Mires*, Scottish Natural Heritage, Edinburgh, 1995.
5 W. Shotyk, S. A. Norton and J. G. Farmer, *Water Air Soil Pollut.*, 1997, **100**, 213.
6 J. G. Farmer, A. B. Mackenzie, C. L. Sugden, P. J. Edgar and L. J. Eades, *Water Air Soil Pollut.*, 1997, **100**, 253.

7 S. A. Norton, G. C. Evans and J. S. Kahl, *Water Air Soil Pollut.*, 1997, **100**, 271.
8 W. Shotyk, D. Weiss, A. K. Cherburkin, P. G. Appleby and J. D. Kramer, *Environ. Sci. Technol.*, 1999, **33**, 1340.
9 M. Krachler, C. Mohl, H. Emons and W. Shotyk, *Environ. Sci. Technol.*, 2003, **37**, 2658.
10 C. Barbante, W. Shotyk, H. Biester, A. Cheburkin, H. Emons, J. G. Farmer, E. Hoffman, A. M. Cortizas, J. Matschullat, S. Norton, J. Schweyer and E. Steinnes, 2000, A peat reference material for trace element analyses, in *Proc. 11th Int. Conf. Heavy Metals Environ.*, ed. J. O. Nriagu, Univ. of Michigan, School of Public Health, Ann Arbor, MI, USA (CD-ROM), Contribution No. 1106, 4 pp.
11 A. M. Ure and C. M. Davidson, *Chemical Speciation in the Environment*, Blackwell Science Inc, Oxford, 2nd edn., 2002.
12 American Society for Testing and Materials, *Standard Practice for Testing Homogeneity of Material for Development of Reference Material*, ASTM Publication E826-85, Philadelphia, PA, 1985, pp. 331.
13 U.S. Environmental Protection Agency, *Method 3052 Microwave Assisted Acid Digestion of Siliceous and Organically Based Matrices*, Office of Solid Waste and Emergency Response, U.S. Government Printing Office, Washington, DC, 1996.
14 Ph. Quevauviller, M. Lachica, E. Boratora, A. Gomez, G. Rauret, A. M. Ure and H. Muntau, *Fresenius J. Anal. Chem.*, 1998, **360**, 505.
15 G. Rauret, J.-F. López-Sánchez, A. Sahuquillo, E. Barahona, M. Lachica, A. M. Ure, C. M. Davidson, A. Gomez, D. Lück, J. R. Bacon, M. Yli-Halla, H. Muntau and Ph. Quevauviller, *J. Environ. Monit.*, 2000, **2**, 228.
16 R. Walker, R. Lawn, P. Roper, G. Holcombe and B. Stuart, *Low-Cost QC Laboratory Reference Materials Investigation of Cost-Effective Production Procedures*, LGC/VAM/2001/009, LGC, London, 2001.
17 U.S. Environmental Protection Agency, *Method 3051 Microwave Assisted Acid Digestion of Sediments, Sludges, Soils, and Oils*, Office of Solid Waste and Emergency Response, U.S. Government Printing Office, Washington, DC, 1994.
18 V. Barwick, S. Burke, R. Lawn, P. Roper and R. Walker, *Application of Reference Materials in Analytical Chemistry*, The Royal Society of Chemistry, Cambridge, UK, 2001.
19 International Organisation for Standardisation, *Certification of Reference Materials – General and Statistical Principles*, ISO Guide 35-1985(E) (1985), ISO, Geneva, 1985.
20 J. Pauwels, A. Lambert and H. Schimmel, *Accred. Qual. Assur.*, 1998, **3**, 180.
21 J. Pauwels, A. M. H. Van der Veen, A. Lambert and H. Schimmel, *Accred. Qual. Assur.*, 2000, **5**, 95.
22 T. P. J. Linsinger, J. Pauwels, H. Schimmel, A. Lambert, A. M. H. Van der Veen, G. Schumann and L. Siekmann, *Fresenius J. Anal. Chem.*, 2000, **368**, 589.
23 A. M. H. Van der Veen and J. Pauwels, *Accred. Qual. Assur.*, 2000, **5**, 464.
24 A. M. H. Van der Veen, T. P. Linsinger and J. Pauwels, *Accred. Qual. Assur.*, 2001, **6**, 26.

Available online at www.sciencedirect.com
SCIENCE DIRECT®
ELSEVIER
International Journal of Mass Spectrometry 232 (2004) 205–215
International Journal of Mass Spectrometry
www.elsevier.com/locate/ijms

Accurate and precise Pb isotope ratio measurements in environmental samples by MC-ICP-MS☆

Dominik J. Weiss [a,b,*], Bernd Kober [c], Alla Dolgopolova [a,b], Kerry Gallagher [a], Baruch Spiro [b], Gaël Le Roux [c], Thomas F.D. Mason [a], Malin Kylander [a], Barry J. Coles [a,b]

[a] *Department of Earth Science and Engineering, Imperial College London, Prince Consort Road, London SW7 2BP, UK*
[b] *Department of Mineralogy, The Natural History Museum, Cromwell Road, London SW7 5BD, UK*
[c] *Institute for Environmental Geochemistry, University of Heidelberg, Im Neuenheimer Feld 234, Heidelberg 69129, Germany*

Received 11 January 2004; accepted 14 January 2004

Abstract

Analytical protocols for accurate and precise Pb isotope ratio determinations in peat, lichen, vegetable, chimney dust, and ore-bearing granites using MC-ICP-MS and their application to environmental studies are presented. Acid dissolution of various matrix types was achieved using high temperature/high pressure microwave and hot plate digestion procedures. The digests were passed through a column packed with EiChrom Sr-resin employing only hydrochloric acid and one column passage. This simplified column chemistry allowed high sample throughput. Typically, internal precisions for approximately 30 ng Pb were below 100 ppm ($\pm 2\sigma$) on all Pb ratios in all matrices. Thallium was employed to correct for mass discrimination effects and the achieved accuracy was below 80 ppm for all ratios. This involved an optimization procedure for the $^{205}Tl/^{203}Tl$ ratio using least square fits relative to certified NIST-SRM 981 Pb values. The long-term reproducibility ($\pm 2\sigma$) for the NIST-SRM 981 Pb standard over a 5-month period (35 measurements) was better than 350 ppm for all ratios. Selected ore-bearing granites were measured with TIMS and MC-ICP-MS and showed good correlation (e.g., $r = 0.999$ for $^{206}Pb/^{207}Pb$ ratios, slope = 0.996, $n = 13$). Mass bias and signal intensities of Tl spiked into natural (after matrix separation) and in synthetic samples did not differ significantly, indicating that any residual components of the complex peat and lichen matrix did not influence mass bias correction. Environmental samples with very different matrices were analyzed during two different studies: (i) lichens, vegetables, and chimney dust around a Cu smelter in the Urals, and (ii) peat samples from an ombrotrophic bog in the Faroe Islands. The presented procedure for sample preparation, mass spectrometry, and data processing tools resulted in accurate and precise Pb isotope data that allowed the reliable differentiation and identification of Pb sources with variations as small as 0.7% for $^{206}Pb/^{207}Pb$.

Keywords: Accuracy; Precision; Pb isotope ratios; MC-ICP-MS; Source assessment; Environmental samples; Sample preparation

1. Introduction

The use of Pb isotopes has had a tremendous effect on our understanding of the geochemical cycling of Pb in the environment and the anthropogenic impact [1]. Lead isotopes in environmental samples, i.e., soil, plant, sediment, peat, surface and subsurface waters, have mainly been measured using thermal ionization mass spectrometry (TIMS) or quadrupole-based inductive coupled plasma source mass spectrometry (ICP-QMS). The advantage of TIMS is that ratios including the least abundant ^{204}Pb isotope are measured with high reproducibility (down to 200 ppm) and it achieves good accuracy also in samples with low [Pb]. However, analytical procedures for TIMS are time consuming and involve intensive sample preparation steps, e.g., two column passages are needed to achieve stable emission of Pb^+ ions from the filament analyzing organic rich matrices, such as lichen or peat. This severely restricts the sample throughput. Yet, many environmental problems require a large sample number to infer statistically significant conclusions. This is due to inherent temporal and spatial variability in the environmental context.

Consequently, most environmental investigations to date use ICP-QMS (e.g., Refs. [2,3]), which performs single mea-

☆ The program code written for the Tl optimization can be obtained from the authors.

* Corresponding author. Tel.: +44-20-7594-6383; fax: +44-20-7594-6464.
E-mail address: d.weiss@imperial.ac.uk (D.J. Weiss).

1387-3806/$ – see front matter © 2004 Elsevier B.V. All rights reserved.
doi:10.1016/j.ijms.2004.01.005

surements at the nominal mass value of each peak using either scanning or peak hopping modes. This results in poor peak shape and consequently in less precise measurements than using multi-collector sector instruments [4]. Typically, precisions of around 0.1–1.0% are achieved [5,6], depending on the concentration or matrix and the ^{204}Pb isotope is seldom measured. However, isotopic ratios including the ^{204}Pb isotope are of crucial importance for source assessments.

Multiple-collector inductively coupled plasma source mass spectrometry (MC-ICP-MS) combines the high ionization efficiency of the Ar-plasma with the precision attainable using multi-collector array. It is thus of great interest for the environmental geochemist as it allows the inclusion of the ^{204}Pb for routine measurements in low [Pb] samples and a large sample throughput with less sample preparation and measurement time is possible. A number of papers have investigated Pb isotope ratio measurements with MC-ICP-MS using different mass spectrometer designs, i.e., double [7–12] or single focussing [13–16] sector field MC-ICP-MS. These papers showed that external precisions achieved are similar to TIMS and that mass fractionation, abundance sensitivity, baseline correction, etc. affect data quality significantly.

With respect to instrumental mass fractionation, arguably a major source of error, the major drawback is that Pb has only one non-radiogenic isotope (^{204}Pb) and mass fractionation cannot be corrected internally. One way to correct for mass bias is to spike the sample with an element of similar mass and with two stable isotopes. In the case of Pb, Tl with isotopes 203 and 205 is the preferred choice [7,12,13]. However, it was shown that the ^{205}Tl/^{203}Tl normalizing ratio of the NIST-SRM 997 Tl (used as dopant) had to be adjusted to higher ratios than the certified value to generate normalized values within error for NIST-SRM 981 Pb determined using double and triple spikes [13]. The latter vary significantly themselves from laboratory to laboratory, i.e., for the ^{206}Pb/^{204}Pb ratios with values of 16.9405 ± 0.0015 [17], 16.9409 ± 0.0022 [18], and 16.9356 ± 0.0023 [19]. White et al. [7] assessed the graphical technique previously developed for Cu and Zn isotope analysis [20], which plots measured ratios of the Tl dopant versus the Pb isotope pair of interest in log–log space. This technique is not applicable on first generation *IsoProbe* instruments due to the small mass bias variations using dry plasma conditions, which consequently results in poor linear fits with high errors and inaccurate isotope ratios [13,21].

To date, most investigations have been limited to synthetic and 'simple' silicate matrices and the Tl mass bias correction procedure has been the object of intense discussions [8,13,15]. Consequently, more investigations on accurate and precise Pb isotope ratio measurements, especially with a focus on environmental samples, are needed. Recent applications of MC-ICP-MS to environmental geochemistry included Pb isotope measurements in seawater matrices [9,16].

The purpose of this contribution is to present a reliable and robust analytical protocol (including sample preparation and mass spectrometry) and data processing methodology for precise and accurate Pb isotope measurements in a wide range of environmental samples. To achieve this, we (i) re-assessed the Tl mass bias correction procedure using a simple optimization procedure, (ii) assessed its analytical merits, and (iii) demonstrated its application in two environmental geochemical studies.

2. Experimental

2.1. MC-ICP-MS and TIMS instrumentation

A Micromass *IsoProbe* MC-ICP-MS based at the Imperial College London/Natural History Museum Joint Analytical Facility (ICL/NHM JAF) was used during the study. The instrument is equipped with seven independently adjustable Faraday cups and a hexapole collision cell. A CETAC Aridus desolvating system (Omaha, NE, USA) with a Tl-H microconcentric nebulizer was used for sample introduction. The optimized data acquisition parameters selected for Pb isotope ratio measurements are summarized in Table 1. For comparative purposes, Pb isotope analyses were also conducted at the Geochronology Laboratory of the University of Heidelberg using a Finnigan *MAT* 261 TIMS with multi-cup system for Pb isotopes and standard sample preparation techniques. Raw TIMS data were normalized to NIST-SRM 981 Pb international standard with reference values of Galer and Abouchami [17] and long-term reproducibility on the 95% confidence level was below 0.03% for ratios normalized to ^{204}Pb. Details of the TIMS procedure have been described in detail before [22].

2.2. Measurement procedures

All isotope measurements were performed by static multiple collection. The ion currents were measured using

Table 1
Typical instrument operating conditions of the *IsoProbe* MC-ICP-MS and the CETAC nebulizer

Instrument settings	
Accelerating voltage (V)	~6000
rf power (W)	~1375
Reflected power (W)	<2
Coolant Ar flow (l min^{-1})	~14
Auxiliary Ar flow (l min^{-1})	1.0–1.2
Nebulizer flow (l min^{-1})	0.6–0.8
Ar collision gas flow (ml min^{-1})	1–2
Abundance sensitivity (ppm)	~25
Analyzer pressure (mbar)	~4.8 × 10^{-8} under full gas load
Sensitivity for Pb (V ppm^{-1})	~300
Cones (skimmer and sample)	Ni
Sample introduction	
Spray chamber temperature (°C)	75
Desolvator temperature (°C)	160
Ar sweep gas flow (ml min^{-1})	~2.8–3.5
Sample flow rate (μl min^{-1})	~40–60

Faraday collectors at masses 200 (Hg), 203 (Tl), 204 (Pb and Hg), 205 (Tl), 206 (Pb), 207 (Pb), and 208 (Pb). The collector efficiencies were calibrated on a daily basis. Ion beam intensities of Pb and Tl were optimized adjusting accelerating voltage, lens system, torch settings, and gas flows. Data collection was made using two blocks with 25 measurements each when analyzing samples and using one block with 20 measurements when analyzing the acid blank before the sample. Internal errors ($\pm 2\sigma$) for synthetic solutions of 50 ng ml^{-1} were below 50 ppm for all ratios. A 10-s integration and 5-s sample admission delay guaranteed stable signals before measurements started. The rinse out time between samples and acid blank was 6 min using 2% (v/v) HNO_3. A typical measurement procedure included five samples taken up in 2% (v/v) HNO_3 and spiked with NIST-SRM 977 Tl and one NIST-SRM 981 Pb standard spiked with NIST-SRM 977 Tl in 2% (v/v) HNO_3 to assess the reproducibility and to optimize the Tl ratio (see below).

Analytical blanks for the total procedure, estimated from intensity data, were below 1 ng and can be accounted for by the Aristar grade acids used during sample preparation. The blank was always below 1% of the total Pb and mixing calculation showed that contributions were insignificant at any time at the level encountered.

2.3. Data reduction and mass discrimination correction

To correct for Faraday cup offset, solvent blank and instrumental blank, averaged acid blank intensities were subtracted from individually measured raw isotope intensities and then the average was calculated. To account for the ^{204}Hg isobaric interference, the ^{200}Hg was measured on L2. This correction was very small and typically amounted to $\leq 0.1\%$. Previous work suggests that average abundance sensitivities are stable on the *IsoProbe* to approximately ± 2 ppm ($\pm 2\sigma$) under same vacuum conditions [16]. Consequently, abundance sensitivity correction during this study was achieved by fixing the Pb/Tl ratio and concentration matching between samples and standards to within 10%.

The run intensities corrected for background and isobaric interference were used to calculate the raw ratios, which then were corrected for instrumental mass bias using Tl as external dopant and the Tl mass fractionation factor f_{Tl}. The ^{205}Tl/^{203}Tl ratio used to calculate the mass fractionation factor f_{Tl} was optimized each measurement session from repeated NIST-SRM 981 Pb standard measurements dispersed between sample measurements (see below details of procedure). The exponential law proved to be the most accurate. The mass fractionation coefficient for Tl (f_{Tl}) was calculated as

$$f_{Tl} = \frac{\ln(R_{Tl}/r_{Tl})}{\ln(M_{205}/M_{203})} \quad (1)$$

where R_{Tl} is the 'true' Tl ratio, r_{Tl} the measured ratio, and M represents the atomic masses of Tl (202.9723 and 204.9745, respectively). The Tl mass correction factor f_{Tl} was used to correct the raw Pb isotope ratios (baseline, interference and abundance sensitivity corrected)

$$R_{Pb} = r_{Pb}\left(\frac{M_1}{M_2}\right)^{f_{Tl}} \quad (2)$$

where R_{Pb} is the 'true' Pb ratio, r_{Pb} is the measured ratio, $M_{1,2}$ are the atomic masses of isotopes 1 and 2, respectively, and f_{Tl} is the mass fractionation coefficient derived from Eq. (1).

2.4. Tl ratio optimization procedure

Instrumental mass fractionation was determined during a measurement session by repeated analyses of the NIST-SRM 981 Pb standard spiked with the NIST-SRM 997 Tl using the same Pb/Tl ratio and concentrations as the samples. The Tl ratio was optimized against the ^{206}Pb/^{204}Pb value of Galer and Abouchami [17]. The optimization was achieved using a least squares method. The approach is based on the logarithmic law, which assumes that the 'true' Tl and Pb ratios are given by

$$R_i^{Tl} = r_i^{Tl}(c^{Tl})^f \quad (3)$$

and

$$R_i^{Pb} = r_i^{Pb}(c^{Pb})^f \quad (4)$$

where f is the mass bias fractionation factor given by $f = \ln(R_i^x/r_i^x)/\ln(c^x)$ (with x = Pb or Tl), R^{Tl} and R^{Pb} are the 'true' ratios, i is a given number of measured NIST-SRM 981 Pb standards, r^{Pb} and r^{Tl} are measured ratios of ^{205}Tl/^{203}Tl and ^{206}Pb/^{204}Pb, respectively, $c^{Tl} = M_2/M_1 = 205/203 = 1.008852$, and $c^{Pb} = M_2/M_1 = 206/204 = 1.009804$.

Using repeated NIST-SRM 981 Pb measurements (between 6 and 12) during a measurement session, we defined $\bar{R}^{Pb}$ (the mean value) as

$$\bar{R}^{Pb} = \frac{1}{N}\sum_{i=1}^{N} R_i^{Pb}, \quad \text{with } R_i^{Pb} = r_i^{Pb}(c^{Pb})^{\ln(R^{Tl}/r_i^{Tl})/\ln(c^{Tl})} \quad (5)$$

where N is the number of NIST-SRM 981 Pb measurements during the measurement session. $\bar{R}^{Pb}$ is a function of the 'true' Tl ratio (R^{Tl}), which we do not know reliably. Given $\bar{R}^{Pb}$ should be close to the certified value for Pb ($R^{Pb}_{cert.}$), we adjusted the unknown R^{Tl}, such that we minimized the prediction error for $\bar{R}^{Pb}$. Therefore, we chose an objective function $\varphi = (\bar{R}^{Pb}/R^{Pb}_{cert.} - 1)^2$, which has a minimum (of zero) when $\bar{R}^{Pb} = R^{Pb}_{cert.}$. The value of R^{Tl} was found by taking the denominator of φ with respect to R^{Tl} and setting this to zero ($\partial\varphi/\partial R^{Tl} = 0$). This leads to the final form

$$R^{Tl} = \ln(c^{Tl})\left(\frac{NR_i^{Pb}}{\sum_{i=1}^{N} r_i^{Pb}(c^{Pb})^{\ln(r_i^{Tl})/\ln(c^{Tl})}}\right)^{\ln(c^{Tl})/\ln(c^{Pb})} \quad (6)$$

2.5. Materials and reagents

Environmental samples included peat from an ombrotrophic bog in the Faroe Islands [23], lichens, vegetables, and chimney dust collected around a Cu smelter in Karabash, Southern Urals [24], and ore-bearing and barren granites from the Orlovka-Spokoine mining district in Eastern Transbaikalia [25]. The acids were of ultra-pure (Merck and sub-boiling acid) or Aristar (Merck) quality. Dilute solutions of acids for mass spectrometry were prepared with purified water obtained from quartz still or an 18 MΩ grade Millipore system (Bedford, MA, USA). Lead, Tl, and mixed Pb–Tl standard solutions were made up from previously prepared stock solutions of NIST-SRM 981 Pb (1240 μg ml^{-1} in 2% (v/v) HNO_3, from S. Bowring, MIT, Cambridge) and NIST-SRM 997 Tl (732 μg ml^{-1} in 2 M HNO_3, from M. Rehkaemper, ETH, Zürich). All solutions and samples were prepared and handled in laminar flow hoods. Solutions were concentration matched to get a signal of ≥100 mV on ^{204}Pb and a Pb/Tl ratio of approximately 5:1.

2.6. Sample preparation of environmental samples

Peat samples were digested using a Milestone high pressure/high temperature microwave oven system [26]. Lichens and vegetables samples from the Karabash smelter were digested using an MARSX high pressure/high temperature microwave oven system [27]. Both microwave digestion methods have been recently developed and showed quantitative recoveries for Pb. The barren and Ta–Nb–W bearing granites from the Orlovka-Spokoine mining district and the chimney dust samples were dissolved using standard HNO_3/HF acid mixtures on a hot plate in closed Teflon beakers [25].

After digestion, all solutions were dried and the residues redissolved in 2 ml of 2.4 M HCl prior to the passage through the column. After conversion to the chloride form, Pb was separated using the Pb selective extraction chromatographic Sr-resin from EiChrom [28] and following the distribution factor dependencies for Pb as reported elsewhere [29]. The method uses only hydrochloric acid and one column pas-

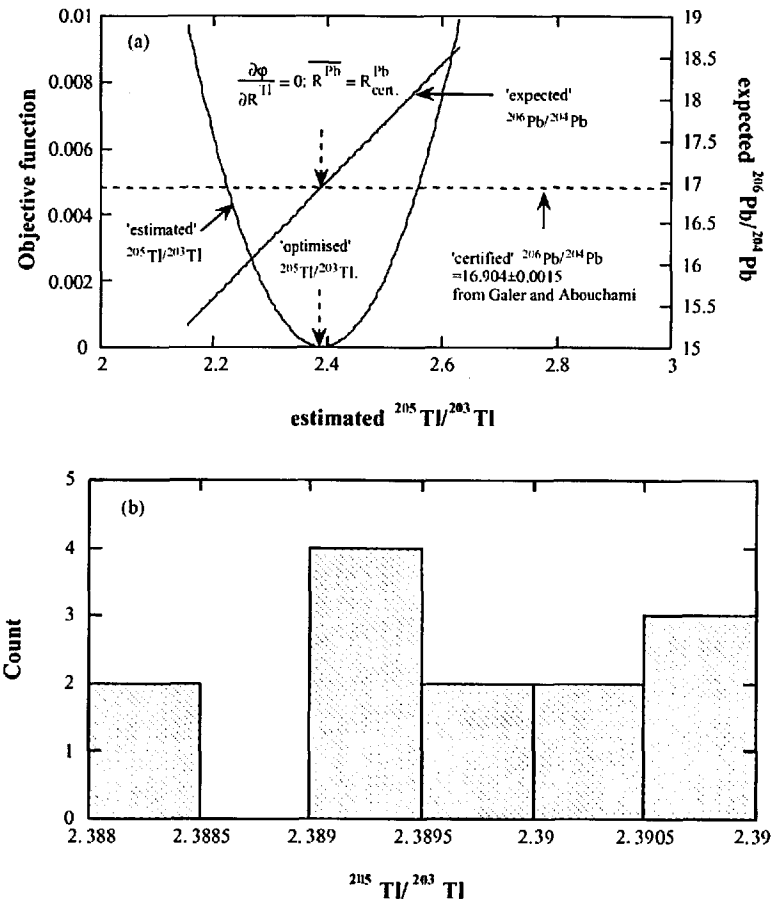

Fig. 1. (a) Distribution of estimated $^{205}Tl/^{203}Tl$ (x-axes) as a function of the expected $^{206}Pb/^{204}Pb$ ratios ($\bar{R}^{Pb}$) and the objective function (φ). The optimized $^{205}Tl/^{203}Tl$ ratio of this measurement session (29.1.03) is given by 2.3905 and fulfills the conditions of $\partial\varphi/\partial R^{Tl} = 0$ and $\bar{R}^{Pb} = R^{Pb}_{cert.}$. (b) The distribution of optimized Tl ratios during 13 measurement sessions at the ICL/NHM JAF during 1 year (August 2002 to August 2003).

Table 2
Ion exchange column procedure for separating Pb from sample matrix

Stage	Acid strength of HCl and volume used
1. Cleaning step	6 M (6 × 1 ml)
2. Conditioning step	2.4 M (2 × 0.5 ml)
3. Sample loading step	2.4 M (1 × 1.5 ml)
4. Matrix elution step	2.4 M (4 × 1 ml)
5. Pb elution step	6 M (3 × 1 ml)
6. Cleaning step	6 M (3 × 1 ml)

The columns were made in-house using Teflon tubing and packed with 600 μl of EiChrom Sr-resin resulting in a bed height of about 0.5 cm.

sage. It consists of a cleaning step with 6 M HCl, a preconditioning and a loading step, both with 2.4 M HCl and an elution step using 6 M HCl (Table 2). The recovery of Pb from the column is quantitative from biological and silicate matrices.

3. Results and discussion

3.1. Assessing the Tl optimization procedure

Fig. 1a shows the results of a Tl optimization calculation from one measurement session (16.8.2002) using 12 individual analyses of NIST-SRM 981 Pb standards doped with NIST-SRM 997 Tl. Plotted is the estimated $^{205}Tl/^{203}Tl$ ratio (R^{Tl}) versus the objective function. Also shown are the corresponding estimated ($\bar{R}^{Pb}$) and certified Pb ratios ($R^{Pb}_{cert.}$). Fig. 1b shows a frequency distribution histogram of optimized Tl ratios determined during 13 individual measurement sessions in a time period of 1 year (August 2002 to August 2003). No systematic trend or bias is visible in the frequency distribution of the optimized Tl ratio. The $^{205}Tl/^{203}Tl$ ranged between 2.3885 and 2.3907 with a mean value of 2.3897 ± 0.0015 (±2σ). The mean value is slightly higher that the originally 'certified' ratio of 2.38714 ± 0.00101 [30] but has a similar error.

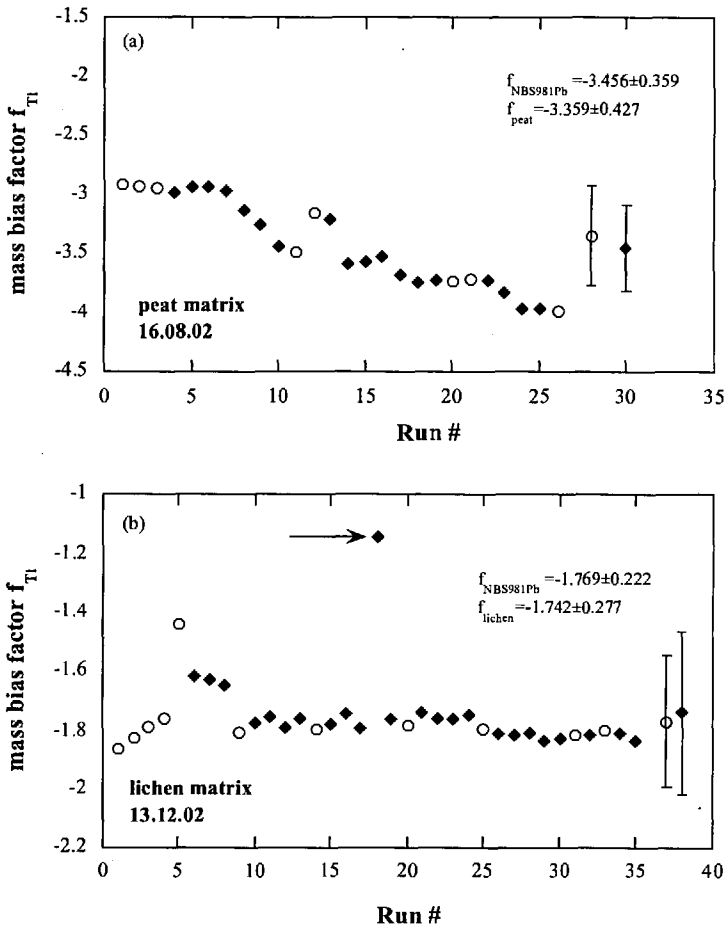

Fig. 2. Changing mass bias factors (f_{Tl}) of the spiked Tl during two measurement sessions in samples and NIST-SRM Pb 981: (a) measuring peat samples from the Faroe Islands, and (b) measuring lichens from the Karabash smelter. Open circles represent the NIST-SRM Pb 981 standard and the closed quadrangles represent the peat and lichen samples. The points with the error bars represent the mean value and the ±2σ standard deviation.

Table 3
Comparison of selected published Pb isotopic composition of NIST-SRM 981 Pb measured by TIMS and MC-ICP-MS

Authors	Mass spectrometer	$^{208}Pb/^{206}Pb$	$^{207}Pb/^{206}Pb$	$^{206}Pb/^{204}Pb$	$^{207}Pb/^{204}Pb$	$^{208}Pb/^{204}Pb$
Todt et al. (1995)	TIMS	2.16701 (43)	0.914585 (132)	16.9356 (23)	15.4891 (30)	36.7006 (112)
Galer and Abouchami [17]	TIMS	2.16771 (10)	0.914750 (35)	16.9405 (15)	15.4963 (16)	36.7219 (44)
Thirlwall [18]	TIMS	2.16770 (21)	0.91469 (7)	16.9409 (22)	15.4956 (26)	36.7228 (80)
Hirata [12]	MC-ICP-MS—*Plasma 54*	2.16636 (82)	0.914623 (37)	16.9311 (90)	15.4856	36.6800 (210)
Rehkaemper and Halliday (1995)	MC-ICP-MS—*Plasma 54*	2.16677 (14)	0.91469 (5)	16.9364 (55)	15.4912 (51)	36.7219 (44)
Belshaw et al. [11]	MC-ICP-MS—Nu *Plasma*	2.1665 (2)	0.91463 (6)	16.932 (7)	15.487	36.683
White et al. [7]	MC-ICP-MS—*Plasma 54*	2.1646 (8)	0.91404	16.9467 (76)	15.4899 (39)	36.6825 (78)
Rehkaemper and Mezger [13]	MC-ICP-MS—*IsoProbe*	2.16691 (29)	0.91459 (13)	16.9366 (29)	15.4900 (17)	36.7000 (23)
Reuer et al. [16]	MC-ICP-MS—*IsoProbe*	2.16639 (304)	0.91460 (18)			
This study	MC-ICP-MS—*IsoProbe*	2.16767 (63)	0.914767 (120)	16.9413 (39)	15.4974 (51)	36.7239 (115)

The Tl ratios used in this study were adjusted to the Galer and Abouchami value. The TIMS data are based on double and triple spike measurements. Errors shown refer to the least significant digits and are all given as $\pm 2\sigma$.

To achieve also accurate Pb isotope measurements in real samples using optimized Tl values derived from repeated NIST-SRM 981 Pb measurements, the mass bias of Tl in standard and samples has to be similar. Fig. 2 shows the calculated mass bias factors f_{Tl} for spiked samples and NIST-SRM 981 Pb standards using the optimized $^{205}Tl/^{203}Tl$ during two measurement sessions: 16.8.02 (Fig. 2a) when peat matrices were measured and 13.12.02 (Fig. 2b) when lichen matrices were measured. The average f_{Tl} in peat (-3.359 ± 0.427; $n = 18$) or lichen

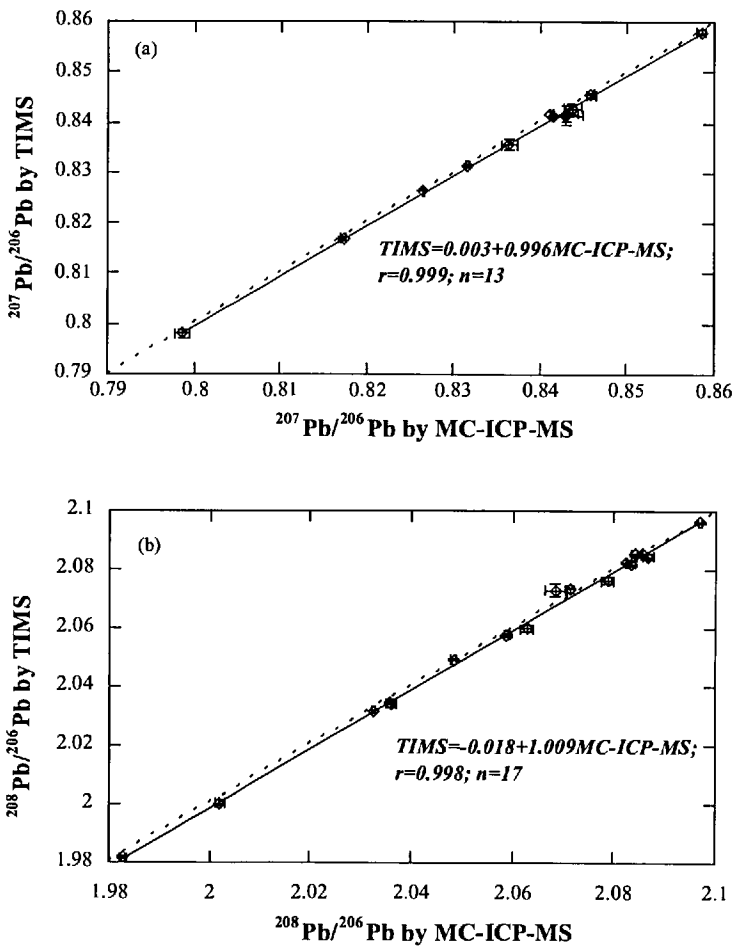

Fig. 3. TIMS and MC-ICP-MS data from selected silicate samples (whole rock and mineral separates from Ta–W ore-bearing granites). Shown is the best linear fit along with the theoretical (dashed) 1:1 line.

Table 4
Complete Pb isotope data set measured during the two environmental geochemical studies

Sample number	Sample ID	Sample type	Pb (μg g)	$^{206}Pb/^{204}Pb$	±2σ (%)	$^{207}Pb/^{204}Pb$	±2σ (%)	$^{208}Pb/^{204}Pb$	±2σ (%)	$^{207}Pb/^{206}Pb$	±2σ (%)	$^{208}Pb/^{206}Pb$	±2σ (%)
Cu smelter near Karabash													
1	I 15 3	Lichen	68.0	17.911	0.0051	15.550	0.0044	37.874	0.0109	0.86816	0.0038	2.11455	0.0051
2	I 17 3	Lichen	120.0	17.897	0.0151	15.535	0.0131	37.847	0.0327	0.86798	0.0038	2.11469	0.0056
5	I 19 3	Lichen	111.0	17.975	0.0032	15.607	0.0028	38.065	0.0070	0.86824	0.0030	2.11767	0.0164
6	I 34 I2 (1)	Lichen	213.0	17.916	0.0025	15.571	0.0020	37.856	0.0050	0.86908	0.0032	2.11293	0.0164
7	I 35 12 (2)	Lichen	151.0	17.906	0.0074	15.549	0.0067	37.830	0.0163	0.86837	0.0051	2.11265	0.0041
8	I 37/C	Lichen	n.d.	17.929	0.0018	15.572	0.0013	37.908	0.0033	0.86852	0.0032	2.11427	0.0042
9	I 1 K1	Lichen	112.8	17.935	0.0036	15.557	0.0029	37.840	0.0073	0.86741	0.0030	2.10983	0.0069
10	I 2 K2	Lichen	64.0	17.801	0.0269	15.457	0.0232	37.635	0.0555	0.86831	0.0065	2.11424	0.0041
11	I 4 K3	Lichen	118.2	17.896	0.0040	15.545	0.0036	37.788	0.0087	0.86860	0.0030	2.11152	0.0040
12	II 5 (D-2)	Vegetable	n.d.	17.831	0.0126	15.506	0.0109	37.684	0.0270	0.86962	0.0036	2.11338	0.0085
13	II 40 3	Lichen	100.6	17.854	0.0144	15.518	0.0130	37.718	0.0322	0.86913	0.0052	2.11251	0.0039
14	II 41/4	Lichen	446.5	17.899	0.0026	15.553	0.0021	37.798	0.0055	0.86890	0.0032	2.11173	0.0059
15	II 42/5	Lichen	1199.9	17.824	0.0142	15.505	0.0127	37.708	0.0313	0.86988	0.0050	2.11558	0.0075
16	II 43/6	Lichen	482.7	17.830	0.0223	15.489	0.0195	37.616	0.0487	0.86871	0.0048	2.10966	0.0045
17	II 44 (2)	Lichen	278.3	17.710	0.0186	15.463	0.0161	37.517	0.0399	0.87313	0.0059	2.11839	0.0071
18	II C1 (D-9)	Chimney dust	n.d.	17.841	0.0014	15.596	0.0007	37.822	0.0019	0.87414	0.0036	2.11990	0.0089
19	II C2 (D-10)	Chimney dust	n.d.	17.844	0.0009	15.599	0.0006	37.833	0.0014	0.87419	0.0028	2.12016	0.0075
20	II C4	Chimney dust	n.d.	17.921	0.0022	15.618	0.0019	37.952	0.0047	0.87149	0.0031	2.11770	0.0044
21	III 46	Lichen	n.d.	17.875	0.0188	15.488	0.0164	37.683	0.0410	0.86646	0.0063	2.10814	0.0047
22	III 49 C/12	Vegetable	175.6	17.913	0.0015	15.574	0.0012	37.864	0.0029	0.86943	0.0036	2.11380	0.0035
23	III 14/1	Vegetable	n.d.	18.044	0.0007	15.727	0.0004	38.342	0.0010	0.87156	0.0021	2.12489	0.0043
24	III 14/2	Vegetable	n.d.	18.003	0.0015	15.599	0.0010	38.015	0.0027	0.86648	0.0035	2.11155	0.0085
25	III KA 26/5	Vegetable	n.d.	17.813	0.0066	15.533	0.0057	37.689	0.0144	0.87201	0.0045	2.11582	0.0045
26	III 26	Vegetable	n.d.	17.901	0.0078	15.527	0.0069	37.776	0.0173	0.86740	0.0034	2.11032	0.0029
27	III KA 4/2	Vegetable	n.d.	17.961	0.0017	15.570	0.0012	37.899	0.0030	0.86687	0.0034	2.11002	0.0045
Average					0.0079		0.0068		0.0169		0.0039		0.0063
Myrarnar peat core													
1	Myr Neo 01	Peat	6	17.738	0.0046	15.583	0.0048	37.606	0.0053	0.87853	0.0015	2.12014	0.0037
2	Myr Neo 02	Peat	14.8	17.688	0.0044	15.582	0.0046	37.577	0.0050	0.88092	0.0018	2.12441	0.0051
3	Myr Neo 03	Peat	45.3	17.657	0.0028	15.562	0.0026	37.503	0.0030	0.88133	0.0046	2.12393	0.0108
4	Myr Neo 04	Peat	65	17.774	0.0061	15.567	0.0054	37.651	0.0054	0.87587	0.0017	2.11838	0.0041
5	Myr Neo 05	Peat	109.1	18.043	0.0030	15.599	0.0029	38.004	0.0036	0.86454	0.0015	2.10633	0.0036
6	Myr Neo 07	Peat	107.1	18.307	0.0078	15.621	0.0086	38.326	0.0094	0.85331	0.0017	2.09358	0.0048
7	Myr Neo 09	Peat	95.9	18.383	0.0124	15.616	0.0161	38.348	0.0203	0.84948	0.0046	2.08601	0.0114
8	Myr Neo 15	Peat	28.1	18.404	0.0018	15.637	0.0020	38.443	0.0022	0.84962	0.0013	2.08879	0.0032
9	Myr Neo 17	Peat	26	18.396	0.0043	15.620	0.0056	38.381	0.0067	0.84911	0.0018	2.08640	0.0043
10	Myr Neo 19	Peat	6.2	18.470	0.0067	15.629	0.0059	38.505	0.0058	0.84618	0.0022	2.08479	0.0062
11	Myr Neo 32	Peat	6.4	18.428	0.0046	15.626	0.0048	38.452	0.0053	0.84796	0.0015	2.08666	0.0035
12	Myr Neo 42	Peat	5.4	18.557	0.0054	15.614	0.0054	38.600	0.0059	0.84137	0.0018	2.08003	0.0043
Average					0.0053		0.0057		0.0065		0.0022		0.0054

The errors shown represent 'with-in run' precisions, which are in general better than the long term reproducibility (see text for details).

211

(-1.742 ± 0.277; $n = 23$) matrix does not differ significantly from the f_{Tl} in the NIST-SRM 981 Pb standards during the same measurement session (-3.456 ± 0.359; $n = 8$, and -1.769 ± 0.222; $n = 11$, respectively). The Tl mass bias is similar in samples and standards, suggesting that the ion exchange chemistry, high plasma temperature and/or the sample dilution prior to the measurements remove any possible interference. The significant different mass bias factors between two measurement sessions reflect the effect of an instrument upgrade which included a new interface.

3.2. Accuracy, precision, and reproducibility

3.2.1. Accuracy

Table 3 shows the average Pb isotope ratio of the NIST-SRM 981 Pb standard from repeated measurements ($n = 35$) during a 5-month period using optimized $^{205}Tl/^{203}Tl$ ratios for mass bias correction (August to December 2002). Also shown are TIMS and MC-ICP-MS data for the NIST-SRM 981 Pb standard from other laboratories. Average accuracy of 48, 70, 55, 41, and 77 ppm for the ratios $^{206}Pb/^{204}Pb$, $^{207}Pb/^{204}Pb$, $^{208}Pb/^{204}Pb$, $^{207}Pb/^{206}Pb$, and $^{208}Pb/^{206}Pb$, relative to the Galer and Abouchami value are achieved.

To get an estimate for the data accuracy for real samples, selected ore-bearing and barren granites (whole rock) from the Orlovka-Spokoine mining district were measured with the *IsoProbe* MC-ICP-MS and with the *MAT* 261 TIMS. Fig. 3 shows the $^{208}Pb/^{206}Pb$ and $^{207}Pb/^{206}Pb$ ratios measured in the same aliquot using the different instruments. Linear regressions ($[^{207}Pb/^{206}Pb]_{TIMS} = 0.003 + 0.996[^{207}Pb/^{206}Pb]_{MC\text{-}ICP\text{-}MS}$; $r = 0.999$; $n = 13$; $[^{208}Pb/^{206}Pb]_{TIMS} = 0.018 + 1.009[^{208}Pb/^{206}Pb]_{MC\text{-}ICP\text{-}MS}$; $r = 0.998$; $n = 17$) and the theoretical 1:1 line are shown. A systematic offset between TIMS and MC-ICP-MS exists, which has been described also with the VG *Plasma 54* [7]. The results agree on average within 0.08% for both $^{207}Pb/^{206}Pb$ and $^{208}Pb/^{206}Pb$ ratios. Similar agreements between MC-ICP-MS and TIMS data for real samples were described for ferromanganese crust [11], volcanic rocks [7], archeological samples [13], and peat samples [31].

3.2.2. Precision and reproducibility

Table 4 shows an entire set of isotope ratios and internal precision expressed in $\pm 2\sigma$ (%) measured during the two environmental studies in various different environmental matrices. The error of the internal isotope measurements is considerably better (on average below 100 ppm) than the errors estimated from the long-term reproducibility. The measured solutions were diluted to a concentration, which allowed a signal of ≥ 100 mV on ^{204}Pb. Typically, that was 50 ng ml^{-1}.

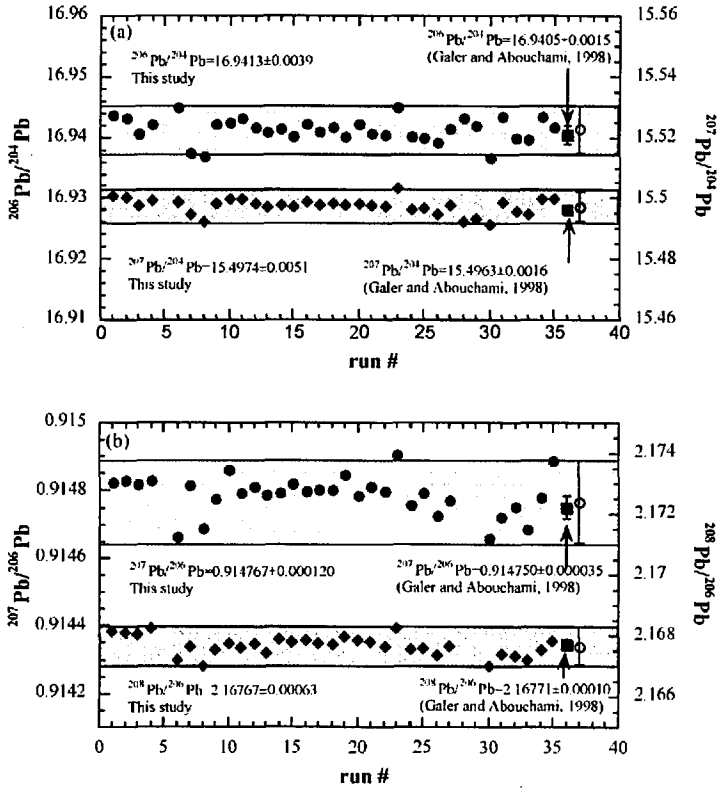

Fig. 4. Typical long-term reproducibility achieved for the ratios (a) $^{208}Pb/^{206}Pb$ and $^{207}Pb/^{206}Pb$, and (b) $^{206}Pb/^{204}Pb$ and $^{207}Pb/^{204}Pb$ ratios on the Micromass *IsoProbe* MC-ICP-MS determined from repeated measurements of NIST-SRM 981 Pb standards spiked with NIST-SRM 997 Tl over the time period of 5 months (August to December 2002).

Fig. 4 shows the long-term reproducibility of the *Iso-Probe* MC-ICP-MS using repeated NIST-SRM 981 Pb measurements over a 5-month period (August to December 2002). Errors (in ppm) are 227 for $^{206}Pb/^{204}Pb$, 326 for $^{207}Pb/^{204}Pb$, 314 for $^{208}Pb/^{204}Pb$, 126 for $^{207}Pb/^{206}Pb$, and 292 for $^{208}Pb/^{206}Pb$. The errors estimated using the long-term reproducibility are significantly higher than the ones estimated from a single measurement session (short-term reproducibility), which was in general below 200 ppm for the $^{208}Pb/^{204}Pb$ ratio and below 150 ppm for all the other ratios (data not shown). The long-term reproducibility of the MC-ICP-MS is similar to the Heidelberg TIMS and agrees well with other laboratories using MC-ICP-MS [7,10–13,32]. Reproducibility estimated from 'true' replicate measurements (different aliquots of same solution) showed similar errors to the ones determined by the repeated measurements of NIST-SRM 981 Pb [31].

3.3. Applications to environmental geochemical studies

Using these new analytical (ion exchange column, high temperature/high pressure microwave digestions) and modified data processing ($^{205}Tl/^{203}Tl$ optimization) procedures, we achieved high precision Pb isotope ratio measurements in peats, lichens, vegetables, and chimney dust during two environmental geochemical projects conducted in London and Heidelberg. One study aimed to assess the local dispersal of Pb and other heavy elements from a Cu smelter using lichen as biomonitors [24], the second study aimed to characterize sources and pathways of Pb and Hg in the sub-Arctic region using a dated peat core in the Faroe Islands [23].

Fig. 5 shows three isotope plots including ^{208}Pb, ^{207}Pb, and ^{206}Pb measured during the two studies. The differences in the isotope ratios among the individual samples are significant on the $\pm 2\sigma$ confidence level and the errors (derived from the long-term reproducibility) plot within the symbols.

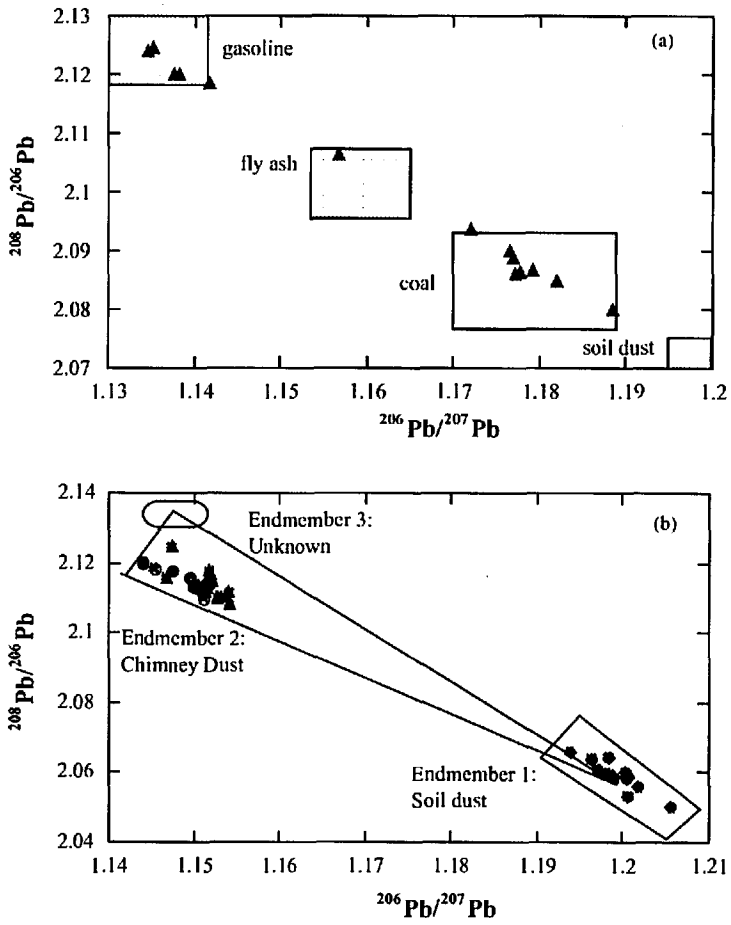

Fig. 5. Three isotope plots including the isotopes ^{208}Pb, ^{207}Pb, and ^{206}Pb of the two different environmental geochemical studies assessing Pb dispersal into the environment: (a) Pb isotope data from chimney dust, vegetable and lichens within the vicinity of a Cu smelter in the Urals (Purvis et al. [24]) and (b) Pb isotope data from a peat core in the Faroe Islands (Shotyk et al. [23]).

3.3.1. Lead sources from long-range atmospheric transport in the sub-Arctic

Fig. 5a represents Pb isotope data measured in a peat bog profile collected in the Faroe Islands (representing ca. 2500 years of atmospheric Pb deposition) with variations of $^{206}Pb/^{207}Pb$ (1.13–1.19) and $^{208}Pb/^{206}Pb$ (2.07–2.12) ratios, which are significantly larger (5 and 2%, respectively) than the estimated long-term reproducibility for these isotope pairs (0.013 and 0.029%, respectively). The large variations of isotope signatures in the peat samples are due to the different Pb sources (gasoline, coal, soil dust, waste incineration, represented as gray fields in Fig. 5a and estimated from data taken from Ref. [33]), which characterized the atmospheric Pb deposition in Europe during the last 2500 years [1,34]. The error bars plot well within the symbols and the individual samples are clearly discernible. The detailed geochemical discussion is given elsewhere [23], but the conclusions agree well with other peat records in Europe covering the last 2500 years of atmospheric Pb deposition [33,35].

3.3.2. Lead sources around a Cu smelter

Fig. 5b shows Pb isotope data measured in lichens, vegetables, and chimney dust around the Cu smelter in Karabash, Southern Urals. The range of $^{206}Pb/^{207}Pb$ and of $^{208}Pb/^{206}Pb$ (1.14–1.15 and 2.11–2.12, respectively) is considerably smaller (0.9 and 0.7%, respectively) than in the peat study, but the variations are still an order of magnitude larger than the estimated errors of the individual data points using the long-term reproducibility. Most ratios of the lichens and vegetables plot on a mixing line between two end members—smelter dust (represented by the isotopic composition of the chimney dust) and natural background Pb (represented by pre-anthropogenic aerosols [36]). However, a statistically significant scatter in the data is revealed and several samples are off the simple two component mixing line, which suggests that a third end member (most likely anthropogenic) with higher ^{208}Pb and higher ^{207}Pb concentrations remains unidentified. The data set shows that with the precision achieved, even on a local scale pollution with small variations, new end members can be identified hinting to additional sources. Such detailed source assessment in a local pollution study has previously been achieved using TIMS [37] but not ICP-QMS [38].

4. Conclusions

A wide range of environmental samples was dissolved using microwave-assisted acid digestion for biological samples or conventional hot plate acid digestion for silicates. After digestion, the solutions were passed through an ion exchange column packed with EiChrom Sr-resin applying a new simple monoacid elution procedure. The column chemistry yielded quantitative recoveries of Pb and allowed a high sample throughput.

Analysis of ^{204}Pb, ^{206}Pb, ^{207}Pb, and ^{208}Pb in 50 ng ml^{-1} solutions on an *IsoProbe* MC-ICP-MS resulted typically in internal precisions of below 100 ppm ($\pm 2\sigma$) on all Pb isotope ratios in all matrices. Mass bias correction using optimized $^{205}Tl/^{203}Tl$ ratios achieved accuracies below 80 ppm for all ratios. The Tl optimization was achieved using repeated measurements of NIST-SRM 981 Pb spiked with NIST-SRM 977 Tl during a measurement session and fitting the $^{205}Tl/^{203}Tl$ ratio using a least square approximation. The optimized Tl ratio used for mass bias correction had to be adjusted for each measurement session up to 2.3907. The long-term reproducibility (expressed as $\pm 2\sigma$) determined over a 5-month period using repeated measurements of the NIST-SRM 981 Pb standard and optimized Tl values was below 350 ppm for all ratios. Ore-bearing granites samples passed through the columns and measured with TIMS and MC-ICP-MS showed excellent correlation. The mass bias of Tl spiked into natural and synthetic samples during a measurement session did not differ significantly, indicating that the complex peat and lichen matrix did not affect the mass bias behavior of the Tl spike.

Acknowledgements

We thank Sara Russell, Eta Mullane, Caroline Smith, Teresa Jeffries, Derek Jones, Mathieu Gounelle, Dietlinde Pingel, and Nicole Rausch for the help in the laboratory and William Shotyk, William Purvis, and Reimar Seltmann for the stimulating collaborative research. Mike Warner, Andy Fleet, and Terry Williams are thanked for support. Financial support from NERC, the Leverhulme Trust, Imperial College London, and The Natural History Museum is gratefully acknowledged. This paper benefited greatly from the discussions with other isotope and environmental geochemists, especially Matthew Thirlwall, Mark Rehkaemper, Ed Boyle, Kevin Foy, Matt Reuer, and Jan Kramers. We also thank the anonymous reviewer and Professor Schwarz for editorial handling. D.W. dedicates this paper to Rosa, Jakob and Claudia.

References

[1] M.K. Reuer, D.J. Weiss, Phil. Trans. R. Soc. Lond. A 360 (2002) 2889.
[2] J.G. Farmer, L.J. Eades, A.B. MacKenzie, A. Kirika, T.E. Bailey-Watts, Environ. Sci. Technol. 30 (1996) 3080.
[3] D. Weiss, V. Chavagnac, E.A. Boyle, J.F. Wu, M. Herwegh, Spectrochim. Acta 55B (2000) 363.
[4] F. Vanhaecke, L. Moens, R. Dams, I. Papadakis, P. Taylor, Anal. Chem. 69 (1997) 268.
[5] I.S. Begley, B.L. Sharp, J. Anal. At. Spectrom. 12 (1997) 395.
[6] C.R. Quétel, T. Bertrand, O.F.X. Donard, F.E. Grousset, Spectrochim. Acta 52B (1997) 177.
[7] W.M. White, F. Albarède, P. Télouk, Chem. Geol. 167 (2000) 257.
[8] J.D. Woodhead, J. Anal. At. Spectrom. 17 (2002) 1381.
[9] S. Ehrlich, Z. Karpas, L. Ben-Dor, L. Halicz, J. Anal. At. Spectrom. 16 (2001) 975.

[10] M. Rehkaemper, A.M. Halliday, Int. J. Mass. Spectrom. 58 (1998) 123.
[11] N.S. Belshaw, P.A. Freedman, K.A. O'Nions, M. Frank, Y. Guo, Int. J. Mass Spectrom. 181 (1998) 51.
[12] T. Hirata, Analyst 121 (1996) 1407.
[13] M. Rehkaemper, K. Mezger, J. Anal. At. Spectrom. 15 (2000) 1451.
[14] M.F. Thirlwall, J. Anal. At. Spectrom. 16 (2001) 1121.
[15] M.F. Thirlwall, Chem. Geol. 184 (2–3) (2002) 255.
[16] M.K. Reuer, E.A. Boyle, B.C. Grant, Chem. Geol. 200 (2003) 137.
[17] S.J.G. Galer, W. Abouchami, Min. Mag. 62A (1998) 491.
[18] M.F. Thirlwall, Chem. Geol. 163 (2000) 299.
[19] W. Todt, R.A. Cliff, A. Hanser, A.W. Hofmann, in: S.R. Hart, A. Basu (Eds.), Earth Processes: Reading the Isotopic Code, vol. 95, American Geophysical Union, 1996, p. 429.
[20] C.N. Maréchal, P.F. Albarède, Chem. Geol. 156 (1999) 251.
[21] T.F.D. Mason, D.J. Weiss, M. Horstwood, R.R. Parrish, S.S. Russell, E. Mullane, B.J. Coles, J. Anal. At. Spectrom., doi:10.1039/b306953b.
[22] B. Kober, M. Wessels, A. Bollhofer, A. Mangini, Geochim. Cosmochim. Acta 63 (9) (1999) 1293.
[23] W. Shotyk, M.E. Goodsite, F. Roos-Barraclough, N. Givelet, G. Le Roux, D.J. Weiss, A.K. Cheburkin, K. Knudsen, J. Heinemeier, W.O. Van der Knaap, S.A. Norton, C. Lohse, Accumulation and predominant atmospheric sources of natural and anthropogenic Hg and Pb on the Faroe Islands since 5,420 ^{14}C yr BP recorded by a peat core from a blanket bog, Geochim. Cosmochim. Acta (submitted).
[24] O.W. Purvis, P.J. Chimonides, G.C. Jones, I.N. Mikhailova, B. Spiro, D. Weiss, B.J. Williamson, Lichen biomonitoring in one of the most polluted areas in the world, Proc. R. Soc. Lond. B 271 (2004) 221.
[25] A. Dolgopolova, R. Seltmann, B. Kober, D. Weiss, P. Dulski, C. Stanley, Geochemical characteristics and Pb isotope systematics of highly fractionated Li-F enriched amazonite granites and related host rocks of the Orlovka-Spokoine mining district, Eastern Tranbsbaikalia (Russia), Trans. Inst. Min. Metall.: Section B: Appl. Earth Sci. (in press).
[26] M. Krachler, C. Mohl, H. Emons, W. Shotyk, J. Anal. At. Spectrom. 17 (8) (2002) 844.
[27] A. Dolgopolova, D. Weiss, R. Seltmann, B. Coles, Improved high temperature/high pressure microwave digestion method for lichens, Int. J. Environ. Anal. Chem. (submitted).
[28] E.P. Horwitz, M.L. Dietz, S. Rhoads, C. Felinto, N.H. Gale, J. Houghton, Anal. Chim. Acta 292 (1994) 263.
[29] E.P. Horwitz, International Workshop on the Application of Extraction Chromatography in Radionucleide Measurements, IRMM, Geel 9-0, Belgium, 1998.
[30] L.P. Dunstan, J.W. Gramlich, I.L. Barnes, W.C. Purdy, J. Res. Nat. Bur. Stand. 85 (1980) 1.
[31] M. Kylander, D.J. Weiss, T. Jeffries, B. Coles, Sample preparation using dry ashing for precise and accurate isotope analysis of Pb by MC-ICD-MS, J. Anal. At. Spectrom. (submitted).
[32] K.D. Collerson, B.S. Kamber, R. Schoenberg, Chem. Geol. 188 (2002) 65.
[33] D. Weiss, W. Shotyk, P.G. Appleby, J.D. Kramers, A.K. Cheburkin, Environ. Sci. Technol. 33 (9) (1999) 1340.
[34] D. Weiss, W. Shotyk, O. Kempf, Naturwissenschaften 86 (1999) 262.
[35] A. Martinez-Cortizas, E. Garcia-Rodeja Gayoso, D. Weiss, Sci. Total. Environ. 292 (1/2) (2002) 1.
[36] W. Shotyk, D. Weiss, J.D. Kramers, R. Frei, A.K. Cheburkin, M. Gloor, S. Reese, Geochim. Cosmochim. Acta 65 (14) (2001) 2337.
[37] C. Gobeil, W.K. Johnson, R.W. MacDonald, C.S. Wong, Environ. Sci. Technol. 28 (1) (1995) 193.
[38] J.M. Blais, Water Air Soil Pollut. 92 (1996) 329.